LAWRENCE RADIATION LABORATORY · UNIVERSITY OF CALIFORNIA · BERKELEY

UCRL-11833
FALL 1964

SEMIANNUAL REPORT BIOLOGY and MEDICINE

TWO-WEEK LOAN COPY

This is a Library Circulating Copy which may be borrowed for two weeks. For a personal retention copy, call Tech. Info. Division, Ext. 5545

DONNER LABORATORY
and DONNER PAVILION

DISCLAIMER

This document was prepared as an account of work sponsored by the United States Government. While this document is believed to contain correct information, neither the United States Government nor any agency thereof, nor the Regents of the University of California, nor any of their employees, makes any warranty, express or implied, or assumes any legal responsibility for the accuracy, completeness, or usefulness of any information, apparatus, product, or process disclosed, or represents that its use would not infringe privately owned rights. Reference herein to any specific commercial product, process, or service by its trade name, trademark, manufacturer, or otherwise, does not necessarily constitute or imply its endorsement, recommendation, or favoring by the United States Government or any agency thereof, or the Regents of the University of California. The views and opinions of authors expressed herein do not necessarily state or reflect those of the United States Government or any agency thereof or the Regents of the University of California.

UCRL-11833
UC-48 Biology and Medicine
TID-4500 (39th Ed.)

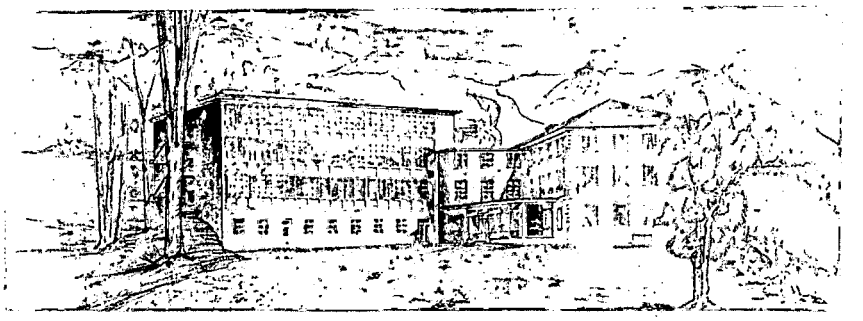

DONNER LABORATORY AND DONNER PAVILION

LAWRENCE RADIATION LABORATORY — UNIVERSITY OF CALIFORNIA

BERKELEY, CALIFORNIA

SEMIANNUAL REPORT — BIOLOGY AND MEDICINE

FALL 1964

John H. Lawrence, M.D., Editor

Tove Neville, Associate Editor

AEC Contract No. W-7405-eng-48

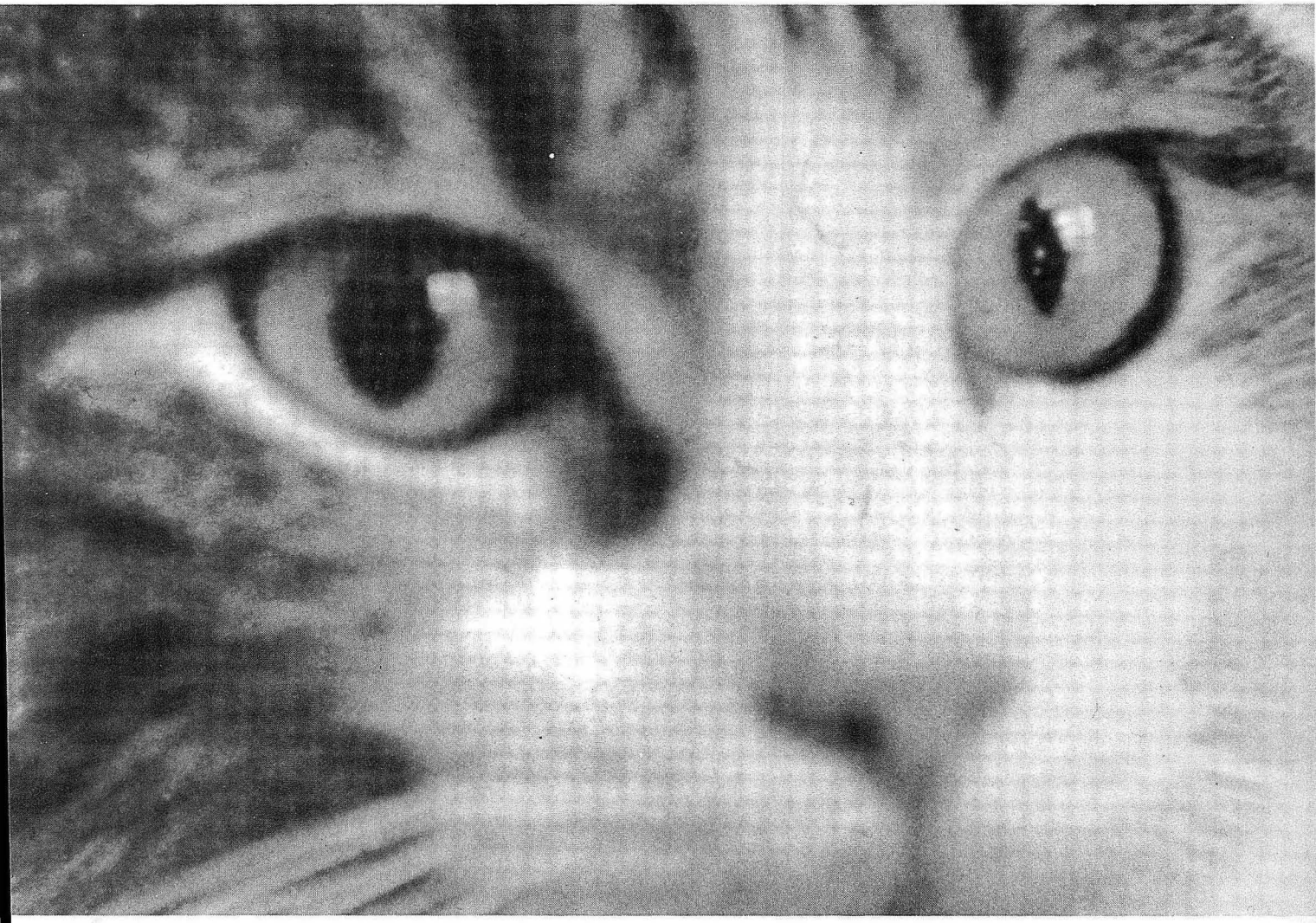

Imbalance of pupil size due to cyclotron irradiation of the brain (see p. 127).

TABLE OF CONTENTS

The Developmental Autonomy of Extra Sex Combs in Drosophila Melanogaster
CHIYOKO TOKUNAGA AND CURT STERN 1

A Novel Method for the Release of Bacteriophage DNA
DAVID FREIFELDER 26

The Effect of Litter Culling, or Family Planning, on the Rate of Natural Selection
JACK LESTER KING 29

On a Single-Tracer Injection Method for C^{14}-Glucose Kinetic Studies in Humans
EDWARD MANOUGIAN 34

C^{14}-Glucose Kinetic Studies in Normal, Diabetic and Acromegalic Subjects
EDWARD MANOUGIAN, MYRON POLLYCOVE, JOHN A. LINFOOT AND JOHN H. LAWRENCE 50

Growth-Hormone Secretion in Treated and Untreated Acromegaly
JOHN A. LINFOOT AND FRED GREENWOOD 73

Effect of Heavy Particles on the Proliferative Capacity of Ascites Tumor Cells (Lymphoma) Grown *In Vivo*
YOLANDA SCHMIDLIN, JOHN H. LAWRENCE, KAREN SILLESEN, GRAEME WELCH AND JOHN LYMAN 80

Production and Chemical Processing of Fe^{52} For Medical Use
YUKIO YANO AND HAL O. ANGER 95

Bone Blood Flow Shown with F^{18} and the Positron Camera
DONALD VAN DYKE, HAL O. ANGER, YUKIO YANO AND CARLOS BOZZINI 100

Improved Liquid Scintillation Counting Method for Fe^{55} and Fe^{59} in Blood
HIROSHI SAITO 112

Blockage of Pupillodilation with Cyclotron-Accelerated Alpha Particles
CORNELIUS T. GAFFEY 121

Serum Lipid-Lipoprotein Interrelationships between Males and Females
NORMAN K. FREEMAN, FRANK T. LINDGREN AND ALICIA M. EWING 134

The Effect of Very Low-Density Lipoproteins on Lipid Transfer in Incubated Serum
ALEX V. NICHOLS AND LESTER SMITH 145

A General Computer Method for Statistical Analysis of Data
ALICIA EWING 154

Staff Publications 158

The Developmental Autonomy of Extra Sex Combs in *Drosophila melanogaster*

Chiyoko Tokunaga and Curt Stern

The forelegs of normal males of Drosophila melanogaster possess a row of about 10 or more heavy bristles on their first tarsal segment (basitarsus). This "sex comb" is lacking on the second and third legs. Several mutants, however, lead to the appearance of a sex comb on the middle and hind legs of the male. Females, whether normal or carrying the mutants lack sex combs on any of their legs.

The restricted, specific area of the male in which a sex comb is formed may be called a regional singularity. An analysis of gynanders, Stern and Hannah (1), showed that this singularity exists in both males and females. Its presence evokes a developmental response toward formation of sex-comb teeth, provided the genotype of the responding cells is male. Female cells lack the competence to form teeth. Insofar as the singularity arises during development before the formation of the visible pattern of differentiation it constitutes part of a "prepattern", Stern (2,3).

The occurrence of extra sex combs on the second and third legs of mutants shows that sex comb singularities can exist also on these legs. The absence of sex combs on them in normal males might mean that the prepatterns of the forelegs and subsequent legs are essentially different so far as the sex comb is concerned. Alternatively, it might signify that all legs, even in normal males, develop essentially the same prepatterns, but that the normal genotype responds only to that of the foreleg whereas certain mutant genotypes may respond to those of all legs.

A morphological analysis by Hannah-Alava (4,5) primarily in terms of the bristle pattern showed that the extra sex-comb mutants not only cause the appearance of sex combs on the middle and hind legs but change the total development of these legs in the direction of that of the first leg. This discovery provided a simple interpretation for the origin of the extra sex combs. If the primary developmental effect of the mutants consists of the homoeotic transformation of the second and third into first legs then, given the fact that first legs have sex combs, it follows directly that sex combs should develop on the transformed legs. Thus, the homoeotic mutants seemed to act by introducing a new, first-leg

prepattern into the embryonic second and third legs, a prepattern to which cells of the male genotype then respond in the usual way by formation of sex-comb teeth.

If the above interpretation is correct, a prediction could be made concerning the phenotypes of mosaic legs. Since a second or third leg made up of cells heterozygous for a recessive extra sex-comb mutant has a normal phenotype it should have the prepattern typical for its kind. A small patch, therefore, of homozygous mutant tissue occuring in the appropriate region of the leg should not produce sex-comb teeth since the leg as a whole had not acquired the prepattern of a foreleg. The experiments to be reported in this paper were undertaken in order to test this supposition of nonautonomy of extra sex-comb mutants in mosaic second and third legs.

In order to lay a basis for the results with mosaic legs, it was necessary to study in some detail the phenotypes of whole, nonmosaic, homozygous extra sex comb legs. The expression of this genotype varies greatly between individuals, and the nature of this variability which affects different parts of the legs in an independent mosaic-like fashion proved to add to the later evidence from genetic mosaics. Another aspect that needed clarification before the mosaics could be evaluated, concerned the appearance of dark-colored sex-comb teeth on heterozygous wild-type second and third legs, which did not seem to arise as the result of mosaic homozygosity for the extra sex comb mutant. A likely cause of differentiation of the dark teeth is a developmental induction of a phenocopy, independent of genetic change. In the Results section, the description and analysis of the phenotypic expression of the extra sex-comb genotype in homozygous nonmosaic legs and of the dark sex-comb teeth will precede the presentation of the genetic mosaics.

MATERIALS AND METHODS

The flies that provide the main data for this report were heterozygous for the recessive autosomal mutant "extra sex combs", Slifer (6). It is located in the left arm of chromosome 2, associated with inversion In(2L)t, Lewis, after Hannah and Strömnaes (7). Usually, the mutant is kept in a balanced stock of the genotype esc/Bl where homozygotes for Bl(Bristle, 2, 54.8) are lethal and homozygotes for esc sterile. The absence of crossovers between esc and Bl in this stock suggests that the two genes are located very close to each other. The recessiveness of esc is not complete. While no third leg of esc/+ males was encountered which had a sex comb, one out of 3,036 second legs of 1,518 y;esc/Bl males from stock cultures had a single sex-comb tooth. In another group of 716 heterozygous males of the genotypes y;esc/Cy and y;esc/sc^{19i}, listed in the third and fourth rows of Table 3, none of the second legs had a comb. Such sex combs, however, did occur in an experiment involving 422 esc/+ and 419 esc/Cy males segregating in pair matings. None of the former had an extra sex comb in

contrast to 6 of the 838 second legs of the latter. It appears from this result that the Cy-carrying chromosome contained an enhancer of the dominance of esc.

In order to obtain esc/esc areas on esc/+ males, somatic crossing-over was induced by means of X radiation of larvae. Homozygous esc areas were recognizable primarily by the color of their bristles or sex-comb teeth, when present. This marking was accomplished by the use of yellow (y, 1, 0.0) in the X chromosome and an insertion into the left arm of the second chromosome of a y^+ carried in a short section of the X chromosome ($T(1;2)sc^{19}$). The complete genotype of the males used in the experiment was $T(1;2)sc^{19}$;$fes\ sc^{19i}\ b\ pr/Cy\ dp^{Th}\ pr$. Of these mutants only b (black body color, 2, 48.5) will be discussed below.

F_1 larvae from the following cross were obtained: y;esc/Bl ♀ x $T(1;2)sc^{19}$ ♂ , the relevant F_1 males being $y;esc/T(1;2)sc^{19i}$. These males have dark setae due to the presence of the insertion. Crossing-over between the locus of esc and the kinetochore results in sister cells of the genotypes y;esc/esc and $y;\ T(1;2)sc^{19i}/T(1;2)sc^{19i}$. The former type leads to yellow areas, the latter to non-yellow areas which are indistinguishable from the heterozygous background. (Crossing-over between the T(1;2) insertion and the locus of esc would result in yellow areas heterozygous for esc and thus not be informative concerning the expression of homozygous esc/esc in mosaic legs. Double crossovers between the loci of T(1;2), esc, and the kinetochore may result in esc/esc cells that have remained heterozygous for T(1;2) and therefore do not lead to yellow areas.)

The age of irradiated larvae varied from 27 to 120 hr at about 25°C (ages in hours are counted from the time of egg deposition). The X-ray dosage varied from 700 R to 2,400 R with a dose rate of about 80 R/min, the youngest larvae receiving the lower dosages. Some prepupae aged 120 to 130 hr were also irradiated, with from 2,100 R to 2,400 R. Irradiation was provided by a 250-kV, 15 MA X-ray tube with 2.5 mm Al tube filtration and 0.25 mm Cu and 1.0 Al external filtration.

The second and third legs of the phenotypically normal males were examined for the presence of mosaic patches under a dissecting microscope at magnifications from 50 to 80 x and occasionally at 160 x. The mosaic legs were mounted in Andre medium between two cover glasses and studied in detail with a compound microscope. Drawings were made with the use of a camera lucida.

Various combinations of esc were made with other mutants that influence features of the sex comb. In this paper only one combination will be discussed. It brings together the dominant allele of esc, designated esc^D, formerly reported as Esc^2, Tokunaga (8), with the recessive mutant en (engrailed, 2, 62.0): esc^D en/+ en. By itself homozygous en causes differentiation of a secondary sex

Table 1. Penetrance and expressivity of extra sex combs in esc/esc males

esc/esc from stock	No. of 2nd or 3rd legs	second legs		third legs	
		sex comb present (%)	mean no. of teeth per comb	sex comb present (%)	mean no. of teeth per comb
Bl/esc	74	35.1 ± 5.5	2.1 ± 1.2	9.5 ± 3.4	1.6 ± 0.8
y;Cy/esc	138	15.9 ± 3.1	2.7 ± 1.4	6.5 ± 2.1	1.4 ± 0.6
y;Bl/esc	60	10.0 ± 3.9	1.7 ± 0.81	0	0

comb on the basitarsus of the first leg, arranged in mirror position to the normal, primary comb, Tokunaga (9).

RESULTS

SOME EFFECTS OF THE ESC/ESC GENOTYPE Apart from the most striking effect of esc in leading to the formation of sex-comb teeth on second and third legs, a series of other effects have been shown to exist, Hannah-Alava (5). These effects on size, shapes and chaetotaxy of the leg segments established the homoeotic nature of the changes produced by the mutant in the second and third legs. A few of these changes will be singled out for the presentation of additional data and discussion since they have bearing on the mosaic experiments.

The effects of homozygous esc/esc are variable. Many second and third legs are unchanged from those of wild-type individuals and a whole range of partially transformed legs is found, from those showing only minor traits of first legs to those having undergone far-reaching transformations.

In many esc males only a single sex-comb tooth is present on a second or third leg. In the following pages the term "sex comb" will be used even for such cases. Specific data on penetrance and expressivity of homozygous esc males relate mostly to the presence or absence of sex combs and, when present, to their number of teeth, Slifer (6), Hannah-Alava (5). Our own data on males from three different unselected nonisogenic stocks show variability of sex-comb penetrance for the second leg from 10 to 35% and for the third leg from 0 to 9.5% (Table 1). In each of the three stocks, the penetrance was higher in the second than in the third leg. This gradient in the frequency of producing sex combs on the three pairs of legs was first observed by Slifer and analyzed in some detail. Her esc/esc males showed higher degrees of penetrance than those listed above. In our own material high penetrance values were also obtained, as a result of selection for a number of generations.

Even when sex combs were present, the mean number of teeth per comb was much lower than that of the normal sex combs on the first leg. For the second

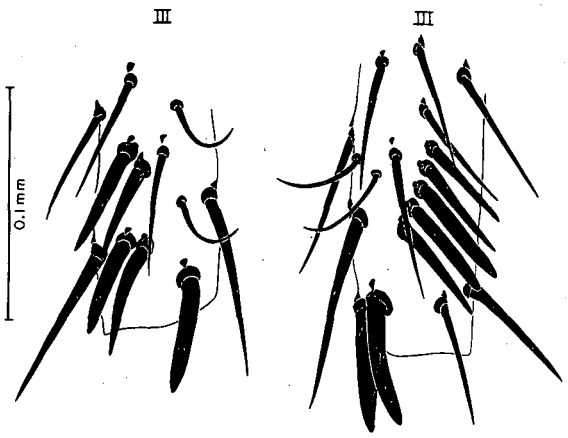

Figure 1. Distal parts of two basitarsi of esc/esc male third legs (III) showing typical bracted bristles characterized by the triangular marking near the base, bractless bristles, sex-comb teeth and various types of chaetae intermediate in form between machrochaetae and teeth.

MUB-3791

leg it varied in the unselected stocks between 1.7 and 2.7 and for the third leg between 1.4 and 1.6, as compared to the usually 10 or more teeth in first-leg combs. In the line selected for high penetrance, the mean numbers of teeth for second and third legs were 6.4 and 3.3, respectively. Apart from the lower mean frequency of differentiation of teeth in the second and third legs, as compared to first legs, the bristle-forming cells in the sex-comb area of the second and third legs not rarely fail to form a typical tooth but do develop into structures that are to varying degrees intermediate between teeth and ordinary macrochaetae (Fig. 1). In determining teeth numbers only those intermediate bristles very similar to full teeth were included in the counts.

The incomplete penetrance of esc in regard to the sex combs on the second and third legs has an important bearing on the expectation concerning the phenotype of y;esc/esc spots in the potentially sex-comb-forming areas of mosaic legs. Absence of sex-comb teeth in relevant yellow spots may signify either nonautonomy of esc or simply lack of penetrance as in many nonmosaic homozygotes. It may also be the result of heterozygosity for esc in consequence of somatic crossing-over to the left of its locus. Presence of sex-comb teeth in even a fraction of small yellow spots would be a demonstration of autonomous expression on mosaic basitarsi.

In addition to the possession of a sex comb, the first leg of normal males differs from the subsequent legs in various ways, at least two of which--the transverse rows on the tibia and those on the basitarsus--can be analyzed in mosaic legs consisting of esc/+ and esc/esc tissues. The approximately six basitarsal transverse rows on the male foreleg lie anterio-ventrally and ventrally between longitudinal rows 7 and 1 and the approximately six distal tibial transverse rows lie in a corresponding region proximally to the basitarsal rows (Fig. 2a). The transverse rows of the foreleg are absent on other normal legs. They are topographically different from the transverse tibial and basitarsal

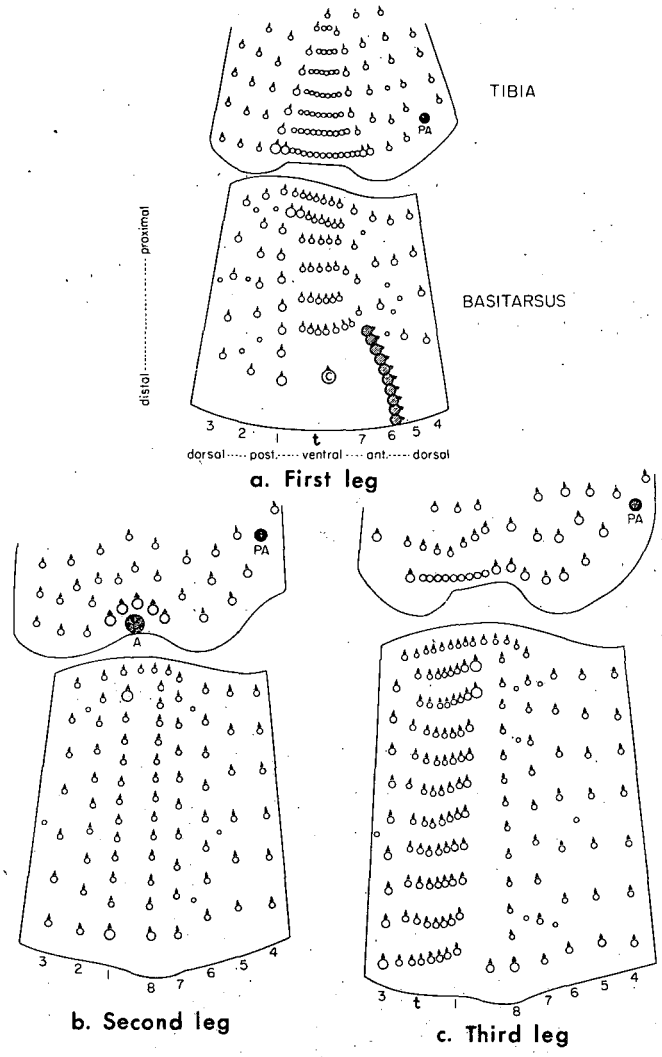

Figure 2. The pattern of chaetae on the distal part of the tibia and the basitarsus of the left three legs of normal males. Circles with triangular markings: bracted bristles. Large shaded circles with markings: sex-comb teeth. Circles without markings: bractless bristles. The proximal and distal bractless bristles between longitudinal rows 6 and 7 are designated in the text as 6.5p and 6.5d, respectively. A: apical bristle surrounded by "spurs" (closed circles). PA: preapical bristle. C: central bristle. Arabic numbers denote longitudinal rows of bristles. (Modified after Hannah-Alava (5)).
MUB-3792

rows formed exclusively on third legs. (Fig. 2c). The rows of the third legs are located posterio-ventrally and posteriorly between longitudinal rows 1 and 3. Interestingly, as found by Hannah-Alava (5), the transformation of third into first legs in whole esc/esc flies does not extend to the area of third-leg transverse rows. They never disappear though their number may decrease somewhat in conformity with a shortening of the basitarsus. This regionally restricted action of esc is similar to that of the bithorax pseudoalleles which can be specified in terms of transformations of anterior and posterior portions of certain body segments, Lewis (10). In the rest of this paper the term transverse rows will refer exclusively to those located between rows 7 and 1. The normal second leg forms none of the various kinds of transverse rows (Fig. 2b).

In mosaics of the second and third legs the presence of transverse rows or parts of them is recognizable morphologically by the fact that bristles are arranged close to one another across the segment in an anterior-posterior

direction. They should also be recognizable by a yellow phenotype produced by the segregated y;esc/esc genotype. However, the bristles of the transverse rows even of whole non-yellow esc/esc flies are sometimes less pigmented than other bristles. This is especially so for the third leg. This makes it at times impossible, or at least uncertain, to distinguish the y/+ from the y genotype by their coloration. In any case, the difference in respect to the presence of transverse rows on first legs and their absence on subsequent legs provides structures in addition to the sex comb for which the problem of autonomy or non-autonomy of action of esc in mosaic legs can be studied.

Investigations on cell lineage have shown that the normal sex comb of a male first leg is equivalent (=homologous) to one of the last transverse rows of the female basitarsus, Tokunaga (11). Developmentally, the transverse row of the male destined to become the sex comb undergoes a rotating shift. This results in a position of the sex comb at an approximately right angle to its original location parallel to the other transverse rows. In gynandromorphs mosaic for the area of the terminal transverse rows of the first leg, small sections of male tissue differentiate sex-comb teeth but may not undergo the tissue shift. It is to be expected that the same absence or incompleteness of the shifting would occur in small sectors of esc/esc tissue on esc/+ second or third legs even when tooth formation can take place autonomously in such mosaics.

The legends of Figs. 2 and 4 of Hannah-Alava's paper (5) are entitled, "Stages in the transformation of a male second [or third] leg into a first leg . . ." A study of these series of legs of different extra sex-comb genotypes shows that some legs are nearly unchanged from the typical appearance of a second or third leg, that others show intermediate types of transformation and that still others are more or less fully transformed into first legs, at least on their ventral parts. Hannah-Alava summarizes her analysis of this variation as follows: "Although there was a considerable range in expression of each of the characters [size, shape and chaetotaxy], a change in any one character was accompanied by a proportional change in another character, that is, the expression(s) of the characters are covariant." (p. 903,l.c). It is made clear, however, that the covariance is a statistical phenomenon rather than one of absolute nature. Many cases are listed in which only one or the other of two variable traits appears, even though there is a significant overall correlation of both traits being absent or both present. Thus, there are second legs that lack tibial and tarsal transverse rows as well as a sex comb, other legs with transverse rows but no sex comb, others without transverse rows but a sex comb and still others with both traits. From our own nonmosaic esc/esc stock material we may cite third legs with tibial and basitarsal transverse rows but without a sex comb or with a sex comb consisting of only one or two teeth, a third leg with one tibial but no basitarsal transverse row and a sex comb of three teeth, a second leg with no tibial but two basitarsal transverse rows and a sex comb of

Table 2. Length and proportions of basitarsi of the three legs in various male genotypes. 100 units of length = 0.65 mm. I, II, III = first, second and third legs

Genotype	Origin	No. of legs*	I	II	II/I	III	III/I
+	Oregon R-C	20	28.2 ± 0.5	44.4 ± 0.7	1.57	48.3 ± 0.8	1.71
pr en	pr en	20	28.2 ± 0.9	44.3 ± 1.3	1.57	49.8 ± 2.0	1.76
esc/esc	Bl/esc	38	23.8 ± 1.3	38.9 ± 1.6	1.63	41.3 ± 2.1	1.73
esc/esc	y;Cy/esc	28	25.6 ± 1.4	40.7 ± 2.2	1.59	44.2 ± 3.1	1.73
y;esc/esc	y;Bl/esc	20	23.4 ± 1.5	39.1 ± 2.5	1.67	40.7 ± 2.9	1.74
y;esc/esc	y;Bl/esc (high select line)	40	24.9 ± 1.0	39.1 ± 2.0	1.57	42.5 ± 1.6	1.71
y;esc/sc^{19i}	†	40	26.2 ± 0.9	42.9 ± 1.4	1.64	46.0 ± 1.3	1.75

*The legs listed in the first and last row were left legs. In all other rows the legs from both sides of half as many males as legs were measured.

†F_1 from y;Bl/esc ♀ x T(1;2)sc^{19}/Cy♂ .

five teeth, another third leg also without tibial but with one basitarsal transverse row and a sex comb of three teeth, and a second leg with no transverse rows but a sex comb of one tooth.

These observations indicate that the various grades of transformation of second and third legs in the direction of first legs do not depend on a gradation of a single primary transformation mechanism. Rather, transformation of a leg occurs in a mosaic fashion so that different legs may show many combinations of changes and absence of changes in the various regions.

A characteristic of whole esc/esc second and third legs apart from their structural properties in regard to sex combs and transverse rows is a shortening of the basitarsus as measured by its actual length and by the tendency toward reduced numbers of bristles in the longitudinal rows, Hannah-Alava (5). Shortening of the basitarsus even seems to affect the first leg and in such a way that the relative lengths of second and third to first basitarsi remain very similar in wild type and esc legs (Table 2). The shortening of the basitarsi of the second and third legs together with the appearance of transverse rows of bristles on these legs suggest that the action of esc consists of a partial change in direction of growth. Instead of primary growth in length in the region of longitudinal rows 7 and 8, as well as in other regions, the esc legs have an additional component of growth in width between rows 7 and 8, including row 7 itself. The basis of this change in growth and differentiation may possibly lie in a change in the direction of cell division. Instead of the divisions occurring in longitudinal direction they would occur transversely.

Table 3. Effect of irradiation on differentiation of sex-comb teeth at abnormal sites

Age at irradiation (hours)	Genotype	Number of males	Number of legs (and %) with one or more teeth: on 2nd tarsal segment, first leg	on basitarsus, second leg	on basitarsus, third leg
Control	y;Bl/Cy	443	0	0	0
	y;Bl/sc^{19i}	360	1 (0.1)	0	0
	y;esc/Cy	404	0	0	0
	y;esc/sc^{19i}	312	0	0	0
37-42	y;Bl/Cy	382	1 (0.1)	2 (0.3)	0
	y;Bl/sc^{19i}	371	0	0	0
	y;esc/Cy	439	0	20 (2.3)	2 (0.2)
	y;esc/sc^{19i}	420	2 (0.2)	10 (1.2)	1 (0.1)
47-52	y;Bl/Cy	500	1 (0.1)	1 (0.1)	0
	y;Bl/sc^{19i}	524	0	0	0
	y;esc/Cy	500	1 (0.1)	28 (2.8)	4 (0.4)
	y;esc/sc^{19i}	1,115	0	27 (1.2)	5 (0.2)
90-95	y;Bl/Cy	170	8 (2.3)	1 (0.3)	0
	y;Bl/sc^{19i}	209	15 (3.6)	0	0
	y;esc/Cy	199	5 (1.2)	5 (1.2)	2 (0.5)
	y;esc/sc^{19i}	255	15 (2.9)	9 (1.8)	0

THE NATURE OF DARK TEETH IN ESC/+ LEGS It will be shown in detail that mosaic yellow areas covering the region of a potential sex comb often differentiate yellowish-brownish teeth corresponding to their genotype. In addition, a considerable number of legs had one or more dark teeth of the wild type. Eighty-seven second legs had a single dark tooth, four had two teeth and one had three teeth (Table 4). Seven third legs had one dark tooth and two had two teeth. In all but five of these cases no indications of yellow tissue were present. In the five exceptions, one bristle of less than normal pigmentation was close to the single dark tooth.

There are several ways in which dark teeth may originate on the second and third legs of y;esc/sc^{19i} males. The most obvious one would be due to the occasional dominance of esc in genetically nonmosaic legs. Another origin of dark teeth would be due to nonautonomy of yellow in the genotypically y;esc/esc cells produced by the prevalent type of somatic crossing-over between esc and the kinetochore. Such nonautonomy has been described before, particularly by Hannah (12) in abdominal mosaics and by Ursprung and Hadorn (13) in wing mosaics (but not in hypodermal mosaics of the mesothorax). It might occur perhaps primarily in very small areas of yellow genotype surrounded by non-yellow tissue either under the influence of the non-yellow surroundings (true nonautonomy) or as the result of the ontogenetically late onset of reactions by the y genotype beginning at the time of somatic segregation. In cases of nonautonomy one might

Table 4. Frequencies of yellow areas, and yellow and dark teeth in sex-comb-forming area after irradiation of y;esc/sc^{19i} male larvae or prepupae. II = second legs; III = third legs

Age at irradiation* (hours)	Number of males	yellow areas (II) Number of teeth								dark teeth (II) Number of teeth			yellow areas (III) Number of teeth				dark teeth (III) Number of teeth	
		0	1	2	3	4	5	6	Total	1	2	3	0	1	2	Total	1	2
27-32	407	0	0	0	0	0	0	0	0	4	0	0	0	0	0	0	0	1
32-42	807	3	1	1	0	0	0	0	5	4	0	0	2	0	0	2	0	0
37-42	420	1	3	1	1	0	0	0	6	6	1	0	2	0	0	2	1	0
42-47	887	5	4	1	0	0	1	1	12	6	0	0	4	3	0	7	1	0
40-52	1,841	8	4	6	1	0	0	0	19	27	1	0	11	4	0	15	0	1
50-60	1,250	6	3	1	0	0	0	0	10	19	1	1	5	1	0	6	4	0
60-67	750	5	3	2	0	0	0	0	10	5	0	0	7	2	0	9	0	0
65-75	605	12	1	0	0	0	0	0	13	1	0	0	9	1	0	10	0	0
75-85	511	6	1	0	0	0	0	0	7	0	0	0	17	1	0	18	1	0
85-95	583	-	0	0	0	0	0	0	0	10	0	0	-	0	0	0	0	0
95-105	137	-	0	0	0	0	0	0	0	0	1	0	-	0	0	0	0	0
105-110	142	-	0	0	0	0	0	0	0	2	0	0	-	0	0	0	0	0
110-120	150	-	0	0	0	0	0	0	0	1	0	0	-	0	0	0	0	0
120-130	324	-	0	0	0	0	0	0	0	2	0	0	-	0	0	0	0	0
Total	8,814	46	20	12	2	0	1	1	82	87	4	1	57	12	0	69	7	2

*The following doses of X rays were used: rows 1 and 2, 700-800 R; row 3, 1,200 R; row 4, 1,600 R; row 5, 1,600-1,800 R; row 6, 1,800 R; row 7, 1,800-2,000 R; row 8, 2,000 R; rows 9 to 14, 2,100-2,400 R.

expect various degrees of darkness of genetically yellow teeth. This kind of variation was indeed found in small spots from larvae irradiated before the age of 85 hr. On the other hand, all dark teeth observed in animals irradiated later were uniformly fully wild type in pigmentation. A special but rather unlikely cause for dark teeth could be nonautonomy of yellow due to interaction, not with the main tissue of the leg but with the twin spot produced by the crossover event. It happened that the sc^{19i} chromosome also carried the mutant b (black body) so that the usual type of somatic crossing-over would lead to two cells, of the genotypes y;esc/esc and $y;sc^{19i}b/sc^{19i}b$. Actually, the darkness of the chitin secreted by b/b cells is not expressed sufficiently in small areas to be recognizable, but it is conceivable that the presence of b/b next to y tissue might darken the latter. An effect of similar kind has been shown to exist when e/e (ebony) cells adjoin y bristles, Hadorn, Anders and Ursprung, (14). In partially dissociated and subsequently mixed wing disks of different genotypes, a narrow zone of y bristles next to e/e bristles takes on dark coloration.

A third possible origin of dark instead of yellow bristles might be based on somatic double crossing-over between sc^{19i} and esc, and esc and the kinetochore leading to a $y;sc^{19i}esc/esc$ genotype which because of the presence of sc^{19i} produces wild type dark setae. Such a probable case will be described below.

A fourth possibility is that the formation of dark teeth on second and third legs is the result of altered differentiation due to the X-ray treatment of genotypically unchanged cells. It was known from earlier work, Tokunaga (9), that irradiation by X rays of various types of male larvae leads to the formation of extra sex-comb teeth on the basitarsus of the first leg and even on its second and more distal tarsal segments. It seemed possible that similar induction by X rays would lead to teeth on the second and third leg. In order to test this hypothesis males of all four genotypes from the cross y;esc/Bl ♀ x $T(1;2)sc^{19};sc^{19i}/Cy$ ♂ were scrutinized for the appearance of teeth outside of the first basitarsus. The material selected consisted of three groups of different larval ages at the time of irradiation and an unirradiated control set (Table 3). Two of the genotypes were hemizygous for yellow, and two were heterozygous for it because of the presence of the sc^{19i} insertion. Only among the $y;esc/sc^{19i}$ legs could a distinction be made between yellow teeth induced in consequence of somatic crossing-over and the dark teeth whose origin is being discussed here. In regard to the second tarsal segment of the first leg, among the 1,519 control individuals a single leg ($y;Bl/sc^{19i}$) showed a dark sex comb tooth. Among the groups irradiated at larval ages 37 to 42 hr and 47 to 52 hr only five legs, representing 0.1 to 0.2% of their genotypes, were found with one or two teeth on the second tarsal segment of the first leg. Two of these five legs came from y;Bl/Cy males, one from a y;esc/Cy male and two (both dark) from

y;esc/sc^{19i} males. In the group irradiated at larval ages 90 to 95 hr there was a striking increase in frequency of teeth on second tarsal segments of first legs of all four genotypes with from one to three teeth present per segment. Phenotypically the teeth were yellow in the classes without sc^{19i} and dark in those with the insertion. The frequencies of teeth varied from 1.2 to 3.6%, the differences between the four genotypes not being statistically significant. In regard to second and third legs, none of the controls had a comb. Among the irradiated males extra sex combs appeared whose frequencies were clearly correlated with their different genotypes (irrespective of the irradiation dosage which did not result in consistent differences). While none of y;Bl/sc^{19i} and only from 0.1 to 0.3% of second legs of the genotype y;Bl/Cy had formed a sex-comb tooth, 1.2 to 2.8% of the two genotypes y;esc/Cy and y;esc/sc^{19i} had one or more teeth. Similarly, though at a lower level of frequencies none of the third legs of the two genotypes y;Bl/Cy and y;Bl/sc^{19i} had any teeth in contrast to 0.1 to 0.5% among y;esc/Cy and y;esc/sc^{19i} legs. For the last named genotype a classification of teeth into yellow and dark was possible. The result indicates an important trend. In the class irradiated between 37 and 42 hr the numbers of cases of yellow and dark teeth, respectively, were five and six on second and third legs, in the 47-to 52-hr class 10 and 22, and in the 90-to 95-hr class zero and nine. It appears from all these data that 1. the production, after irradiation, of teeth on the second tarsal segment of the first leg is not increased in the presence of esc heterozygosity as compared to esc^{+} homozygosity and that there is in both genotypes a rise in the frequency of these teeth with irradiation at late larval stages; 2. the production after irradiation of teeth on the second and third legs is much more frequent in esc/+ than +/+ genotypes; and 3. in y;esc/sc^{19i} males the proportion of legs with dark teeth to those with yellow teeth increases greatly with increasing age, at irradiation.

The proportions of the two kinds of legs with dark and with yellow teeth have been studied over the whole range of irradiation ages from 27- to 32-hr-old larvae to early prepupae (Fig. 3). It is seen that no yellow teeth on second legs were produced by irradiation during the periods 27 to 32 hr and after 85 hr. For the five time intervals from 37 to 67 hr the frequencies of second legs with yellow teeth show an irregularly elevated level. After that they fall toward zero. Second legs with dark teeth occur over the whole range of irradiation ages. Their frequencies are high for the period corresponding to that of the elevated frequencies of second legs with yellow teeth and are, on the whole, higher than these. They are low for two subsequent periods and then rise to a peak and subsequent relative elevation for the late irradiation ages beginning with 85 to 95 hr.

The trend towards much lower frequencies of third legs with sex-comb teeth than of second legs gives a less clear picture. The curve for third legs with yellow teeth seems similar to that for yellow-toothed second legs. Dark

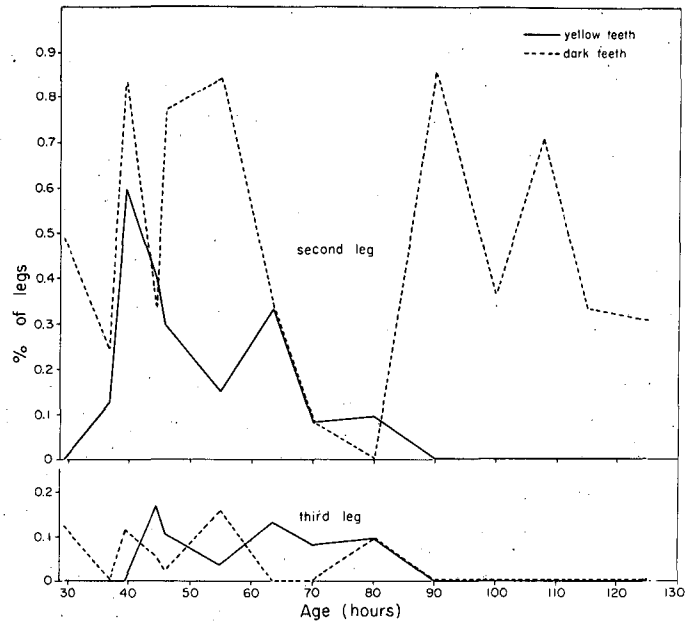

Figure 3. Frequencies of second and third legs with yellow or dark teeth from y;esc/T(1;2)sc^{191} males irradiated at different larval stages. Age signifies hours after egg deposition when irradiation was applied.

MUB-3793

teeth on third legs vary greatly at low frequencies, and there is a complete absence of legs with dark teeth in the older age groups which show such a striking second rise for dark toothed second legs.

It seems difficult to reach a conclusion from these data concerning the nature of the dark teeth. It is possible that they are all the result of somatic crossing-over and segregation followed in development by nonautonomous pigmentation. In this case, one would have to assume that there are at least two periods in larval life sensitive to the induction of somatic crossing-over, and that a majority of early induced segregant cells and all late induced ones do not divide sufficiently to produce large enough areas to include chaetae which would be yellow. A more likely alternative possibility is that the induction of dark teeth in most cases is a purely developmental phenomenon, not connected with somatic crossing-over. It would correspond to the induction by metaborate of phenocopies in Drosophila melanogaster for eyeless which is facilitated in heterozygotes carrying a recessive ey allele as compared to normal homozygotes, Sang and McDonald (15); see also Goldschmidt and Piternick (16,17).

If the appearance of dark teeth on second and third legs is primarily a phenomenon unrelated to a segregational genetic change, then their significance for the prime problem of this paper, that of the expression of esc/esc spots on esc/+ legs, is very limited. Alternatively, if the dark teeth are products of esc/esc cells then they are examples for autonomy of extra sex-comb-tooth differentiation in mosaics. They then could be added to the unequivocal examples

which are characterized by their yellow phenotype. It seems advisable to exclude the cases of dark teeth from further consideration. Their inclusion with proven mosaics would add to the number of cases and lend even further support to the conclusions to be reached, rather than detract from them.

CELL LINEAGE IN LEGS Specific examples of mosaic second and third legs will be described below. Legs with yellow bristles, including teeth, usually possess a single segregant area marked by them. Wherever this area is large enough to include more than very few bristles it consists of a long, narrow strip often extending over several segments and sometimes over nearly the whole length of the leg. This strip is not always continuous but may be interrupted by dark bristled parts. Such two or more separate mosaic areas on the same leg may be either derived from a single or from more than one crossover event. It seems nearly certain that the first alternative is valid. Somatic crossovers in leg disks are very rare so that only four out of 7,478 males with mosaic areas on a sex-comb site on more than one of the total of four second and third legs have been found. A higher coincidence of independent crossover cells within one leg than between separate legs is unlikely. Another argument in favor of a single initial yellow cell in cases of several yellow areas is based on the topography of the separate yellow areas on the same leg. They lie always along the same longitudinal strip of surface of the leg, be it a single or several leg segments. Preliminary studies of cell lineage, made independently of the material on the developmental genetics of esc, further strengthen the view that the original yellow cells produced from a single crossover event either divide primarily in the proximal-distal direction of the future leg or that the cell groups derived from them by division are stretched out and result in a narrow strip of tissue which may be broken up into separate consecutive parts. In detail the cell lineage within the legs varies from one specimen to another as shown by the variations of outlines of mosaic patches.

THE DIFFERENTIATION OF SEX-COMB TEETH IN MOSAICS For purposes of standardization, the sex-comb-forming area was defined as that part of the basitarsus which is occupied by the two most distal bristles of longitudinal rows 6, 7 and 8. It includes the bractless bristle 6.5d. Among a total of 17,616 second legs of 8,814 irradiated y;esc/sc^{19i} males, 82 cases were found in which a patch of yellow tissue covered the region of a potential sex comb, wholly or partially. Of these patches, 46 did not differentiate any teeth (including intermediary bristles) but 36 did. Of the latter cases, only one tooth was formed on 20 legs, the other 16 legs having from two to six teeth (Table 4).

Among a total of 17,616 third legs from 8,814 males, 69 had their potential sex-comb-forming area covered, at least partially, by yellow tissue. On 57 legs no teeth had formed. The remaining 12 legs had one tooth each (see Table 4).

The radiation induction of somatic crossing-over leading to the appearance of yellow patches at the sex-comb site occurs over a rather long period of larval life beginning at about 32 hr and ending about 85 hr (Table 4). In detail the data from different age groups are not strictly comparable since the X-ray dosage used varied with the age of irradiated larvae. The absence of yellow segregants at the sex-comb site in the groups of earliest irradiation is perhaps more a reflection of the low radiation dosage and of the presumably low number of cells that make up the young imaginal disks than of intrinsic absence of crossing-over. On the other hand, the absence of yellow segregants with sex combs among flies irradiated after 85 hr may be the result of reduced frequencies of cell division, thus lowering the possibility of segregation as well as reducing the size of spots derived from segregant cells. A relation between size of spots and time of irradiation is reflected in the table for the number of sex-comb teeth in yellow areas of second legs: the larger sex combs arose from early irradiated larvae. While the designation "0" in Table 4 signifies that no specimens of the type concerned were observed, the designation "-" means that no classification of the types concerned was attempted. The reason for this procedure is that bristles with low amount of pigmentation as well as some morphological abnormalities occur at increasing frequencies after irradiation later than 85 hr. These bristles, which are often like those of yellow genotype, are probably not products of somatic crossing-over but of abnormal development.

The formation of teeth by esc/esc areas shows that it is not necessary for a whole second or third leg to be of the homozygous genotype in order to form a sex comb. Indeed, 44% of the second legs and 17% of the third legs whose potential comb-forming area was wholly or partly covered with y;esc/esc tissue actually possessed a sex comb. The overall penetrance of the homozygous genotype in mosaic legs thus compares well with (and even surpasses) that in wholly homozygous individuals of our nonselected stocks.

As documented in Table 4, the proportions of yellow areas with sex-comb teeth to the total number of such areas for second legs were as follows: ages (in hours) 32 to 42, 7/11; 40 to 52, 18/31; 50 to 60, 4/10; 60 to 67, 5/10; 65 to 75, 1/13; and 75 to 85, 1/7. For third legs the proportions were 0/4; 7/22; 1/6; 2/9; 1/10; and 1/18 for the same age groups. These proportions signify that the penetrance for sex-comb formation for the different ages in which the larvae were irradiated varies for the second legs between 40 and 83.3%, except for the last two periods when the penetrance was 7.6 and 14.2%. Similarly, penetrance in third legs varied from 16.6 to 42.8%, except for the last two periods in which the percentages were 10 and 5.5. Much of the variability of penetrance for the different age groups is clearly due to the small number of mosaics involved, but the combined penetrance for the second legs in the two relatively oldest age groups is significantly lower than that of the combined younger group

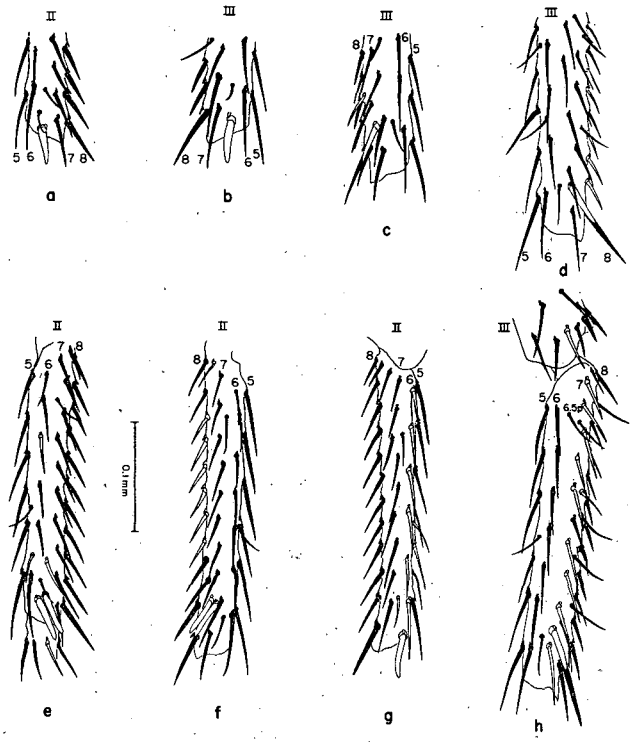

Figure 4. Basitarsi from second (II) and third (III) mosaic male legs with yellow bristles and yellow sex combs on mainly not yellow y;esc/T (1;2)sc^{19i} legs. Solid bristles: wild type; setae in outline: yellow.

MUB-3794

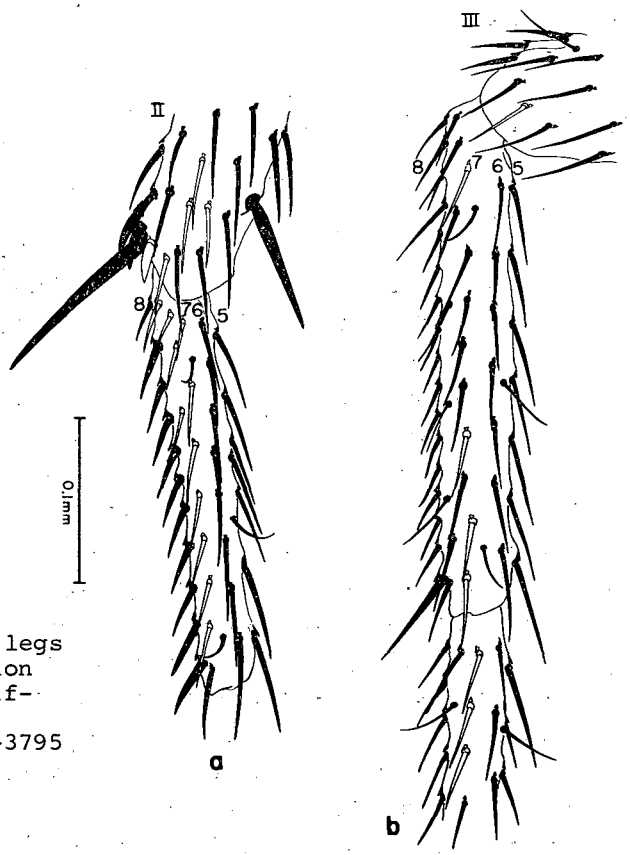

Figure 5. Basitarsi from mosaic male legs in which yellow tissue covers the region of a potential sex comb but did not differentiate a comb.

MUB-3795

($P < 0.01$). For the third legs the difference is not significant, though it is in the same direction. The cause of the low penetrance in the oldest age groups is not known. The observations on abnormally pigmented bristles quoted above suggest that many yellow areas induced as early as 65 to 85 hr are not products of somatic crossing-over but of abnormal development. This agrees with the fact that often a yellow area consists of one bristle only. If such yellow areas are the result of abnormal development then the low proportions of yellow areas with teeth at the two latest ages considered above are not relevant as measures of penetrance.

The expressivity of esc/esc in homozygous individuals is measured by the number of teeth per sex comb. In the mosaic legs the number of teeth only partly reflects the expressivity since it is often clear that only a fraction of the sex-comb-forming area was covered by esc/esc cells. The mean number of teeth on mosaic second legs was 1.7, on third legs 1.0 . Compared to the mean numbers reported in Table 1 for whole esc/esc legs (between 1.7 and 2.7 for second and 1.4 and 1.6 for third legs) the expressivity in mosaics may be regarded as relatively high, in line with the high penetrance.

The differentiation of teeth occurred on legs with a great range of sizes of esc/esc areas. A number of second and third legs on which teeth had differentiated but which had no transverse rows on either tibia or basitarsus are depicted in Fig. 4. In (a) and (b) the esc/esc areas are so small as to comprise only a single seta, the sex-comb tooth. In (c) two setae are yellow and one of them is a tooth. In (e) the area comprises five setae, two of them teeth. Among the other mosaics figured (Fig. 4, d, f-h) the one with the largest number of yellow setae, (h), had 10 bristles and one tooth. These various mosaics show that differentiation of an extra sex comb frequently occurs even on overwhelmingly normal esc/+ second and third legs if the esc/esc patch occupies the potential sex-comb area. Additional examples of this kind are represented in some legs of Figs. 6 and 7, which were selected for features concerned with the transverse rows. Before discussing these, attention is directed to some of the mosaic basitarsi without sex combs (Fig. 5), which presumably correspond to whole esc homozygotes in which the extra comb has not been penetrant.

THE DIFFERENTIATION OF TRANSVERSE ROWS IN MOSAICS The transformation by esc of second and third legs in the direction of first legs comprises the differentiation of transverse rows present in first legs but absent in the other legs. The tibiae shown in Fig. 6 give evidence of autonomy in differentiation of tibial transverse rows in small as well as larger esc/esc areas if they cover the region of such potential transverse rows. Differentiation of small sections of tibial transverse rows is seen in different degrees in the basitarsi of Fig. 6 (a-c). In all three the esc/esc tissue extends in a single line to the basitarsus and in two of them leads to differentiation of sex-comb teeth. Well

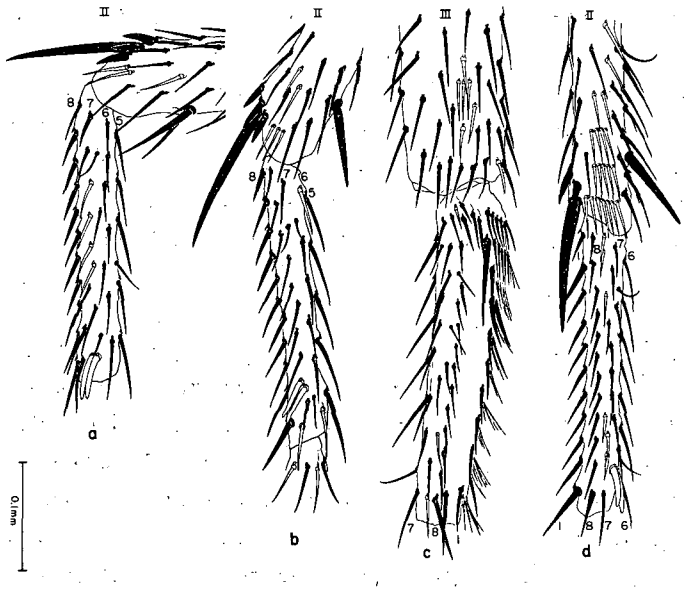

Figure 6. Distal parts of the tibia and basitarsus of mosaic male legs in which the yellow tissue differentiated into transverse tibial rows.
MUB-3796

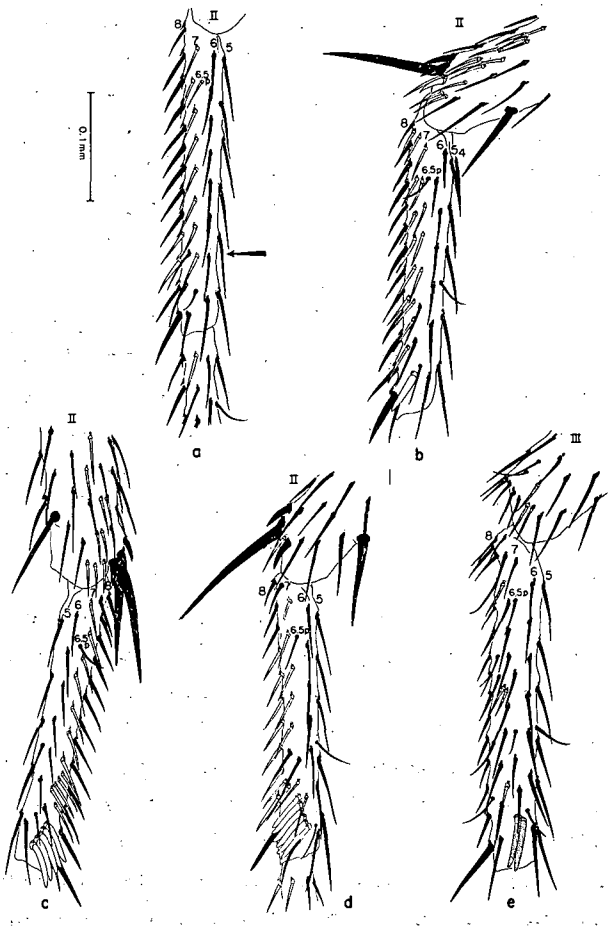

Figure 7. Basitarsi and adjoining parts of mosaic male legs in which the yellow tissue differentiated in various degrees into transverse basitarsal rows. In (a) a single yellow bristle marked by the arrow gives an indication of transverse row formation. Transverse tibial rows are present in (b), (c), and (e). In (d) the single yellow bristle located between two spurs surrounding the apical bristle is an indication of transverse tibial row formation. In (e) the stippled sex-comb teeth are fully pigmented. The stippled bristles indicate by their positions and their lighter pigmentation that they correspond to bristles in homoeotic transverse tibial and basitarsal rows of transformed third legs. See text.
MUB-3797

differentiated rows are present on the tibia of Fig. 6d, on which a single longitudinal line of seven yellow bristles lies proximally to the transverse rows and where an interrupted line of six yellow bristles, which lies between longitudinal rows 6 and 7, continues along the basitarsus, ending with two teeth.

Corresponding to the self differentiation of tibial transverse rows is that of basitarsal ones. The single yellow bristle to the right of a row of seven yellow bristles of longitudinal row 7 and of two in longitudinal row 8 in Fig. 7a is perhaps a borderline case of beginning formation of a transverse row. (Another possible borderline case was shown earlier in Fig. 4h, in which a yellow tooth and a neighboring dark bristle of longitudinal row 7 are placed so as to suggest a transverse row). A whole series of well-defined, though narrow rows is shown in Fig. 7b, and still other variations in 7c and 7d. Special discussion is required for 7e. Here a seemingly interrupted strip of tissue with light-colored bristles extends from the tibia to the basitarsus, ending in two dark teeth. A two-bristle transverse row occurs in the middle of the basitarsus and a similar one on the tibia. It is assumed that the tissue in question is--as the result of a double crossover--of the genotype $y;sc^{19i}esc/esc$. This would account for the dark teeth and would make it likely that a continuous or at least less interrupted strip of dark bristles has the same constitution. The light color of the thin bristles indicating formation of transverse rows would have to be regarded not as of the genetically yellow type but rather as of the very lightly pigmented kind often seen in transverse rows of normal, wild type third legs.

DISCUSSION

The main result of our experiments is the establishment of the autonomy in differentiation of three homoeotic traits characteristic for *esc* second and third legs: sex comb teeth, tibial transverse rows and basitarsal transverse rows. These findings are in contrast to a theoretical expectation outlined in the introduction. If *esc* were a prepattern-determining gene that causes a prepattern of the second and third leg anlagen different from those in normal nonmutant individuals then one would have predicted nonautonomy in the expression of small *esc/esc* patches. The observed autonomy leads to the assignment of *esc* to the group of genes controlling only a terminal pattern. In this way *esc* joins other genotypes of *Drosophila melanogaster* with terminal effects on the sex combs such as maleness (vs. femaleness, Stern and Hannah, 1950), *en* (engrailed, Tokunaga (9)), and *sx* (sexcombless, Mukherjee (18)), as well as genotypes affecting bristle patterns such as *ac* (achaete, Stern (2,3), Roberts (19)), Theta (Stern (20)) and *sc* (scute, Stern and Swanson (21)). The description of these genotypes as not changing a prepattern but only the final pattern implies that they endow the cells with specific competences to react to an invariant prepattern whose development preceded their specific differentiation. Maynard Smith and Sondhi (22) (see also the review of other papers by these authors in

Sondhi (23)), on the basis of pattern changes produced by selection in the mutant ocelliless of Drosophila subobscura, conclude that both prepattern and terminal pattern changes were involved. In Drosophila melanogaster the effects of Hw (hairy wing, Gottlieb (24)) on bristle patterns and of dp (dumpy, King (25)) on vortex and bristle positions have aspects of a similar double influence. A predominantly prepattern effect has been suspected in the action on the sex comb of ey^D (eyeless dominant). In regard to the tarsus the main effect of this genotype is an abnormality of segmentation which so changes the area of potential sex-comb formation as to lead to the differentiation of multiple sex combs (Stern and Mukherjee (26)). Studies of genetic mosaics involving ey^D are needed to show whether small areas express their genotype autonomously.

The autonomy of esc in mosaics first reported by Tokunaga (27) is not unique among homoeotic mutants. It has been described for bithorax mutants by Lewis (10) and for aristapedia by Roberts (28). Autonomy in homoeotic differentiation poses interesting problems in developmental genetics. Within a nonmosaic wild-type embryo or larva, imaginal disks even of serially homologous organs, such as the three pairs of legs, are different as seen by the development of different appendages. The differentiation of sex combs on the first basitarsus and their absence on the second and third basitarsi of wild-type males may depend on the ability of the first basitarsus to call into action special genes and the inability of the other basitarsi to do the same. This view would imply that the prepatterns of the leg disks differ from one another. An alternative interpretation would be that the prepatterns are alike but that the competence of cells in the three leg disks varies. Experiments with embryos, particularly in amphibians, have shown that there may be orderly time sequences during which tissues first acquire and then lose the competence to react to an inductor. It is possible that the cells of the leg disks go through such a time sequence which might be specific for the cells of each disk, thus leading to different end results. An epigenetic difference in competence of serially homologous organs has been demonstrated in the moth Ephestia. Kröger (29) joined together larval imaginal disks of fore- and hind-wings and transplanted the combined disks into a caterpillar host. The transplanted disks were able to create a unified prepattern system as seen by the differentiation of a unified system of wing sclerites (hinges), which often lie across the borderline between the fore- and hind-wing tissue. Although the overall differentiation results in a unified system, the specific differentiation of sclerite parts depends on the nature of the tissue of which they are composed. Accordingly, in sclerite systems composed of fore- and hind-wing tissue, mosaic sclerites develop, showing fore-wing sclerite parts from fore-wing tissue and hind-wing parts from hind-wing tissue. The common prepattern singularity for sclerite formation evokes different responses from the genetically identical but epigenetically diversified cells. The striking differences among the three kinds of wild-type legs originally suggested essential differences in the prepatterns of

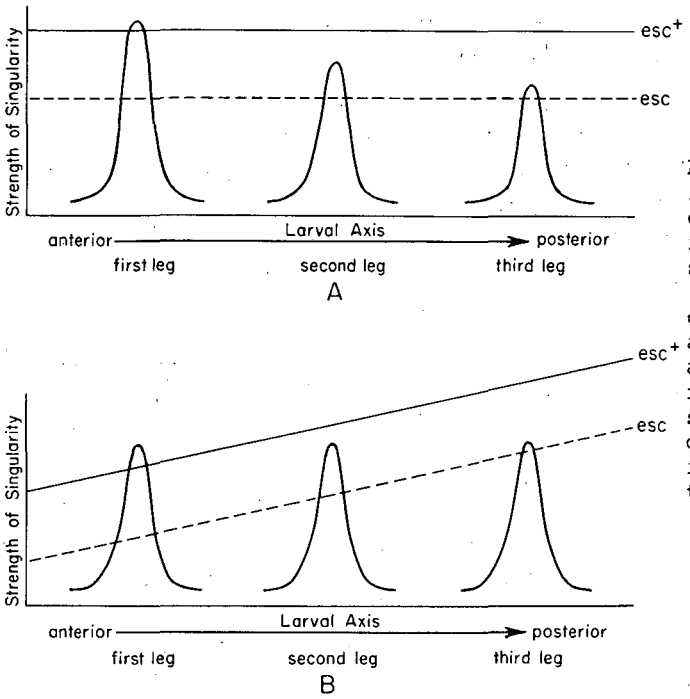

Figure 8. Two diagrams illustrating alternative modes of the action of genetic and epigenetic factors in the development of homoeotic structures on second and third legs. (a) Epigenetically variable strengths of prepatterns in the three legs and constant threshholds for esc$^+$ and esc action along the body axis for differentiation of first-leg structures. (b) Invariant strengths of prepatterns and epigenetically increasing threshholds for differentiation. See text.

MUB-3798

the corresponding leg disks--essential in the sense that second and third legs might lack the singularities that are present in the first leg and lead to differentiation of sex combs and transverse rows. The experiments with mosaics for esc show that this is not the case. The autonomy in differentiation of structures characteristic for first legs by small esc/esc patches on morphologically wild-type second or third legs shows that these legs possess prepatterns with the same kind of singularities as those of first legs. This suggests that the differences between the disks of the three serially homologous legs in *Drosophila*, similar to the differences between the disks of the two serially homologous wings in *Ephestia*, are based on a differentiated response of the cells composing them to an invariant prepattern. The invariance is not necessarily absolute. It may well be that the singularities present in each disk nevertheless show differences of degree in their ability to evoke genic reactions.

The autonomous action of esc in mosaics is based on a mutant response different from that of wild-type esc$^+$. Cells with the latter allele seem to acquire epigenetic differences in competence or react differentially to minor differences in the prepatterns of the three leg disks whereas esc/esc cells often do not. A variety of interpretations can be fitted to the property of the mutant esc gene as opposed to that of esc$^+$. In Fig. 8a, the evoking strength of the singularity for a first leg structure is indicated by a peak, high in the first leg and successively lower in the second and third legs. In addition, two horizontal lines indicate threshhold levels of strength for esc$^+$ and esc respectively, which have to be surpassed to result in first leg differentiation.

As drawn, the esc^+ threshhold permits formation of first-leg structures in the first leg only while the esc threshhold permits formation of such structure in all legs. This model assumes identical response potentialities of the esc^+ and esc allele, respectively, in the three different disks. An alternative model (Fig. 8b) would ascribe identical peaks of prepattern singularities to the three disks but different epigenetic response potentialities of the cells. As shown in the diagram, for esc^+ it would involve a rise from first to subsequent legs in the threshhold level required for first leg differentiation. It would permit such differentiation in the first leg only but be above that for the other legs. For the esc allele either no epigenetic changes in level would occur or, as assumed in the figure, the rise of the threshhold level in second and third legs would still permit response to each of the invariant peaks. The two alternative models just outlined assume a decrease in factors favoring differentiation of first-leg structures from anterior to posterior imaginal disks. Very similar models can be fitted to the assumption of an increase in factors inhibiting such differentiation. There are no means at present by which to discriminate between the hypotheses of promotion vs. inhibition.

Applied to the sex comb, the preceding discussion concerns the primary comb. Consideration of the secondary sex comb adds to the analysis. As reported earlier in this paper, homozygous en males possess a secondary comb on their first legs without this condition leading to either a primary or secondary comb on the subsequent legs. Correspondingly, the production by esc of primary combs on the subsequent legs is not accompanied by an appearance of a secondary comb on first legs. This suggests that there are qualitative differences involved in the causation of primary and secondary combs. If the differentiation of the two kinds of combs would involve completely independent processes one would expect that the homozygous esc en compound would, additively, have both combs on the first leg but only primary combs on the subsequent legs. The data from esc^D en homozygotes, esc^D en/+ en males, (equivalent to esc en homozygotes) do not fit this expectation since they show the existence of both combs on first and second legs (the third legs with their low level of penetrance for extra sex combs do not contribute relevant information). Thus the facts confirm the action of esc as a homoeotic mutant in the sense that it transforms a second leg into a first, which would be expected to form a secondary comb if homozygous for en. This implies an interaction between esc and en. Perhaps, esc as compared to esc^+ changes the level of competence of cells, not only for the primary but also for the secondary comb singularity. Or, the action of esc precedes that of en in differentiation so that esc changes the pattern of the developing secondary leg and provides a changed prepattern for the subsequent response of en.

The autonomy in response of esc/esc cells in mosaics suggests that the homoeosis produced by esc in nonmosaic, whole esc/esc individuals is the result of separate responses independently occurring in each area of the

developing second or third leg. If penetrance in these esc legs is high, these homoeotic responses take place everywhere on the anlage, and a more or less complete homoeotic transformation is accomplished. If, otherwise, penetrance is low so that the homoeotic response does not occur in every region, transformation is incomplete in an epigenetically mosaic pattern that varies from leg to leg as it is observed in esc and other homoeotic genotypes.

The three autonomous traits studied in esc mosaics have in common a multiplication of setae in transverse rows, on the tibia, along a strip of the basitarsus and in the configuration of the sex comb which itself originates as a transverse row. The autonomy of esc in mosaics thus consists in the expression of a tendency in specific regions towards growth in a transverse direction coupled with differentiation, in a closely packed row, of bristles or teeth. In this sense the effect of esc can be regarded as a late prepattern effect intercalated between the usual prepattern and the terminal pattern.

The basic effect of esc is modulated in specific ways in different parts of the legs. Not only do the tibia and basitarsus differentiate transverse rows of bristles and the basitarsus a sex comb, but the transverse rows themselves are of different width along the proximal-distal axis. Thus, the various singularities of the leg prepattern which, independently from one another, call esc into action result in a variety of effects.

SUMMARY

In males of Drosophila melanogaster the first legs possess a sex comb, certain tibial transverse rows of bristles and certain basitarsal transverse rows. These structures are absent on the second and third legs. The recessive autosomal mutant esc (extra sex comb) transforms certain features of the second and third into those of first legs. In different legs the transformation may be incomplete. The different parts may be transformed independently of each other, resulting in an array of partially transformed legs which are epigenetic mosaics of changed and unchanged areas. Genetic mosaics consisting of esc/esc patches on esc/+ legs were obtained in consequence of X-ray induced somatic crossing-over. By means of a translocation, the esc/esc areas were marked by genetically yellow pigmentation on the background of wild-type esc/+. In the genetic mosaics esc acts autonomously in causing the appearance of sex combs and both types of transverse rows even in very small esc/esc areas. Wild-type colored sex-comb teeth on second and third legs were induced by irradiation of esc/+ males. The second legs of males with the combination esc^D en/+ en of esc^D, a dominant allele of esc, and en (engrailed) had a typical (primary) sex comb as well as the secondary comb normally placed by en on the first leg only. The gene esc as compared to esc^+ controls the terminal pattern of leg differentiation by changing the competence of imaginal disk cells to respond to a prepattern that is alike for both alleles. The changed response consists in a tendency in

certain areas towards growth in a transverse direction coupled with differentiation in a closely packed row of bristles or teeth.

ACKNOWLEDGMENTS

We wish to thank Norman Arnheim for his critical comments during the preparation of the manuscript and Emily Reid for preparation of the figures.

This work was carried out under the auspices of the United States Atomic Energy Commission and supported in part by National Science Foundation Grant G 18057.

REFERENCES AND NOTES

1. Stern, C., and Hannah, A.; Portugaliae Acta Biologica Series A:798-812, 1950.
2. Stern, C.; Caryologia, Suppl. 6:355-369, 1954.
3. Stern, C.; American Scientist 42:213-247, 1954..
4. Hannah-Alava, A.; J. Morphol. 103:281-310, 1958.
5. Hannah-Alava, A.; Genetics 43:878-905, 1958.
6. Slifer, E.; J. Exptl. Zool. 90:31-40, 1942.
7. Hannah, A., and Strömnaes, Ø.; Drosophila Information Service 29:121-123, 1955.
8. Tokunaga, C.; Drosophila Information Service 38:80, 1963.
9. Tokunaga, C.; Genetics 46:157-176, 1961.
10. Lewis, E. B.; Am. Zoologist 3:33-56, 1963.
11. Tokunaga, C.; Develop. Biol. 4:489-516, 1962.
12. Hannah, A.; J. Exptl. Zool. 123:523-560, 1953.
13. Ursprung, H., and Hadorn, E.; Develop. Biol. 4:40-66, 1962.
14. Hadorn, E.; Anders, G., and Ursprung, H.; J. Exptl. Zool. 142:159-175, 1959.
15. Sang, J. H., and McDonald, J. M.; Genetics 52:392-412, 1954.
16. Goldschmidt, R. B., and Piternick, L.; J. Exptl. Zool. 135:127-202, 1957.
17. Goldschmidt, R. B., and Piternick, L.; J. Exptl. Zool. 136:201-228, 1957.
18. Mukherjee, A. S.; Ph.D. Thesis, University of California, Berkeley, 1958.
19. Roberts, P.; Genetics 46:1241-1243, 1961.
20. Stern, C.; Cold Spring Harbor Symp. Quant. Biol. 21:375-382, 1956.
21. Stern, C., and Swanson, D. L.; J. Faculty of Sci., Hokkaido University 13: 303-307, 1957.
22. Maynard Smith, J., and Sondhi, K. C.; Genetics 45:1039-1050, 1960.
23. Sondhi, K. C.; Quart. Review Biol. 38:289-327, 1963.
24. Gottlieb, F. J.; Genetics 49:739-760, 1964.
25. King, J. L.; Genetics 49:425-438, 1964.
26. Stern, C., and Mukherjee, A. S.; Proc. Natl. Acad. Sci., India Section B, 34:19-26, 1964.
27. Tokunaga, C.; Genetics Today 1:170-171, 1963 (abstract) Proceedings of XI International Congress of Genetics.

28. Roberts, P.; Genetics 49:593-598, 1964.
29. Kröger, H.; Roux's Arch. 151:113-135, 1959.

Dr. Curt Stern is Professor of Zoology and Genetics, University of California, Berkeley.

Received September, 1964.

A Novel Method for the Release of Bacteriophage DNA

David Freifelder

Ideally, a procedure for the isolation of undamaged DNA from bacteriophage should have the following characteristics: (i) it should be rapid, (ii) the extracting material should show no optical absorption at 260 mμ (OD_{260}), (iii) nucleases should be inactivated, (iv) no adverse chemical effects should result, (v) the method should be applicable to semimicro samples, e.g., 10 μl, and to samples of low concentration, i.e., 1 to 10 μg/ml, and (vi) it should work for all phages. Of the methods in current use, phenol extraction by Mandell and Hershey (1) requires additional procedures to remove the high OD_{260} left by residual phenol and does not satisfy criteria (iii) and (v); release by alkali or heating, Davison and Freifelder (2), fails for items (iii) and (vi) and possibly for (iv). This report describes a new technique which seems to satisfy all six criteria and which is probably also useful for extraction of nucleic acids from animal and plant viruses and bacteria.

In the new procedure, DNA is extracted from coliphages T4, T7 and λ, and Pseudomonas aeroginosa phage B3 by adding a phage suspension to a 5 M $NaClO_4$ solution containing 5×10^{-3} M EDTA, mixing, and waiting until DNA release occurs. Release can be stopped at any time after addition of the phage by dilution with sodium phosphate, pH 7.8, to a perchlorate concentration of 1 molar. The rate of release has been measured by determining in the analytic ultracentrifuge the relative amounts of material sedimenting in both the phage and DNA boundaries after various times of exposure to high perchlorate concentrations. It was found that the rate of release varies with the phage species and is dependent on the perchlorate concentration. At 5 M the process is complete in 10 sec for B3, 20 sec for λ and T7, and 1 min for T4. The concentration dependence of the rate of release for phage T7 is shown in Table 1. It should be noticed that for both 2.3 M and 3.7 M the kinetics are peculiarly biphasic. This enables the phage population to be fractionated in a way not yet understood.

DNA isolated by perchlorate extraction from T7 and T4 is intact by the criterion of sedimentation velocity homogeneity, Davison and Freifelder (2). For λ and B3, but not for T4 or T7, an unexpected phenomenon occurs: the DNA is released stepwise--first, as a rapidly sedimenting form and then (only if the high concentration of perchlorate is maintained) as the form with the usual

Table 1. Percentage of DNA released from phage T7 as a function of time for various concentrations of $NaClO_4$

Concentration	Time, sec	% Release
5.0 M	5	50
"	10	90
"	20	100
3.7 M	10, 20	65
"	30	70
"	40	80
"	50	100
2.3 M	20	40
"	50,60,90,100,150, 270,600,900	50
"	30 min	100

sedimentation coefficient. This will be described in detail in a subsequent publication. For each of these phages it has also been possible to extract the DNA in the denatured state simply by raising the perchlorate concentration and adding HCHO. This result was not unexpected in view of the denaturing effect on DNA of very high concentrations of $NaClO_4$, Hamaguchi and Geiduschek (3), and of HCHO, Freifelder and Davison (4).

If T7 phage is mixed with 10 μg/ml of pancreatic DNAase in 10^{-3} M $MgSO_4$ - 10^{-2} M PO_4, pH 7.8, and the DNA is released by incubating for 10 min either at pH 7.8, 70°C or at pH 11.5, 25°C, enough DNAase survives the extraction procedure so that the DNA is severely damaged. In a typical experiment the $S_{20,w}$ was 20 instead of the normal value of 29. Treatment of a similar sample with 5 M $NaClO_4$ yielded DNA with no indication of nuclease damage. Whether the DNAase is irreversibly inactivated or the result is a consequence of the insolubility of $Mg(ClO_4)_2$ is not yet clear.

The mechanism of action of $NaClO_4$ is not known. It is not simply osmotic shock because 1) NaCl at equivalent concentrations has no effect, 2) the procedure works for T4 O^r, the osmotic shock-resistant form of T4 and 3) the effect is independent of dilution rate and, in fact, does not even require dilution, i.e., if the phage is added to 2.3 M $NaClO_4$ and the undiluted solution centrifuged, the sedimentation boundary is that of DNA.

In preliminary experiments, transforming DNA has been extracted with 2 M $NaClO_4$ from B. subtilis phage SP50 (Trautner, personal communication). Experiments in progress include detailed studies of the concentration dependence

and kinetics of release, the use of perchlorate as a denaturing agent for DNA and RNA and as an extracting agent of DNA in bacteria and animal cells, and electron micrographic studies of perchlorate-released DNA.

ACKNOWLEDGMENTS

The author wishes to thank Katherine Le Blanc who prepared the purified phages used in these studies.

REFERENCES

1. Mandell, J. P., and Hershey, A. D.; Anal. Biochem. 1:66, 1960.
2. Davison, P. F., and Freifelder, D. M.; J. Mol. Biol. 5:643, 1962.
3. Hamaguchi, K., and Geiduschek, E. P.; J. Am. Chem. Soc. 84:1329, 1962.
4. Freifelder, D. M., and Davison, P. F.; Biophys. J. 3:49, 1963.

Received November, 1964.

The Effect of Litter Culling, or Family Planning, on the Rate of Natural Selection

Jack Lester King

In his classic paper on mathematical theory of natural and artificial selection, Haldane (1) devotes some space to the consideration of those cases in which the struggle occurs between members of the same family. Haldane terms this familial selection, citing as an example the matings of yellow by yellow mice from which litters are no smaller than normal, although one quarter of the embryos die in the blastula stage. The criteria for familial selection are that the number of survivors in each family is unchanged, and differential genetic deaths occur within families.

Haldane states that ". . . familial selection occasionally occurs through natural causes, but never through human agency." However, the criteria are met whenever any arbitrary limitation of family size is regularly imposed. Genetic deaths that occur prior to such arbitrary limitation constitute familial selection. Compensation, the replacement of genetic losses with viable full sibs, is implicit in all such cases. Four general instances suggest the need for review and further consideration of the effects of familial selection on the rate of change in gene frequencies:

1. The practice by commercial and laboratory animal breeders of culling litters to uniform sizes.
2. The use of certain breeding methods that reduce genetic drift through equal representation of each sibship, Gowe et al. (2), Luning (3) and King (4).
3. Certain plant genetics studies in which thinning is regularly employed.
4. The arbitrary limitation of human family size through contraception (i.e., family planning).

It was demonstrated by Haldane that in the case of recessives with small unfavorable effects on fitness, the rate of elimination in familial selection is expected to be half that in ordinary selection, and that sex-linked recessives are selected against at from one-third to one-half the ordinary rate.

THEORY

FAMILIAL SELECTION: SELECTION WITH COMPLETE COMPENSATION Haldane's approach, with changes in nomenclature and symbolism, will be used to repeat his

Table 1. Genotypes surviving with familial selection

Mating	Mating frequency	Surviving genotypic frequencies AA	Aa	aa
AAxAA	D^2	D^2	-	-
AAxaa	2DR	-	2DR	-
aaxaa	R^2	-	-	R^2
AaxAA	4DH	$4DH(\frac{a}{a+b})$	$4DH(\frac{b}{a+b})$	-
AaxAa	$4H^2$	$4H^2(\frac{a}{a+2b+c})$	$8H^2(\frac{b}{a+2b+c})$	$4H^2(\frac{c}{a+2b+c})$
Aaxaa	4HR	-	$4HR(\frac{b}{b+c})$	$4HR(\frac{c}{b+c})$
Total:	1	D_{n+1}	$2H_{n+1}$	R_{n+1}

[AA] $D_{n+1} = D^2 + 4Ha\,[\frac{D}{a+b} + \frac{H}{a+2b+c}]$

[Aa] $H_{n+1} = DR + 2Hb\,[\frac{D}{a+b} + \frac{2H}{a+2b+c} + \frac{R}{b+c}]$

[aa] $R_{n+1} = R^2 + 4Hc\,[\frac{H}{a+2b+c} + \frac{R}{b+c}]$

finding with regard to deleterious recessives and to extend consideration to some other classes of alleles. It should be noted that the Hardy-Weinberg distribution does not hold where familial selection operates. For this reason it is necessary to use discrete symbols for the genotypic frequencies as well as for gene frequencies. Let q represent the frequency of allele a and $1-q$ that of allele A. The frequencies of genotypes AA, Aa, and aa are represented by D, $2H$, and R; their respective fitnesses by a, b, and c. Then the frequency of allele a is $q = H + R$; the frequency of A is $1-q = D + H$. The generation subscript n is implicit except where generation $n + 1$ is explicit. In addition, the coefficient of selection s is defined such that for every normal zygote surviving to the age at which family size limitation is imposed, 1-s affected zygotes survive. If the matings in generation n are at random, the adult genotypes of generation $n + 1$ are as shown in Table 1.

CHANGES IN GENE FREQUENCY

1. Recessive Alleles with Small Deleterious Effects on Fitness.

Let a = b = 1; c = 1-s. Then

$$H_{n+1} = DR + DH + \frac{4H^2}{4-s} + \frac{2HR}{2-s} = (D+H)(H+R) + sH\left[\frac{H}{4-s} + \frac{R}{2-s}\right] = q(1-q) + sH\left[\frac{H}{4-s} + \frac{R}{2-s}\right]$$

$$R_{n+1} = R^2 + \frac{4H^2}{4-s} + \frac{4HR}{2-s} - 4sH\left[\frac{H}{4-s} + \frac{R}{2-s}\right] = (H+R)^2 - sH\left[\frac{3H}{4-s} + \frac{2R}{2-s}\right] =$$

$$q^2 - sH\left[\frac{3H}{4-s} + \frac{2R}{2-s}\right]$$

$$q_{n+1} = H_{n+1} + R_{n+1} = q - sH\left[\frac{2H}{4-s} + \frac{R}{2-s}\right] ;$$

$$\Delta q = - sH\left[\frac{2H}{4-s} + \frac{R}{2-s}\right] .$$

Since H differs from q(1-q) and R differs from q^2 by amounts less than sH, for small values of s

$$\Delta q \cong -sq^2 (1-q)\left[\frac{2-2q}{4-s} + \frac{q}{2-s}\right] \cong - 1/2\ sq^2(1-q) - \frac{s^2q^2(1-q^2)}{8} \cong -1/2\ sq^2(1-q) .$$

This is one half the rate of selection without compensation. It should be mentioned that these equations are identical to those derived by Haldane (1).

2. Recessive Lethal Alleles.

Let a = b = 1; c = 0. Then R = 0; H = q; D = 1 - 2q; and

$$q_{n+1} = H_{n+1} = q(1-2q)+ \frac{4q^2}{3} = q - \frac{2q^2}{3}$$

$$\Delta q = - \frac{2q^2}{3} .$$

The rate of selection without compensation is:

$$\Delta q = - \frac{q^2}{1+q} .$$

With familial selection, recessive lethals are eliminated about two thirds as rapidly as under ordinary selection, or more precisely 2/3 (1+q) as rapidly.

3. Dominant Deleterious Alleles with Recessive Lethality.

Let a = 1; b = 1-s; c = 0. Then D = 1-2q; H = q; R = 0; and

$$q_{n+1} = H_{n+1} = 2q(1-s)\left[\frac{1-2q}{2-s} + \frac{2q}{3-2s}\right] = q -q\left[\frac{4q+s-4qs}{2-s} - \frac{4q-4qs}{3-2s}\right]$$

$$\Delta q = - \frac{sq}{2-s} - \frac{2q^2}{3} + sq^2\left[\frac{2}{2-s} - \frac{5}{9-6s}\right] .$$

The corresponding rate of change in a population without compensation is:

$$\Delta q = - \frac{sq}{1+q} - \frac{q^2}{1+q} + \frac{2sq^2}{1+q-2sq} .$$

Thus, in both types of selection Δq can be expressed as the sum of three terms of the order of sq, q^2, and sq^2. If q is small relative to s, the first terms are operative, and the allele is selected against as a heterozygote; the relative efficiency of familial selection is $\frac{1+q}{2-s}$. If s is small relative to q, the allele is selected against primarily as a recessive lethal homozygote, the second terms are operative and the relative efficiency of familial selection is $\frac{2}{3}(1+q)$.

4. Additive Alleles Affecting Fitness. In noncompensating panmictic populations the within-sibship component of additive genetic variance is half the total additive genetic variance; one might expect then that limiting

selection to within sibships should reduce the rate of selection by half. The Haldane method confirms this. Let a = 1+s; b = 1; c = 1-s. Then, with familial selection,

$$H_{n+1} = DR + 2H\left[\frac{D}{2+s} + \frac{H}{2} + \frac{R}{2-s}\right] = (D + H)\ (H + R) - sH\left[\frac{D}{2+s} - \frac{R}{2-s}\right] ;$$

$$R_{n+1} = R^2 + 4H(1-s)\left[\frac{H}{4} + \frac{R}{2-s}\right] = (R + H)^2 - sH\left[H + \frac{2R}{2-s}\right]$$

$$q_{n+1} = H_{n+1} + R_{n+1} = q(1-q) + q^2 - sH\left[\frac{D}{2+s} + \frac{2H}{2} + \frac{R}{2-s}\right]$$

$$\Delta q = -\frac{sH}{2} + \frac{s^2H}{2}\left[\frac{D}{2+s} - \frac{R}{2-s}\right] .$$

For small values of s, H = q(1-q) and

$$\Delta q \cong -1/2\ sq(1-q) ,$$

or half the corresponding rate with ordinary selection.

DISCUSSION

Familial selection on a population level, as calculated above, requires complete and rigorous compensation for every genetic loss. Obviously, this is rarely possible. There will always be some matings that will never produce the predetermined numbe of living offspring, with the possibility of direct genetic losses without compensation. Furthermore, not all genetic effects on fitness are subject to compensation. Those causing deaths prior to the arbitrary culling of litters (animals) or deaths prior to the termination of the parental reproduction period (humans) are subject to compensation; those affecting adult longevity or causing complete sterility are not.

Aside from complete sterility, however, genotypes that affect fertility are even more drastically affected by compensation. This applies also to genetically based maternal effects on early survival--and, surprisingly, includes the semi-sterility of translocation heterozygosis. Familial selection acts only on the genetic differences between sibs; deleterious parental genotypes are not selected against at all so long as the predesignated number of viable progeny is attainable. For these genetic effects, so long as full compensation occurs, $\Delta q = 0$.

Some measure of compensation is present in all mammalian populations. In animals with large litters, the embryonic and perinatal deaths of a few individuals increase the survival chances of their sibs, and the number of reproducing adults from that sibship may be unchanged. In human populations, even in the absence of deliberate progeny-limiting practices, there is probably a high degree of compensation for preimplantation losses, since the female then becomes able to conceive again sooner than would have been the case had implantation been successful. Family planning frequently has other objectives than the limitation of progeny number to an arbitrary size. It is often employed in consideration of parental physical or mental health, or even in consideration

of known familial genetic defects. In such cases, contraception should often have the effect of increasing the rate of selection against deleterious alleles.

SUMMARY

Familial selection, or the arbitrary limitation of the number of progeny of each mating pair in a population (as by litter culling or family planning), reduces the rate of natural selection by eliminating between-family selection. Selection against recessive early lethals is reduced to about two-thirds of the rate predicted with true panmixis; the rates of selection against rare recessive, additive and dominant deleterious alleles, with small individual effects on viability, are nearly halved. Selection rates against alleles affecting fecundity are likely to be still more sharply reduced.

ACKNOWLEDGMENTS

I wish to express my gratitude to Dr. James F. Crow who assisted me with advice in the mathematical portion of this paper.

This study was supported by a National Institutes of Health Postdoctoral Fellowship and in part by the United States Atomic Energy Commission.

REFERENCES

1. Haldane, J. B. S.; Trans. Camb. Phil. Soc. 23:19-41, 1924.
2. Gowe, R. S.; Robertson, A., and Latter, B. D. H.; Poultry Sci. 38:462-471, 1959.
3. Luning, K. G.; Hereditas 46:668-674, 1960.
4. King, J. L.; Genetics 50:1211, 1964.

Received September, 1964.

Further Development of a Single-Tracer Injection Method for C^{14}-Glucose Kinetic Studies in Humans

Edward Manougian

In 1954 Baker et al. (1) proposed a model for the kinetics of glucose metabolism in humans after the injection of a single tracer dose of glucose, the sites of experimental measurement being the blood and the expired breath. Some data were presented to support the plausibility of their model and to set forth temporary values of the various parameters for normal individuals. Subsequently Shreeve et al. (2) modified these normal values and extended the results to include persons with diabetes mellitus. Tolbert et al. (3) in 1956 improved the experimental method of Baker and co-workers so continuous monitoring of the expired CO_2 and $C^{14}O_2$ became possible. Pollycove (4) then applied Tolbert's instrumentation and Baker's theory in order to study the effects of insulin, tolbutamide, and phenethylbiguanide on normal individuals.

Concomitant with this study of the effects of hypoglycemic agents on normal subjects, an investigation of glucose kinetics was initiated in this laboratory on patients with diabetes mellitus and on patients with acromegaly. Most of these patients subsequently received heavy-particle irradiation to the pituitary gland for treatment of their acromegaly or diabetic retinopathy. Several of these patients had a repeat glucose kinetic study performed some time after therapy. It is the purpose of this paper to elucidate and to amplify the theory of Baker et al. A subsequent communication will present the results of these studies.

THEORY

The theory is that of Baker (1). Essentially, a steady-state two-compartmental model with unidirectional flow is assumed (Fig. 1). If the glucose pool (or compartment) is defined operationally to be that glucose of the body which dilutes the injected C^{14} glucose (5) and if the bicarbonate pool is defined similarly, then the assumptions are those of Baker (1) and Reichard (6):

(A-1) The tracer dose of glucose C^{14} injected intravenously mixes with a homogenous non-labeled glucose pool without affecting glucose metabolism.

(A-2) The amount of glucose in the glucose pool remains constant. This means that labeled glucose molecules in the glucose pool are replaced in time by nonlabeled glucose molecules at a rate that maintains a constant concentration of glucose in the glucose pool.

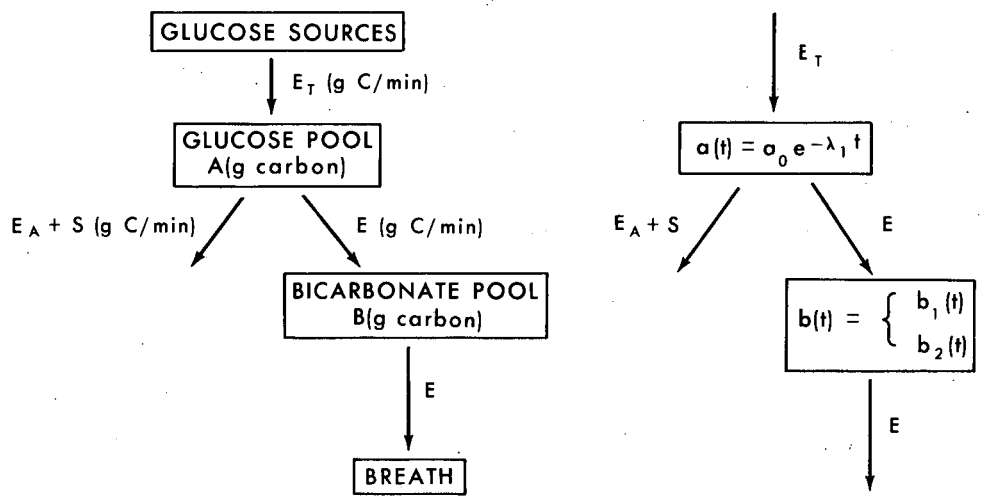

Figure 1. In the Baker et al. model for glucose C^{14} kinetics, (a) represents the various pools and their interrelationships, (b) represents the equations for the specific activity in the corresponding pools.

MUB-2933

(A-3) The rate at which glucose or CO_2 carbon leaves either the glucose or bicarbonate pool (and hence enters either pool) is proportional to the amount of carbon present in that pool.

(A-4) Some glucose is oxidized "rapidly" and irreversibly to CO_2 by some pathway(s), which will be called "the immediate oxidative pathway."

(A-5) The newly formed CO_2 mixes rapidly with the body bicarbonate pool and this CO_2 is produced at a rate that is constant and equal to that of its loss via the lungs.

(A-6) The "volumes" of these two pools remain constant.

(A-7) The theoretical CO_2 specific activity curve (which is equation E-15) reaches its maximum point at the same time as does the experimental CO_2 specific activity curve for expired breath.

These assumptions have been incorporated into Fig. 1. Assumption (A-2) implies that there is no feedback of labeled glucose into the glucose pool during the time interval of the experiment once it has left this pool. It will be seen that under the experimental conditions of this study a single exponential decay curve for glucose-pool specific activity is obtained in the time period under observation, provided a short period of time is allowed for mixing, thus supporting the plausibility of assumption (A-2).

In assumption (A-3), "rapidly" means rapid in relation to other pathways whereby C^{14} originally in glucose appears as C^{14} in CO_2. The pathways bringing about this rapid oxidation of glucose to CO_2 are combined under one title and called "the immediate oxidative pathway." Whether this "pathway" is the

hexose-monophosphate shunt or the Embden-Meyerhof-Tricarboxylic acid pathway or a summation of these or other pathways is not of importance in the theory. The work of Wrenshall and Hetenyi (7) suggests that assumption (A-6) is a fair approximation to reality. Assumption (A-7) is partially justified in Baker's report (1).

Certain definitions are now needed in order to proceed with the mathematical expression of the model. These definitions differ slightly from Baker's in that here μCi per gram of carbon (either in glucose or CO_2) is used for expressing specific activity whereas Baker et al. (1) use percent of injected activity per milligram of either glucose carbon or CO_2 carbon. Let

(D-1) $\alpha(t)$ = μCi of C^{14} in the glucose pool at any time $t \geq 0$. Then $\alpha(0) = \alpha_o$ is taken to be the dose of C^{14} injected as C^{14} glucose.

(D-2) $\beta(t)$ = μCi of C^{14} in the bicarbonate pool at any time $t \geq 0$.

(D-3) $a(t)$ = μCi per gram of C in the glucose pool at any time $t \geq 0$. $a(t)$ will be used to denote both the theoretical and experimental specific activities in the glucose pool since the theory is thought to approximate closely the experimental results.

(D-4) $b(t)$ = μCi per gram of C in the bicarbonate pool at any time $t \geq 0$ under the assumption that all of the CO_2 in the bicarbonate pool is derived from glucose. This will be referred to as the "theoretical specific activity" in the bicarbonate pool as distinct from the experimental specific activity, $E^{SA}_{CO_2}$, in that pool. The reason for this distinction will become apparent later.

(D-5) A = grams of glucose carbon in the glucose pool.

(D-6) B = grams of CO_2 carbon in the bicarbonate pool.

(D-7) E = grams of CO_2 carbon exhaled per minute in the breath.

(D-8) λ_1 = fraction of the glucose pool which turns over each minute.

(D-9) λ_2 = fraction of the bicarbonate pool which turns over each minute.

(D-10) t denotes time in minutes measured from the time of injection of C^{14} glucose.

(D-11) t_{max} = time at which CO_2 specific activity reaches its maximum value. (This will sometimes be denoted t_m.)

(D-12) $t_{\frac{1}{2}}$ = half-life of the specific activity in the glucose pool.

(D-13) $E_A + S$ = grams of glucose carbon removed from the glucose pool per minute by paths other than the immediate oxidative route.

(D-14) E_T = rate at which carbon enters and leaves the glucose pool, in grams per minute.

As immediate consequences of the foregoing definitions we have:

(E-1) $$a(t) = \frac{\alpha(t)}{A}$$, by (D-1), (D-3) and (D-5).

(E-2) $$b(t) = \frac{\beta(t)}{B}$$, by (D-2), (D-4) and (D-6).

(E-3) $\lambda_1 = \frac{E_T}{A}$, by (D-5), (D-8), (D-1) and (D-4).

(E-4) $\lambda_2 = \frac{E}{B}$, by (D-6), (D-7) and (D-9).

(E-5) $E_T = E + E_A + S$ by (D-7), (D-13) and (D-14).

Clearly all of these are non-negative quantities.

The equation for the specific activity in the glucose pool is derived as follows: by assumption (A-3), at any time t, the rate of disappearance of radioactivity from the glucose pool is proportional to the radioactivity present in that pool. Thus

(E-6) $$\frac{d\alpha(t)}{dt} = -\lambda_1 \alpha(t), \ \lambda_1 \geq 0 \ , \ \alpha(t) \geq 0 \ ,$$

where λ_1 denotes the constant of proportionality and the minus sign indicates that the radioactivity decreases with time. Hence,

$$\frac{d\alpha(t)}{\alpha(t)} = -\lambda_1 \, dt$$

so that integration over the interval [0,t] yields $[\ln \alpha(t)]_0^t = -\lambda_1 t$. Thus,

$$\ln \frac{\alpha(t)}{\alpha(0)} = -\lambda_1 t \text{ and}$$

(E-7) $$\alpha(t) = \alpha(0) e^{-\lambda_1 t} \ .$$

By (E-1) it follows that

(E-8) $$a(t) = \frac{\alpha(t)}{A} = a_o e^{-\lambda_1 t} \ .$$

a(t) is expected to represent the actual specific activity in the glucose pool at any time $t \geq \tau$, where τ is the "mixing time" and where assumptions (A-1), (A-2), (A-3) and (A-6) hold.

The analysis for the bicarbonate pool differs from that for the glucose pool because the objective of the analysis for the bicarbonate pool is not to establish what actually happens in it but rather what would happen if all the CO_2 of this pool were to come from glucose. Then the experimentally obtained CO_2 specific activity can be compared with this theoretical CO_2 specific activity in order to obtain the fraction of CO_2 derived from glucose. This means that if the situation for the bicarbonate pool were as depicted in Fig. 2 where k is the fraction of CO_2 derived from glucose, then the specific activity in the bicarbonate pool would actually be kb(t), rather than b(t). Thus it is clear that if we want to determine k we need only take the ratio $\frac{kb(t)}{b(t)}$, i.e., the ratio of the experimental specific activity over the theoretical specific activity. This, in essence, is the purpose for the following analysis. Hence, in order to derive the theoretical expression for b(t) the following additional assumption is made:

(A-8) All of the CO_2 in the bicarbonate pool comes from glucose.

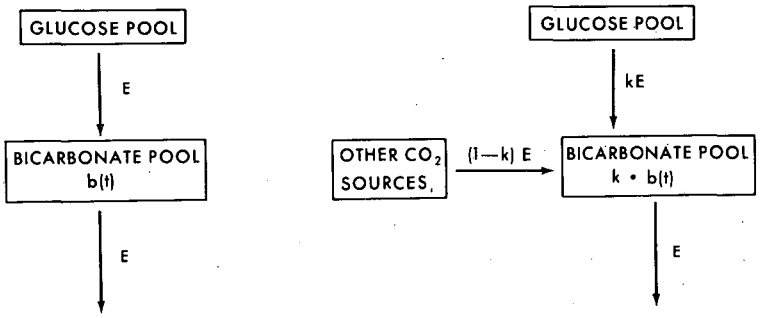

Figure 2. (a) Theoretical situation: all of the CO_2 is assumed to come from glucose. (b) actual situation: only a fraction k of the CO_2 comes from glucose.

MUB-2934

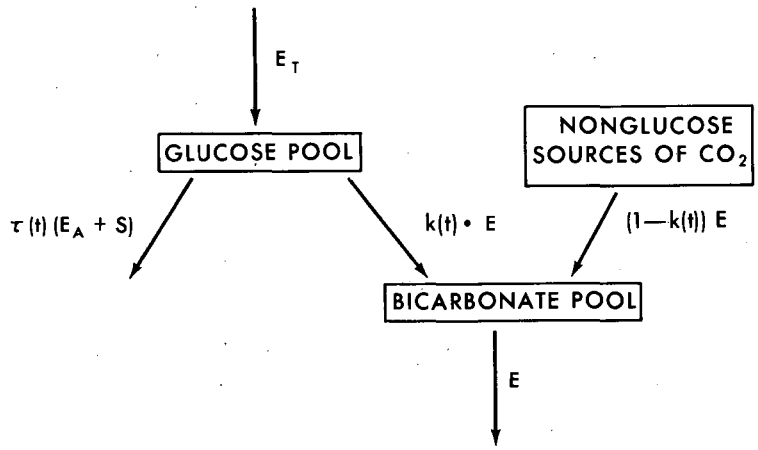

Figure 3. An example to show k need not be constant.

MUB-2935

By assumptions (A-3) and (A-8) the rate at which radioactivity enters the bicarbonate pool from the glucose pool is proportional to the amount of radioactivity present in the glucose pool. Thus, $\frac{E}{A}\alpha$ μCi of C^{14} enters the bicarbonate pool from the glucose pool each minute. Likewise, $\frac{E}{B}\beta$ μCi of C^{14} leaves the bicarbonate pool each minute via the breath. Thus the total rate of change in the amount of radioactivity in the bicarbonate pool is

(E-9) $$\frac{d\beta(t)}{dt} = \frac{E}{A}\alpha(t) - \frac{E}{B}\beta(t) .$$

Let $k_1 = \frac{E}{A}$ and $\lambda_2 = \frac{E}{B}$ (see (E-4)) so that

(E-10) $$\frac{d\beta}{dt} = k_1\alpha - \lambda_2\beta .$$

Equation (E-10) can be solved by the method of variation of parameters as follows: consider the homogeneous equation $\frac{d\beta}{dt} + \lambda_2\beta = 0$ and assume $\beta(t) = Ce^{-\lambda_2 t}$. If we allow C to vary with t, this assumed solution may be differentiated with the rule for differentiation of products of functions

(E-11)
$$\frac{d\beta}{dt} = \frac{dC}{dt} e^{-\lambda_2 t} - \lambda_2 C e^{-\lambda_2 t}$$
$$= \frac{dC}{dt} e^{-\lambda_2 t} - \lambda_2 \beta \ .$$

By comparing this with equation (E-10) we see that
$$\frac{dC}{dt} e^{-\lambda_2 t} = k_1 \alpha \ .$$

That is, $dC = k_1 \alpha e^{\lambda_2 t}\, dt$
so that by integrating over the interval $[0,t]$ yields
$$C(t) - C(0) = k_1 \int_0^t \alpha e^{\lambda_2 \tau}\, d\tau \ .$$

Substituting $\alpha(\tau) = \alpha_o e^{-\lambda_1 \tau}$ gives

(E-12)
$$C(t) = k_1 \int_0^t \left(\alpha_o\, e^{-\lambda_2 \tau} \cdot e^{\lambda_2 \tau}\right) d\tau + C(0)$$
$$= \alpha_o k_1 \int_0^t e^{(\lambda_2 - \lambda_1)\tau} d\tau + C(0) \ .$$

Hence, $\beta(t) = \left(\alpha_o k_1 \int_0^t e^{(\lambda_2 - \lambda_1)\tau}\, d\tau + C(0)\right) \cdot e^{-\lambda_2 t}$.

Since at $t = 0$ the bicarbonate pool contains no C^{14}, it all being in the glucose pool, $\beta(0) = 0$. Thus
$$0 = C(0)$$
so that

(E-13)
$$\beta(t) = \left(\alpha_o k_1 \int_0^t e^{(\lambda_2 - \lambda_1)\tau}\, d\tau\right) \cdot e^{-\lambda_2 t} \ .$$

Two cases must be considered, namely $\lambda_1 = \lambda_2$ and $\lambda_1 \neq \lambda_2$.

If $\lambda_1 = \lambda_2$ then
$$\beta(t) = \alpha_o k_1 t e^{-\lambda_2 t} \ .$$

If $\lambda_1 \neq \lambda_2$ then
$$\beta\ (t) = \left[\alpha_o k_1 \left[\frac{e^{(\lambda_2 - \lambda_1)\tau}}{\lambda_2 - \lambda_1}\right]_0^t\right] \cdot e^{-\lambda_2 t}$$
$$= \left[\alpha_o k_1 \left(\frac{e^{(\lambda_2 - \lambda_1)t} - 1}{\lambda_2 - \lambda_1}\right)\right] \cdot e^{-\lambda_2 t}$$
$$= \frac{\alpha_o k_1}{\lambda_2 - \lambda_1} \left(e^{-\lambda_1 t} - e^{-\lambda_2 t}\right) .$$

Hence

$$\text{(E-14)} \qquad \beta(t) = \begin{cases} \alpha_o k_1 t e^{-\lambda_2 t} & , \text{ if } \lambda_1 = \lambda_2 \\ \dfrac{\alpha_o k_1}{\lambda_2 - \lambda_1} (e^{-\lambda_1 t} - e^{-\lambda_2 t}) & , \text{ if } \lambda_1 \neq \lambda_2 \ . \end{cases}$$

By the definition of k_1 and consequences (E-1), (E-2) and (E-4) it follows that for the case $\lambda_1 = \lambda_2$, $b(t)$ is given by

$$b(t) = \frac{\beta(t)}{B} = \frac{\alpha_o}{A} \cdot \frac{E}{B} \cdot te^{-\lambda_2 t} = a_o \lambda_2 t e^{-\lambda_2 t}$$

and in the case $\lambda_1 \neq \lambda_2$

$$\begin{aligned} b(t) &= \frac{\beta(t)}{B} = \frac{\alpha_o k_1}{B(\lambda_2 - \lambda_1)} (e^{-\lambda_1 t} - e^{-\lambda_2 t}) \\ &= \frac{a_o \cdot A \cdot E/A}{B(\lambda_2 - \lambda_1)} (e^{-\lambda_1 t} - e^{-\lambda_2 t}) \\ &= a_o \frac{\lambda_2}{\lambda_2 - \lambda_1} (e^{-\lambda_1 t} - e^{-\lambda_2 t}) \end{aligned}$$

so that the complete solution for $b(t)$ is

$$\text{(E-15)} \qquad b(t) = \begin{cases} a_o \lambda_2 t e^{-\lambda_2 t} & , \text{ for } \lambda_1 = \lambda_2 \qquad \text{(C-1)} \\ a_o \dfrac{\lambda_2}{\lambda_2 - \lambda_1} (e^{-\lambda_1 t} - e^{-\lambda_2 t}) & , \text{ for } \lambda_1 \neq \lambda_2 \qquad \text{(C-2)} \ . \end{cases}$$

In order to simplify the notation and show the dependence of b on λ_1 and λ_2 write equation (E-15) as follows

$$\text{(E-16)} \qquad b(\lambda_1, \lambda_2, t) = \begin{cases} b_1(\lambda_2, t) & , \text{ for } \lambda_1 = \lambda_2 \\ b_2(\lambda_1, \lambda_2, t) & , \text{ for } \lambda_1 \neq \lambda_2 \ . \end{cases}$$

By L'Hôpital's rule, for each fixed λ_2 and t

$$\lim_{\lambda_1 \to \lambda_2} b_2(\lambda_1, \lambda_2, t) = b_1(\lambda_2, t)$$

so that $b(t)$ is continuous at $\lambda_1 = \lambda_2$.

A test to determine whether $\lambda_1 = \lambda_2$ or $\lambda_1 \neq \lambda_2$, i.e., whether case (C-1) or (C-2) holds, can be made using assumption (A-7). By this assumption, the time, t_{max}, required for $b(t)$ to reach its maximum value can be obtained from the experimental data for the bicarbonate pool, see (D-11). Likewise λ_1 can be obtained directly from the experimental data for the glucose pool. Hence the following lemma can be used to determine whether or not $\lambda_1 = \lambda_2$.

(E-17) <u>Lemma</u>: $\lambda_1 = \lambda_2$ if and only if $t_{max} = \frac{1}{\lambda_1}$.

<u>Proof</u>: t_{max} is the time t such that $b'(t) = 0$. Letting primes denote derivatives with respect to t, (E-15) yields:

$$\text{(E-18)}\quad b'(t) = \begin{cases} b_1'(t) = a_o\lambda_2 e^{-\lambda_2 t}(1 - \lambda_2 t) & , \text{ for } \lambda_1 = \lambda_2 \\ b_2'(t) = a_o\frac{\lambda_2}{\lambda_2 - \lambda_1}(\lambda_2 e^{-\lambda_2 t} - \lambda_1 e^{-\lambda_1 t}) & , \text{ for } \lambda_1 \neq \lambda_2 . \end{cases}$$

Suppose $\lambda_1 = \lambda_2$. Then to find t_{max} the equation $0 = b_1'(t) = a_o\lambda_2 e^{-\lambda_2 t}(1 - \lambda_2 t)$ must be solved for t. This yields $t_{max} = \frac{1}{\lambda_2} = \frac{1}{\lambda_1}$.

Suppose $\lambda_1 \neq \lambda_2$. It must be shown that in this case $t_{max} \neq \frac{1}{\lambda_1}$. Since $\lambda_1 \neq \lambda_2$, t_{max} is the solution of

$$0 = b_2'(t) = a_o \frac{\lambda_2}{\lambda_2 - \lambda_1}(\lambda_2 e^{-\lambda_2 t} - \lambda_1 e^{-\lambda_1 t}) .$$

Thus, $t_{max} = \frac{1}{\lambda_2 - \lambda_1} \ln \frac{\lambda_2}{\lambda_1}$. Now it must be demonstrated that $\frac{1}{\lambda_1}$ cannot equal $\frac{1}{\lambda_2 - \lambda_1} \ln \frac{\lambda_2}{\lambda_1}$. To show this, one may argue by contradiction, i.e., show that $\frac{1}{\lambda_1} = \frac{1}{\lambda_2 - \lambda_1} \ln \frac{\lambda_2}{\lambda_1}$ implies that $\lambda_1 = \lambda_2$ and thus obtain a contradiction to the supposition that $\lambda_1 \neq \lambda_2$.

If $\frac{1}{\lambda_1} = \frac{1}{\lambda_2 - \lambda_1} \ln \frac{\lambda_2}{\lambda_1}$, then $\frac{\lambda_2 - \lambda_1}{\lambda_1} = \ln \frac{\lambda_2}{\lambda_1}$, or $\frac{\lambda_2}{\lambda_1} - 1 = \ln \frac{\lambda_2}{\lambda_1}$.

Let $x = \frac{\lambda_2}{\lambda_1}$. Then this equation is equivalent to $x - \ln x = 1$. But $x = 1$ is the unique solution to this equation, because:

1) $x = 1$ clearly is a solution $(1 - \ln 1 = 1 - 0 = 1)$

2) all values of $x - \ln x$ are greater than 1 for values of $x \neq 1$.

To see this let $\phi(x) = x - \ln x$. Then $0 = \phi'(x) = 1 - \frac{1}{x}$ implies $x = 1$. So ϕ has an extremum at $x = 1$. To see that this extremum is a minimum we note that $\phi''(x) = \frac{1}{x^2} > 0$. Hence $\frac{\lambda_2}{\lambda_1} = 1$ so that $\lambda_2 = \lambda_1$ contradicting the supposition that $\lambda_2 \neq \lambda_1$. Q.E.D.

This result is important in the calculation of λ_2 from the data and will be expanded later (see discussion following Lemma 3).

Equation (E-18) represents the specific activity of the bicarbonate pool under the proviso that all of the CO_2 in the bicarbonate pool originates from glucose. To further clarify the use of this expression for b(t), suppose that only kE grams of glucose carbon enter the bicarbonate pool each minute, k being the fraction of CO_2 carbon that originates from glucose, $0 < k < 1$. Then, by theory, the specific activity in the bicarbonate pool should be

(E-19) $$p(t) = kb(t)$$

since, in the derivation of b(t), E appeared in the numerator. k here need not be constant. The following example will show that the assumption of "steady-stateness" for the glucose and bicarbonate pools does not imply that k is constant. Consider the situation in Fig. 3 where E_T, E, E_A and S are positive constants. Steady-stateness of the glucose and bicarbonate pools implies that

(E-20) $$E_T = kE + \tau(E_A + S) \ .$$

Solving for τ,

$$\tau = \frac{E_T - kE}{E_A + S} \ .$$

From this it can be seen that if k depends on time, then for each $t \geq 0$, τ can be chosen to be

$$\tau(t) = \frac{E_T - k(t)E}{E_A + S} \ .$$

Thus, at any time t, the inflow rate E_T and the outflow rate $k(t)E + \tau(t)\ (E_A + S)$ for the glucose pool are equal (by (E-20)) and constant as are the inflow rate $k(t)E + (1 - k(t))E$ and the outflow rate E for the bicarbonate pool. Hence, steady-state conditions hold for both the glucose and the bicarbonate pools but k is not constant. It should be noted that the nonglucose precursors of CO_2 need not be in a steady state; tnis, however, has no bearing on the present analysis. The supposition that only kE grams of glucose carbon enter the bicarbonate pool per minute is not in reality a "supposition." It is well known that the carbon of CO_2 in the bicarbonate pool can originate from nonglucose precursors (8).

It should be noticed that during the experimental procedure, the specific activity of CO_2 is not measured in the bicarbonate pool but in the breath. Heuristically one would expect that in time both of these would have nearly the same specific activity since homogeneous mixing seems plausible and since $C^{14}O_2$ and $C^{12}O_2$ behave quantitatively approximately the same in physiologic processes. Nonetheless, there is a lag period before these two sites of CO_2 develop nearly the same specific activity (9).

With these words of caution, the gap between the experimentally observed specific activity in the breath, denoted $E^{SA}_{CO_2}$, and the modified theoretical specific activity of the bicarbonate pool, p, is hurdled. That is, p is taken to be equal to $E^{SA}_{CO_2}$ so that for each $t \geq 0$

(E-21) $$k(t) = \frac{p(t)}{b(t)} = \frac{E^{SA}_{CO_2}(t)}{b(t)} \ .$$

In calculating the data, k is determined at t_{max} thus allowing time for mixing and for diminution in the error due to lag.

Calculation of b(t) requires knowledge of a_o, λ_1 and λ_2. The experimental data for the glucose pool readily provide a_o and λ_1. a_o is the intercept on the specific-activity axis of the straight-line fit to the points obtained by plotting experimental glucose-pool specific activity versus time, for $t \geq 15$, on semilogarithmic paper. λ_1 is the slope of this line. To determine λ_2 the following results may be used.

Lemma 1: λ_2 must satisfy the equation $\lambda_1 e^{-\lambda_1 t_m} = \lambda e^{-\lambda t_m}$.

Proof: If $\lambda_1 = \lambda_2$ then clearly $\lambda_1 e^{-\lambda_1 t_m} = \lambda_2 e^{-\lambda_2 t_m}$. If $\lambda_1 \neq \lambda_2$ then b_2 holds in (E-16), and since at t_m, $b_2'(t_m) = 0$, the lemma follows from (E-18) and the fact that $a_o \neq 0$ and $\lambda_2 \neq 0$.

Corollary 1: λ_2 must satisfy $Ce^{\lambda t_m} - \lambda = 0$ where $C = \lambda_1 e^{-\lambda_1 t_m}$.

Proof: Immediate from lemma 1.

Definition 1: Let ϕ be the function defined on $[0,\infty)$ by $\phi(\lambda) = Ce^{\lambda t_m} - \lambda$ where $C = \lambda_1 e^{-\lambda_1 t_m}$. (See Fig. 4a)

Lemma 2: If $\phi(\lambda_o)$ is the minimum value of ϕ, that is, $\phi(\lambda) \geq \phi(\lambda_o)$, for all $\lambda \epsilon [0,\infty)$ then, $\phi(\lambda_o) = 0$ implies $\lambda_2 = \lambda_1$, and, $\phi(\lambda_o) < 0$ implies that there exists a unique $\lambda_2 \neq \lambda_1$, such that $\phi(\lambda_2) = 0$.

Proof: The properties of ϕ which make this lemma possible are:

(P-1) $\lim_{\lambda \to 0} \phi(\lambda) = C > 0$. This is clear since ϕ is a continuous function of λ.

(P-2) $\lim_{\lambda \to \infty} \phi(\lambda) = \infty > 0$.

(P-3) ϕ has a unique minimum. To see this, the rules of differential calculus for finding extrema require that

(E-22) $$0 = \phi'(\lambda) = t_m Ce^{\lambda t_m} - 1$$

be satisfied by any λ for which $\phi(\lambda)$ is an extremal. (E-22) has the unique solution, λ_o, given by

$$\lambda_o = \frac{1}{t_m} \ln \frac{1}{Ct_m}$$

the uniqueness being a result of the constancy of t_m and C. That $\phi(\lambda_o)$ is a minimum follows from

$$\phi''(\lambda_o) = t_m^2 Ce^{\lambda_o t_m} > 0 .$$

These properties of ϕ are incorporated into Fig. 4b.

From these properties it follows that ϕ can have at most two zeros, and the condition that must hold for ϕ to have two zeros is $\phi(\lambda_o) < 0$. Since λ_1 is always one of these zeros (as is clear from the nature of C), it follows that when $\phi(\lambda_o) < 0$, there exists a unique $\lambda_2 \neq \lambda_1$, such that $\phi(\lambda_2) = 0$. When $\phi(\lambda_o) = 0$, there is only one solution, this being $\lambda_1 = \lambda_o$.

Lemma 3: $$\phi(\lambda_o) = \frac{1 - \lambda_1 t_m + \ln \lambda_1 t_m}{t_m} .$$

Proof: $\phi(\lambda_o) = Ce^{\lambda_o t_m} - \lambda_o$ (by definition 1)

$$= Ce^{\left(\frac{1}{t_m} \ln \frac{1}{Ct_m}\right) \cdot t_m} - \frac{1}{t_m} \ln \frac{1}{Ct_m} \qquad \text{(by (E-25))}$$

$$= \frac{1 + \ln Ct_m}{t_m}$$

$$= \frac{1 + \ln \left((\lambda_1 e^{-\lambda_1 t_m}) \cdot t_m\right)}{t_m} \qquad \text{(by definition 1)}$$

$$= \frac{1 - \lambda_1 t_m + \ln \lambda_1 t_m}{t_m} \qquad \text{Q.E.D.}$$

Lemma 4: (a) If $\lambda_1 t_m = 1$, then $\phi(\lambda_o) = 0$

(b) If $\lambda_1 t_m \neq 1$, then $\phi(\lambda_o) < 0$.

Proof: (a) follows immediately from lemmas 3 and 2. This result was expressed earlier as part of (E-17).

(b) follows from noticing that the function

$$\psi(x) = 1 - x + \ln x \ , \ x \geq 0$$

has a unique extremum, it being a maximum, at $x = 1$. In order to see this, observe that $0 = \psi'(x) = -1 + \frac{1}{x}$ has a unique solution, it being $x = 1$, and that $\psi(1) = 0$. Thus, since $\psi''(1) = -\frac{1}{x^2}\Big|_{x=1} < 0$, it follows that for all $x \neq 1$, $\psi(x) < 0$. Since $\phi(x) = \frac{1}{t_m}\psi(x)$, the lemma follows.

To determine λ_2, then, one should first calculate $\lambda_1 t_m$. If $\lambda_1 t_m = 1$ then $\lambda_2 = \lambda_1$ by (E-17) and also by lemma 2. If $\lambda_1 t_m \neq 1$ then, by lemma 4, $\phi(\lambda_o) < 0$, and, by lemma 2 , the existence of a unique $\lambda_2 \neq \lambda_1$, is assured. Since in this case $\lambda_2 \neq \lambda_1$, and since λ_1 is known, the unknown λ_2 can be calculated from $\lambda_1 e^{-\lambda_1 t_m} = \lambda e^{-\lambda t_m}$ by successive approximations carried out by substituting various values of λ in this equation until $\lambda e^{-\lambda t_m}$ approximates $\lambda_1 e^{-\lambda_1 t_m}$ as closely as desired.

METHOD

The experimental technique and instrumentation are described in detail in the articles of Tolbert et al. (3) and Pollycove (4). For purposes of measuring the glucose-pool specific activity, a polyethylene catheter is inserted into a forearm vein and serial blood samples of 5 to 10 ml are withdrawn in heparinized syringes, starting before and continuing after a single rapid intravenous injection of approximately 10 to 15 μCi universally labeled C^{14} glucose (Nuclear - Chicago Corporation) in the opposite arm. These samples are collected at 15-min intervals for the first hour and at 60-min intervals thereafter until a maximum point is discernible on the CO_2 specific-activity curve produced by the recorder. This usually requires 3 to 5 hr. The blood samples are analyzed for glucose and glucose radioactivity with a glucose oxidase method of glucose determination

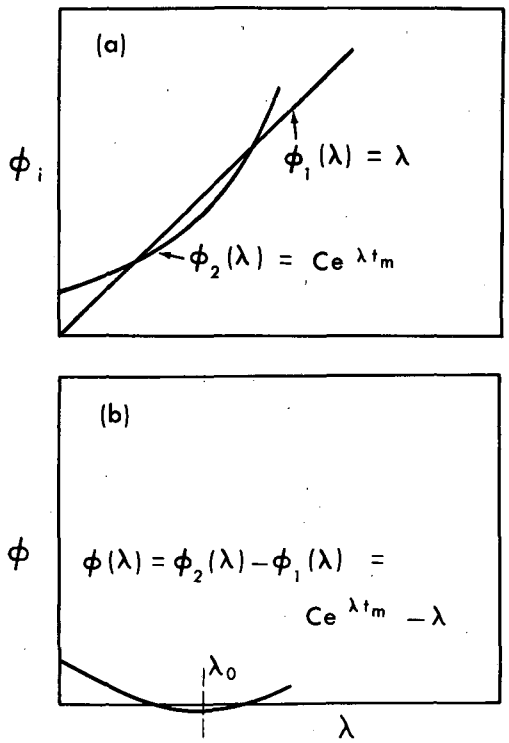

Figure 4. (a) Graphs of $\phi_1(\lambda) = \lambda$ and $\phi_2(\lambda) = Ce^{\lambda t_m}$. (b) Graph of $\phi(\lambda) = Ce^{\lambda t_m} - \lambda$ illustrates the case $\phi(\lambda_o) < 0$ where $(\lambda_o, \phi(\lambda_o))$ is the minimum point of ϕ. In this case there are two points where ϕ takes on the value 0.

MUB-2936

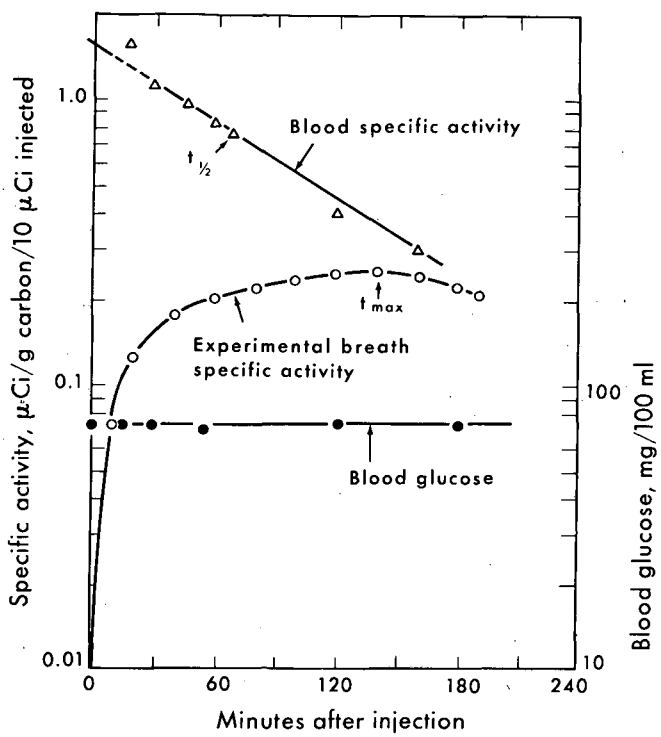

Figure 5. Example of graphs of the data for a(t), the blood-glucose specific activity in μCi/gC adjusted to an injected dose of 10 μCi, for $E^{SA}_{CO_2}(t)$, the experimental specific activity of the expired breath in μCi/gC, and for $B_S(t)$, the blood sugar in milligram percent.

MUB-2937

(Glucostat, Worthington Biochemical Corp., Freehold, N.J.) on protein free filtrate obtained by the method of Somogyi (10) and the method of Searle and Chaikoff (11) respectively.

In the present experimental method the breath is analyzed for CO_2 and CO_2 radioactivity every 12 sec with an infrared CO_2 gas analyzer and a 21-liter ionization chamber having a vibrating reed electrometer, a 95% theoretical efficiency and a calibration constant of 1.40 μCi of C^{14} per 10^{-11} amperes. These instruments receive the expired air from a plastic helmet placed over the subject's head. A recorder produces tracings of the radioactivity and the CO_2 content of the expired breath as well as the ratio between these two quantities. During the course of the procedure, the subjects sit in a reclining chair and are permitted to drink black coffee, to converse, and to remove the helmet for a few minutes.

CALCULATIONS

The theory presented earlier was synthesized to allow the calculation of certain quantities from data obtained through the application of the foregoing method. An orderly approach to these calculations is as follows:

(Q-1) Recall that $\alpha(0) = \alpha_o$ is the injected dose of C^{14} glucose in μCi. See (D-1).

(Q-2) Plot a(t) versus time on semilogarithmic paper, see (D-3). Extrapolate to t = 0 and obtain a_o. This is μCi/g C in the glucose pool. In order to get μCi/g glucose, divide a_o by 2.5 (because, for each gram of carbon in glucose there are 2.5 g of glucose) and define $A_o = \frac{a_o}{2.5}$: this then is μCi/g glucose in the glucose pool. In Fig. 5, $\underline{a}(t)$ has been plotted instead of a(t), $\underline{a}(t)$ being a(t) adjusted to an initial injected dose of 10 μCi, i.e., $\underline{a}(t) = \frac{10}{\alpha_o} a(t)$.

(Q-3) $t_{\frac{1}{2}}$ is readily obtained from plot (Q-2) since it is the time required for a_o to drop to $\frac{1}{2}a_o$.

(Q-4) The glucose pool in grams, denoted by P_G, is obtained from $P_G = \frac{\alpha_o}{A_o}$. Let W represent body weight in kilograms. Then the glucose pool in grams per kilogram, denoted P_G^W, is $P_G^W = \frac{\alpha_o}{A_o W}$. Note that A, see (D-5), is given by $A = \frac{P_G}{2.5}$.

(Q-5) λ_1, the fractional turnover rate for the glucose pool, see (D-8), is the slope of the line plotted in (Q-2). It can also be obtained from $t_{\frac{1}{2}}$ by using $\lambda_1 = \frac{0.693}{t_{\frac{1}{2}}}$ which is obtained from $a(t) = a_o e^{-\lambda_1 t}$ by taking logarithms and substituting $\frac{1}{2}a_o$ for a(t) and $t_{\frac{1}{2}}$ for t.

(Q-6) To obtain the glucose turnover rate in g/kg/hr, denoted T_G, use

$$T_G = \lambda_1 \cdot P_G^W \cdot 60 .$$

(Q-7) The "glucose volume" in liters, denoted V_G, and in liters per kg of body weight, denoted V^W, and in percent body weight, denoted V_G^W, may be obtained as follows: Since V_G is defined to be the volume, in liters,

which contains the P_G grams of glucose, $\frac{P_G}{V_G} = B_G \cdot 10^{-2}$ where B_G is the fasting blood glucose and the factor 10^{-2} enters in the conversion of mg/100 ml to g/liter. Thus, $V_G = \frac{P_G}{B_G} \cdot 10^2$ liters and $V^W = \frac{P_G}{B_G} \cdot \frac{10^2}{W}$ liters/kg. If it is assumed that one liter is equivalent to one kilogram, then V^W is the fraction of body weight devoted to glucose and $V^W \cdot 100\%$ is the percent of body weight comprising the glucose pool. Thus $V_G^W = \frac{P_G \cdot 10^4}{B_G \cdot W}$ % body weight.

(Q-8) λ_2 is obtained as described in the discussion following lemma 4.

(Q-9) The mean milligrams of CO_2 expired per minute, denoted $\left\langle \frac{d[CO_2]}{dt} \right\rangle$, was obtained by integrating the CO_2 experimental curve with the assistance of a mechanical integrator. This "mean" is an average over time. Note that this quantity is almost E, see (D-7), the difference being essentially in units. E is in terms of g C/min and $\left\langle \frac{d[CO_2]}{dt} \right\rangle$ is in terms of mg CO_2/min.

(Q-10) t_{max}, see (D-11), is read off the experimental CO_2 specific-activity curve, t_{max} being the time at which this curve reaches its maximum value.

(Q-11) The experimental CO_2 specific activity, denoted $E_{CO_2}^{SA}$, is obtained at t_{max} directly by reading it off the experimental CO_2 specific-activity curve at this point.

(Q-12) Since λ_1, λ_2, and t_{max} are known, from (E-15),

$$b(t_{max}) = \begin{cases} b_1(t_{max}) \ , & \text{for } \lambda_1 = \lambda_2 \\ b_2(t_{max}) \ , & \text{for } \lambda_1 \neq \lambda_2 \end{cases}$$

can be calculated.

(Q-13) The percent CO_2 derived from glucose, denoted $_{\%}CO_2^G$, is obtained by (E-21),

$$_{\%}CO_2^G(t_{max}) = \frac{E_{CO_2}^{SA}(t_{max})}{b(t_{max})} \cdot 100 \ .$$

(Q-14) The mg of glucose oxidized to CO_2 per minute, denoted G_{CO_2}, is

$$G_{CO_2}(t) = \frac{_{\%}CO_2^G(t)}{100} \cdot \left\langle \frac{d[CO_2]}{dt} \right\rangle \cdot \frac{180}{6 \cdot 44}$$

because:

(fraction of CO_2 derived from glucose) $\cdot$ (mg CO_2/min) = (mg CO_2 derived from glucose/min) and one mg of CO_2 is equivalent to $\frac{180}{6 \cdot 44}$ mg of glucose as can be seen from

$$6O_2 + C_6H_{12}O_6 \rightarrow 6CO_2 + 6H_2O$$

$$180 \text{ mg} \quad 6 \cdot 44 \text{ mg} \ .$$

Since the fraction of CO_2 derived from glucose is $\frac{_{\%}CO_2^G(t)}{100}$, the desired equation follows.

In terms of g/kg/hr, denoted $G_{CO_2}^W$, this is

$$G^{W}_{CO_2}(t) = \frac{G_{CO_2}(t)}{W} \cdot 60 \cdot 10^{-3} .$$

Notice that G_{CO_2} is again almost E, the difference once more being essentially in the units.

(Q-15) The CO_2 turnover in g/hr per kg of body weight, denoted by T_{CO_2}, is

$$T_{CO_2} = \frac{\left\langle \frac{d[CO_2]}{dt} \right\rangle}{W} \cdot 60 \cdot 10^{-3} \quad \text{g/kg/hr.}$$

(Q-16) The CO_2 pool size in g/kg, denoted by P_{CO_2} is

$$P_{CO_2} = \frac{T_{CO_2}}{\lambda_2} \cdot \frac{1}{60}$$

because:

(fraction of pool which turns over/min) · (pool size) = (total turnover/min) implying that

$$\lambda_2 \cdot (\text{pool size}) = T_{CO_2} \cdot \frac{1}{60}$$

that is

$$(\text{pool size}) = \frac{T_{CO_2}}{\lambda_2} \cdot \frac{1}{60} .$$

These then, are the various parameters measured or calculated.

DISCUSSION

Three methods of glucose kinetic studies using universally labeled C^{14} glucose are presently in vogue. One method, originating with Baker et al., was described in this article. Another method, developed by Steele et al. (5,9), consists of simultaneously injecting a priming dose of C^{14} glucose and starting a continuous I.V. infusion of this tracer. The objective here is to maintain a constant blood glucose specific activity in order to simplify the determination of the asymptotic value of this specific activity. But even if this specific activity is not maintained at a constant value, fairly good results can be obtained by an approximation method outlined by Steele and co-workers. This method also allows a determination of the fraction of CO_2 derived from glucose, but again an asymptote is needed, this time of the ratio of the blood glucose specific activity to the specific activity of the expired breath.

The third method is that of Wrenshall and Hetenyi (7). It consists of giving successive intravenous injections of C^{14} glucose and determining the glucose volume after each injection by means of an isotope dilution equation. This method was originated to study the changes induced in glucose volume by modifications in the physiological state of the organism under study. In addition, rates of glucose appearance and disappearance from the blood can be

calculated. However, this method has not been used to answer questions regarding conversion of glucose to CO_2.

Each of these methods has its limitations, which have been discussed by their own authors. Baker's method has the following in its favor: 1) It is relatively simple to perform. 2) The equations involved are simple and fit the data sufficiently well to give consistent results. 3) It provides a means for analyzing data regarding conversion of glucose to CO_2. 4) In the dog it gives results quite comparable to those obtained by the other two methods.

SUMMARY

The model for the study of glucose kinetics originated by Baker et al. has been expanded and refined both in its theory and in its realization. The present paper is concerned with the refinements in theory. A subsequent report will present the data obtained when this method was applied to the study of normal individuals as well as patients with acromegaly or diabetes mellitus.

REFERENCES

1. Baker, N.; Shreeve, W.; Shipley, R.; Incefy, G., and Miller, M.; J. Biol. Chem. 211:575, 1954.
2. Shreeve, W.; Baker, N.; Miller, M.; Shipley, R.; Incefy, G. E., and Craig, J. W.; Metabolism 5:22, 1956.
3. Tolbert, B. M.; Kirk, M., and Baker, E. M.; Am. J. Physiol. 185:269, 1956.
4. Pollycove, M.; Semiannual Report, Donner Laboratory, Lawrence Radiation Laboratory, UCRL-9897:188, 1961.
5. Steele, R.; Wall, J. S.; deBodo, R. C., and Altszuler, N.; Am. J. Physiol. 187:15, 1956.
6. Reichard, G. A., Jr.; Jacobs, A. E.; Kimbel, P.; Hochella, N. J., and Weinhouse, S.; J. Appl. Physiol. 16(5):789, 1961.
7. Wrenshall, G. A., and Hetenyi, G., Jr.; Metabolism 8:531, 1959.
8. West, E. S., and Todd, W. R.: Textbook of Biochemistry, New York, The Macmillan Co., 1961, pp. 910-911.
9. Steele, R.; Altszuler, N.; Wall, J. S.; Dunn, A., and deBodo, R. C.; Am. J. Physiol. 196(2):221-230, 1959.
10. Somogyi, M.; J. Biol. Chem. 86:655, 1939.
11. Searle, G. L., and Chaikoff, I. C.; Am. J. Physiol. 170:456, 1952.

Received September, 1964.

C^{14}-Glucose Kinetic Studies in Normal, Diabetic and Acromegalic Subjects

Edward Manougian, Myron Pollycove, John A. Linfoot and John H. Lawrence

In the past few years several methods have been introduced for the study of the kinetics of C^{14} glucose in humans or laboratory animals. Among these methods, the most popular ones presently appear to be the priming dose-continuous infusion (1), the successive tracer injection (2) and the single tracer injection methods (3). The priming dose-continuous infusion method consists of giving an initial dose of C^{14} glucose and simultaneously starting a constant continuous infusion of this tracer. It provides a means of calculating various parameters for both the glucose compartment and the bicarbonate compartment, but the determination of an asymptote required for some of these calculations sometimes presents a difficulty. The successive tracer injection method is performed by giving injections of C^{14} glucose at various times, the time of each injection depending on the preceding events. This method was devised to study the characteristics of the glucose compartment. It has not been extended to include the bicarbonate compartment. The simplest method, which allows the calculation of parameters for both the glucose and bicarbonate compartments, is the single tracer injection method. It, however, relies on the steady-state of these two compartments, a situation not always attained in patients with abnormalities in carbohydrate metabolism. These methods along with the cautions required in their use are discussed by their respective authors.

The method used in the present study is a modification of the single tracer injection method introduced by Baker _et al_. in 1954 (3). The technique they used required the periodic collection of CO_2 via a face mask whereas the newer version, developed by Tolbert _et al_. (4,5), allows "continuous" monitoring of expired CO_2 and $C^{14}O_2$. The theoretical model as presented by Baker and coworkers had some minor gaps that were bridged recently (6). Further support of this model, when properly applied, will be presented here. The present report, however, is concerned primarily with the results obtained when this method was applied to normal subjects (Table 1), patients with either adult or juvenile type diabetes mellitus (Table 2) and patients with active acromegaly (Table 4). The characteristic differences of glucose kinetics in the diabetics and in the acromegalics as compared to the normals will be indicated. Similarities between these groups will also be noted. It will be seen that the abnormalities in glucose kinetics that frequently accompany acromegaly are similar to those seen in

Table 1. Normal subjects

Study no. (different subjects)	Bs (FBS) mg%	$t_{\frac{1}{2}}$ min	Glucose-pool size P_G g	Glucose-pool size P_G^w g/kg	Glucose turnover λ_1 1/min	Glucose turnover T_G g/kg/hr	Glucose vol. V_G^w % B.W.	t_{max} min	$\left\langle \frac{d[CO_2]}{dt} \right\rangle$ mg/min	$B^{SA}_{CO_2}(t_{max})$ µCi/gC	$b(t_{max})$ µCi/gC	$\%^{CO_2^G}$ %CO_2 via glucose	Oxidation of glucose to CO_2: G_{CO_2} mg/min	Oxidation of glucose to CO_2: $G^w_{CO_2}$ g/kg/hr	CO_2 turnover λ_2 1/min	CO_2 turnover T_{CO_2} g/kg/hr	CO_2 pool size P_{CO_2} g/kg
6	79	90	21.5	0.364	0.0077	0.168	36.0	140	287	0.168	0.397	42.3	89.2	0.085	0.0065	0.294	0.758
7	77	77	20.8	0.311	0.0090	0.168	42.0	95	302	0.153	0.538	28.7	88.0	0.054	0.0135	0.268	0.332
9	82	78	16.6	0.236	0.0089	0.126	28.8	50	391	0.060	0.096	63.3	168.9	0.144	0.0380	0.333	1.460
10	--	108	21.7	0.289	0.0064	0.111	--	120	373	0.107	0.528	19.8	50.4	0.040	0.0030	0.296	0.448
12	61	95	23.8	0.370	0.0073	0.162	42.0	125	309	0.152	0.400	38.2	80.5	0.075	0.0083	0.288	0.581
13	--	77	17.9	0.226	0.0090	0.122	--	125	305	0.150	0.450	34.0	70.8	0.054	0.0070	0.232	0.554
28	81	88	20.4	0.232	0.0079	0.110	28.6	120	304	0.165	0.478	34.5	71.6	0.049	0.0090	0.207	0.383
30	69	90	19.2	0.256	0.0077	0.118	37.1	100	317	0.165	0.604	27.3	59.1	0.047	0.0129	0.254	0.329
31	71	117	15.6	0.215	0.0059	0.076	30.3	135	325	0.189	0.720	26.2	58.2	0.048	0.0092	0.268	0.486
33	80	90	14.7	0.240	0.0077	0.111	30.0	112	265	0.250	0.716	34.9	63.1	0.062	0.0105	0.260	0.413
48	94	97	17.2	0.240	0.0071	0.103	25.6	120	356	0.188	0.614	30.6	75.0	0.063	0.0096	0.302	0.524
50	86	110	27.6	0.234	0.0063	0.089	27.2	130	487	0.090	0.401	22.4	74.5	0.038	0.0092	0.249	0.451
51	88	112	18.3	0.192	0.0062	0.071	21.8	140	329	0.248	0.576	43.1	96.8	0.060	0.0082	0.204	0.414
Average	79	95	19.6	0.262	0.0075	0.118	31.8	116	330	0.169	0.535	31.8	73.1	0.056	0.0089	0.260	0.473

(excluding study 9 for averages of the CO_2 data)

Table 2a. Diabetic patients without pituitary irradiation and off hypoglycemic agents

Study no. (different subjects)	Bs (FBS) mg%	$t_{\frac{1}{2}}$ min	Glucose-pool size P_G g	Glucose-pool size P_G^w g/kg	Glucose turnover λ_1 1/min	Glucose turnover T_G g/kg/hr	Glucose vol. V_G^w % B.W.	t_{max} min	$\left\langle \frac{d[CO_2]}{dt} \right\rangle$ mg/min	$E^{SA}_{CO_2}(t_{max})$ µCi/gC	$b(t_{max})$ µCi/gC	$\%CO_2^G$ %CO_2 via glucose	Oxidation of glucose to CO_2: G_{CO_2} mg/min	Oxidation of glucose to CO_2: $G^w_{CO_2}$ g/kg/hr	CO_2 turnover λ_2 1/min	CO_2 turnover T_{CO_2} g/kg/hr	CO_2 pool size P_{CO_2} g/kg
3 (J)*	550	610	88.4	1.610	0.0011	0.118	29.0	120	308	0.250	0.246	10.2	20.4	0.022	0.0280	0.336	0.200
15 (J)	472	381	90.8	1.320	0.0018	0.144	27.9	110	288	0.183	2.250	8.1	16.0	0.014	0.0260	0.252	0.162
32 (J)	---	350	83.3	1.350	0.0020	0.160	---	250	259	0.060	0.183	32.9	58.1	0.056	0.0071	0.419	0.989
39 (A)	200	447	43.5	0.660	0.0016	0.061	33.0	225	254	0.126	0.406	31.0	53.8	0.049	0.0097	0.232	0.398
40 (A)	84	129	16.2	0.248	0.0054	0.080	29.5	135	254	0.312	0.786	39.7	68.8	0.064	0.0099	0.236	0.395
41 (J)	167	200	26.6	0.426	0.0035	0.089	25.5	210	193	0.148	0.452	32.7	43.1	0.041	0.0063	0.183	0.488
44 (J)	371	225	78.1	1.130	0.0031	0.210	30.4	155	338	0.032	0.200	16.0	36.9	0.032	0.0116	0.293	0.419
61 (A)	127	198	30.4	0.496	0.0035	0.104	34.1	220	226	0.145	0.381	38.1	49.1	0.048	0.0058	0.185	0.532
64 (A)	153	210	35.2	0.484	0.0033	0.096	31.6	125	300	0.119	0.470	25.3	51.8	0.043	0.0159	0.249	0.216
76 (A)	120	280	33.8	0.442	0.0025	0.066	36.8	200	229	0.167	0.450	37.1	57.9	0.046	0.0088	0.180	0.341
Average	249	303	52.6	0.817	0.0028	0.113	30.9	175	255	0.154	0.582	27.1	45.6	0.042	0.0129	0.257	0.414

*(A) Adult-type diabetes, (J) juvenile-type diabetes.

Table 2b. Diabetic patients on insulin

Study no. (different subjects)	Bs (FBS) mg%	$t_{\frac{1}{2}}$ min	Glucose-pool size P_G g	Glucose-pool size P_G^w g/kg	Glucose turnover λ_1 1/min	Glucose turnover T_G g/kg/hr	Glucose vol. V_G^w % B.W.	t_{max} min	$\left\langle \frac{d[CO_2]}{dt} \right\rangle$ mg/min	$E^{SA}_{CO_2}(t_{max})$ µCi/gC	$b(t_{max})$ µCi/gC	$\%CO_2^G$ %CO_2 via glucose	Oxidation of glucose to CO_2: G_{CO_2} mg/min	Oxidation of glucose to CO_2: $G^w_{CO_2}$ g/kg/hr	CO_2 turnover λ_2 1/min	CO_2 turnover T_{CO_2} g/kg/hr	CO_2 pool size P_{CO_2} g/kg
3	80	34	12.7	0.230	0.0099	0.281	29	70	405	0.185	0.475	39.0	109.5	0.120	0.0096	0.449	0.366
15	98	71	15.4	0.224	0.0098	0.131	22	105	361	0.170	0.575	29.6	73.0	0.064	0.0089	0.316	0.589
32		360	52.6	0.852	0.0019	0.099		170	280	0.131	0.344	38.1	72.8	0.070	0.0133	0.454	0.569
34		164	34.0	0.398	0.0042	0.101		175	283	0.156	0.352	44.3	85.6	0.060	0.0074	0.199	0.446
39	200	425	43.5	0.660	0.0016	0.064	33	190	252	0.109	0.421	25.9	44.5	0.041	0.0123	0.230	0.313
41	109	325	31.2	0.501	0.0021	0.064	46	235	233	0.140	0.485	28.9	46.0	0.044	0.0075	0.223	0.492
44	191	420	62.1	0.898	0.0017	0.089	47	320	320	0.074	0.237	31.2	68.2	0.059	0.0053	0.277	0.871
Average	135	257	35.9	0.5385	0.0045	0.118	35	181	305	0.138	0.413	33.9	71.4	0.066	0.0092	0.307	0.521

diabetes mellitus but usually with a lesser degree of deviation from normal. Preliminary results of glucose kinetic studies on patients after the administration of suppresive doses of heavy-particle irradiation to their pituitary glands will also be presented. At the time of pituitary irradiation, these patients had either diabetes mellitus with retinopathy (Table 3) or active acromegaly (Table 5). It will be seen that the diabetic state sometimes accompanying acromegaly can be reversed with heavy-particle irradiation to the pituitary. The effects on adult-type diabetes are yet unclear. It appears, however, that the diabetic state is not improved in this disorder. Included in this report is a study performed on a patient with Cushing's syndrome due to an adrenal carcinoma. Interestingly, this patient had a normal glucose kinetic study in spite of a markedly elevated excretion rate of urinary adrenocortical steroids.

THEORY AND METHOD

The method, in brief, consisted of giving a single tracer dose (10 to 15 μCi) of universally labeled C^{14} glucose (Nuclear-Chicago Corporation) intravenously and by subsequently following the blood-glucose specific activity, blood-glucose concentration, expired CO_2 and expired CO_2 radioactivity for 3 to 6 hr (6). These studies were performed either after an overnight fast or, as in the case of some diabetics, immediately after breakfast preceded by a dose of insulin or an oral hypoglycemic agent. The diet of the acromegalic subjects contained more than 200 g of carbohydrates. The diabetic subjects, however, were on individual diets as given in Table 7. The use of heavy-particle pituitary irradiation in the treatment of diabetic retinopathy and acromegaly has been reported previously (7-9). The theory is that of Baker et al. (3,6). It is based on a unidirectional two compartmental (glucose compartment and bicarbonate compartment) steady-state model, in which glucose is oxidized to CO_2 by an "immediate oxidative pathway". The equations describing this model are:

$$a(t) = a_o e^{-\lambda_1 t}$$

$$b(t) = \begin{cases} a_o \lambda_2 t e^{-\lambda_2 t}, & \text{for } \lambda_1 = \lambda_2 \\ a_o \dfrac{\lambda_2}{\lambda_2 - \lambda_1} (e^{-\lambda_1 t} - e^{-\lambda_2 t}), & \text{for } \lambda_1 \neq \lambda_2 \end{cases}$$

where $\lambda_1 = \lambda_2$ if and only if $t_{max} = \frac{1}{\lambda_1}$, and where the quantities in these equations are defined to be:

$a(t)$ = μCi/g C in the glucose compartment at any time $t \geq 0$, ($a_o = a(0)$).
$b(t)$ = μCi/g C in the bicarbonate compartment at any time $t \geq 0$.
λ_1 = fraction of the glucose compartment which turns over each minute.
λ_2 = fraction of the bicarbonate compartment which turns over each minute.
t = time in minutes. $t = 0$ is the time of injection of C^{14} glucose.
t_{max} = time when the specific activity of the bicarbonate compartment (or breath) reaches its maximum value.

Table 3. Diabetic patients after pituitary irradiation

Study no. (different subjects)	Bs (FBS) mg%	$t_{\frac{1}{2}}$ min	Glucose-pool size P_G g	Glucose-pool size P_G^w g/kg	Glucose turnover λ_1 1/min	Glucose turnover T_G g/kg/hr	Glucose vol. V_G^w % B.W.	t_{max} min	$\left\langle \frac{d[CO_2]}{dt} \right\rangle$ mg/min	$E^{SA}_{CO_2}(t_{max})$ µCi/gC	$b(t_{max})$ µCi/gC	$\%^{CO^G_2}$ $\%CO_2$ via glucose	Oxidation of glucose to CO_2: G_{CO_2} mg/min	Oxidation of glucose to CO_2: $G^w_{CO_2}$ g/kg/hr	CO_2 turnover λ_2 1/min	CO_2 turnover T_{CO_2} g/kg/hr	CO_2 pool size P_{CO_2} g/kg
34	255	209	83.3	0.976	0.0033	0.194	38.3	190	320	0.046	0.160	28.9	63.1	0.044	0.0079	0.225	0.478
62 (40)*	127	195	34.4	0.528	0.0036	0.113	41.6	170	254	0.188	0.399	47.1	81.7	0.076	0.0091	0.236	0.432
63	132	90	44.4	0.519	0.0077	0.240	39.0	165	324	0.103	0.158	65.2	144.2	0.101	0.0047	0.227	0.805
69	127	240	59.9	0.771	0.0029	0.134	60.7	260	289	0.097	0.198	48.9	96.5	0.074	0.0051	0.221	0.729
71 (40)	80	75	19.5	0.304	0.0092	0.168	38.0	160	132	0.388	0.392	99.0	89.2	0.084	0.0030	0.124	0.689
78	78	151	33.8	0.332	0.0046	0.091	42.7	240	196	0.206	0.259	79.5	106.4	0.062	0.0042	0.114	0.456
Average	133	160	45.9	0.571	0.0052	0.157	43.4	198	252	0.171	0.278	61.4	96.9	0.073	0.0057	0.191	0.598
	Diabetic after pituitary irradiation on chlorpropamide									Diabetic after pituitary irradiation on chloropropamide							
63	120	129	23.1	0.270	0.0054	0.0087	22.3	170	295	0.143	0.438	32.7	66.0	0.046	0.0066	0.206	0.520

*Figures in parentheses indicate corresponding preirradiation studies (see Table 2a).

Table 4. Acromegalic patients without pituitary irradiation

Study no. (different subjects)	Bs (FBS) mg%	$t_{\frac{1}{2}}$ min	Glucose-pool size P_G g	Glucose-pool size P_G^W g/kg	Glucose turnover λ_1 1/min	Glucose turnover T_G g/kg/hr	Glucose vol. V_G^W % B.W.	t_{max} min	$\left\langle \frac{d[CO_2]}{dt} \right\rangle$ mg/min	$E^{SA}_{CO_2}(t_{max})$ µCi/gC	$b(t_{max})$ µCi/gC	$\%^{CO_2^G}$ %CO_2 via glucose	Oxidation of glucose to CO_2: G_{CO_2} mg/min	Oxidation of glucose to CO_2: $G^W_{CO_2}$ g/kg/hr	CO_2 turnover λ_2 1/min	CO_2 turnover T_{CO_2} g/kg/hr	CO_2 pool size P_{CO_2} g/kg
8	108	117	52.1	0.527	0.0059	0.187	48.8	180	321	0.065	0.162	39.4	87.0	0.0528	0.0055	0.196	0.602
35*	92	133	38.4	0.443	0.0052	0.138	48.2	155	292	0.104	0.290	35.9	71.5	0.049	0.0078	0.202	0.431
38	96	165	28.6	0.370	0.0042	0.093	38.2	165	224	0.134	0.437	30.6	46.9	0.0364	0.0084	0.174	0.346
45	76	98	26.2	0.311	0.0071	0.132	40.9	115	409	0.122	0.424	28.8	80.4	0.057	0.0105	0.290	0.460
47	87	110	28.4	0.388	0.0063	0.147	44.6	150	418	0.108	0.346	31.1	88.7	0.073	0.0072	0.344	0.796
49	95	134	25.0	0.260	0.0052	0.081	27.4	180	432	0.098	0.391	25.0	73.7	0.046	0.0059	0.270	0.763
52	91	101	24.5	0.359	0.0069	0.148	39.5	115	397	0.146	0.468	31.2	84.6	0.074	0.0108	0.347	0.536
55	95	118	18.4	0.324	0.0059	0.114	34.1	145	302	0.156	0.574	27.2	56.1	0.0593	0.0079	0.319	0.673
74	72	81	18.0	0.247	0.0086	0.127	34.3	140	199	0.249	0.042	16.9	23.0	0.0189	0.0058	0.163	0.467
75	99	118	34.7	0.402	0.0059	0.142	46.5	145	278	0.149	0.306	48.7	92.4	0.0642	0.0080	0.193	0.405
79	89.8	128	30.9	0.395	0.0054	0.128	44.0	170	238	0.257	0.309	83.2	135.2	0.1040	0.0059	0.183	0.519
Average	91	118	29.6	0.366	0.0060	0.131	40.6	151	319	0.144	0.341	36.2	76.3	0.0577	0.0076	0.244	0.545

*This study performed eight months after pituitary irradiation.

Table 5. Acromegalic patients after pituitary irradiation

Study no. (different subjects)	Bs (FBS) mg%	$t_{\frac{1}{2}}$ min	Glucose-pool size P_G g	Glucose-pool size P_G^W g/kg	Glucose turnover λ_1 1/min	Glucose turnover T_G g/kg/hr	Glucose vol. V_G^W % B.W.	t_{max} min	$\left\langle \frac{d[CO_2]}{dt} \right\rangle$ mg/min	$E^{SA}_{CO_2}(t_{max})$ µCi/gC	$b(t_{max})$ µCi/gC	$\%^{CO_2^G}$ %CO_2 via glucose	Oxidation of glucose to CO_2: G_{CO_2} mg/min	Oxidation of glucose to CO_2: $G^W_{CO_2}$ g/kg/hr	CO_2 turnover λ_2 1/min	CO_2 turnover T_{CO_2} g/kg/hr	CO_2 pool size P_{CO_2} g/kg
16 (8)*	142	185	35.1	0.363	0.0037	0.082	25.5	185	325	0.057	0.356	16.2	35.8	0.022	0.0073	0.202	0.464
45 (45)	77	104	24.0	0.261	0.0067	0.104	33.8	100	438	0.139	0.537	25.8	77.1	0.050	0.0143	0.278	0.324
65 (35)	79	84	28.1	0.359	0.0083	0.178	45.4	120	376	0.112	0.308	36.4	93.4	0.071	0.0083	0.287	0.574
68 (49)	87	108	30.5	0.305	0.0064	0.117	35.1	185	384	0.080	0.253	31.6	82.8	0.050	0.0046	0.232	0.841
Average	96	120	29.4	0.322	0.0063	0.120	35.0	148	381	0.097	0.364	27.5	72.3	0.048	0.0086	0.250	0.551

*Figures in parentheses indicate corresponding preirradiation studies (see Table 4).

a (t) is assumed to describe the actual situation in the glucose compartment. b (t) is the theoretical specific activity of the bicarbonate compartment, assuming all of the CO_2 in this compartment comes from glucose. But, not all of the CO_2 in this compartment is derived from glucose. Hence the ratio between the experimentally observed breath specific activity, $E^{SA}_{CO_2}$, and this theoretical bicarbonate compartment specific activity, b (t), namely

$$\frac{E^{SA}_{CO_2}(t)}{b\ (t)}$$

is taken to be the fraction of CO_2 derived from glucose. The reader is referred to reference (6) for further details regarding the calculation of these and other quantities presented in the results. The words "pool" and "compartment" will be used synonymously.

RESULTS

The time required for uniform mixing of the injected radioactive glucose was defined to be the time when the exponential decay curve for blood specific activity fell on the straight line (using semilogarithmic paper) drawn through the later points. This ranged from 15 to 60 min but was usually 30 min. Reichard et al. (10), had similar results. The glucose pool was considered to be in a steady state in all patients who had a constant blood glucose throughout the procedure. In all but seven instances, the variation in blood glucose was within 20 mg %. However, in these seven studies numbered 3, 16, 28, 32, 34 ("on insulin" study), 39 and 61, there was a change in blood glucose from 550 to 420, 180 to 70, 69 to 95, 340 to 240, 100 to 30, 200 to 110 and from 150 to 100 mg %, respectively, over the course of the procedure (3 to 6 hr).

In a few instances the blood-glucose specific activity curves, plotted on semilog paper, could be better fitted using two straight lines rather than one. The point of intersection in these cases was between 90 to 180 min. The angle between the two lines was never more than 10 deg. Further support of assumption (A-7) (6), namely, that $E^{SA}_{CO_2}$ and b reach their maximum values at the same time, was provided by data on patients who had steady blood-glucose levels. t_{max}, the time at which $E^{SA}_{CO_2}$ had its maximum value, and $t_m = \frac{1}{\lambda_2 - \lambda_1} \ln \frac{\lambda_2}{\lambda_1}$, the time at which b had its maximum value, differed, on the average, by only 2%. This suggests that steady-state conditions are reached between the bicarbonate compartment and the expired breath within the time interval $[0, t_{max}]$. The results of the remainder of the experimental findings and calculations are presented in Tables 1-5. In what follows, the ranges of variations of these parameters will be represented by intervals written as ordered pairs, [a, b], where a is the least member and b the greatest member of the interval. Numbers in double parentheses, (( )) refer to the studies being discussed. Tables 6 and 7 provide the clinical background as well as some of the laboratory results on the patients studied.

Table 6. Diabetic patients, clinical data

Study number: Pre-pituitary irradiation	Study number: Post-pituitary irradiation	Age yr	Wt kg	Sex	Type of diabetes	Duration of Diabetes yr	Diet: cal	Diet: g CHO	Daily medication	Result of C^{14} glucose study: Off hypoglycemic agents	Result of C^{14} glucose study: On hypoglycemic agents	Years after pituitary irradiation
3	--	57	55.0	♂	surgical pancreatectomy	1/6	--	--	insulin	abnormal	abnormal	0
15	--	48	68.6	♂	juvenile	21	1,600	155	insulin	abnormal	abnormal	0
32	--	25	61.8	♀	juvenile	13	1,200	--	insulin	abnormal	abnormal	0
39	--	35	65.9	♀	adult	13	1,300	90	tolbutamide	abnormal	abnormal	0
40	see 62, 71 below	61	65.0	♀	adult	9/12	1,200	100	none	abnormal		0
41	--	26	61.5	♀	juvenile	15	1,800	--	insulin	abnormal	abnormal	0
44	--	40	69.1	♂	juvenile	21	2,400	200	insulin	abnormal		0
61	--	47	61.3	♀	adult	14	1,400	140	none	abnormal		0
64	--	55	72.7	♂	adult	10/12	1,800	180	tolbutamide	abnormal		0
76	--	65	76.4	♂	adult	5 10/12	2,100	114	tolbutamide	abnormal		0
--	34	37	85.0	♂	juvenile	23	2,200	180	insulin	abnormal	abnormal	1/2
see 40 above	62	63	65.0	♀	adult	3 3/12	1,200	100	none	abnormal		2 1/2
--	63	50	85.0	♂	adult	11	1,600	130	chlorpropamide	abnormal	abnormal	1 1/2
--	69	56	77.7	♂	adult	24	2,000	150	none	abnormal		1
see 40 above	71	64	65.0	♀	adult	4	1,000	100	none	abnormal		3 1/4
--	78	63	101.8	♂	adult	5	1,200	92	none	abnormal		3 5/6

Table 7. Acromegalic patients

Study number					
Pre-pituitary irradiation	Post-pituitary irradiation	Oral-glucose tolerance test	Disease status	Yr after heavy-particle irradiation	C^{14} glucose study
8	see 16 below	abnormal	active	X ray Rx to pituitary 4 yr previously	abnormal
35	see 65 below	abnormal	active	4/6	abnormal
38		normal	questionable activity	0	abnormal
45	see 45 below	normal	active	0	normal
47		normal	active	0	normal
49	see 68 below	abnormal	active	0	abnormal
52		normal	questionable activity	1/12	normal
55		abnormal	active	0	normal
74		normal (flat)	active	3 months after surgical partial hypophysectomy	normal
75		abnormal	active	0	abnormal
79		abnormal	active	0	abnormal
see 8 above	16	abnormal	active	1/2	abnormal
see 45 above	45	abnormal	active	9/12	normal
see 35 above	65	abnormal (improved)	active	4 1/4	normal
See 49 above	68	abnormal	active	1 1/2	abnormal

(R-1) $t_{\frac{1}{2}}$: Half-life of C^{14}-glucose in the glucose pool.

The radiobiological half life, $t_{\frac{1}{2}}$, of the glucose pool in diabetic subjects was strikingly different from normal in almost all instances. The normal range [77, 117] minutes, was relatively narrow with a mean of 95'. In sharp contrast, the juvenile diabetic patients without insulin therapy had $t_{\frac{1}{2}}$ values in the range [200, 610]. All individuals having $t_{\frac{1}{2}}$ values below the normal range were again juvenile diabetics but they had at this time received insulin and eaten breakfast. Only one diabetic patient ((63)) had a $t_{\frac{1}{2}}$ in the normal range, but he had not only taken his usual dose of chlopropamide up to and including the morning of the test but also had received pituitary irradiation 18 months prior to the test. However, when off medication for three days his $t_{\frac{1}{2}}$ was elevated above normal. Another adult diabetic subject--studies ((40, 62)) and ((71)), see Fig. 1--had a slightly abnormal glucose tolerance test, a strikingly abnormal cortisone-modified glucose-tolerance test, and this subject was well controlled on diet alone. She had a nearly normal $t_{\frac{1}{2}}$ before pituitary irradiation, but, 2 1/2 years after irradiation her $t_{\frac{1}{2}}$ became definitely abnormal, rising from 129 min to 195 min. At the time of this second study she was recovering from an episode of thrombophlebitis. Nine months later her thrombophlebitis had cleared and her $t_{\frac{1}{2}}$ value had returned to normal. Two other adult diabetic patients and one juvenile diabetic patient, ((69, 78, 34)) respectively, had post-pituitary irradiation studies, all with prolonged $t_{\frac{1}{2}}$ values.

The acromegalic patients tended to have normal or slightly elevated $t_{\frac{1}{2}}$ values. One ((45)) stayed essentially unchanged nine months after pituitary irradiation, another ((8)) developed a prolongation of his $t_{\frac{1}{2}}$ six months after irradiation, and two ((35, 49)), who had elevated $t_{\frac{1}{2}}$'s experienced a drop to normal in 3 7/12 and 1 1/12 years, respectively.

(R-2) P_G: glucose-pool size in grams of glucose.

Eleven of our 13 normal subjects had P_G values in the range [14.5, 22.0] with the range for the whole group being [14.5, 28] and average 19.6 . When insulin was withheld, all juvenile diabetic patients, except one ((41)), had markedly elevated glucose-pool sizes, the highest being four times normal. These same patients on insulin had low to low-normal glucose-pool sizes. One adult diabetic patient before irradiation ((40)) and again 3 1/4 years after irradiation ((71)), and another adult diabetic patient 1 1/2 years after irradiation ((63)) had normal glucose-pool sizes. All other adult diabetic studies demonstrated elevated glucose-pool sizes.

Acromegalic individuals had P_G values that ranged from high-normal to definitely high values. Among the four acromegalic patients who had pre- and post-pituitary-irradiation studies, see studies ((8, 35, 45, 49)) of Table 4 and studies ((16, 65, 45, 68)) of Table 5, respectively, two experienced a drop in their glucose-pool size from high to normal, ((8, 16)) and ((35, 65)),

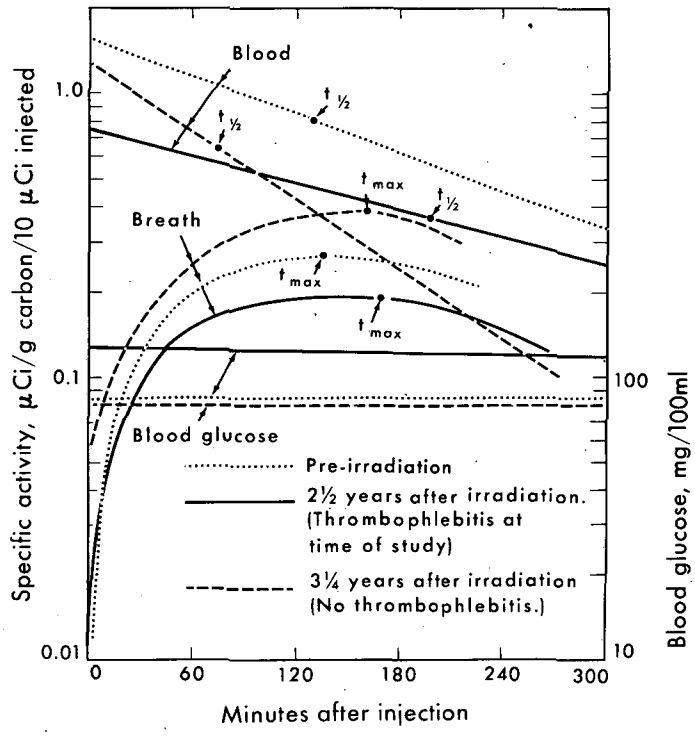

Figure 1. Graphs of data obtained in three successive studies on a patient with adult-type diabetes mellitus. These are studies numbered 40 (pre-irradiation), 62 (2 1/2 years post irradiation) and 71 (3 1/4 years post irradiation).

MUB-2939

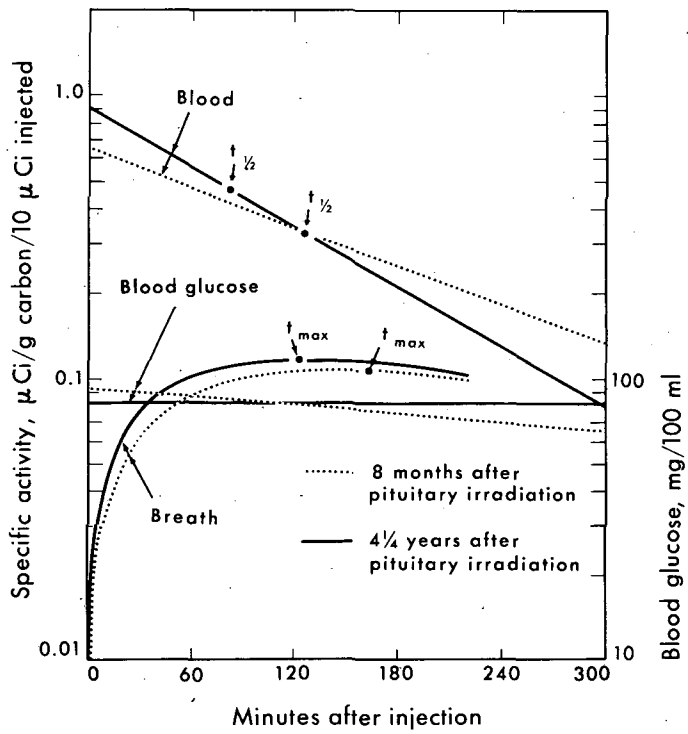

Figure 2. Graphs of data obtained in two successive studies on an acromegalic patient. The first study, number 35, was performed eight months after pituitary irradiation. The second study, number 65, was performed 4 1/4 years after therapy.

MUB-2938

another remained unchanged in the normal range ((45, 45)), whereas the fourth had a rise in P_G from a normal value to a high value ((49, 68)).

(R-3) P_G^W: glucose-pool size in g glucose/kg body weight.

This paralleled the glucose-pool size in grams rather closely. The normal range was [0.19, 0.37].

(R-4) λ_1: fraction of the glucose pool which turns over each minute.

The normal group had λ_1 values in the interval [0.0059, 0.0090]. Only one diabetic subject ((63)) (with or without diabetic medication, before or after pituitary irradiation) had a λ_1 value inside this range. Only juvenile diabetic patients who had received insulin the morning of the test were above 0.0090/min. The remainder were below 0.0059 .

Acromegalic subjects had λ_1 values in the low to low-normal range. The two, ((35,49)), who had studies performed more than one year following pituitary irradiation improved to normal.

(R-5) T_G: glucose turnover in g/kg/hr.

For normal subjects, the range was [0.071, 0.168]; but, 10 out of 13 were in the much narrower interval [0.071, 0.126] with an average of 0.118 for the whole group. T_G values for juvenile diabetic patients without insulin replacement were almost always in the normal range indicating that their low fractional turnover per minute and their high glucose-pool size resulted in a normal glucose turnover in terms of grams glucose leaving or entering the glucose pool per hour per kilogram of body weight. The one adult diabetic patient who had pre- and post-pituitary-irradiation studies ((40, 62, 71)) had low, mid-normal, and borderline high T_G values, in that order.

All acromegalic patients except two ((8, 35)) had normal glucose turnover rates. One of these had a high turnover rate before irradiation but a normal one six months later ((8)). The other had a normal T_G eight months after irradiation but a high turnover rate 3 7/12 years later, when he had evidence of mild hypopituitarism.

(R-6) V_G^W : Glucose pool's volume in percent of body weight.

V_G^W for normal individuals was in the range [21, 42]. This range also includes the V_G^W values for almost all other individuals studied. The acromegalic subjects, however, tended to have high normal V_G^W values whereas the diabetic patients tended toward low normal V_G^W values.

(R-7) t_{max}: the time in minutes required for the expired breath to reach maximum specific activity.

[95, 140] was the normal range. For diabetic patients, t_{max} tended to be

above normal. All post-pituitary-irradiation studies on diabetic subjects were associated with elevated t_{max} values.

Acromegalic patients tended to behave as the diabetic patients with regard to t_{max} but with less divergence from normal. Pituitary irradiation was followed by a shortening of t_{max} in the two acromegalic patients whose post-pituitary-irradiation studies were performed 4 1/4 and 1 1/12 years following pituitary irradiation ((35, 49)). The patients ((8, 45)), studied six and nine months following irradiation, experienced no change in t_{max}.

(R-8) λ_2 : fraction of the bicarbonate pool which enters and leaves that pool per minute.

Normal subjects had λ_2 values in [0.0030, 0.0135]. The only diabetic subjects outside this range were two nonirradiated juvenile diabetics ((3, 15)) and one adult diabetic ((64)), all of whom had elevated λ_2 values. The one diabetic patient ((40)) who had studies performed before and after pituitary irradiation had essentially no change in λ_2.

All acromegaly patients had λ_2 values in the normal range both before and after pituitary irradiation. However, two acromegalic subjects ((8, 45)) had an increase in λ_2 following pituitary irradiation, whereas, of the other two, one ((35)) remained unchanged, and one ((49)) had a decrease in λ_2.

(R-9) $\left\langle \frac{d[CO_2]}{dt} \right\rangle$: mean mg CO_2 entering and leaving the bicarbonate pool each minute.

Normal values, with one exception, were in [265, 391]. Six out of ten diabetic subjects had values below 265. However, 8 out of 10 diabetic patients had studies resulting in $\left\langle \frac{d[CO_2]}{dt} \right\rangle \leq 300$ (Table 2a) whereas this was true for only 2 out of 13 normal subjects (Table 1). Pituitary irradiation did not significantly alter $\left\langle \frac{d[CO_2]}{dt} \right\rangle$ in the acromegalic group. The lowered value in study 71 on an adult diabetic patient is probably not valid.

(R-10) $E^{SA}_{CO_2}(t_{max})$: the experimental specific activity of expired CO_2 at t_{max}.

Eight out of 13 studies on normal subjects resulted in values in the interval [0.150, 0.190]. If these values are taken as normal, then 10 out of 17 studies on nonirradiated diabetic patients produced values below normal and all but three acromegalic patients ((55, 74, 79)), either before or after pituitary irradiation, had values below normal. However, in order to include all normal subjects the range must be taken to be [0.060, 0.250] and this range includes nearly all the $E^{SA}_{CO_2}(t_{max})$ values. Still, one untreated juvenile diabetic patient off of insulin ((44)) had a value below 0.060.

(R-11) $b(t_{max})$: the theoretical specific activity at t_{max}, of the

bicarbonate pool. $b(t_{max})$ had a wide spread for normal individuals, its range being [0.096, 0.720]. This range included all but one patient, an adult diabetic ((40)) who after pituitary irradiation reverted to a normal value. However, Table 1 shows that 12 of the 13 normal studies produced $b(t_{max}) \geq 390$ whereas from Table 2a it can be seen that four out of five untreated juvenile diabetic patients off of insulin had $b(t_{max}) < 0.390$. The one irradiated juvenile diabetic patient ((34)) had $b(t_{max}) < 0.390$ for both his studies, both while on and off insulin.

The acromegalic patients were split almost equally by $b(t_{max}) = 0.390$. Five studies resulted in values above 0.390 and six studies resulted in values below this figure. Pituitary irradiation had mixed effects on $b(t_{max})$ relative to this value. Among the four acromegalic patients who had both pre- and post-pituitary-irradiation studies, two of the three ((8, 35)) with $b(t_{max}) < 0.390$ remained unchanged while the other ((49)) dropped 0.138 units. The one ((45)) with $b(t_{max}) \geq 0.390$ had a rise in $b(t_{max})$ by 0.113 units.

(R-12) ${}_{\%}CO_2^G$: $\%CO_2$ derived from glucose.

If [20, 43] is taken as the normal range, then almost all studies resulted in normal ${}_{\%}CO_2^G$ values. The ones digressing most significantly from this range were of untreated juvenile diabetic patients off of insulin. These had low values. Pituitary irradiation had no significant effect on the value of ${}_{\%}CO_2^G$ for the one adult diabetic patient ((40)) or for three of the acromegalic patients with sequential studies. The remaining acromegalic patient in this group had a drop in ${}_{\%}CO_2^G$ to below normal.

(R-13) G_{CO_2}: The mg of glucose oxidized to CO_2 per minute.

Normal values, with one exception, were found to lie in the interval [50, 97] with a mean of 73.1 . This range includes most other G_{CO_2} values. However, four out of five nonirradiated juvenile diabetic patients had values below 50 when off insulin, but when on insulin their G_{CO_2} values were higher and ranged from low normal to above normal. The one juvenile diabetic subject ((34)) who had a post-pituitary-irradiation study showed G_{CO_2} values in the normal range both when on and off insulin. One adult diabetic subject ((40)) developed a low G_{CO_2} 2 1/2 years after pituitary irradiation, at which time she was convalescing from an episode of thrombophlebitis ((62)). Nine out of 13 normal individuals had $G_{CO_2} \geq 70$ whereas all 10 nonirradiated diabetic subjects had $G_{CO_2} < 70$.

Almost all acromegalic patients had normal G_{CO_2} values before irradiation. In fact, eight out of 11 preirradiation studies resulted in $G_{CO_2} \geq 70$. An acromegalic patient with frank diabetes before irradiation ((8)) had a normal preirradiation G_{CO_2}, but, six months after irradiation, his G_{CO_2} had fallen to below normal values. Another acromegalic patient ((35)) who had diabetes

(requiring 80 units of insulin) before irradiation but who, at the time of his first C^{14} glucose study, eight months after irradiation, was controlled on diet alone, had normal G_{CO_2} values for both his post-pituitary-irradiation studies eight months and 4 1/4 years later.

(R-14) $G^{w}_{CO_2}$: Oxidation of glucose to CO_2 in g/kg/hr.
The results here were much like those for G_{CO_2}, the normal range being [0.038, 0.085] with average 0.056.

(R-15) T_{CO_2}: CO_2 turnover in g/kg/hr.
The interval, which includes T_{CO_2} values for all normal subjects, is [0.204, 0.333]. However, nine out of 13 studies on normal subjects resulted in T_{CO_2} values lying approximately in the interval [0.250, 0.300]. Only three out of 10 studies on diabetic subjects had T_{CO_2} values in this interval (Table 2a). The highest values of T_{CO_2} were obtained from diabetic patients on insulin (Table 2b). Pituitary irradiation resulted in a decrease in T_{CO_2} in the adult diabetic patient with sequential studies ((40, 62, 71)).

The acromegalic patients had T_{CO_2} values in the range [163, 347]. Pituitary irradiation resulted in no significant change in three cases ((8, 45, 49)) and a rise from below normal to normal values in one case ((35)).

(R-16) P_{CO_2}: The CO_2 pool in gCO_2/kg of body weight.
The normal range for P_{CO_2} was taken to be [0.329, 0.581]. Two untreated juvenile diabetic patients ((3, 15)) off insulin had $P_{CO_2} < 0.329$ as did one adult diabetic ((64)). Pituitary irradiation resulted in a rise in this parameter in the one adult diabetic subject studied before ((40)) and after ((62, 71)). Two other adult diabetics ((63, 69)), who were studied only after pituitary irradiation, also had high P_{CO_2} values.

Four acromegalic patients ((8, 47, 49, 55)) had high P_{CO_2} values before irradiation. Two of these ((8, 49)) had postirradiation studies ((16, 68)) and of these one ((49, 68)) had no significant change in P_{CO_2} while the other had a return to normal values ((8, 16)).

The one patient with Cushing's syndrome secondary to adrenal carcinoma had a normal glucose-C^{14} study, although two oral-glucose-tolerance tests were slightly abnormal. This patient had moderately elevated urinary 17-hydroxycorticosteroids and very high urinary 17-ketosteroids.

DISCUSSION

The parameters presented in the results can be divided into two classes. The first class consists of those parameters whose values for the diabetic subjects differ from normal. The second class consists of those parameters that

show no significant difference in any of the groups of subjects studied. The most distinctive members of the first class are $t_{\frac{1}{2}}$, P_G, P_G^W, λ_1 and t_{max}. But in addition, since $E_{CO_2}^{SA}$ (t_{max}), $b(t_{max})$, G_{CO_2} and $\left\langle \frac{d[CO_2]}{dt} \right\rangle$ are of help in diagnosing abnormalities in glucose kinetics, they belong to this class. However, T_G, V_G^W, λ_2, $\%CO_2^G$, T_{CO_2} and P_G are of no assistance in this regard and therefore do not belong to this class. Nonetheless, the fact that these latter quantities are normal, except in the severest diabetics after fasting, is of some significance and will be discussed.

By using the first class of parameters, it is possible to distinguish individuals with adult or juvenile diabetes mellitus from normal individuals because when not receiving therapy the diabetic patients have a prolonged $t_{\frac{1}{2}}$, an increased P_G and P_G^W, a diminished fractional turnover rate for the glucose pool, λ_1, and a delayed t_{max}. They also frequently have a low $E_{CO_2}^{SA}$ (t_{max}), a low $b(t_{max})$, a low G_{CO_2} and a low $\left\langle \frac{d[CO_2]}{dt} \right\rangle$. All diabetic patients studied had an abnormal outcome to this test, abnormality being defined as having two or more of these parameters outside their normal range.

The lowered λ_1 values in these diabetic patients were accompanied by elevated P_G^W values so that the glucose turnover rates, T_G $(T_G = \lambda_1 \cdot P_G^W \cdot 60)$, were almost always in the normal range, see (R-5). However, there was a general increase in T_G with increasing values of B_s or P_G^W over a limited range (see Figs. 3 and 4). This phenomenon is discussed by Soskin and Levine (11) who describe a linear relationship between fasting blood-sugar concentration, B_s, in the range [100, 500] mg %, and dextrose utilization, T_G, in eviscerated dogs. For $B_s \geq 500$ mg % they display a nearly constant value for T_G. Although the present data are consistent with a linear relationship between T_G and B_s for a range B_s in [70, 370], they do not support the constancy of T_G for larger values of B_s. In fact, there was a sharp decrease in T_G for values of $B_s \geq 370$ (Fig. 3). A plot of T_G vs P_G^W was even more revealing (Fig. 4). Again there was a general increase in T_G with P_G^W for diabetic subjects, but this increase appeared to be non-linear. Normal subjects also had a general increase in T_G with P_G^W, the exact relationship being obscure. Furthermore, for the diabetic subjects, T_G reached a maximum for P_G^W in the interval [1.000, 1.200] and thereafter declined. These findings suggest that, directly or indirectly, glucose at high levels inhibits pathways involved in its production or utilization.

Reichard et al. (10) found T_G values to be decreased in "mild diabetes mellitus" whereas Shreeve et al. (12) reported slightly elevated T_G values for such patients. The results (R-5) (table 2a) in the present report lend support to those of Reichard and co-workers because T_G for adult-type diabetic subjects prior to pituitary irradiation were in general in the low-normal range. The one subject in this group who had post-pituitary-irradiation studies performed had an elevation of this parameter to a borderline high level. The cause for

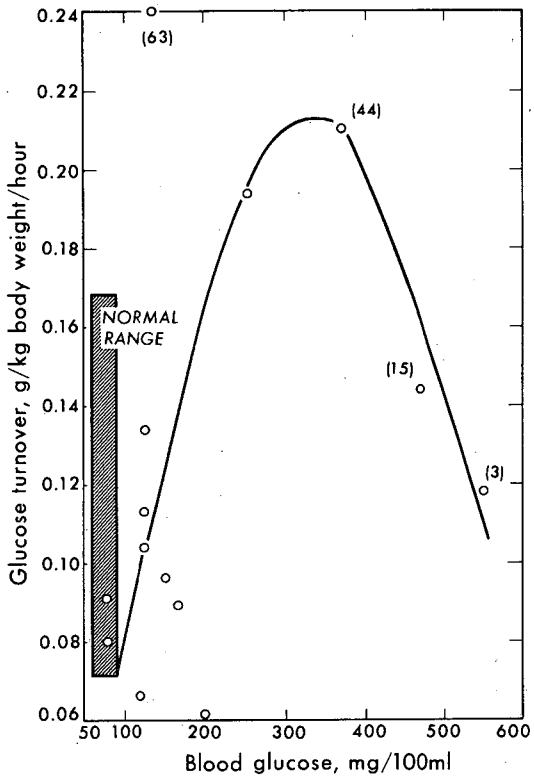

Figure 3 A graph of T_G, the glucose turnover rate, versus Bs, the blood glucose concentration.

MUB-2940

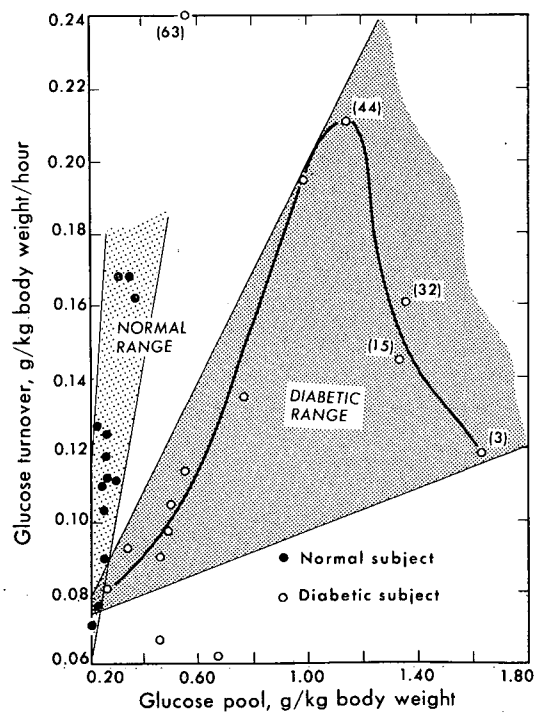

Figure 4. A graph of T_G, glucose turnover rate, versus P_G^W, the glucose pool size.

MUB-2941

this rise in T_G is unknown. One may conjecture, on the basis of known growth hormone effects, that it was due to an increase in insulin sensitivity resulting from diminution in growth hormone (13).

The general decrease in oxidation of glucose to CO_2 in the diabetic subjects, in spite of approximately normal values of T_G, indicates that although glucose utilization is near normal, less of it is being converted to CO_2 by the "immediate oxidative pathway". This means that in diabetic individuals a larger portion of the glucose utilized is going by way of pathways other than the "immediate oxidative pathway", which probably consists of the hexose monophosphate pathway and the Embden-Meyerhof-Tricarboxylic acid pathway. One would thus expect a greater rate of appearance of C^{14} in fats and amino acids (14,15).

The tendency toward a decreased expiratory specific activity, $E^{SA}_{CO_2}(t_{max})$, in the diabetic patients is consistent with the delay in reaching t_{max}. If G_{CO_2}, the oxidation of glucose to CO_2, is normal or less than normal, then the total amount of $C^{14}O_2$ expired in time t_{max} is normal or less than normal; hence, the area under the expiratory $C^{14}O_2$ curve must be normal or less than normal. Under these conditions a delay in t_{max} implies a lower $E^{SA}_{CO_2}(t_{max})$. The data in Table 2a or, in condensed form, Table 9 support this statement.

Generally, diabetic subjects without therapy had lower $\left\langle \frac{d\,[CO_2]}{dt} \right\rangle$ values than normal. Surprisingly, a depancreatized patient ((3)) and a brittle juvenile diabetic patient ((15)) had normal $\left\langle \frac{d\,[CO_2]}{dt} \right\rangle$ values. This will be discussed. The cause for the lower CO_2 expiration rate in the remainder of the diabetics is unknown. It may, however, be hypothesized that it is due to an increase in CO_2 assimilation in diabetic subjects (e.g. CO_2 assimilation in fatty acid synthesis via acetyl coenzyme A).

Distinguishing acromegalic individuals from normal subjects on the basis of this glucose kinetic study was considerably more difficult than in the case of patients with diabetes mellitus. Although the changes in the two disorders were similar, they were less marked in the acromegalic subjects unless overt diabetes was present. Table 7 shows that prior to pituitary irradiation all but two ((38, 55)) abnormal C^{14}-glucose studies were associated with abnormal oral-glucose-tolerance tests (using the criteria of Fajans and Conn ((16)). In study ((38)) the glucose C^{14} test was abnormal whereas the glucose-tolerance test was normal. This patient had questionable activity of her disease, as measured by clinical and biochemical methods (including a normal plasma level of growth hormone as assayed by C. H. Li). Study ((55)), on the other hand, resulted in an abnormal glucose-tolerance test and a normal C^{14}-glucose-kinetic study. Ikkos _et al_. (17) found no correlation between decreased intravenous glucose tolerance and activity of acromegaly. As seen from Table 7 the C^{14}-glucose studies as well as the oral-glucose-tolerance tests performed in the present study also did

not correlate satisfactorily with activity of the disease. This method of evaluating glucose metabolism appears to have diagnostic merit. It must, however, be emphasized that until a more precise method of measuring these parameters becomes available, each laboratory will have to determine its own set of standards for normal subjects. The values reported for these parameters by various investigators are listed in Table 8. Although this method is simple to perform, it gives valid results only if the system remains in a steady state. In the 52 studies reported here the blood-glucose levels during the test remained fairly constant except in seven cases. Furthermore, no perturbance such as insulin injection or appreciable glucose injection was made during the studies. The post-pituitary-irradiation studies were performed on individuals who may have had a new "steady-state" due to modified homeostatic control, but no changes were induced during the test itself.

The parameters, which are of little if any help in distinguishing normal, diabetic, and acromegalic individuals, are T_G, V_G^W, λ_2, $_{\%}CO_2^G$, T_{CO_2} and P_{CO_2}. T_G was discussed earlier. V_G^W, the glucose space per kg body weight, has been thought to correspond well with the extra-cellular fluid volume (1,11). Hence, it is not surprising that all individuals had comparable values for this parameter. The remainder of these parameters refer to the bicarbonate compartment.

Since most patients were in a good nutritional state prior to the initiation of the test, the CO_2 compartments in most cases were normal. However, the overnight fast as well as abstinence from their daily dose of insulin were sufficient to modify the bicarbonate compartments of two of the juvenile diabetic patients, ((3 and 15)). They experienced a lowering of their bicarbonate-pool size probably because of metabolic acidosis resulting from poor diabetic control. In spite of this lowered bicarbonate pool they were able to maintain a normal output of CO_2, i.e., $\left\langle \frac{d[CO_2]}{dt} \right\rangle$, by elevating their fractional turnover rates λ_2. These two patients also had markedly diminished $_{\%}CO_2^G$ values indicating, again, that much of their CO_2 was coming from non-glucose sources.

The effect of pituitary suppression on the diabetic state in acromegaly, as measured by this method, can best be exemplified by studies ((35, 65)). Figure 2 illustrates reactions in this acromegalic patient who received a relatively large dose of α-particle radiation to the pituitary gland and who waited the longest period, 4 1/4 years, between his irradiation and his kinetic study. Prior to irradiation, this patient had frank diabetes and eight months after therapy he still had an abnormal kinetic study ((35)). However, approximately four years after therapy his kinetic study was normal ((65)).

Pituitary irradiation, however, did not produce such a clear effect on the adult diabetic patient studied before ((40)) and three years after ((71)) a comparable dose of radiation (see Fig. 1). Both tests ((40)) and ((71)) were

Table 8.

Investigators	$t_{\frac{1}{2}}$ min	Glucose turnover λ_1 fraction/min	Glucose turnover T_G g/kg/hr	P_G g	P_G^w g/kg	V_G liters	V_G^w % B.W.	t_{max} min	Bicarbonate turnover λ_2 fraction/min	Bicarbonate turnover T_{CO_2} g/kg/hr	P_{CO_2} g/kg	$\left\langle \frac{d[CO_2]}{dt} \right\rangle$ mg/min	$E_{CO_2}^{SA}(t_{max})$ µCi/gC	$b(t_{max})$ µCi/gC	$G_{CO_2}^w$ g/kg/hr	$\%CO_2^G(t_m)$
NORMAL SUBJECTS																
Baker et al. (3)		0.0069	0.062		0.15		17		0.0086	0.27	0.54				0.038	20
Shreeve et al. (12)		0.0069	0.085		0.21		24		0.0084	0.27	0.53				0.055	
Hlad et al. (18)							23.3									
Hlad et al. (19)							22.6									
Elrick et al. (20)							21.3									25
Reichard et al. (10)		0.0064	0.120		0.31		30	120								
Segal et al. (21)*																
U-C^{14}								100								
1-C^{14}								127								
2-C^{14}								107								
6-C^{14}								145								
Pollycove (22)		0.0080	0.130		0.28		33		0.0090	0.27	0.51				0.52	28
Present study	95	0.0075	0.118	19.6	0.262		31.8	116	0.0089	0.26	0.47	330	0.169	0.535	0.056	31.8
DIABETES MELLITUS																
Hlad et al. (19)							19.0									
Reichard et al. (10)		0.0058	0.109		0.51		29									22
Shreeve et al. (12)																
Stable D.M.†		0.0019	0.10		0.87		26		0.0094	0.36	0.72				0.059	
Labile D.M.		0.0030	0.19		1.08		30		0.0107	0.24	0.40				0.031	
Present study	303	0.0028	0.113	52.6	0.817		30.9	175	0.0129	0.26	0.41	255	.154	.582	0.042	27.1
ACROMEGALY																
Present study	118	0.0060	0.131	29.6	0.366		40.6	151	0.0076	0.24	0.55	319	0.144	0.341	0.058	36.2
HYPOPHYSECTOMIZED SUBJECTS																
Ikkos et al. (13)		0.0107		16.3		17.6										

*Figures taken from graphs presented in article.

†D.M. = diabetes mellitus.

Table 9.

Studies having prolonged t_{max} and normal or low G_{CO_2}											
Study	34		32		41		39		44		61
Insulin	off	on	off	on	off	on	off	on	off	on	----
$E^{SA}_{CO_2}(t_{max})$	↓	n	↓	↓-n	n	n	n	n	↓	↓	n

Studies having normal t_{max} and normal or low G_{CO_2}					
Study	3	15		64	40
Insulin	off	off	on	----	----
$E^{SA}_{CO_2}(t_{max})$	↑-n	n	n	n	↑

nearly normal, but since each had two abnormal "diagnostic parameters", both were classified as abnormal. Nonetheless, there was a major distinction between the two tests. The first study revealed low T_G and λ_1 values, whereas these parameters were elevated in the second study. This effect on T_G and λ_1 parallels the effect of pituitary irradiation on the acromegalic patient discussed in the previous paragraph.

SUMMARY

The results obtained by using the single injection tracer method of Baker et al., as modified by Tolbert et al., for the study of glucose kinetics in humans are presented for normal subjects, diabetic patients and acromegalic patients. The latter two categories contain individuals who had studies performed before and/or after heavy-particle irradiation to the pituitary gland. The results indicate similar deviations from normal for both the diabetic and the acromegalic patients. These deviations are more marked in diabetes mellitus than in uncomplicated acromegaly and consist of prolongation of the radiobiological half-life of glucose C^{14}, diminution of the fractional turnover rate of glucose, enlargement of the glucose-pool size and lowering of the oxidation rate of glucose to CO_2. The deviations in acromegaly can be reversed by heavy-particle pituitary irradiation. However, the effect of pituitary irradiation on the C^{14}-glucose kinetic pattern of adult diabetic subjects seems to be an elevation in glucose turnover without other significant changes. Further studies are required on irradiated diabetic and acromegalic subjects before more definite statements can be made. The rise in glucose turnover that accompanies the rise in blood glucose appears to be limited, a decline in turnover being observed for blood-glucose values above 370 mg/100 ml. Further support for the model of Baker et al. was obtained through the agreement of the theoretically predicted t_{max} and the actually observed t_{max} for the CO_2 specific activity curves.

REFERENCES

1. Steele, R.; Wall, J. S.; deBodo, R. C., and Altszuler, N.; Am. J. Physiol. 187:15, 1956.
2. Wrenshall, G. A., and Hetenyi, G., Jr.; Metabolism 8:531, 1959.
3. Baker, N.; Shreeve, W.; Shipley, R.; Incefy, G., and Miller, M.; J. Biol. Chem. 211:575, 1954.
4. Tolbert, B. M.; Kirk, M., and Baker, E. M.; Am. J. Physiol. 185:269, 1956.
5. Tolbert, B. M.; Kirk, M., and Upham, F.; Lawrence Radiation Laboratory Report, UCRL-3920, 1957.
6. Manougian, E.; this report, p. 34.
7. Tobias, C. A.; Lawrence, J. H.; Born, J. L.; McCombs, R. K.; Roberts, J. E.; Anger, H. O.; Low-Beer, B. V. A., and Huggins, C. B.; Cancer Res. 18:121-134, 1958.

8. Lawrence, J. H.; Tobias, C. A.; Linfoot, J. A.; Born, J. L.; Gottschalk, A., and Kling, R. P.; Diabetes 12:490-501, 1963.
9. Lawrence, J. H.; Tobias, C. A.; Born, J. L.; Sangalli, F.; Carlson, R. A., and Linfoot, J. H.; Acta Radiol. 58:337, 1962.
10. Reichard, G. A., Jr.; Jacobs, A. G.; Kimbel, P.; Hochella, N. J., and Weinhouse, S.; J. Appl. Physiol. 16:789, 1961.
11. Soskin, S., and Levine, R.; in Carbohydrate Metabolism; University of Chicago Press, 1952, pp. 163, 165.
12. Shreeve, W.; Baker, N.; Miller, M.; Shipley, R.; Incefy, G. E., and Craig, J. W.; Metabolism 5:22, 1956.
13. Ikkos, D., and Luft, R.; Endocrinol. 39:567-583, 1962.
14. Fine, M.; Michaels, G.; Shah, S.; Chai, B.; Fukayama, G., and Kinsell, L.; Metabolism 11:893, 1962.
15. Geiger, A.; Horvath, N., and Kawakita, Y.; J. Neurochem. 5:311-322, 1960.
16. Fajans, S. S., and Conn, J. W.; Am. J. Med. 31:839, 1961.
17. Ikkos, D.; Luft, R.; Gemzell, C., and Almquist, S.; Acta Endocrinol. 39:547-566, 1962.
18. Hlad, C. J., Jr.; Elrick, H., and Witten, T. A.; J. Clin. Invest. 35:1139, 1956.
19. Hlad, C. J., Jr., and Elrick, H.; J. Clin. Endocrinol. and Metab. 20:1120, 1960.
20. Elrick, H.; Hlad, C. J., Jr., and Arai, Y.; J. Clin. Endocrinol. and Metab. 21:387, 1961.
21. Segal, S.; Berman, M., and Blair, A.; J. Clin. Invest. 40:1263, 1961.
22. Pollycove, M.; Semiannual Report, Donner Laboratory, Lawrence Radiation Laboratory, UCRL-9897:188, 1961.

Received September, 1964.

Growth-Hormone Secretion in Treated and Untreated Acromegaly

John A. Linfoot and Fred C. Greenwood

The development of sensitive radio-immunological techniques for the assay of human growth hormone (1,2) has been extremely valuable in elucidating the important role of growth hormone in a number of physiological processes (3). The hypersecretion of growth hormone in pituitary gigantism and acromegaly has been recognized for many years (4), and in some cases it has been possible to measure blood elevations by less sensitive and less specific forms of assay (5,6). Unfortunately, the less sensitive assays which we had previously used have not been suitable for determining the effectiveness of a given form of therapy in acromegaly (7,8) and have not provided information about the role of the level of growth hormone in many of the metabolic abnormalities found in the disease. Thus, the evaluation of the effectiveness of a given form of therapy has been largely based on a number of clinical and laboratory findings that have not been completely reliable in many cases. The correlation of these findings with growth-hormone levels, however, has helped to define the more precise clinical criteria to be used for evaluating therapy (9,10).

The use of heavy-particle pituitary irradiation was first employed in the treatment of acromegaly in 1958. Several publications have reported the effectiveness of this therapy in producing cessation of acral growth, soft tissue and bony regression, as well as improvement in diabetic glucose tolerance and other biochemical changes associated with acromegaly (7,8,11). The present study indicates that the levels of circulating growth hormone, measured by a radioimmunological method, fall to normal following this treatment.

MATERIALS AND METHODS

Plasma specimens were obtained from 33 acromegalic patients. Fourteen patients were studied prior to receiving heavy-particle pituitary irradiation, and 19 patients were studied six months to five years after treatment. In addition, assays were performed on patients with a variety of other diseases (panhypopituitarism, mammary carcinoma) and on several normal subjects. These groups served as a control group and their values corresponded to those previously reported by one of the authors (12,13). All of the patients were hospitalized in the Donner Pavilion, and fasting blood specimens were drawn at the patient's bedside prior to breakfast. The blood was placed in heparinized tubes

and the plasma promptly separated, frozen, stored at minus 20°C and transported by air in a thermos containing cardice to the Division of Chemistry and Biochemistry, Imperial Cancer Research Fund in London. All specimens were kept frozen until the time of assay. The radio-immunoelectrophoretic assays for growth hormone were performed using the method of Hunter and Greenwood (12), without prior information on diagnoses.

The changes in plasma growth-hormone concentrations during insulin- (0.1 unit/kg) and oral-glucose (100 g) tolerance tests in one patient, M.H., and during an intravenous glucose tolerance (0.5 g/kg given in a single injection of 50% glucose) performed on patient M.S., are also described.

RESULTS

Figure 1 compares the plasma-growth-hormone (HGH) concentrations in a group of 14 patients with varying degrees of active acromegaly who were being considered for pituitary irradiation. The mean value was 40.8 mμg/ml with the range from 9 to 99. While four patients, indicated by the open circles in Fig. 1, were not considered to have highly active disease by our clinical criteria, in general there was little correlation between the level of circulating growth hormone and the other features of acromegaly in the remainder of the group. These hormone levels appear to be higher than the levels reported for normal subjects (2,3,12,13). However, the data on normal subjects were not obtained under the standardized conditions noted above, i.e., at the bedside after an overnight fast. Exercise has been shown to stimulate growth-hormone secretion, and the mild exercise of travelling to an outpatient department may explain the high values (50 mμg/ml) found in two such normal subjects after an overnight fast (3,12). Subsequent experience suggests that levels in samples from normal adults taken at the bedside after an overnight fast do not exceed 1 to 2 mμg/ml. The values reported here for acromegalic subjects may then be interpreted as abnormal. Nevertheless we would consider that a single sample from a patient, rested after an overnight fast, is insufficient to help confirm a diagnosis of acromegaly.

The mean HGH level in 19 patients studied six months to five years after pituitary irradiation was 11.6 mμg/ml with a range from $<$ 1.0 to 39 mμg/ml. Furthermore, if one removes the values of the three patients indicated by the open triangles and by an open circle, the mean value of the group is 6.8 mμg/ml. It should be noted that the two patients designated by open triangles received less than 4,000 rads over 11 days (now considered less than optimal treatment), and the other patient's value was obtained only six months after treatment (HGH having fallen by 35%). Thus only one of the 16 patients who had received optimal therapy, had an elevated HGH level two years after treatment. Again, it is not possible to state unequivocally whether all of the remaining values fall within the range for normal adults.

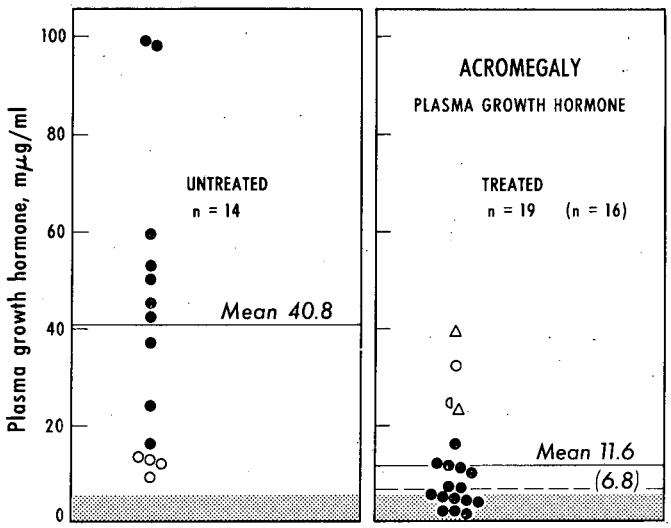

Figure 1. Plasma growth-hormone concentrations in acromegalic patients. The group on the left had received no treatment; those on the right had received heavy-particle pituitary irradiation. (Open circle on the right: six months after treatment. Triangles: treated with less than 4,000 rads. Open half-circle: only patient in group that had optimal treatment and persistently elevated growth hormone.)
MUB-3629

Figure 2. The effect of insulin hypoglycemia on plasma growth hormone in a 23-year-old male with acromegaly. Note that breakfast failed to suppress growth-hormone secretion, despite the partial suppression by oral glucose, see Fig. 3.
MUB-3634

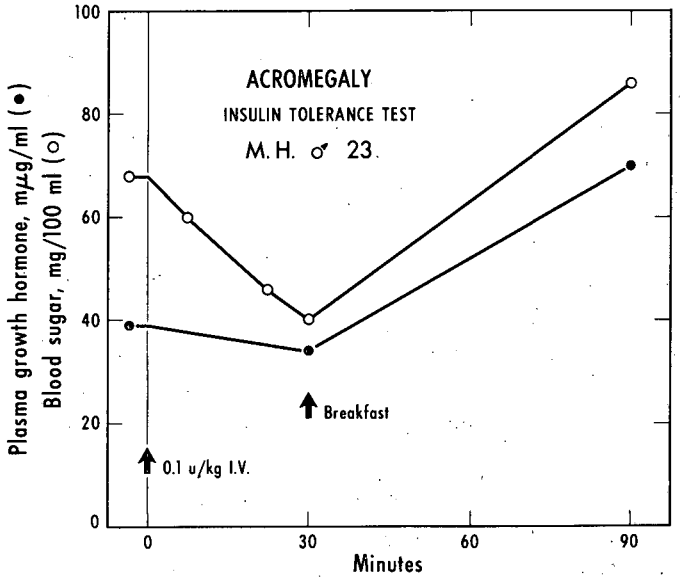

The behavior of the plasma growth hormone during insulin- and oral glucose-tolerance tests is shown in Figs. 2 and 3. Following the administration of insulin, the blood sugar fell from a fasting level of 68 to 40 mg per 100 ml in 30 min. The patient had mild hypoglycemic symptoms and was permitted to eat breakfast. Initially, the HGH fell from 39 to 34, but the hypoglycemic stimulus produced a marked secretion of HGH that was still detectable 90 min after the test was started. The same patient had a normal glucose-tolerance test (see Fig. 3), and during the test the HGH level fell progressively from a fasting level of 45 to 12 mμg/ml 180 min after the ingestion of 100 g of glucose.

In contrast, another patient, M.S., represented by an open circle in the preirradiation group in Fig. 1, showed a different response when an intravenous glucose-tolerance test was performed. This patient differed from the previous case in several respects. The patient was a postmenopausal female who had long-standing, slowly progressive acromegaly. The fasting HGH level was 13.0 and it was not altered appreciably by the intravenous glucose load.

DISCUSSION

As previously noted, since heavy-particle pituitary irradiation was first employed in the treatment of acromegaly in 1958, it has been found superior, compared to X-ray or gamma-ray therapy, for producing cessation of acral growth, soft tissue and bony regression, as well as symptomatic improvement and other biochemical changes (14).

This present study shows that there is a marked difference in the level of circulating growth hormone in patients with acromegaly who have received heavy-particle pituitary irradiation. While this study does not compare the pre- and postirradiation values in the same patients, the nearly sevenfold difference in mean level for these groups is striking and illustrates the effectiveness of heavy-particle therapy in treating acromegaly.

No attempt was made to establish the relationship of the level of circulating HGH and other clinical features of acromegaly; however, it was of interest to observe that a female patient (Fig. 4) with long-standing, slowly progressive disease and HGH levels only slightly more than twice normal, did not show suppression of growth hormone during an intravenous glucose-tolerance test. This lack of suppression is quite different from that observed in normal persons, in whom there is a prompt fall in pituitary growth-hormone release with glucose (3,12), and has also been reported by Roth _et al_. (9) in acromegaly. On the other hand, a young male patient, whose HGH level was increased eightfold and who clinically had highly active acromegaly of relatively recent onset, showed a fall from 45 to 12 mμg/ml during an oral glucose-tolerance test. This does not represent complete suppression but is a striking contrast to the other patient. It is possible that the degree of suppression of endogenous growth

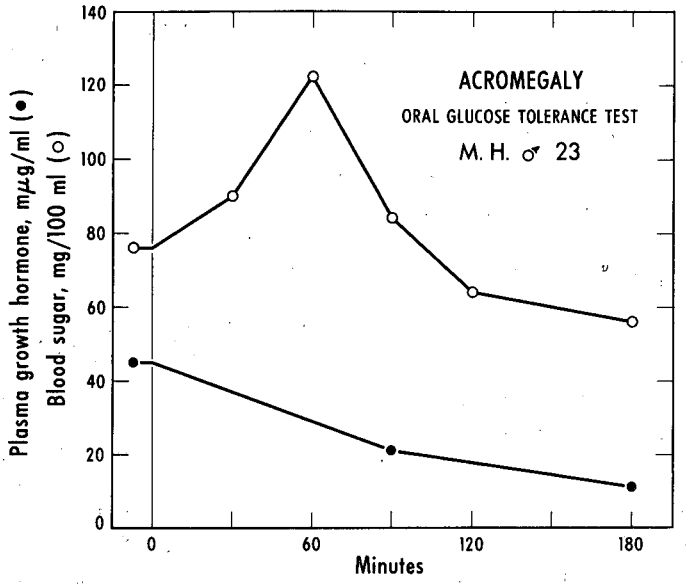

Figure 3. Partial suppression of plasma growth hormone during an oral glucose-tolerance test in a 23-year-old male with acromegaly.

MUB-3635

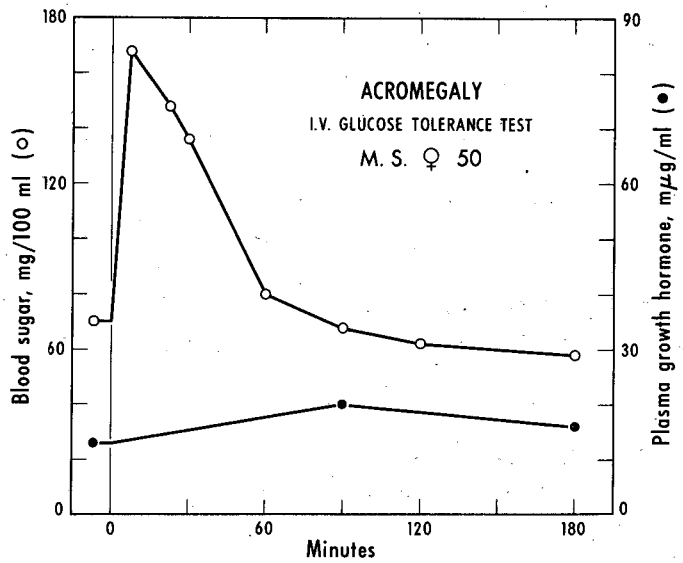

Figure 4. Failure of intravenous glucose to suppress plasma-growth-hormone concentrations in a 50-year-old female with long-standing acromegaly.

MUB-3633

hormone from a meal or from oral glucose might be more important in reflecting the clinical activity of acromegalic subjects than the absolute level in a sample from a fasted, rested subject. Insulin hypoglycemia was associated with a twofold increase in HGH, although the total increase amounted to 40 mμg/ml 90 min after the injection of the insulin. The failure of a normal breakfast to suppress this stimulated response is curious since the half-life of circulating immunological active HGH is known to be approximately 30 min (12,15,16) and oral glucose had partially suppressed the high fasting level of HGH. This effect might be attributed to delayed absorption or perhaps to the mixture of carbohydrate, protein and fat in the diet; protein has been shown to be less potent than carbohydrates in "switching off" growth-hormone secretion (13). In any event, these differences in response to suppression and stimulation of pituitary growth hormone in these acromegalic subjects suggest that there are metabolic as well as other clinical differences in patients with acromegaly. These findings are consistent with previous observations during carbohydrate tolerance tests in our patients (10,17) and those recently reported by others (18,19).

Further studies currently in progress of HGH, plasma insulin, and the other factors involved in metabolism of glucose before and after the effective treatment of acromegaly with heavy-particle pituitary suppression should improve our knowledge of the pathophysiology of this disease.

SUMMARY

A sensitive radio-immunoelectrophoretic assay has been used to determine the effects of heavy particles delivered to the sella turcica on levels of circulating growth-hormone in a series of acromegalic patients. In 14 untreated patients, the HGH level ranged from 9 to 99 mμg/ml with a mean of 40.8 mμg/ml, whereas the mean was 6.8 mμg/ml in 16 patients who had received heavy-particle therapy. The changes in HGH during insulin- and glucose-tolerance tests in two acromegalic patients who differed clinically as well as metabolically, is also described.

ACKNOWLEDGMENTS

The authors wish to acknowledge with gratitude the encouragement and helpful consultations with Dr. John H. Lawrence throughout our studies.

REFERENCES AND NOTES

1. Hunter, W. M., and Greenwood, F. C.; Biochem. J. 85:39, 1962.
2. Glick, S. M.; Roth, J.; Yallow, R. S., and Berson, S. A.; Nature 119:784, 1963.
3. Roth, J.; Glick, S. M.; Yallow, R. S., and Berson, S. A.; Metabolism 12:577, 1963.
4. Atkinson, F. R. B.: Acromegaly, London, John Bale, Sons and Daniellson, Ltd., 1932, p. 5.

5. Camsell, C. A.; J. Clin. Endocrinol. 19:1049, 1959.
6. Daughaday, W. H.; Salmon, W. D., Jr., and Alexander, F. J.; J. Clin. Endocrinol. 19:743, 1959.
7. Lawrence, J. H.; Tobias, C. A.; Born, J. L.; Sangalli, F.; Carlson, R. A., and Linfoot, J. A.; Acta Radiol. 58:337, 1962.
8. Lawrence, J. H.; Tobias, C. A.; Born, J. L.; Wang, C. C., and Linfoot, J.A., J. Neurosurg. 19:717, 1962.
9. Roth, J.; Glick, S. M.; Yallow, R. S., and Berson, S. A.; Diabetes 13:355, 1964.
10. Linfoot, J. A.; Manougian, E.; Born, J. L.; Tobias, C. A., and Lawrence, J. H.; 2nd International Congress of Endocrinology, London, Aug. 17-21, 1964.
11. Lawrence, J. H.; Tobias, C. A., and Born, J. L.; Trans. Am. Clin. Climatol. Assoc. 73:176, 1961.
12. Hunter, W. M., and Greenwood, F. C.; Biochem. J. 91:43, 1964.
13. Hunter, W. M., and Greenwood, F. C.; Brit. Med. J. 1:804, 1964.
14. Lawrence, J. H.; Tobias, C. A.; Born, J. L.; Gottschalk, A.; Linfoot, J.A., and Kling, R. P.; J. Am. Med. Assoc. 186:236, 1963.
15. Parker, M. L.; Utiger, R. D., and Daughaday, W. H.; J. Clin. Invest. 41: 262, 1962.
16. Glick, S. M.; Roth, J., and Lonergan, E. T.; J. Clin. Endocrinol. 24:501, 1964.
17. Linfoot, J. A.; Manougian, E.; Born, J. L.; Garcia, J., and Lawrence, J. H., Clin. Res. 13:107, 1965.
18. Cerasi, E., and Luft, R.; Lancet 2:769, 1964.
19. Hartog, M.; Gaafar, M. A.; Meisser, B., and Prasex, T. R.; Brit. Med. J. 2:1229, 1964.

Fred C. Greenwood is biochemist in charge of protein hormones, Division of Chemistry and Biochemistry, Imperial Cancer Research Foundation, London, W. C. 2, England.

Received December, 1964.

Effect of Heavy Particles on the Proliferative Capacity of Ascites Tumor Cells (Lymphoma) Grown *In Vivo*

Yolanda Schmidlin, John H. Lawrence, Karen Sillesen, Graeme Welch and John Lyman

The present study represents an attempt to obtain further information concerning the relative biological effect (RBE) of heavy-particle-induced ionization in living cells grown in vivo. The effects of varying densities of ionization (including X rays and various heavy particles from both the Heavy Ion Linear Accelerator (HILAC) and the 88-inch cyclotron) on ascites tumor cells irradiated in vivo or in vitro were studied, the irradiated cells then being injected into living mice to test their proliferative capacity. In 1935, when Wilson cloud-chamber pictures first made us aware of the dense tissue ionization produced by heavy particles (1), our interest was not only in the safety of the workers around the early cyclotrons but also in understanding the effect of this dense ionization in tissue, and its possible medical applications. Using both transplanted mouse tumors and normal mice, the greater biologic effect of the dense ionization produced in tissue by neutrons (than that of X rays) was observed (2,3). During the intervening years our interest has continued in several aspects of densely ionizing radiations, and for the past 10 years we and our associates have had considerable success utilizing heavy particles in several areas of medical therapy (4). The work of Hewitt and Wilson with ascites tumor cells has made it possible to quantitate more accurately the relative biologic effect of radiations of various linear energy transfers (LET) (5). By the use of such methods we have carried out the present study with an ascitic form of a lymphoma (6), which is similar to the lymphoma used in our very early studies (7,8,9). These neoplastic cells grow very rapidly in a genetically uniform strain of mice after the injection of only a few cells intraperitoneally and are lethal in approximately one week; therefore, in general we are not concerned with the problem of any immunity that might develop in the recipient animal and thus interfere with the interpretation of the results (10).

MATERIALS AND METHODS

The studies reported here concern 35- to 45-MeV protons from the 88-in. cyclotron and 40-MeV alpha particles from the HILAC. As in previous studies 200-kV X rays were used as a baseline for the comparison of various LET's as related to RBE. Thus the LD_{50}, calculated by method of Reed and Muench (11), of 200-kV X rays administered at a dose rate of 80 to 100 R per minute was compared to the LD_{50} of each of the heavy particles used; for the 35- to 45-MeV protons

and the 40-MeV alphas the dose rate averaged 600 rads/min. The RBE was taken as the ratio of the X-ray dose to the heavy-particle dose to produce the same effect on proliferative capacity of the neoplastic cells.

As in the previously described experiments (12,13) we used a transplantable lymphoma (diploid) which "takes" after administration of very few cells intraperitoneally, the LD_{50} being 1 to 10 cells. For these experiments only one strain of mice was used, LAF_1, which is a hybrid between $C_{57}L$ and A/Heston. The lymphoma line was passed in A/Heston mice rather than LAF_1 mice because a tendency for the tumor to change in virulence after several passages in LAF_1 mice had been noted (the animals dying earlier); however, this was not noted when it was passed in A/Heston mice. The tumor was passed weekly in ascites form by inoculating 10^6 cells into adult A/Heston mice; the tumor "took" in 100% of the mice, usually causing the animal's death eight days later. The cells used in the present experiments were cells from approximately the 75th to the 130th passage of the tumor used by us during the past two and one-half years. In these experiments (except when the whole animal carrying the ascites tumor cells was irradiated) four to six LAF_1 mice were injected with 10^6 tumor cells intraperitoneally one week prior to each experiment; at the time of the experiment the ascitic fluid from these mice was pooled, 1 to 2 ml of ascites being obtained from each mouse with the tumor-cell concentration usually amounting to about 2×10^8 cells/ml.

Some attempts have been made to develop a technique similar to that of Hewitt and Wilson (5) in which the whole animal carrying the ascites tumor cells is irradiated *in vivo*, and then after varying doses of radiation the tumor cells are titrated in recipient animals. However, especially in studying the effect of the Bragg peak, this is not possible because of the narrówness of the peak with the energy and particles used; therefore the cells had to be placed in sufficiently thin chambers so that fairly uniform irradiation was given to the entire sample. Thus, in some experiments the cells were irradiated *in vivo* in either adult or infant mice, whereas in other experiments the cells were irradiated *in vitro* in chambers; in both cases, the irradiated cells were transplanted into adult animals.

The whole-body experiments were carried out as follows:

1) In one group the mice were irradiated while breathing air.
2) In another group the mice were sacrificed a few minutes prior to irradiation in order to be certain of anoxic tumor cells.
3) In a third group the mice were irradiated after injection of H_2O_2 intraperitoneally to provide well-oxygenated neoplastic cells. Each mouse was given 0.2 ml of a 1:10 dilution of concentrated H_2O_2, providing a final concentration of approximately 0.1*M* in the ascitic fluid of an adult mouse. Deschner and Gray (14), and Gray *et al*. (15),

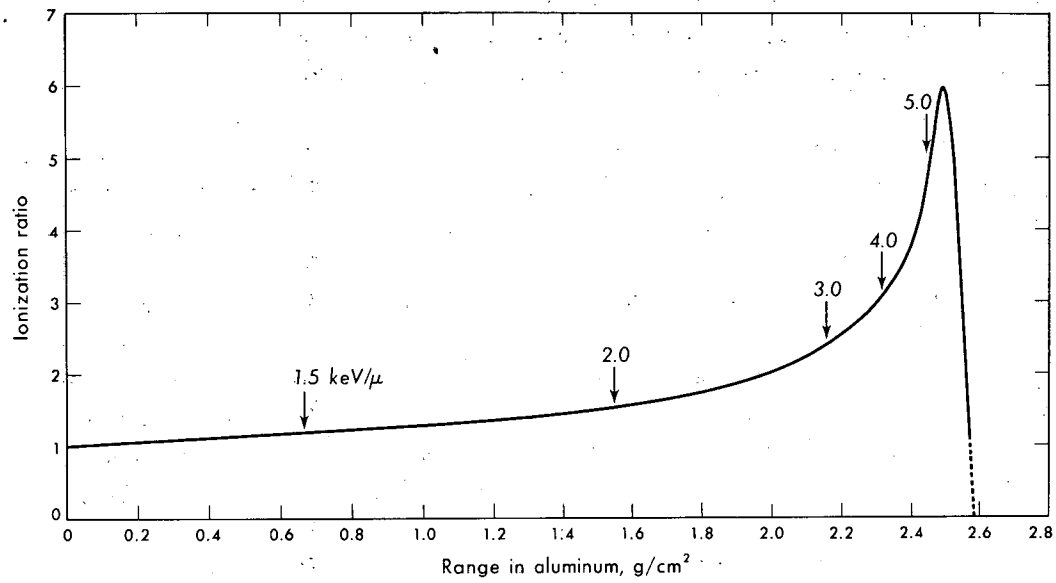

Figure 1. Bragg curve of 45-MeV protons showing the LET's at various positions along the curve. For the experiments using the plateau portion of the proton beam the LET was 1.5 to 2 keV/μ; using the peak portion the LET's were 3 and 5 keV/μ.

MUB-4886

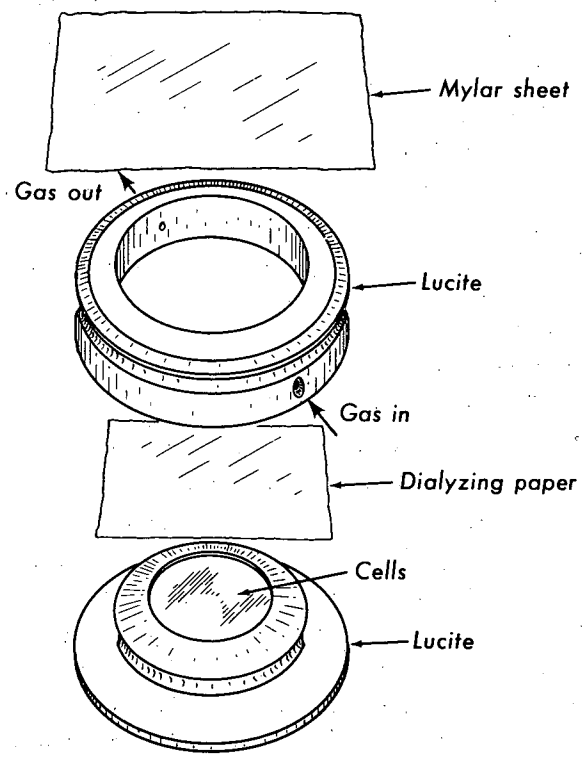

Figure 2. Diagram of chamber used for *in vitro* studies of oxygen effect. Pictured is the 0.125-mm-deep lucite chamber that contains the cells. The cells are covered with a sheet of dialyzing paper held in place with an "O" ring. The lucite gas chamber, covered with a Mylar sheet, fits into place on top of the cell chamber. The gas (either oxygen or nitrogen) is then flushed through the system, going in and out of the chamber as indicated.

MUB-4618

Table 1.

Accelerator	Energy	Particle	LET (keV/μ)
X ray	200 kV		1.5 - 3
88" cyclotron	35 - 45-MeV	protons (plateau)	1.5 - 2
88" cyclotron	35 - 45-MeV	protons (peak)	3 - 7
HILAC	40-MeV	alpha particles (plateau)	18.6

have shown that such concentrations of H_2O_2 do oxygenate the ascites cells because catalase present in the red blood cells decomposes the H_2O_2, producing diffuse small oxygen bubbles in the ascitic fluid.

These three types of experiments were carried out with X rays (LET 1.5 to 3 keV/μ) using both adult and infant mice. In addition, in a few experiments 12-day-old infant mice carrying the ascites tumor were irradiated while breathing either oxygen or nitrogen. As in the case of adult mice they had been injected with tumor cells seven days prior to the experiment, but only 500,000 cells were injected. To provide oxygenation of the ascites tumor cells, the infant mice were given intraperitoneally 0.05 ml of 1:10 dilution of concentrated hydrogen peroxide just prior to irradiation.

Because of the small size of the 12-day-old mouse it was also possible to irradiate them with the plateau portion of the proton beam from the 88-in. cyclotron. The energy of these particles varies from 35 to 45 MeV; the LET is 1.5 to 2 KeV/μ at the plateau and 3 to 7 keV/μ at the peak (see Table 1). The particles have a distance of penetration into tissue of about 2 cm (see Fig. 1). As already mentioned, the Bragg-peak portion of the beam is a very narrow region of the Bragg curve, and so in order to study the effect of the Bragg-peak ions the cells had to be irradiated _in vitro_, using very thin lucite chambers 0.125 mm deep (see Fig. 2). The cells in the chambers were covered with dialyzing paper which when kept moist permits water-saturated gas to pass through. The gas is continuously flushed through a gas chamber which fits over the lucite chamber and is covered with mylar. Thus, by using oxygen or nitrogen for flushing we hoped to study the difference in radiosensitivities of oxygenated and anoxic cells.

For the studies with the particles from the HILAC, 0.3-mm-deep chambers covered with mylar were used. All of these studies were performed in air only, and the chamber was placed only in the plateau portion of the alpha-particle beam, the energy being 40 MeV and the LET 18.6 keV/μ. These particles have a distance of penetration into tissue of 1.3 mm.

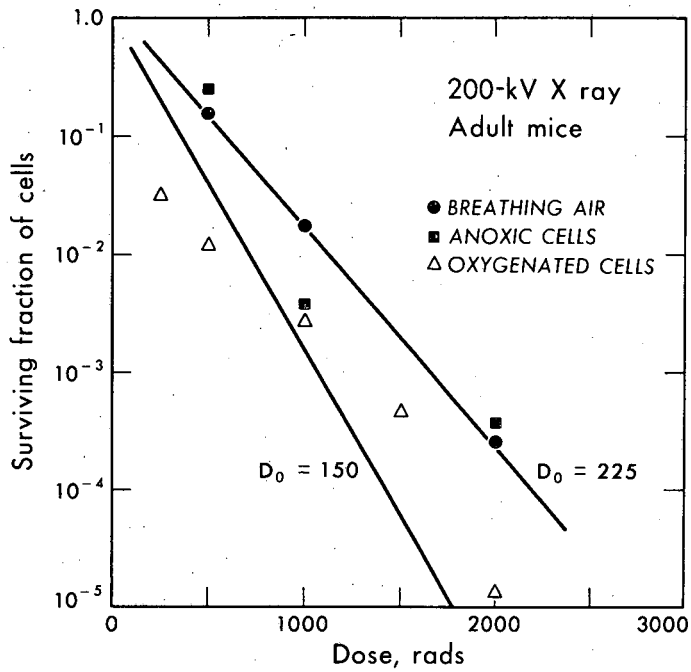

Figure 3. Surviving fraction of lymphoma cells injected intraperitoneally into LAF_1 mice. Irradiation was given in vivo (adult mice) with 200-kV X rays (LET 1.5 to 3 keV/μ). The mice were breathing air, or were killed just prior to irradiation (anoxic cells), or were given injections of H_2O_2 intraperitoneally just prior to irradiation (oxygenated cells).

MUB-4883

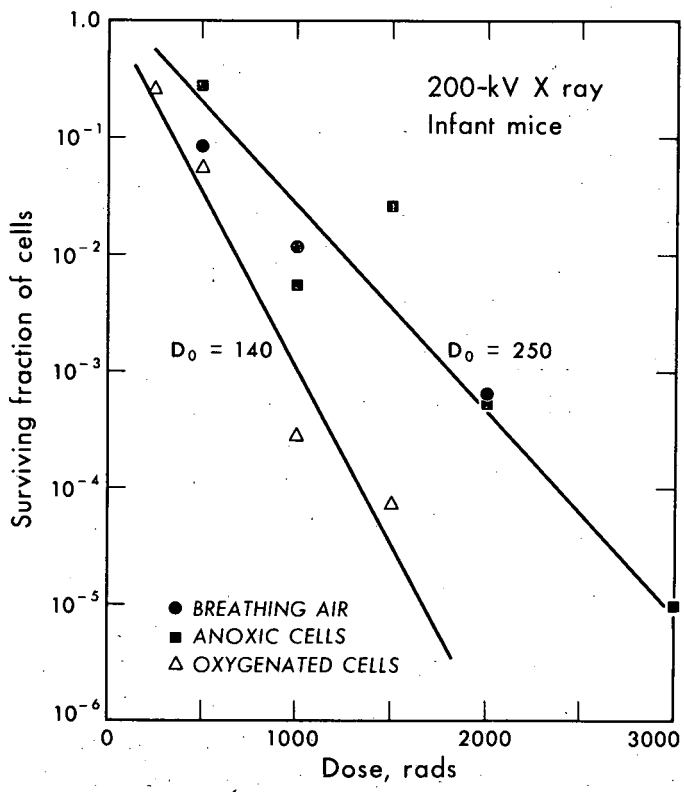

Figure 4. Surviving fraction of lymphoma cells injected intraperitoneally into LAF_1 mice. Irradiation was given in vivo (infant mice) with 200-kV X rays (LET 1.5 to 3 keV/μ). The mice were breathing air, or were killed just prior to irradiation (anoxic cells), or were given injections of H_2O_2 intraperitoneally just prior to irradiation (oxygenated cells).

MUB-4885

After exposure to the various radiations, the tumor cells were taken from the animal or the chamber and added to an ice-cold TC-199 solution (16). After counting, serial dilutions were made for each radiation dose and the cells were injected into adult recipient animals, using five animals for each dose and titration level. In other words, there were four or five groups of five animals at each radiation dose. Most of the experimental titrations included a group with zero mortality as well as a group with 100% mortality. Thus, for each experiment with the control included we used about 100 to 300, or more, mice. Proliferative capacity was determined by the percentage positive or negative animals at the end of eight weeks.

RESULTS AND DISCUSSION

1. CELLS IRRADIATED IN VIVO WITH X RAYS (LET 1.5 TO 3 keV/μ) OR PLATEAU PORTION OF THE 35- TO 45-MeV PROTON BEAM (LET 1.5 TO 2 keV/μ) Figure 3 shows the results with cells irradiated *in vivo* in 11 X-ray experiments (whole-body irradiation of adult mice): three were done with animals breathing air; three with animals sacrificed just prior to irradiation (anoxic tumor cells); and five with animals having received H_2O_2 intraperitoneally immediately before exposure (oxygenated tumor cells). The surviving fraction on a log scale is plotted as a function of radiation dose. This fraction is determined by the ratio of the number of cells that cause 50% mortality in the control group to the number of cells that cause 50% mortality at the given dose of radiation. D_o (D_{37}) is defined as the dose of radiation necessary to reduce any surviving fraction along the straight-line portion of the curve by 0.37 (17). In the Figure there is clearly a difference between the survival fraction of anoxic and oxygenated cells; D_o's calculated from the graph are 225 and 150, respectively, indicating an oxygen enhancement ratio of approximately 1.5. It is also seen that when the animals are breathing air during radiation the dose-response curve for the ascites cells is similar to that for the anoxic cells. This is expected since a mouse bearing a seven-day-old ascitic tumor contains 1.5 to 2 ml of fluid, in which there are approximately 2×10^8 cells per milliliter; this means that only a few cells will be within the distance of approximately 150 μ of the vascularized tissues within the abdominal cavity and where the oxygen tension will be sufficiently high to give adequate oxygenation (18). Furthermore, these results agree with those of Berry and Andrews (19) to be discussed below.

In Fig. 4 are shown the dose-response curves calculated from 11 experiments made under the same conditions as those for Fig. 3 but using infant mice. In two experiments the animals breathed air, in four the animals were killed just prior to irradiation, and in five the animals had received intraperitoneally H_2O_2 just prior to irradiation. With H_2O_2 the LD_{50} for the unirradiated control cells tended to be higher than in those experiments in which H_2O_2 was not used, indicating some toxic effect of the hydrogen peroxide in the infant mice. There had been no such sign of toxic effect in the adult mice. If one relates the

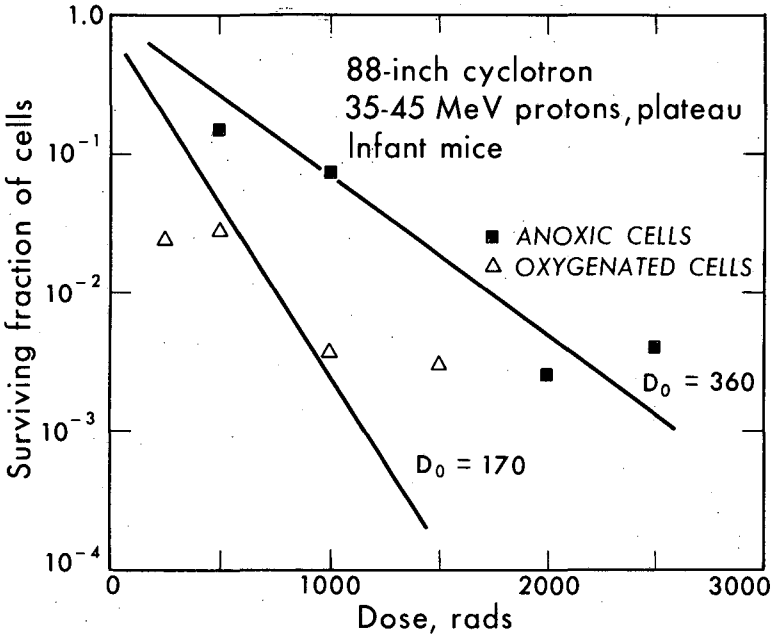

Figure 5. Surviving fraction of lymphoma cells injected intraperitoneally into LAF_1 mice. Irradiation was given in vivo (infant mice) with 35- to 45-MeV protons using the plateau portion of the beam (LET 1.5 to 2 keV/μ). The mice were either killed just prior to irradiation (anoxic cells) or were given injections of H_2O_2 intraperitoneally just prior to irradiation (oxygenated cells).

MUB-4888

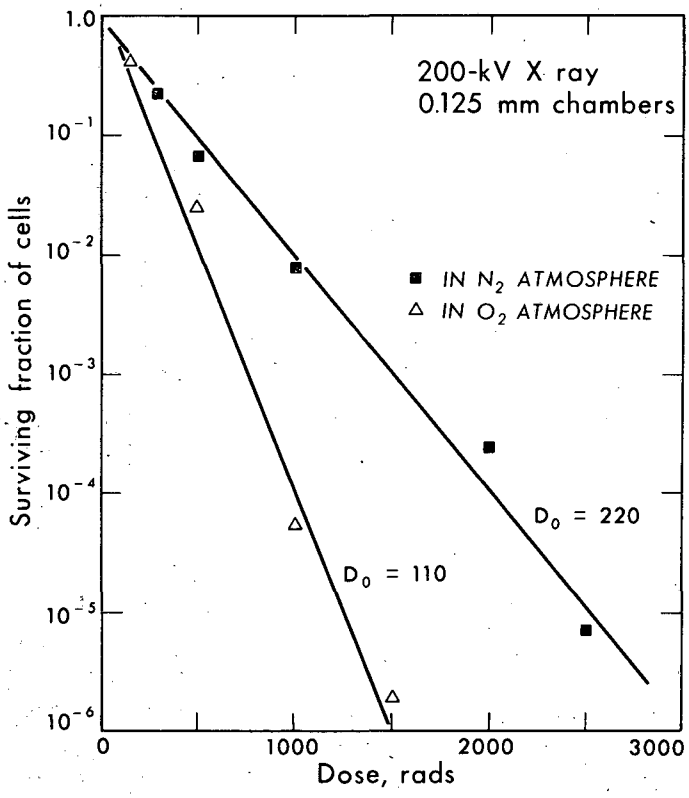

Figure 6. Surviving fraction of lymphoma cells injected intraperitoneally into LAF_1 mice. Irradiation was given in vitro in 0.125-mm-deep chambers with 200-kV X rays. (LET 1.5 to 3 keV/μ). The gas chamber was flushed with either oxygen or nitrogen during irradiation, the cells being oxygenated or anoxic, respectively.

MUB-4887

dose of H_2O_2 administered to the amount of ascites present in the animals, it is noted that the infant mice received the larger dose; the final concentration in their case was about 0.25M compared to 0.1M for the adult mice. However, the dose-response curves for the infant mice are about the same as were those for the adult, and again the curve for the ascites tumor cells irradiated in animals breathing air was similar to that for the anoxic tumor cells. D_o anoxic is 250 and D_o oxygenated is 140, giving an oxygen enhancement ratio of approximately 1.8 . A few experiments, in which the infant mice breathed either oxygen or nitrogen during exposure to X rays, showed that when the mice were breathing pure oxygen the survival fraction of the tumor cells corresponded best to the anoxic dose-response curve. This occurred in spite of the fact that the amount of ascites in the infant mice is only 0.1 to 0.3 ml and would lead one to expect a somewhat better oxygenation.

Our observed oxygen enhancement ratios may turn out to be higher in future experiments since according to Berry and Andrews (20) well-oxygenated conditions in the abdominal cavity after H_2O_2 intraperitoneally lasts only for 8 to 10 min. In the present experiments, however, the time interval between H_2O_2 and the completion of irradiation was unfortunately often 30 to 40 min, especially when using the higher irradiation doses. Thus the oxygenation was probably not always adequate. Hewitt and Wilson (21) found no difference in the radiosensitivity of leukemic cells irradiated *in situ* in livers of leukemic mice, whether the host animal was breathing air or oxygen. However, they found a reduction in sensitivity amounting to a factor of 2.3 when the animal had been killed 2 min before irradiation. This indicated that the tumor cells in even a heavily tumor-infiltrated liver exist under fairly well-oxygenated conditions, whereas most cells in ascitic fluid are apparently anoxic. These results agree with those of Berry and Andrews who found that the radiosensitivity of ascitic tumor cells was the same whether the host animal was killed a few minutes prior to radiation, was breathing air during radiation or was breathing pure oxygen during radiation.

Figure 5 presents the dose-response curves in experiments where tumor-bearing infant mice were irradiated with the plateau portion of the proton beam (LET 1.5 to 2 keV/μ) from the 88-in. cyclotron. Again anoxic cells (in dead animals) were compared with oxygenated cells (in animals injected with H_2O_2). The data are more scattered than in the previous graphs. One finds a D_o anoxic of 360 rads, and a D_o oxygenated of 170 rads, which gives an oxygen enhancement ratio of 2.1 . When these data are compared to the X-ray data, the RBE for the plateau portion of the beam is 0.8 for oxygenated cells and 0.7 for anoxic cells (see Table 2). The accuracy of methods used here, however, does not lead us to believe that these findings prove any difference between the two forms of radiation, which actually have similar LET's.

Table 2.

Radiation	LET (keV/μ)	Experiment	Figure	D_o Anoxic	D_o Oxygen	$D_o(An)^*$ / $D_o(Ox)$	RBE Anoxic	RBE Oxygen
200-kV X ray	1.5 - 3	*in vivo* adult mice	3	225	150	1.5		
200-kV X ray	1.5 - 3	*in vivo* infant mice	4	250	140	1.8		
200-kV X ray	1.5 - 3	*in vitro* 0.125-mm chamber	6	220	110	2		
35 - 45-MeV protons (plateau)	1.5 - 2	*in vivo* infant mice	5	360	170	2.1	0.7	0.8
35 - 45-MeV protons (peak)	3 - 7	*in vitro* 0.125-mm chamber	8	180	130	1.4		
35 - 45-MeV protons (plateau)	1.5 - 2	*in vitro* 0.125-mm chamber	7	180	125	1.4	1.2	0.9
40-MeV alphas (plateau)	18.6	*in vitro* 0.3-mm chamber	9	220			1	

*Oxygen enhancement ratio.

2. CELLS IRRADIATED *IN VITRO* WITH X RAYS (LET 1.5 TO 3 keV/μ) OR THE PLATEAU PORTION OF THE 35- TO 45-MeV PROTON BEAM (LET 1.5 TO 2 keV/μ) Figure 6 presents experiments in which the cells were placed in 0.125-mm-deep chambers (see Fig. 2) during irradiation with 200-kV X rays. The chambers were kept in either an oxygen (five experiments) or a nitrogen (five experiments) atmosphere during irradiation. In this case the D_o anoxic was 220 and the D_o oxygenated was 110 giving an oxygen enhancement ratio of 2. This ratio agrees rather closely with the results of Hewitt and Wilson (who, as mentioned previously, found a ratio 2.3) and reflects the better oxygenation of the tumor cells irradiated *in vitro* during continuous flushing with oxygen than was obtained with tumor cells irradiated in the whole-body experiments where H_2O_2 was injected intraperitoneally prior to irradiation.

The same chambers were used to contain the cells while they were placed in the plateau portion of the proton beam (LET 1.5 to 2 keV/μ). Figure 7 shows the results of 15 experiments (seven in nitrogen and eight in oxygen). In this case D_o anoxic was 180 and D_o oxygenated was 125, giving an oxygen enhancement ratio of 1.4 . Again we can calculate the RBE for the protons compared to X rays; RBE for anoxic cells is 1.2, and RBE for oxygenated cells is 0.9, both thus being close to 1. Again, we do not interpret these results as indicating any significant difference between X rays and protons of these energies.

3. CELLS IRRADIATED *IN VITRO* WITH THE PEAK PORTION OF THE 35- TO 45-MeV PROTON BEAM (LET 3 TO 7 keV/μ) On the Bragg curve shown in Fig. 1 the LET's for

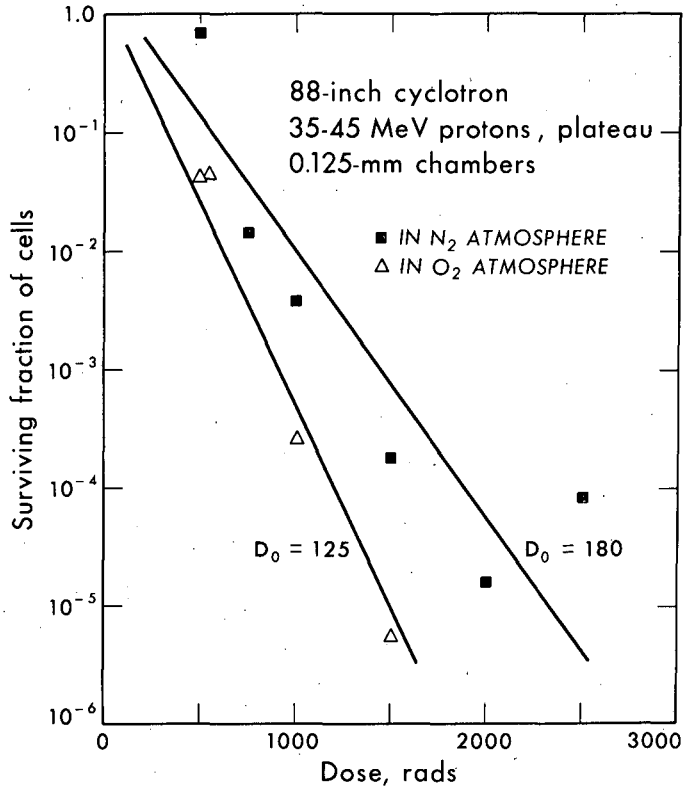

Figure 7. Surviving fraction of lymphoma cells injected intraperitoneally into LAF_1 mice. Irradiation was given in vitro in 0.125-mm-deep chambers with 35- to 45-MeV protons using the plateau portion of the beam (LET 1.5 to 2 keV/μ). The gas chamber was flushed with either oxygen or nitrogen during irradiation, the cells being oxygenated or anoxic, respectively.

MUB-4884

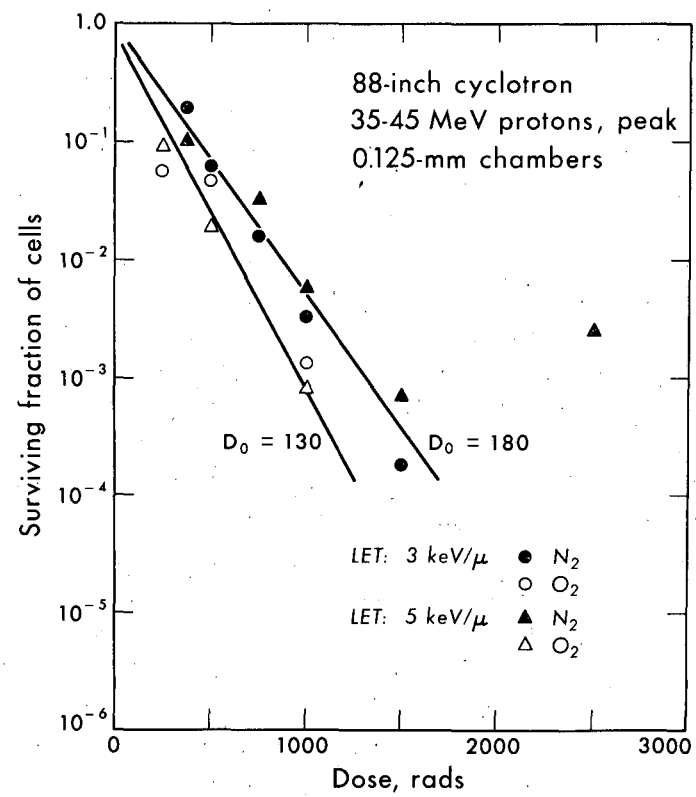

Figure 8. Surviving fraction of lymphoma cells injected intraperitoneally into LAF_1 mice. Irradiation was given in vitro in 0.125-mm-deep chambers with 35- to 45-MeV protons using the peak portion of the beam (two positions were used, the LET being 3 or 5 keV/μ). The gas chamber was flushed with either oxygen or nitrogen during irradiation, the cells being oxygenated or anoxic, respectively.

MUB-4890

different positions along the curve are indicated, and it is seen that the LET increases towards the Bragg peak. As already mentioned the Bragg peak is very narrow; however, we attempted to move the sample toward the Bragg peak and thus expose the cells to higher LET irradiation. Figure 8 shows the results of six such experiments in which cells were irradiated in vitro in the 0.125-mm-deep chambers and were flushed with either oxygen or nitrogen during the exposure (see Fig. 2). In three of these experiments the cells were placed so they were irradiated with heavy particles having an LET of 3 keV/μ (see Fig. 1 for position on Bragg curve); in the other three experiments the LET was 5 keV/μ.

As would be expected, both sets of data follow the same curves, giving a D_o (anoxic) of 180 and a D_o (oxygenated) of 130, and an oxygen enhancement ratio of 1.4. This is very close to the data obtained with plateau portion of the same beam (see Table 2), again showing that with these rather low LET's we do not get an RBE greater than 1, as compared with X rays.

4. CELLS IRRADIATED IN VITRO WITH THE PLATEAU PORTION OF THE 40-MeV ALPHA PARTICLE BEAM (LET 18.6 keV/μ) Figure 9 shows the average of 11 experiments in which lymphoma ascites cells were irradiated in the plateau portion of the 40-MeV alpha-particle beam (LET 18.6 keV/μ). We used 0.3-mm-deep chambers containing the undiluted ascites tumor cells, without flushing with oxygen or nitrogen. From the graph we obtain a D_o of 220. As of this date the corresponding data from the X-ray experiments using the same kind of chambers have not been completed. However, since the tumor cells were irradiated as undiluted ascites it is probably fair to compare the results to those obtained with tumor cells irradiated with X rays using the 0.125-mm-deep chambers in a nitrogen (anoxic) atmosphere (Fig. 6). The reason for this assumption is discussed below. D_o (anoxic) for 200-kV X ray was 220; using this as a baseline the RBE for 40-MeV alpha particles (LET 18.6 keV/μ) is 1. This is the same as that found at our laboratory for haploid yeast and bacteria (22,23) and close to the 1.5 for human kidney cells in vitro (24). In addition, the Yale group found the RBE's of 40-MeV alpha particles to be close to 1 for virus (dried T1 bacteriophage), for bacteria (Escherichia coli WP2), and for haploid and diploid interdivisional yeast cells (25).

The reason for assuming that we are dealing with anoxic cells in undiluted ascites is based on the experiments shown in Fig. 10. The dose-response curves from Fig. 6 (X-ray data) are again shown, these having been calculated from experiments in which tumor cells were irradiated as undiluted ascites in 0.125-mm-deep chambers kept in either pure oxygen or nitrogen atmospheres. Superimposed are the data from experiments in which undiluted ascites tumor cells in 0.125-mm chambers were kept in air during exposure to 200-kV X rays and the data from experiments in which undiluted ascites tumor cells were irradiated in test tubes. Both sets of data correspond fairly well to the data obtained from cells

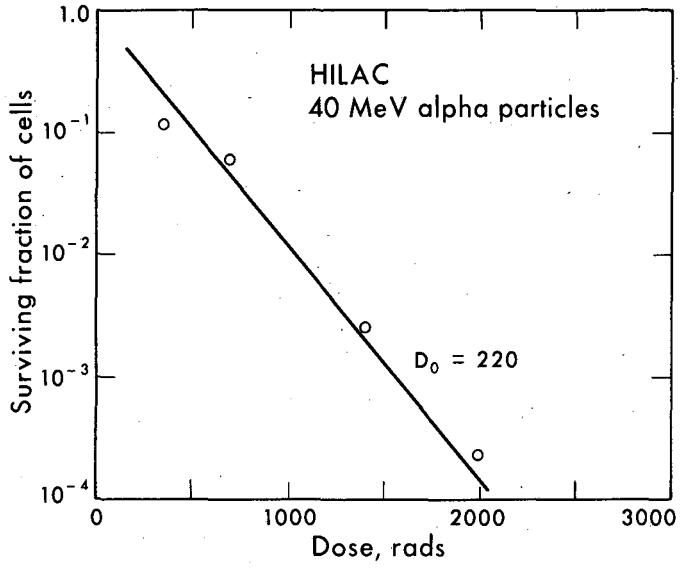

Figure 9. Surviving fraction of lymphoma cells injected intraperitoneally into LAF_1 mice. Irradiation was given *in vitro* in 0.3-mm-deep chambers with 40-MeV alpha particles (LET 18.6 keV/μ). The chambers were in air during irradiation.

MUB-4889

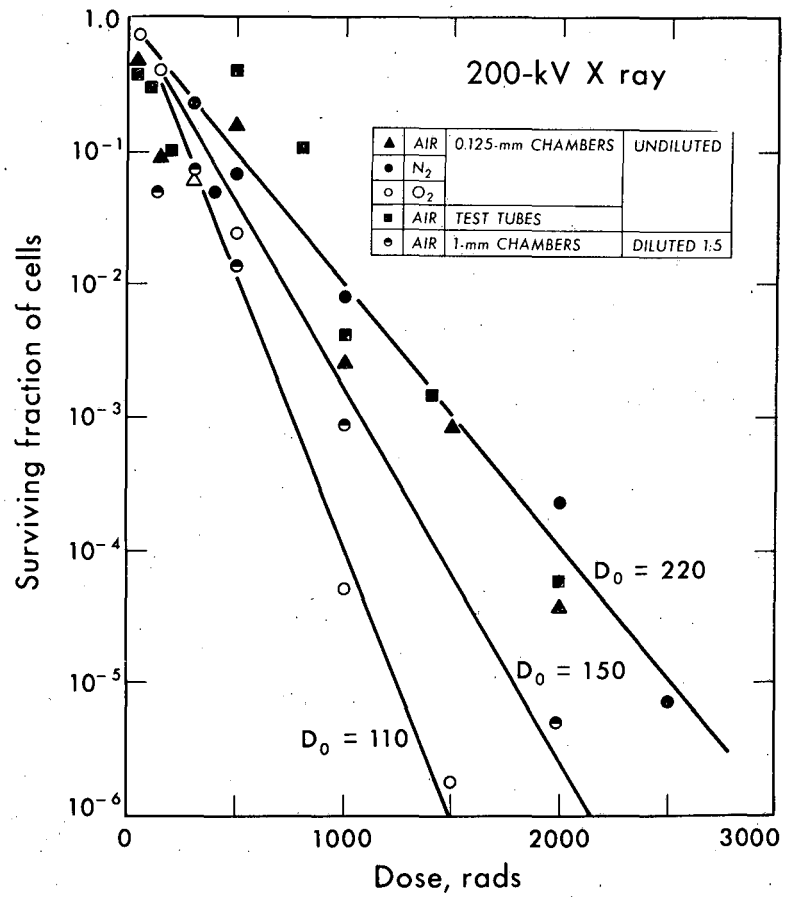

Figure 10. Surviving fraction of lymphoma cells injected intraperitoneally into LAF_1 mice. The data from several types of *in vitro* X-ray experiments are shown: ascites tumor cells irradiated in 0.125-mm-deep chambers in an atmosphere of oxygen, nitrogen, or air; undiluted ascites tumor cells irradiated in a test tube; diluted (1:5) ascites tumor cells irradiated in 1-mm-deep lucite chambers.

MUB-4882

irradiated in the nitrogen atmosphere (anoxic). The middle line in Fig. 10 presents the dose-response curve for cells in diluted ascites (approximately 1:5) irradiated in 1-mm-deep lucite chambers; in this case we seem to have a mixture of oxygenated and anoxic cells.

CONCLUSIONS AND SUMMARY

These investigations are still in the preliminary stages and complete data are not yet available. However, on the basis of the results described and discussed in the previous section we can make the following statements.

1) The radiosensitivity of lymphoma-ascitic-tumor cells to 200-kV X rays (LET 1.5 to 3 keV/μ) was like that of anoxic cells whether the animal was killed a few minutes prior to irradiation, was breathing air during irradiation or was breathing pure oxygen during irradiation.
2) The oxygen enhancement ratio for 200-kV X rays in the *in vitro* experiments was 2; however, when using whole-body irradiation of the animal carrying the cells it was lower, probably because of the long time interval between the intraperitoneal injection of H_2O_2 and the completion of irradiation and thus the incomplete oxygenation of the cells.
3) The RBE of 35- to 45-MeV protons approaches 1 when using both the plateau portion (LET 1.5 to 2 keV/μ) and certain portions of the Bragg-peak (LET 3 to 7 keV/μ) of the beam.
4) In the *in vitro* experiments the oxygen enhancement ratios for both the plateau and peak portions (low LET) of the 35- to 45-MeV proton beam are smaller than that for the 200-kV X rays.
5) The RBE of 40-MeV alpha particles (LET 18.6 keV/μ) was approximately 1.

Further studies are now under way using particles with higher LET's continuing our investigations of the relationship of LET to RBE. In addition, further studies are being done to find out how high an LET is required before the oxygen effect disappears. These problems have important implications for the treatment of certain human diseases (26,27). In our earlier studies (12,13) we could not demonstrate any oxygen effect with boron ions (LET 124 keV/μ) whereas there seemed to be a definite oxygen effect with lithium ions (LET 43.2 keV/μ). Manney *et al*. (22), and Tobias and Todd (23) in studying kidney cells in tissue cultures, find that an even higher LET is required before the oxygen effect disappears; when the LET is above 200 keV/μ it is 10% or less, and at LET's above 300 keV/μ it disappears completely. In tissue culture the cells lose their normal appearance, unlike the original explant, whereas in our studies such is not the case. It remains to be seen whether the findings with reference to RBE and oxygen effect are similar. Finally, in these studies we are dealing with neoplastic cells and not normal cells. In our previous work (12,13) millipore filters were used and it was difficult to prevent drying of the cells. New experiments are in progress now using a 0.125-mm-deep lucite chamber (see

Fig. 2) as the container for the tumor cells. The cells are then bombarded in either an oxygen or a nitrogen atmosphere with various heavy ions accelerated with the HILAC, including helium, lithium, boron, and carbon ions, the latter having an LET of 185 keV/μ and being the heaviest ion now available which has a range long enough to give a uniform irradiation throughout the 0.125-mm-deep chamber. Within this range of LET's we also wish to study the relationship between LET and RBE.

According to Storer et al. (28), for most test objects the RBE generally starts increasing at an LET of 5 keV/μ and reaches a maximum at about 50 keV/μ, after which it decreases again. However, as described in part 3 of the discussion, we were not able to demonstrate any rise in RBE using 35- to 45-MeV protons and placing the sample at a position where the LET was 5 keV/μ (see Fig. 1), nor is there an increase of RBE at LET as high as 18.6 keV/μ as in the case of 40-MeV alpha particles. Manney ét al. (22), Tobias and Todd (23), Todd (24), and Deering and co-workers (25,29) indicated that with carbon ions the maximum RBE is not reached before a considerably higher LET than that reported by Storer and co-workers.

All these are interesting and important problems, and hopefully the present studies will assist in our better understanding of therapeutic aspects of heavy particles and lead to the further development of therapy with heavy particles. However, the great difficulties in carrying out the experiments described here, largely owing to the poor penetration of these relatively low-energy heavy particles, indicate the desirability of having available heavy particles of very high energy and high atomic number, particles not now produced by any accelerator in the world. We believe the greater RBE and the relative absence of the oxygen effect and other characteristics of such very high LET radiations, which are not now available in a penetrating form, may be of great importance in the therapy of disease, including neoplastic disease, in which an equalization of effect of radiation on both normal and neoplastic cells may be important.

ACKNOWLEDGMENTS

The authors wish to express their appreciation to Alice Beckman for her valuable technical assistance in performing these experiments.

REFERENCES AND NOTES

1. Lawrence, J. H., and Lawrence, E. O.; Proc. Natl. Acad. Sci. U.S. 22:124-133, 1936.
2. Lawrence, J. H.; Aebersold, P. C., and Lawrence, E. O.; Proc. Natl. Acad. Sci. U.S. 22:543-557, 1936.
3. Axelrod, D., Aebersold, P. C., and Lawrence, J. H.; Proc. Soc. Exptl. Biol. Med. 48:251-256, 1941.

4. Lawrence, J. H.; Tobias, C. A.; Linfoot, J. A.; Born, J.L.; Manougian, E., and Lyman, J. T.; Ann. Internal Med. 62:400-407, 1965.
5. Hewitt, H. B., and Wilson, C. W.; Ann. N. Y. Acad. Sci. 95:818-827, 1961.
6. Amos, D. B.; Ann. N.Y. Acad. Sci. 63:706-710, 1956.
7. Lawrence, J. H., and Gardner, W. U.; Am. J. Cancer 33:112-119, 1938.
8. Graff, W. S.; Scott, K. G., and Lawrence, J. H.; Am. J. Roentgenol. Radium Therapy 55:44-54, 1946.
9. Lawrence, J. H., Horn, R., and Strong, L. C.; Yale J. Biol. Med. 10:145-154, 1938.
10. Scott, O. C. A.; Radiation Res. 14:643-652, 1961.
11. Reed, L. J., and Muench, H.; Am. J. Hyg. 27:493-497, 1938.
12. Sillesen, K.; Lawrence, J. H., and Lyman, J. T.; Semiannual report, Donner Laboratory, Lawrence Radiation Laboratory, UCRL-11033:139-151, 1963.
13. Sillesen, K.; Lawrence, J. H., and Lyman, J. T.; Acta Isotopica 3:107-126, 1963.
14. Deschner, E. E., and Gray, L. H.; Radiation Res. 11:115-146, 1959.
15. Gray, L. H.; Chase, H. B.; Deschner, E. E.; Hunt, J. W., and Scott, O. C. A.; Proceedings Second International Conference on Peaceful Uses of Atomic Energy, 22:413-419, 1958.
16. Morgan, J. F.; Morton, H. J., and Parker, R. C.; Proc. Soc. Expertl. Biol. Med. 73:1, 1950.
17. Alper, T.; Gillies, N. E., and Elkind, M. M.; Nature 186:1062-1063, 1960.
18. Thomlinson, R. H., and Gray, L. H.; Brit. J. Cancer 9:539-549, 1955.
19. Berry, R. J., and Andrews, R.; Radiology 77:824-830, 1961.
20. Berry, R., and Andrews, J. R.; Brit. J. Radiol. 36:49-55, 1963.
21. Hewitt, H. B., and Wilson, C. W.; Brit. J. Cancer 13:675-684, 1959.
22. Manney, T. R.; Brustad, T., and Tobias, C. A.; Radiation Res. 18:374-388, 1963.
23. Tobias, C. A., and Todd, P. W.; Semiannual Report, Donner Laboratory, Lawrence Radiation Laboratory, UCRL-11387, 1964.
24. Todd, P. W.; Ph.D. Thesis, University of California, Lawrence Radiation Laboratory, UCRL-11614, 1964.
25. Deering, R. A.; Hutchinson, F., and Schambra, P. E.; Aerospace Med. 32:915-924, 1961.
26. D'Angio, G. J., and Lawrence, J. H.; Nucleonics 21, No. 11, 56-61, 1963.
27. Lawrence, J H , and Tobias, C. A.; in Progress in Atomic Medicine, edited by J. H. Lawrence, New York, Grune & Stratton, 1965, in press.
28. Storer, J. B.; Payne, S. H.; Furchner, J. E., and Langham, W. H.; Radiation Res. 6:188-288, 1957.
29. Deering, R. A., and Rice, R., Jr.; Radiation Res. 17:774, 1962.

Dr. Yolanda Schmidlin's present address is: Hallen Str. Dübendorf 13, Zürich, Switzerland.

Received January, 1965.

Production and Chemical Processing of Fe^{52} for Medical Use

Yukio Yano and Hal O. Anger

The radioisotope iron 52 is produced by the nuclear reaction $Cr^{50}(\alpha\ 2n)Fe^{52}$. In the production method described here, natural chromium, containing 4.3% Cr^{50}, 83.8% Cr^{52}, 9.6% Cr^{53} and 2.4% Cr^{54}, is bombarded with 65-MeV α particles from the 88-in. spiral-ridge cyclotron at the Lawrence Radiation Laboratory, Berkeley. The usual yield of processed Fe^{52} is 100 to 200 μCi for a 3-hr bombardment.

Iron 52 has a half-life of 8.2 hr and decays 56.5% by positron emission and 43.5% by electron capture to metastable Mn^{52m}, accompanied by a 165-keV γ ray. The Mn^{52m} decays with a 21.3-min half-life, 99+% by positron emission to stable Cr^{52}(1). Since iron is incorporated into newly forming red cells and because of the suitable half-life and decay by positron emission of Fe^{52}, this tracer is very advantageous for <u>in vivo</u> localization of functioning red bone marrow with the positron scintillation camera (2).

MATERIALS AND METHODS

CYCLOTRON TARGET PREPARATION AND IRRADIATION High-purity chromium with an iron content of less than 100 ppm is used for the cyclotron irradiation targets. A 100- to 300-mesh powder is compressed under a pressure of 80,000 psi to form a solid cohesive disk. Higher beam current can be applied to these pressed targets than to loose powder targets because of their improved heat conductivity. Average specifications of the targets are shown in Table 1. The deviation of any one target from the average of 30 targets prepared was less than ± 5% for any specification. Targets consisting of chromium electroplated on copper foil were also tried, but they have two disadvantages. First, the activity induced in the copper is very high, and second, the thickness of the plated chromium layer was limited to about 0.008 in., resulting in a lower yield of Fe^{52} per run.

The pressed chromium target is placed between a 0.01-in. aluminum backing foil and a 0.001-in. Dural cover foil. The backing foil is in contact with circulating water for cooling. The effective diameter of the alpha beam on the chromium target varies from 1/2 to 5/8 in. The average beam current is 12 μA. At this current there is some blackening of the chromium but no burn-through of the cover foil.

Table 1. Target specifications

Weight Cr	0.826 g
Diameter	1.68 cm
Area	2.20 cm^2
Thickness	0.024 in.
Density	0.366 g/cm^2
Density compared to solid metal	86.8%

For a yield of 150 μCi of Fe^{52} at the conclusion of the chemistry a 40-μAhr bombardment at 65 MeV is necessary. The yield of Fe^{52} as a function of α-particle energy is shown in Fig. 1. This yield curve is for irradiation of a thick target, where the α particles are degraded by passage through the target to about 20 MeV. This is near the threshold energy for the $Cr^{50}(\alpha\ 2n)$ Fe^{52} reaction.

CHEMICAL SEPARATION OF FE^{52} The radioactive iron is separated from the chromium and from other radioactive isotopes by ether extraction. In a highly acidic medium of 8 N hydrochloric acid, ferric chloride extracts into the ether phase as $FeCl_4^-$. All of the iron must be in the oxidized ferric state because iron in the ferrous state, as well as manganese and chromium, can not be appreciably extracted into the ether phase. A very satisfactory separation of iron from copper, cobalt, manganese, nickel, aluminum, chromium, zinc, quadrivalent vanadium, and titanium can be achieved by repeated ether extractions and washings with ether-saturated 8 N hydrochloric acid (3). By using redistilled diisopropyl ether and maintaining the HCl concentration near the optimum of 8 N, we found that the efficiency of the extraction reaches about 99% in the presence of carrier iron. The ferric chloride is recovered from the ether phase by back extraction with water.

A considerable amount of short half-life activity decays away within 30 to 60 min after irradiation. Three hours after irradiation, the βγ radiation 12 in. from the chromium target and the aluminum target holder is 5 R/hr.

All the chemical processing is done in an enclosure shielded with 2 in. of lead. The processing is done by remote handling with tongs. An automated system of specially fitted "goose neck" pipettes and vacuum stirring is used for the ether extraction.

PROCEDURE FOR ISOPROPYL ETHER EXTRACTION OF IRON

1. Place the pressed chromium target in a 250-ml round-bottom boiling flask and pulverize into fine particles.
2. Wash down with 25 ml of concentrated HCl acid.

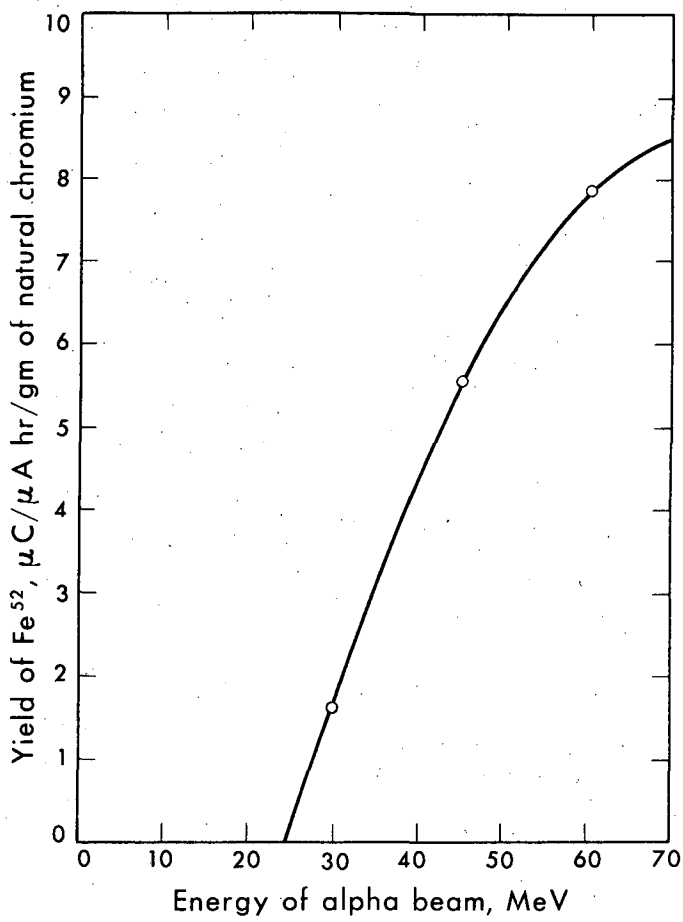

Figure 1. Fe^{52} yield vs. energy of alpha beam.

MUB-3500

3. Heat the acid solution of chromium at 50°C for 1 hr under reflux. (Initial heating should be just sufficient to maintain the dissolution of Cr.)
4. Increase the heating temperature to 125°C and heat the chromium solution for 1 hr to give a complete solution of the chromium and to achieve a constant boiling mixture of about 7 N HCl. (The refluxed Cr and HCl acid solution was found to be near 7 N by titration with a standard NaOH solution.)
5. Add carrier Fe^{+2} (2.0 μg) and Mn^{+2} (4.0 μg) in 8 N HCl to the Cr solution.
6. Add 10 drops of concentrated HNO_3 acid to the target solution.
7. Continue heating the Cr solution at 125°C for an additional 30 min to oxidize Fe^{+2} to Fe^{+3}.
8. Remove the Cr solution from the heating mantle and cool in a circulating water bath at 10°C.
9. In an ice bath precool the diisopropyl ether and the 8 N HCl acid to be used for the extraction procedure.

10. By vacuum draw the cooled Cr-HCl acid solution into separating pipet #1 and add 35 ml of precooled diisopropyl ether.
11. Agitate for 1 min with vacuum applied to the goose-neck pipet.
12. Allow the two phases to separate for 1 min and expel the acid layer back into the round-bottom flask. Retain the ether layer in pipet #1.
13. Repeat steps #10 through 12 with goose-neck pipet #2.
14. Discard the acid layer of pipet #2 and combine the ether layer in pipet #2 with the ether layer in pipet #1.
15. Acid wash the combined ether layers in pipet #1 with 20 ml of 8 N HCl. Repeat for a total of five washings.
16. Back extract the $Fe^{52}Cl_3$ into 15 ml of distilled H_2O. Repeat for a total of three back extractions. Collect the aqueous phases in a 125-ml Erlenmeyer flask fitted with a ground-glass stopper. The $Fe^{52}Cl_3$ is passed into an adjoining enclosure for further processing.

CONVERSION OF $FE^{52}Cl_3$ TO FE^{52} CITRATE (4)

1. Evaporate the aqueous solution of $FeCl_3$ to near dryness on a hot plate under a heated N_2 stream.
2. Make a dilute solution of $Fe^{52}Cl_3$ by adding 6 ml of O_2-free distilled H_2O.
3. Add 1.0×10^{-2} mM of ascorbic acid to reduce Fe^{+3} to Fe^{+2}.
4. Add 1.0×10^{-1} mM of sodium citrate to form the ferrous citrate.
5. Adjust the solution to pH 6 by dropwise addition of 2 N NaOH.
6. Dilute to 10 ml to give a nearly isotonic solution of Fe^{52} citrate.
7. Pass the ferrous citrate solution through a sterile millipore filter (pore size 0.22 μ) and into a sterile serum vial.

DISCUSSION

The time required for the chemical processing of Fe^{52} is 6 to 7 hr. Ferrous citrate solution for intravenous injection with a concentration of about 15.0 μCi/ml is obtained from this process. The Fe^{52} is assayed by counting the 511-keV positron annihilation gammas with a γ-ray spectrometer. The assay is done about 2 hr after the chemical separation to allow the Mn^{52m} daughter to build into equilibrium.

Of the total amount of radioiron produced about 5 to 6% is Fe^{55}, mostly by the reaction $Cr^{52}(\alpha, n)Fe^{55}$. The half-life of Fe^{55} is 2.94 years. It decays by electron capture, producing 5.6-keV X rays. The permitted continuous body burden of Fe^{55} is 1 mCi (5), so the small amount given with Fe^{52} is of no consequence as far as irradiation of the patient is concerned. The presence of the contaminant (Fe^{55}) may be important if Fe^{55} is used as a tracer isotope in the same patient. About 0.05% Mn^{52} is also present in the tracer as a contaminant. This has a half-life of 5.6 days and decays 65% by electron capture and 35% by positron emission to stable Cr^{52}. Mn^{52} is produced by isomeric

transition of 0.05% of the metastable Mn^{52m} (6). The separzted Fe^{52} has a straight-line decay curve through about nine half-lives when the Fe^{55} is excluded from the counting.

Spectrographic analysis of the Fe^{52} citrate solution shows there is less than 1.0 μg of Cr, 300 μg of Fe, and 1.0 μg of Mn in the total solution. The rather large amount of iron is due to iron in the chromium target material and in the chemical reagents. The specific activity is about 0.5 μCi of Fe^{52} per μg of iron, however, which is high enough for the intended use. By the use of enriched Cr^{50} as the target material, we could increase the yield of Fe^{52} by a factor of about 20.

SUMMARY

A method is described for the production and chemical separation of radioactive Fe^{52} for clinical use. Iron 52 in the form of ferrous citrate is being used to determine the distribution of erythropoietic bone marrow in both animal and human subjects with the positron scintillation camera. Detailed descriptions of the target preparation, cyclotron irradiation and chemical processing of the Fe^{52} are given.

ACKNOWLEDGMENTS

The authors wish to thank Will D. Phillip and the Health Chemistry Group for design of the shielding and remote handling apparatus, and Bill Abrams for preparation of the pressed Cr targets. We are grateful to the 88-in. cyclotron group for carrying out the bombardments.

REFERENCES

1. Juliano, J. O.; Kocher, W. C.; Naiman, T. O., and Mitchell, A. C.; Phys. Rev. 113:602, 1959.
2. Anger, H. O., and Van Dyke, D. C.; Science 144:1587-1589, 1964.
3. Hillebrand, W. F., and Lundell, G. F.: Applied Inorganic Analysis, New York, Wiley and Sons, 1953, p. 134.
4. Glen, H. W.; private communication, 1962.
5. National Bureau of Standards Handbook, No. 69, 1959, p. 30.
6. Strominger, D.; Hollander, J. M., and Seaborg, G. T.; Rev. Phys. 30:627, 1958.

Received July, 1964.

Bone Blood Flow Shown with F^{18} and the Positron Camera

Donald Van Dyke, Hal O. Anger, Yukio Yano and Carlos Bozzini

The use of the short-lived positron-emitting isotope of fluorine (F^{18}) and the positron camera (1) provides a unique method for demonstrating the distribution of fluoride in the living animal or human subject. Fluoride ion taken into the body is promptly deposited in the skeleton or excreted via the kidneys. The uptake by other tissues is very low (2,3,4). The initial uptake of fluoride by bone occurs primarily by exchange (5). The incorporation of fluoride within the bone lattice is a much slower process (3). Since the blood level is high for only a short time following intravenous injection, the rapid process of exchange dominates, and the distribution of the tracer within the skeleton depends on its rate of delivery to bone, i.e., on the blood supply to bone, and on the extraction efficiency of different parts of the skeleton. Bauer and Wendeberg (6) have proposed that the uptake of Ca^{47} and Sr^{85} can be used to quantitate the accretion rate of bone crystal in normal bone or bone lesions. Blau et al. (7) have concluded: "Uptake of these agents has been found in areas of bone activity whether osteolytic or osteoblastic, suggesting that the mechanism of localization involves exchange with exposed bone crystal rather than a metabolic process." Copp (8) states: "There is also very rapid movement of Ca^{47} into bone, the limiting factor apparently being the bone blood flow." Frederickson et al. (9) conclude that the clearance of bone-seeking radioisotopes from the blood provides an estimate of bone blood flow, the validity of which is dependent upon the efficiency of removing the isotopes from the blood as it passes through the skeleton. This paper correlates skeletal F^{18} distribution with skeletal growth rate, hypophysectomy, experimentally induced changes in temperature, fracture healing and with Paget's disease.

MATERIALS AND METHODS

The positron camera (1) and the method of preparation of F^{18} (4,10) have been described elsewhere. The distribution of F^{18} in the skeleton is determined by taking positron-camera pictures one hour after intravenous administration of the tracer in the form of sodium fluoride. At this time uptake by the skeleton is maximum, and the blood level has fallen sufficiently so as not to interfere.

Because of its short half-life, F^{18} delivers a relatively small radiation dose to the patient. Fifty percent of the administered dose is excreted via the urine. Assuming an intravenously administered dose of 200 μCi and a urine

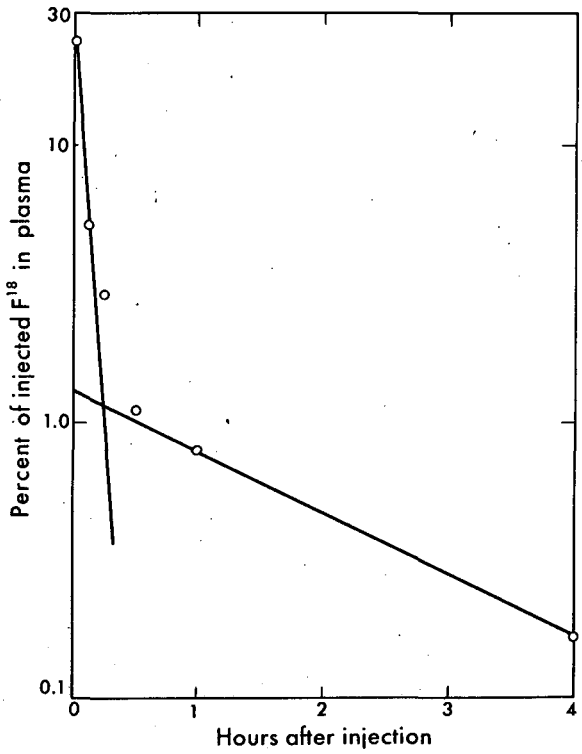

Figure 1. The disappearance of F^{18} from the plasma of normal rats. The curve can be approximated by two components with 3.5-min and 89-min half-times.

MUB-2853

output at the normal rate of 1,500 ml per day, and that the bladder is empty at the time of administration (the condition that results in the highest radiation dose), the integral radiation dose to the bladder is about 0.5 to 1 rad. If F^{18} is administered orally, the stomach receives a comparable dose. The average dose received by the rest of the body, excluding bone, is less than 20 mr. Areas of bone that concentrate F^{18} receive a higher dose that is difficult to estimate. However, assuming an extreme case where one-tenth of the administered dose is taken up by 10 g of bone, the radiation dose is still below 1 rad. These estimates are similar to those of Blau et al. (7).

For the animal studies, rats of the Long-Evans strain were used. After lightly anesthetizing them with Pentomeph, heating or cooling of their tails was accomplished by immersing the tails in water heated to 45°C or in a mixture of ice and water. This was done for a period starting one minute before and ending one hour after intravenous administration of F^{18}. Abdominal implantation of the distal portion of the tail was done as described by Huggins and Blocksom (11).

When quantitative information on the distribution of fluoride was desired, F^{18} was given intravenously, and one hour later the animal was anesthetized and thoroughly perfused with saline until the heart stopped beating. The bone was cleaned of all soft tissue and counted in a well-type scintillation counter. Hypophysectomy was performed by the parapharyngeal approach, and

completeness of hypophysectomy was determined at autopsy by examination of the pituitary site and by weighing the pituitary target organs.

RESULTS

EFFECT OF SKELETAL GROWTH ON F^{18} DISTRIBUTION IN RATS In normal adult rats, F^{18} was found to leave the plasma at a rate that could be approximated by two exponentials, as shown in Fig. 1. The curve has an initial component with a half-time of approximately 3.5 min and an intercept indicating dilution in compartments larger than the plasma volume. The second component had a half-time of 89 min. The curve was not followed long enough to determine whether or not there were other slower components. The plasma disappearance found in this study is similar to that previously reported by Wallace-Durbin (4). The uptake of F^{18} by the tibiae of rats was approximately exponential with a half-time of 10 min. Maximum uptake by the tibia was 2.5% of the injected dose in young rats (50 days of age) and 1% in adult rats.

Positron-camera pictures demonstrated that the distribution of F^{18} in the skeletons of three young, rapidly growing rats was not different from the distribution in rats of various ages up to advanced senility. Moreover, the normal pattern was not altered by hypophysectomy. Rats three days, three weeks, three months and one year after hypophysectomy showed a distribution pattern that was indistinguishable from the normal rats.

In Fig. 2 positron-camera pictures are shown of the F^{18} distribution in a) a rat hypophysectomized at age 28 days (pictures taken a year later), b) a 28-day-old normal rat, c) a one-year-old normal rat and d) a 2.5-year-old normal rat. The quantitative distribution of F^{18} in the tibiae of the hypophysectomized rat and the 28-day-old normal rat shown in Fig. 2 was determined by removing the tibiae, cutting them into transverse sections, and counting the sections in a well-type counter. The osteogenically active epiphysis in the tibia of the rapidly growing young rat took up no greater proportion of the fluoride than the osteogenically inactive epiphysis of the hypophysectomized rat. No activity was found in the marrow in either rat. Subsequent studies in children have shown that the situation in human beings is different, with marked accumulation of F^{18} in the area of active epiphyses in children.

EFFECT OF ACUTE TEMPERATURE ELEVATION ON F^{18} UPTAKE BY BONE The experiment described in MATERIAL AND METHODS, in which a rat's tail was heated or cooled, was designed to determine the effect of temperature on F^{18} uptake by the caudal vertebrae. The fraction of injected dose taken up by the caudal vertebrae of rats with tails heated in water at 45°C and by controls with tails left at room temperature is shown in Fig. 3. Heating the tail for a period starting one minute before and ending one hour after F^{18} administration resulted in a marked increase in uptake by the caudal vertebrae. The uptake in the caudal

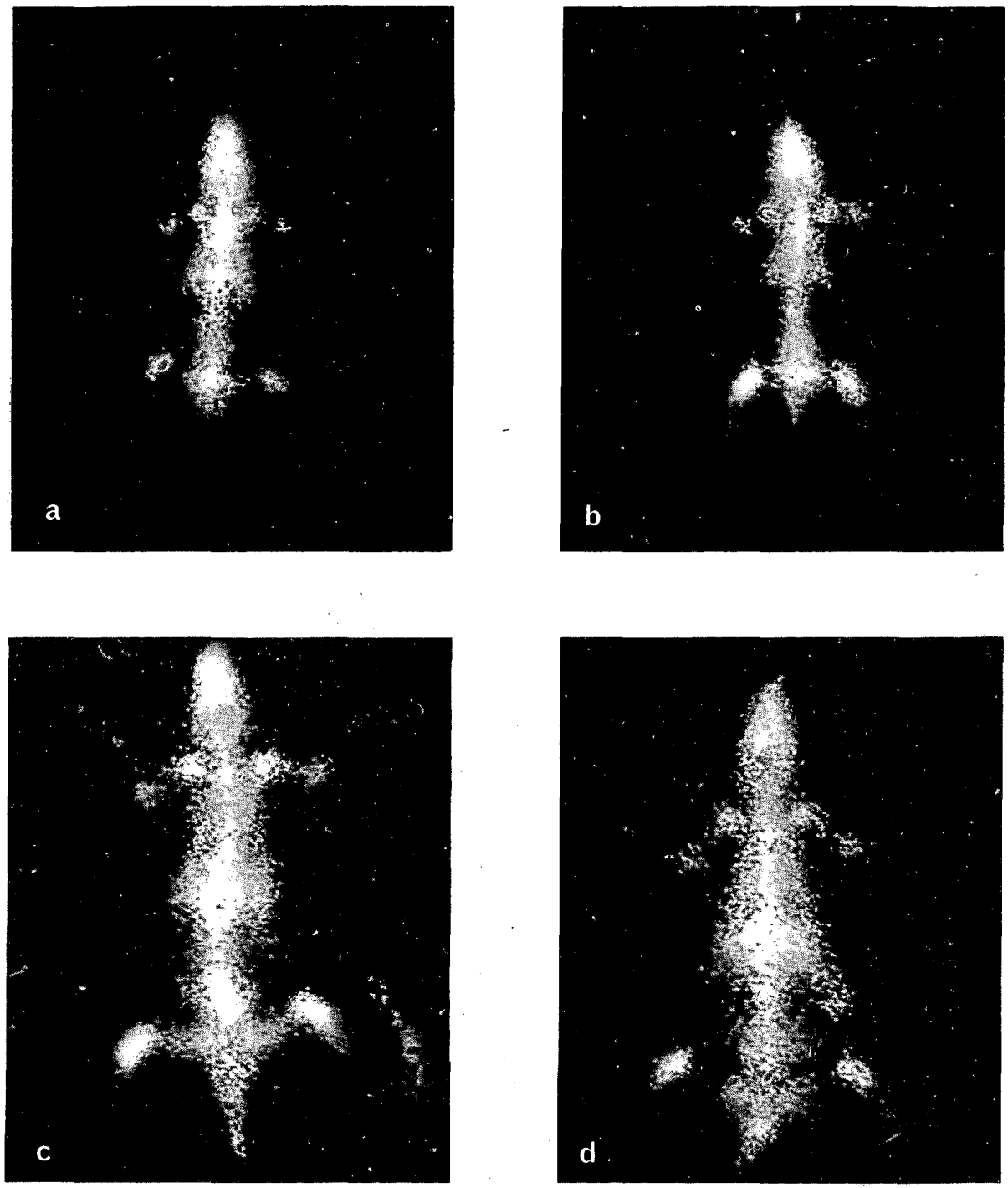

Figure 2. Positron-camera pictures of F^{18} distribution in rats with markedly different skeletal growth rates: (a) a rat hypophysectomized at age 28 days (pictures taken a year later); (b) 28-day-old normal; (c) one-year-old normal; and (d) 2.5-year-old normal. The pictures were taken with the rats under ether anesthesia one hour after intravenous administration of F^{18}.

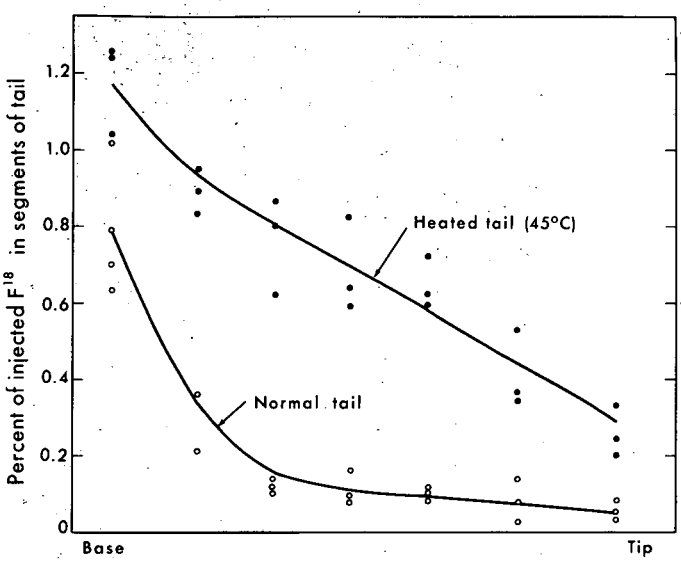

Figure 3. Uptake of F^{18} into the caudal vertebrae of rats with tails that had been immersed in warm water. Normals are shown for comparison.

MUB-2851

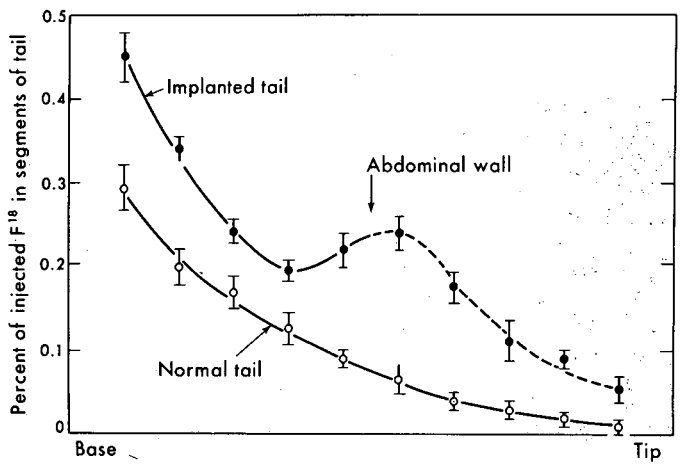

Figure 4. Effect of abdominal implantation of F^{18} uptake by caudal vertebrae of the rat. The broken line indicates the implanted segment. The bars indicate standard error of the mean of five rats. F^{18} uptake was determined 28 days after implantation.

MUB-4896

vertebrae of rats with tails immersed in ice water was only slightly less than that of the controls kept at room temperature.

EFFECT OF CHRONIC TEMPERATURE ELEVATION ON F^{18} UPTAKE BY BONE The classic experiments of Huggins and Blocksom (11), in which hemopoiesis was induced in the distal caudal vertebrae by implanting the tip of the tail in the abdominal cavity, was repeated in order to determine the effect on F^{18} uptake. After 28 days of implantation, F^{18} was administered intravenously and one hour later the rats were anesthetized with ether and perfused with saline until the heart stopped beating. Dilation of the caudal veins in the implanted segment was apparent when the abdomen was opened. The percentage of F^{18} taken up by the caudal vertebrae is shown in Fig. 4. The uptake of fluoride was increased to some

extent along the entire length of the tail and was markedly increased in the implanted segment. The implanted segment took up approximately three times as much fluoride as the corresponding segment in a normal rat. Presumably, the reason for increased uptake in the unimplanted length of tail, as suggested by Huggins and Blocksom (11), is the elevation of temperature of the entire tail through being held closely to the body. When the vertebrae in the implanted segment were cleaned and dried, they weighed 20% more than the corresponding bones of the controls. The soft tissue of the tail contained a negligible amount of F^{18} compared to the bone.

DISTRIBUTION OF F^{18} IN SKELETONS OF DIFFERENT SPECIES The distribution of F^{18} in the skeleton of five New Zealand white rabbits, three dogs, three cynomolgous monkeys and one opossum was studied. All were normal adults and all pictures were taken one hour after intravenous injection of 50 μCi of F^{18}. The distribution of F^{18} in the skeleton of a) a New Zealand white rabbit, b) a beagle dog, c) an opossum and d) a cynomolgous monkey is shown in Fig. 5. The distribution in the various species shows interesting variations. In the rabbit, F^{18} is fairly evenly distributed throughout the skeleton except for slight concentration in some of the joints of the extremities and heavy concentration in the skull. In the dog, F^{18} is heavily concentrated in the joints of the extremities and in the jaw. The bladder containing F^{18} is also visible. The distribution in the opossum is similar except for heavier uptake in the skull. The monkey differs from the other animals shown, in that F^{18} is heavily concentrated in the spine with relatively little uptake in the extremities. The autoradiograms presented by Appelgren et al. (12) show a heavy accumulation of F^{18} in the upper and lower jaws of the rat.

ACCUMULATION OF F^{18} AT FRACTURE SITES In human beings F^{18} has been found to concentrate at the site of fractures studied from two weeks to three years post-fracture when healing was normal. The same high uptake is found at the site of fractures with non-union of two to three years. Positron-camera pictures of the distribution of F^{18} in a 19-year-old girl four months after a fracture of the middle of the right femur are shown in Fig. 6. The bones of the pelvis and lower extremities and the callus at the healing fracture site can be seen. The fractured femur took up more F^{18} along its entire length than did the uninvolved femur. The bright circular area is the bladder. The rate of mixing and clearance of F^{18} from the blood of the same subject is shown in Fig. 7. The concentration fell to 20% of its maximum value in 100 min. The maximum counting rate over the knee occurred at 20 min. Approximately 25% of the injected dose was excreted in the urine in two hours.

F^{18} DISTRIBUTION IN PAGET'S DISEASE Positron-camera pictures of the distribution of F^{18} in four patients with Paget's disease have shown that the distribution in the skeleton corresponds to the distribution of the bone involvement

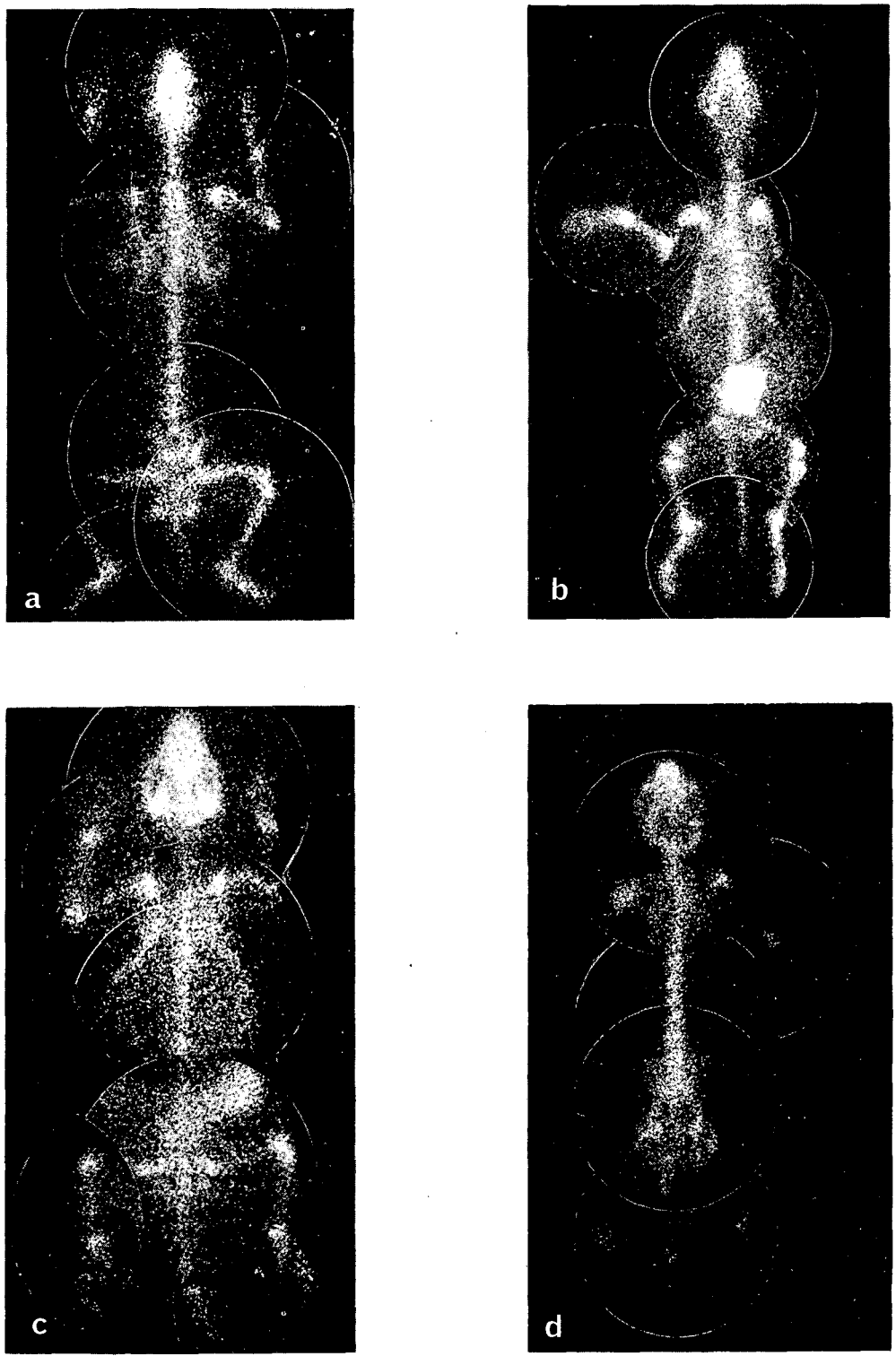

Figure 5. Distribution of F^{18} in the skeleton of a rabbit (a); dog (b); opposum (c); and monkey (d). All were normal adults.

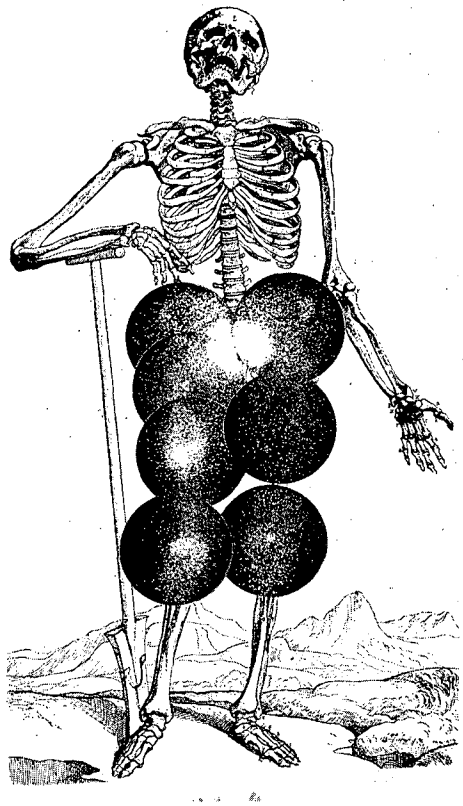

Figure 6. Positron-camera pictures of the distribution of F^{18} in a 19-year-old girl four months after a mid-femoral fracture. The distribution of erythropoietic marrow (Fe^{52}) in this same patient has been published (1).

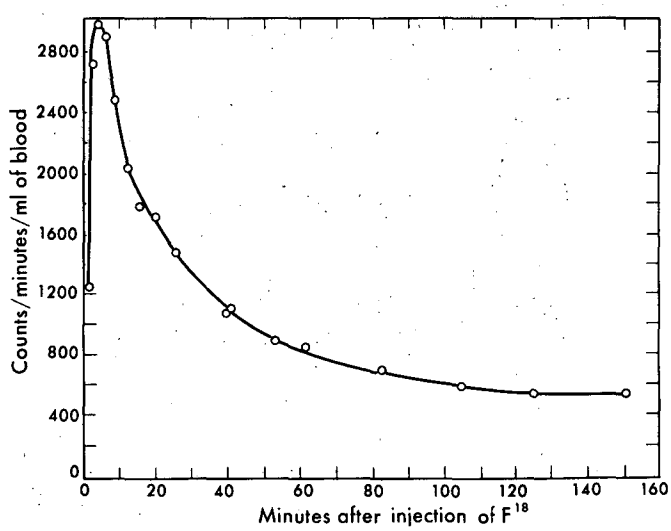

Figure 7. Rate of mixing and clearance of F^{18} from the blood of subject shown in Fig. 6.
MUB-2852

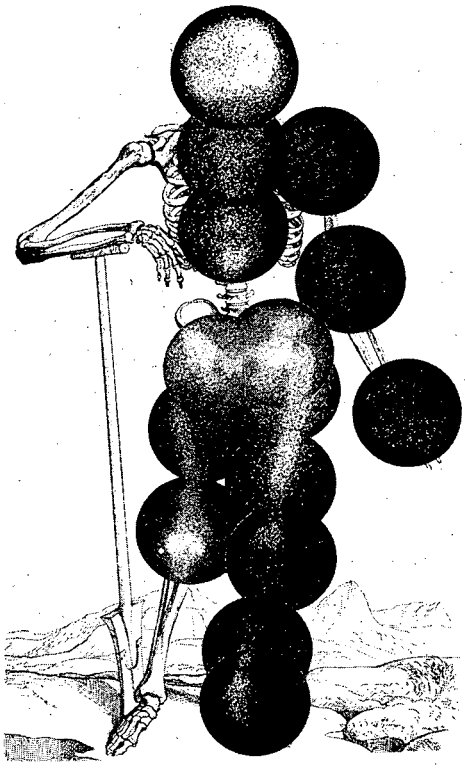

Figure 8. Positron-camera pictures of the distribution of F^{18} in a patient with advanced Paget's disease.

as demonstrated by roentgenograms. Pictures of the distribution in a patient with far advanced Paget's disease are shown in Fig. 8. Abnormal uptake is shown in the skull, pelvis, left femur and ankle, right knee, and two areas in the spine.

DISCUSSION

The amount of F^{18} deposited in bone after a period of time is the product of three factors: rate of blood flow, efficiency of extraction of F^{18}, and the integral with respect to time of the concentration of F^{18} in blood, assuming no loss of F^{18} from the bone and no saturation effects. This can be expressed in the following equation:

$$F^{18} \text{ deposited in bone } \left[\frac{\mu Ci}{g}\right] = \text{Blood flow } \left[\frac{ml}{g\ sec}\right] \times \text{fraction exchanged in each passage} \times \int_0^t \text{concentration of } F^{18} \text{ in blood} \left[\frac{\mu Ci}{ml}\right] dt .$$

If one is concerned only with the relative distribution of F^{18} in different parts of the skeleton, the time integral of concentration of F^{18} in blood is not a factor, assuming that rapid and complete mixing occurs in the blood. Then the amount of F^{18} deposited in different bones is determined by the rate of

blood flow and the efficiency of extraction. If the efficiency of extraction is uniform throughout the skeleton, then the rate of blood flow becomes the determining factor in the distribution.

An estimation of total skeletal blood flow can be obtained from the F^{18} plasma-disappearance curve and the skeletal-uptake curve if the assumption is made that the bone clears 100% of the F^{18} in each passage. Integration of the plasma-disappearance curve for rats in Fig. 1 shows that the average concentration of F^{18} in the plasma during the first hour after intravenous injection was 2.9% of the injected dose. Total uptake by the skeleton at the end of one hour was 30% of the injected dose. Therefore, during one hour the skeleton cleared slightly over 10 times the plasma volume, or 17% of the plasma volume per minute. Since the plasma volume of the rats was probably about 7.8 ml (2.8% of 277 g), the blood flow to the skeleton was 1.3 ml of plasma or 2.4 ml of blood per minute. If the extraction efficiency of bone for F^{18} is less than 100%, the skeletal blood flow estimated by this method will be proportionately higher, so the figure given here, based on complete clearance, represents a minimum value.

If the cardiac output of rats is taken as 21 ml of blood/100 g/min (13), the rats in this study had a cardiac output of 58 ml/min of blood or 31 ml/min of plasma. The minimum value for skeletal blood flow is therefore 4.3% of cardiac output.

Other researchers have measured skeletal blood flow by methods based on the assumption that the clearance of bone-seeking isotopes from the blood is complete on a single passage through the skeleton, an assumption that has not yet been proved. Weinman *et al*. (14) estimate from skeletal clearance of Ca^{47} and Sr^{85} that the minimum fraction of cardiac output going to the skeleton ranged from 7.7% to 10.1% in immature dogs, and from 5.2% to 6.9% in mature dogs. Frederickson *et al*. (9) measured the initial uptake of Ca^{45} in the skeleton of rats and obtained a value for bone blood flow of 5% to 8% of cardiac output. Copp *et al*. (15) using Ca^{45} estimate 5% in the dog, and Ray and co-workers (16) estimate 3.5% to 9.3% in the dog.

If one could isolate an artery supplying only bone and a vein draining the same region of the bone, skeletal fluoride-extraction efficiency could be measured directly. Since the nutrient arteries going to bones supply the marrow as well (17), and the distribution of blood between bone and marrow is not known, direct measurements of bone extraction efficiency are not possible. Branemark (18) states that the bone-marrow arteriole divides dichotomously into capillaries. These run to sinusoids within the marrow which are drained by venules into collecting venules which empty into the central vein. Blood cells may bypass a sinusoid by flowing through a shunting capillary directly into a venule,

thus avoiding all contact with bone. Capillaries stemming from marrow arterioles enter the Haversian canals to supply endosteal parts of diaphyseal bone. The capillaries then swing back into the marrow to empty into sinusoids or directly into collecting venules.

We have not been able to demonstrate conclusively whether differences in extraction efficiency are partly responsible for the uneven skeletal uptake of intravenously administered F^{18}. However, if one assumes that differences in extraction efficiency are largely responsible for F^{18} distribution, one must assume that the bone chemistry varies as a result of the various pathological and experimental conditions described here. Although immersing the tail of rats in warm water could conceivably alter bone chemistry sufficiently in a few minutes to result in a fourfold increase in extraction efficiency, a more likely explanation would seem to be an increase in blood flow. Although there are marked changes in bone structure in Paget's disease that might be associated with changes in bone chemistry, it is well known that the lesions of Paget's disease are associated with extreme vascularity (19).

SUMMARY

Development of the positron camera has made it possible to obtain rapidly pictures of the distribution of radioactive fluorine 18 in the living animal or human being. The distribution of F^{18} administered intravenously as fluoride ion is uneven in the normal skeleton. Furthermore, it is markedly altered in pathological conditions and accumulates at fracture sites, tumor sites, and in the lesions of Paget's disease. The initial uptake of fluoride in bone is dependent on the rate of delivery of the isotope to each bone (blood-perfusion rate) and the extraction efficiency of that bone. Evidence is presented indicating the fluoride distribution in the skeleton is determined by differences in blood-perfusion rate to the various bones rather than differences in extraction efficiency. We suggest that F^{18} distribution is an indicator of blood flow to bone.

ACKNOWLEDGMENTS

The authors are indebted to Dr. C. W. Asling of the Department of Anatomy, University of California, for providing the hypophysectomized rats used in these studies.

This work was supported in part by the United States Atomic Energy Commission and by Cancer Research Funds of the University of California.

REFERENCES

1. Anger, H. O.; Van Dyke, D.; Gottschalk, A.; Yano, Y., and Schaer, L. R.; Nucleonics 23, No. 1, 57-62, 1965.
2. Carlson, C. H.; Singer, L., and Armstrong, W. D.; Proc. Soc. Exptl. Biol.

Med. 103:418-420, 1960.
3. Hodge, H. C.; Metab. Interrelations 4:250-262, 1952.
4. Wallace-Durbin, P.; J. Dental Res. 33:789-800, 1954.
5. Neuman, W. F., and Neuman, M. W.: The Chemical Dynamics of Bone Mineral, Chicago, University of Chicago Press, 1958.
6. Bauer, G. C. H., and Wendeberg, B.; J. Bone and Joint Surg. 41B:558-580, 1959.
7. Blau, M.; Nagler, W., and Bender, M. S.; J. Nucl. Med. 3:332-334, 1962.
8. Copp, D. H.; Am. J. Med. 22:275-285, 1957.
9. Frederickson, J. M.; Honour, A. J., and Copp, D. H.; Federation Proc. 14: 49, 1955.
10. Thomas, C. C., Jr.; Sondel, I. A., and Kerns, R. C.; personal communication.
11. Huggins, C., and Blocksom, B. H., Jr.; J. Exptl. Med. 64:253-274, 1936.
12. Appelgren, L. E.; Ericsson, Y., and Ullberg, S.; Acta Physiol. Scand. 53:339-347, 1961.
13. Bullard, R. W.; Federation Proc. 15:28, 1956.
14. Weinman, D. T.; Kelley, P. J.; Owen, C. A., and Orvis, A. L.; Proc. Staff Meetings Mayo Clinic 38:559-570, 1963.
15. Copp, D. H.; Mensen, E. D., and McPherson, G. D.; Clin. Orthopaed. 17:288-296, 1960.
16. Ray, R. D.; Aouad, R., and Galante, J.; Soc. Internat. de Chir. Orthop. de Traumatol Symposium Presentis au IX Congres 1:6-9, 1963.
17. Root, W. S.; in Handbook of Physiology, Section 2. Circulation, Vol. 2, edited by W. F. Hamilton and P. Dow, Washington, D. C., Am. Physiol. Soc., 1963.
18. Branemark, P. I.; Scand. J. Clin. Lab. Invest. 11:Suppl. 38, 1959.
19. Edholm, O. G.; Howarth, S., and McMichael, J.; Clin. Sci. 5:249-260, 1945.

Carlos Bozzini is a postdoctoral fellow from the University of Buenos Aires, Argentina.

Received December, 1964.

An Improved Liquid Scintillation Counting Method for Fe^{55} and Fe^{59} in Blood

Hiroshi Saito

The simultaneous use of Fe^{55} and Fe^{59} was introduced by Peacock and co-workers (1) in 1946. Saylor and Finch (2) applied the two isotopes of iron for the study of iron absorption in 1952, and further studies (3,4) were later reported. However, counting of the weak 5.9-KeV X ray from the Mn^{55} daughter of Fe^{55} required time-consuming and laborious processing, such as wet ashing (1), purification by repeated sedimentation and electroplating on a copper planchet (5). The poor counting efficiency in Geiger-Muller or gas-flow counters was also a great disadvantage of this method.

High counting efficiency was reported by Dern, using a liquid scintillation counter (6-8). However, Dern's procedure is complex and leaves an uncertainty as to the degree of decolorization and the amount of excess perchloric acid remaining in each sample after the reaction. Moreover, when his method is used a yellowish color often reappears, in spite of the addition of ascorbic acid, a strong chemical quenching agent. In the method reported here these problems are largely eliminated.

MATERIALS AND METHODS

COUNTER AND COUNTING SOLUTION A Nuclear-Chicago 720 series liquid scintillation counter was used. The primary solute of the counting solution consisted of 4.0 g PPO with toluene to bring the final volume to one liter. Counting vials were of low-activity glass by Packard. One milliliter of human whole blood or serum, radioiron-labeled *in vivo*, was used for each sample.

DRY ASHING Three milliliters of concentrated HNO_3 was added to each sample in a 20-ml Erlenmeyer pyrex flask and dried at 100°C (with an infra-red lamp or an oven) and was then ashed in an oven at 600°C for about 4 hr. No loss in activity of the samples tested was observed in dry ashing, as seen in Table 1a and b.

However, ashing of plasma alone without carrier iron sometimes resulted in poor recovery. Therefore the addition of an adequate amount of elemental iron was required to stabilize the recovery after ashing. If the subject's red cells are not radioactive, and his hematocrit stays constant, the subject's

Table 1a. Recovery of radioiron in the erythrocytes of 1 ml blood after ashing

Whole blood sample	% Recovered
1	98.0
2	103.9
3	99.2
Average	100.3±2.5

Table 1b. Recovery of serum-bound radioiron after ashing with 2.5 mg of $FeCL_3$ and 1 ml of HNO_3

Plasma sample	% Recovered
1	101.3
2	99.0
3	98.7
Average	99.7±2.0

whole blood should be used instead of adding carrier iron to his plams. The percent utilization figure can then be obtained comparing the zero-time plasma activity with the red-cell activity after utilization.

PURIFICATION OF IRON One milliliter of concentrated hydrochloric acid was added to the ash in the flask. After the sample was completely dissolved, the solution was transferred to a 15-ml centrifuge tube. (Slight warming shortens the dissolving time.) Then sodium hydroxide solution in sufficient amount to convert $FeCl_3$ into $Fe(OH)_3$ was added and the sample was centrifuged for 5 min. Carrier solution containing 1.0 mg of $FeCl_3$ was added to the supernatant and the sample was centrifuged again. (If this procedure is omitted, recovery decreases to 90%.) The supernatant was decanted and the precipitate rinsed with neutral distilled water. Loss of radioiron from three samples averaged 2.7±1.6% in the process of purification (Table 2). The loss was 1.1± 2.4% in transferring the sample from a test tube to a vial. Use of a siliconized centrifuge tube was not adequate to prevent this loss.

Table 2. Percent loss by purification

Whole blood sample	% Loss
1	1.7
2	5.0
3	1.3
Average	2.7±1.6

DECOLORIZATION One milliliter of diluted phosphoric acid solution, equivalent to 0.025 ml of 85% phosphoric acid, was added to the $Fe(OH)_3$ at the bottom of the centrifuge tube. The material was stirred and warmed until it

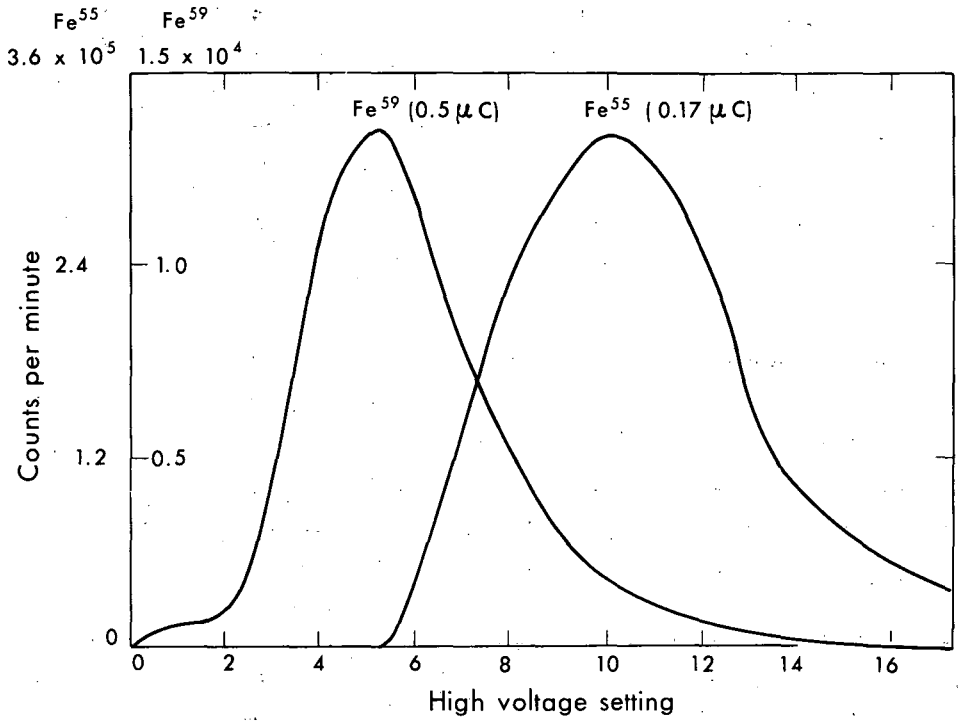

Figure 1. Energy spectra of Fe^{55} and Fe^{59}, from which the voltage to maximize counts of each isotope is obtained.

MUB-3757

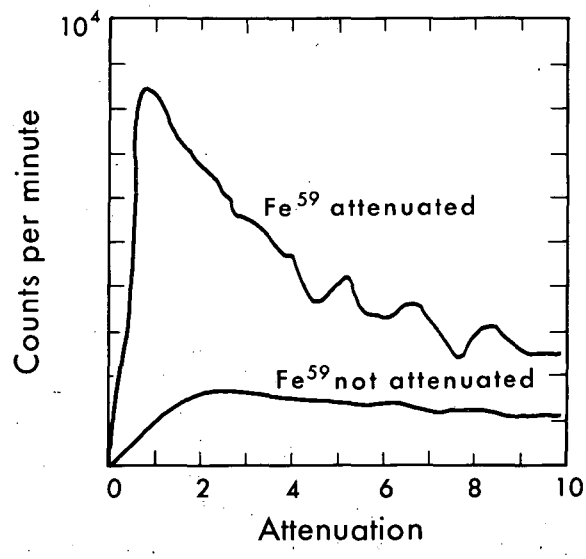

Figure 2. Fe^{59} spectra attenuated and not attenuated at the optimal voltage for Fe^{55} counting.

MUB-3754

dissolved in the phosphoric acid. This was transferred, rinsing twice, to a counting vial that was then heated on an electric hot plate until the water was thoroughly evaporated. (To prevent boiling, splashing and over-drying of the sample, mild heating is important. If the sample is not dried completely, it becomes cloudy when alcohol is added. If cloudiness does occur, the alcohol and water are evaporated by heating, and then cloudiness will not appear when alcohol is added. If the sample is dried excessively, addition of water and re-evaporation will save the sample.) The vial was then cooled and one milliliter of absolute alcohol added to dissolve the material. The vial was then shaken by hand for complete mixing, and 10 ml of scintillator solution added to the vial. This was then counted in the liquid scintillation counter.

The process of purification and decolorization can be summarized as follows:

$$\text{Iron in dry ash} \xrightarrow{HCl} FeCl_3 \xrightarrow{NaOH} Fe(OH)_3 \xrightarrow{H_3PO_4} FePO_4 .$$

PREPARATION FOR THE COUNTING OF TWO ISOTOPES OF IRON SIMULTANEOUSLY The high voltage was varied with the standard sample of each isotope to obtain energy spectra as shown in Fig. 1. From these curves, an optimal voltage was obtained to maximize the count of each isotope. At the optimal voltage for Fe^{55} counting, Fe^{59} counts were maximized by using the attenuator. The effect of attenuation is shown in Fig. 2.

SIMULTANEOUS COUNTING OF FE^{55} AND FE^{59} The channels ratio method makes possible the counting of two isotopes simultaneously (9,10). The discriminator settings used here for Fe^{55} and Fe^{59}, and the corresponding channels in which counts were recorded, are shown in Fig. 3. The discriminator L_2 for channel A (L_2-L_5) and channel B (L_2-L_4) was set at 0.9 so that only 0.1% of the Fe^{55} counts appeared in channels A and B.

If quenching occurs, a shift in the spectrum results, and the ratio $R_1 = \frac{B}{A}$ (the ratio of counts in channel B to those in channel A) is an index of the degree of quenching. A setting of 3.0 for discriminator L_4 was found to yield a value of $R_1 = 0.5$, which keeps channel B sufficiently sensitive to quenching and also minimizes the effect of shifting of the spectrum when counting samples of varied activity. An increase in R_1 indicates a shift of the spectrum by quenching and a corresponding increase of counts from Fe^{59} appearing in channel C. The total counts in channel C consist of the Fe^{59} counts (C_{59}) and counts from Fe^{55} (C_{55}). The curve in Fig. 4a was obtained from an iron 59 standard at varying degrees of quenching. For any sample counted, R_1 and A_{59} are known, and C_{59} is obtained from Fig. 4b. A value for C_{55}, uncorrected for quenching, is then obtained from the total counts in C less C_{59}. A quenching curve was obtained with a series of increasingly quenched standards as shown in Fig. 4b. It was not possible to achieve a completely unquenched sample, but the

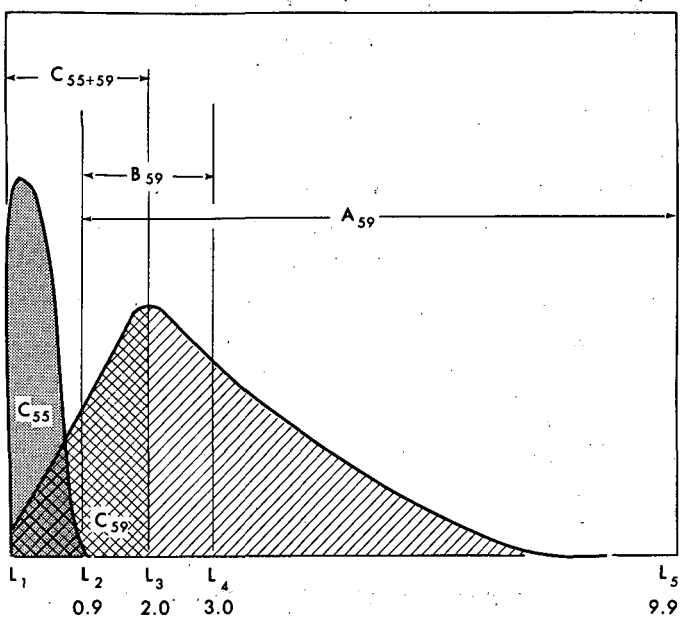

Figure 3. Discriminator settings used in this study.

MUB-4229

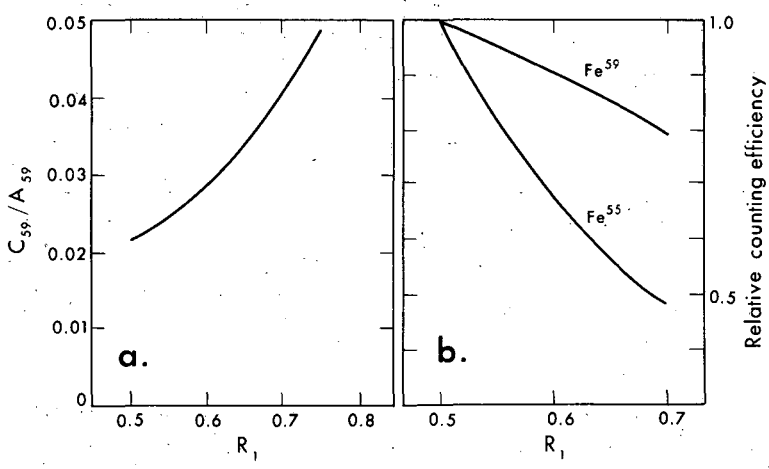

Figure 4a. Fraction of Fe^{59} counts in channel A appearing in channel C (C_{59}) at various grades of quenching.

Figure 4b. Relative counting efficiency of Fe^{59} and Fe^{55} obtained by quenching samples.

MUB-3753

value of R_1 for the least quenched sample was 0.48. For each sample then, the value of R_1 is used to obtain a relative counting efficiency for Fe^{55} from Fig. 4b. The net Fe^{55} count, C_{55}, is then divided by the relative counting efficiency from Fig. 4b to yield a value corrected for quenching.

A sample of Fe^{55} containing 0.0025 ml of 85% phosphoric acid, 0.2 ml alcohol and 3 lambda of water was successively quenched by the addition of increments of alcohol, as shown in Fig. 5. By extrapolation of this curve to zero milliliter of alcohol, a theoretical, maximum-possible counting efficiency of 19% is obtained for Fe^{55}.

More Fe^{55} counts may be obtained by setting the upper discriminator for channel C (L_3) at its maximum value of 9.9. With the attenuation settings used for these experiments, about 10% of the Fe^{59} counts in channel A appeared in C when L_3 = 9.9, but only 2.4% when L_3 = 2.0, the latter a little higher than the upper end of the Fe^{55} spectrum. Thus, it is possible to reduce C_{59} with a small sacrifice in the net counts of C_{55} to improve the accuracy in the value of R_1. If the counts in channel A are too low, R_1 is not accurate. In such a case, counting without attenuation at the optimal voltage for Fe^{55} effectively eliminates the small fraction of Fe^{59} counts appearing in channel C.

Another method of obtaining net Fe^{55} counts from Fe^{59} counts in channel A is shown in Fig. 6. Samples with various relative amounts of Fe^{55} and Fe^{59} were counted, then each was quenched stepwise. Measured increments of acetone were added and the samples counted at each addition. A family of curves was then drawn with R_1 as a function of R_2, where $R_1 = \frac{B}{A}$ as before, and $R_2 = \frac{B}{C}$. Each curve of the family represents a different value of $\frac{C_{55}}{A_{59}}$. By using this graph, an estimation of Fe^{55} counts in an unknown sample is directly obtained from R_1, R_2 and A_{59}. Decay factors and internal standards may also be used to check the results obtained by the channels ratio method.

DISCUSSION

Ashing did not cause any loss of erythrocyte-bound P^{32} and Cr^{51}. However, the process of purification caused 97.7% loss of P^{32} and 4.9% of Cr^{51}.

A small amount of phosphoric acid and alcohol present in a sample causes chemical quenching. However, the amount of phosphoric acid and alcohol in our samples was reduced as far as is possible in the present method. Although there is a small amount of phosphoric acid in excess after the reaction with iron, this is not as strong a quenching agent as the amount of perchloric acid required for decolorization. Therefore, phosphoric acid has an advantage over perchloric acid for the decolorization of iron. In contrast to the method reported by Dern, water was practically eliminated by evaporation in this experiment. Furthermore, ascorbic acid was not needed here, since decolorization was complete.

The use of dioxane instead of toluene does not require ethyl alcohol to dissolve phosphoric acid and iron phosphate. However, turbidity was often observed when dioxane was added to a sample. This turbidity disappeared with the addition of water, but the addition of water caused quenching. Addition of water to dioxane caused more quenching than addition of alcohol to toluene in an amount sufficient to clear turbidity. Therefore dioxane was not used. POPOP was not used as a secondary solute because it did not increase counting efficiency significantly. Nitrogen gas to lessen oxygen content in a sample was not used in the present study.

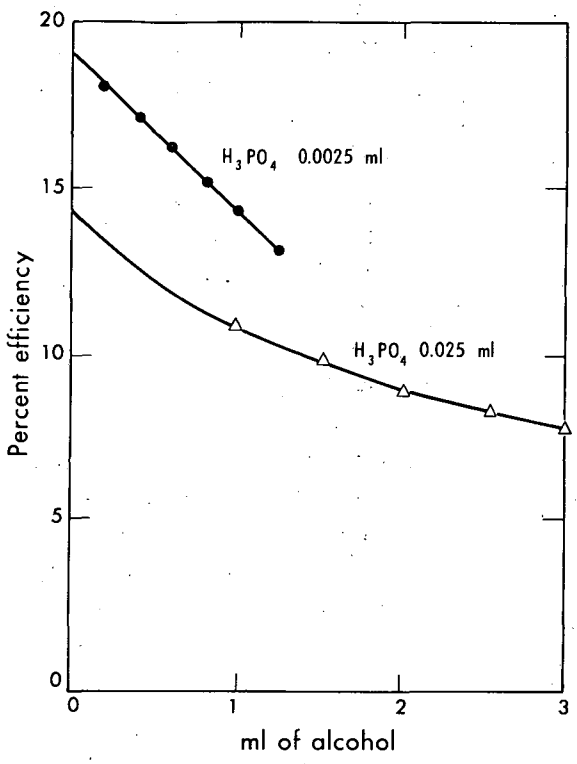

Figure 5. Curves of quenching with alcohol.

MUB-3749

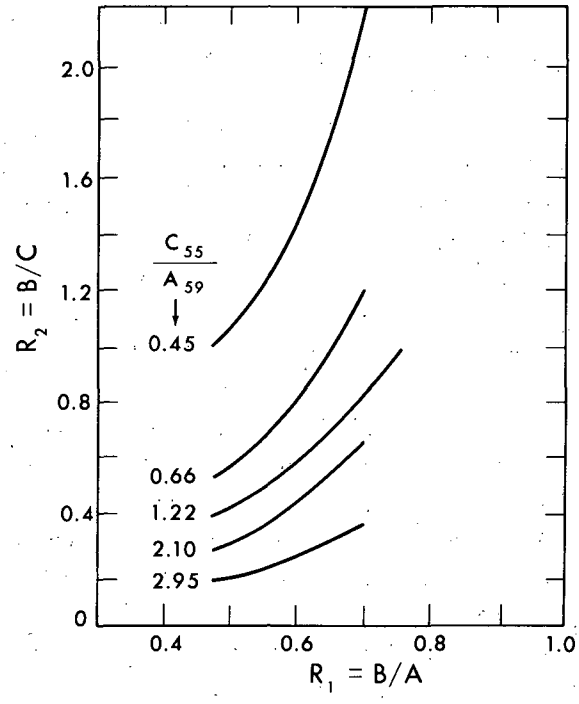

Figure 6. Ratio of Fe^{55} counts in C to Fe^{59} counts in A, at various values of R_1 and R_2.

MUB-3751

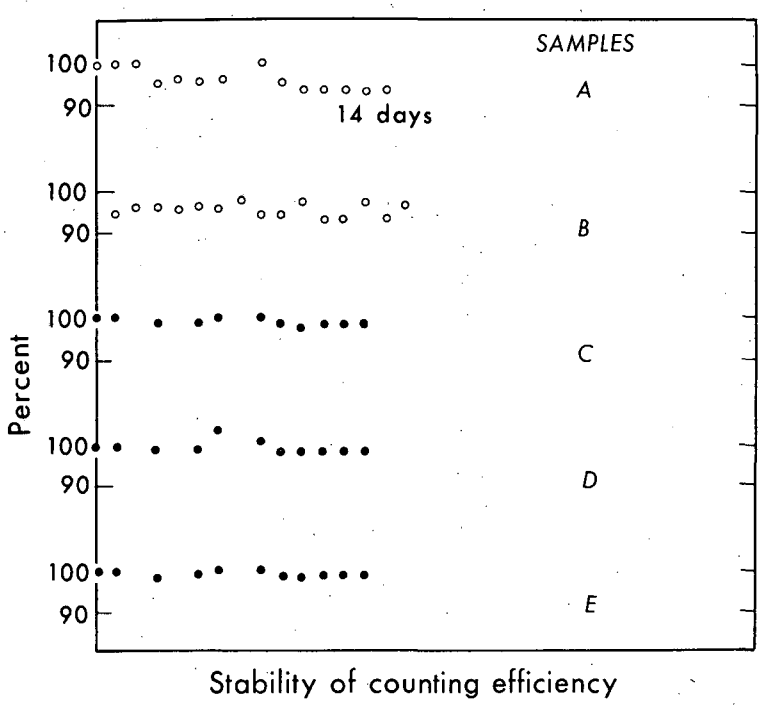

Figure 7. Samples A and B Contain 1 ml alcohol to 14 ml toluene. Samples C, D and E contain 1 ml alcohol to 10 ml toluene. Fe^{55}: open circles; Fe^{59}: closed circles.

MUB-3750

The samples prepared by this method were stable, as shown in Fig. 7. No development of color was observed after six months. The counting efficiency for Fe^{55} was always about 10% and for Fe^{59} 70% when a standard solution of 2.5 mg carrier $FeCl_3$, 0.025 mg of 85% phosphoric acid, 1.0 ml of C_2H_5OH, and toluene-PPO was used. In some cases, because of carrier iron and probably impurities, a small amount of transparent or nebula-like precipitate was observed. A slight decrease of counting efficiency after several weeks was also observed in such cases. Usually these quenched samples showed restoration of initial activities by shaking. The channels ratio method is also useful to correct back to a least quenched value.

By the present method, results can be known within eight hours after sampling. Fast processing and high counting efficiency combined with accuracy and stability have not been possible by other methods so far reported.

ACKNOWLEDGMENTS

Suggestions and encouragements given by Dr. Thornton Sargent, Professor Motoharu Tanaka and William E. Siri are appreciated as is the technical assistance of Akio Miki, Patricia J. Blanche and Rosemary A. Hughes.

REFERENCES AND NOTES

1. Peacock, W. C.; Evans, R. D.; Irvine, J. H., Jr.; Good, W. M.; Kip, A. F.; Weiss, S., and Gibson, J. G.; J. Clin. Invest. 25:605, 1946.
2. Saylor, L., and Finch, C. A.; Am. J. Physiol. 172:372, 1953.

3. Bothwell, T. H.; Pirzio-Biroli, G., and Finch, C. A.; J. Lab. Clin. Med. 51:24, 1958.
4. Hallberg, L., and Sölvell, L.; Acta Med. Scand. 168, Suppl. 358, 1960.
5. Vosburgh, G. J.; Flexner, L. B., and Lowie, D. B.; J. Biol. Chem. 175:391, 1948.
6. Dern, R. J.; in Liquid Scintillation Counting, London, New York, Paris and Los Angeles, Pergamon Press, 1958, p. 205.
7. Dern, R. J., and Hart, W. L.; J. Lab. Clin. Med. 57:322, 1961.
8. Dern, R. J., and Hart, W. L.; J. Lab. Clin. Med. 57:460, 1961.
9. Nuclear Chicago Liquid Scintillation Manual, November, 1963.
10. Handler, R. W.; Dual Isotope Counting by Channels Ratio Method, Preliminary Technical Bulletin attached to the Nuclear Chicago Corporation Manual, November, 1963.

This study was performed in part at Radioisotope Laboratory, Nagoya University, School of Medicine, Nagoya, Japan.

Received September, 1964.

Blockage of Pupillodilation with Cyclotron-Accelerated Alpha Particles

Cornelius T. Gaffey and Anne K. Kelley

High energies are imparted to charged atomic nuclei by repeated accelerations across an electric field in the cyclotron, Lawrence and Livingston (1). After being extracted from the cyclotron, the ionic particles travel through evacuated tubes and are steered by magnets into selected targets. The particles travel nearly parallel and are approximately monoenergetic. The velocity of the accelerated particles approaches the speed of light (59%) and therefore they proceed with very little scattering. These physical properties of cyclotron-accelerated particles are of special value to the biologist. In 1952 Tobias, et al. (2) demonstrated that 190-MeV deuterons were capable of producing radiolesions. The nonscattering characteristic of energy-rich nucleons permitted well-defined volumes of tissue to be irradiated without appreciable damage to circumscribed cells, Tobias et al. (2,3). This newly available technique for local irradiations was used in the study of the radiosensitivity of parts of the central nervous system. Protons (Leksell (4), Lawrence (5), Tobias, et al. (6), Larsson, et al. (7), Leksell, et al. (8), Rexed, et al. (9), Andersson, et al. (10), Siegbahn and Howard (11), Larsson, et al. (12)), deuterons (Tobias, et al. (3), Anderson, et al. (13), Van Dyke and Simpson (14), Zeman, et al. (15,16)) and alpha particles (Tobias, et al. (2), Lawrence (5), Constable, et al. (17), Lawrence, et al. (18,19)) were used as neurosurgical tools for generating discrete lesions within the brain. The knowledge gained about the radiovulnerability of biological tissue lead to the therapeutic use of cyclotron-accelerated particles in the treatment of malignant tumors, Tobias, et al. (2), and radiation-hypophysectomy of cancer patients, Lawrence (5) and Lawrence, et al. (19).

Cyclotron-accelerated particles are approximately monoenergetic and thus have an almost identical range in tissue. Prior to stoppage, the ionization per unit length of track is maximized (Bragg-ionization peak). For certain types of biological studies this offers an advantage. In deep-brain irradiations the dose at the terminal of the tract is about seven times the skin dose. This variation of dose-with-distance permits internal lesions to be induced in desired sites within the brain. The Bragg-peak effect has been utilized for the investigation of connections and functions of the cerebral cortex by the production of laminar lesions with protons and deuterons, Malis, et al. (20-23), and alpha particles, Jansen, et al. (24). Rose, et al. (25) have given attention to

the regrowth process of nerve fibers in the cerebral cortex after laminar destruction with ionizing particles.

The present work was undertaken in an attempt to determine the sensitivity of the cat's pupillodilation center to cyclotron-accelerated alpha particles. A combination of techniques permitted a unique assay of the influence of 910-MeV alpha particles on this control center in the brain. The stereotaxic technique of implanting chronic electrodes into structures within the brain made possible a study of the response of the pupillodilation center to electric stimulation, Hess (26). High-energy radiation was concentrated in and restricted to the pupillodilation center by using an animal-rotational technique. An assay of the influence of radiation by electrophysiological methods has been late in arriving. Tisljar-Lentulis (27) dealt with the influence of 900-MeV alpha particles on the electroencephalographic activity of the brain of the rat. Other investigations have been concerned with the effect of alpha particles and deuterons on the bioelectric properties of sciatic nerve, Gaffey (28). The bioelectric sensitivity of components of the visual system, such as the retina, optic tract and optic chiasma to localized, alpha-particle irradiation has been reported, Gaffey (29). It was of interest to compare the present findings with data concerning lesion production by ionizing radiation.

METHODS

STEROEOTAXIC IMPLANTATION PROCEDURE Contact with the pupillodilation center (nucleus perifornicalis of the hypothalmus, Hess (26)), was made by the insertion of bipolar electrodes through burr holes in the skull of anesthetized cats, immobilized in the Lab-Tronics (Model No. 4) stereotaxic instrument. Bipolar needle electrodes, (nichrome wire 0.0089 in. in diameter) were insulated with Formvar except for 1 mm at the tips. Twin wires were attached with Epoxylite #6001 varnish to supportive steel tubing that separated the wires by 2 mm. During the implantation procedure (Delgado (30)) the cat was electrically stimulated and the bipolar electrode was finely adjusted to produce a maximum pupil size for a minimum current strength. A stimulator (Grass, Model S-4) delivered biphasic pulses at 40 cps, each pulse being 1 msec in duration. The leads from the left and right hemisphere's pupillodilation center were soldered to a radio socket (Amphenol Corp.). The wires and socket were held securely by dental plastic (a mixture of Kadon resin powder and liquid methyl methacrylate monomer from the L. D. Caulk Company) anchored to the skull by bone screws. Control and postirradiation-evoked pupillodilation responses were induced by sending current from the stimulator through a cable attached to the cat's head socket. The threshold voltage to evoke maximum pupil size was measured in a field of fixed illuminance (10^4 lumen/ft^2) which induced pupillar constriction.

IRRADIATION PROCEDURE The 184-in. frequency-modulated cyclotron supplied accelerated alpha particles for irradiations in these experiments. The

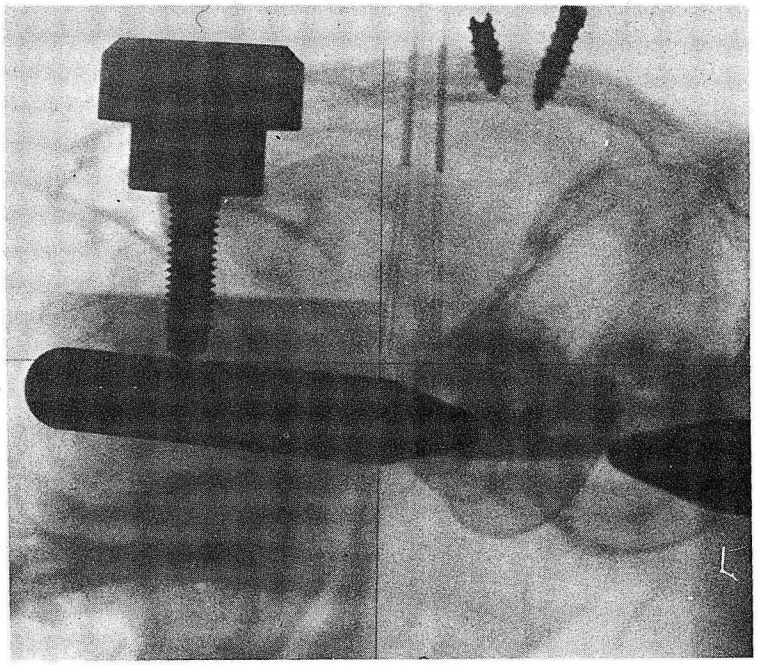

Figure 1. An X-ray photograph of the lateral view of a cat's head taken at a slant angle. The bipolar electrodes are implanted in the nucleus perifornicalis of the hypothalmus. The tip of one electrode is being aligned on the reference cross-hairs of the cyclotron beam. The head of the cat is held securely by a rigid frame with ear bars in the external auditory meatus, which are seen in this photograph as dark rods with a large set-screw.

JHL-4413

specifications of these high-energy beams have been reported by Tobias, et al. (6) and Gaffey (28). By magnetic focusing and columating techniques, alpha particles travelling at 59% of the speed of light were limited to parallel paths of approximately monoenergetic beams. The average alpha-particle-beam energy was 910-MeV/N. An ionizing chamber designed by Birge, Anger and Tobias (31) was placed immediately in front of the experimental animal and was used to measure the delivered dose. In pupillodilation experiments the mean dose rate was 1,000 rad/min. For conversion purposes we may note that 1 rad is equivalent to 1.07 R or 100 ergs absorbed per gram of tissue.

In our nucleus perifornicalis irradiation, the cat was immobilized in a stereotaxic instrument locked to a precision-machined alignment apparatus, Born et al. (32) and Welch and Tobias (33). Prior to irradiation, bipolar electrodes were implanted in the nucleus perifornicalis of the left and right hemispheres. Using the tips of the electrodes as targets at which to aim, the authors aligned the cat by means of orthogenal X rays (Figs. 1 and 2) so that the terminals of the electrodes were at the focus of a mechanical rotator and located in the center of a circular, alpha-particle beam. The electrode tips, having been uniquely located at a rotation focus, remained in the center of the irradiated volume

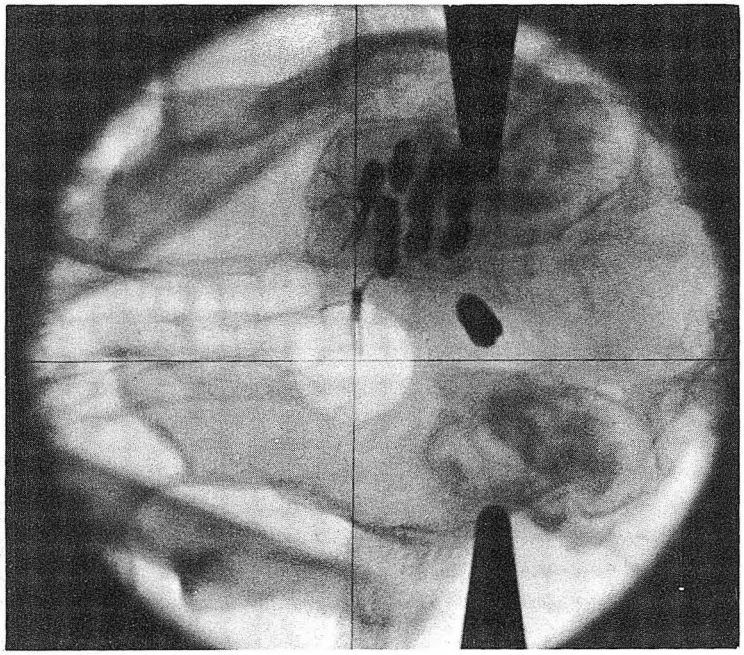

Figure 2. An X-ray photograph of the dorsal view of a cat's head taken at an acute angle. Regardless of the angle of rotation, the tip of the implanted electrode in the nucleus perifornicalis remains at the center of 1/4-in. radius 910-MeV alpha-particle beam. Nine dark dots in one quadrant of the X-ray photograph represent the pins in the radio socket on the head of the chronically implanted cat. The tilt of the cat's head makes it appear as if the ear bars are not properly inserted.

JHL-4414

when the mechanical rotator passed the head of the cat through a procession of planes and angles. By this procedure, Tobias, et al. (2), Tobias, et al. (6), it was possible to irradiate a discrete volume of brain tissue and avoid irradiating surrounding cells with a damaging dose. The range of 910-MeV alpha particles was 7 in. in aluminum and the linear-energy transfer (LET), also referred to as stopping power and rate of energy loss, was 15 MeV-cm^2 per gram, Born, et al. (32). The particles were generated in pulses averaging 500 μsec in duration at a frequency of 64 pulses per sec. The radius of the high-energy alpha-particle beam was 1/4 in. In these studies 19 adult cats were used as test animals.

RESULTS

The nucleus perifornicalis of the cat was irradiated with a beam of 910-MeV alpha particles. With dorsal X rays, the head of the cat was adjusted in the horizontal plane (Fig. 1) so that the chronically implanted electrode in the nucleus perifornicalis coincided with the cross hairs of the cyclotron's beam. In a similar manner lateral X rays were used to position the tips of the implanted electrode in the vertical plane (Fig. 2) on the reference cross hairs of the cyclotron's beam. By design, the point of intersection of the horizontal

and vertical reference cross hairs was a focus of mechanical rotation. A multiplane, translational procedure concentrated ionizing radiation within a spherical volume equivalent to the dimension of the aperture, 1/4 in. radius, of the high-energy particle beam. Each X-ray picture delivered 0.5 R to the head of the cat. Approximately six X-ray exposures were required to insure proper electrode positioning in the path of the cyclotron's beam.

On the fifth week after electrode implantation each cat was studied for responses to brain stimulation. A signal was sent from the stimulator (Grass, Model S-4) and isolation unit through a cable (Microdot Inc.) into the head socket of the cat. A 1-msec biphasic pulse delivered at 40 cps was increased in voltage until there was a maximum pupil dilation within 2 sec. This stimulus strength was referred to as threshold voltage. Both pupils were enlarged at this amplitude regardless of whether the left or right hemisphere was stimulated. Two weeks before irradiation the threshold voltage for each cat was studied for stability. All animals were stimulated in the alert state. If the variance in four tests per day proved small, the animal was considered satisfactory for experimentation.

In Fig. 3 the threshold voltage for pupillodilation before and after irradiation is presented. In this example, 24,000 rads of 910-MeV alpha particles were delivered to the nucleus perifornicalis. Immediately after exposure to the high-energy particles there was a rise in the threshold voltage, but this was held to be caused by nembutal anesthesia (Fig. 3) required for irradiation procedure. On the sixth day after irradiation the threshold voltage rose sharply to almost four times the preirradiated value and after 6 1/2 days the biological response to electrical stimulation was lost irreversibly. The electrode in the nonirradiated hemisphere did not undergo variation in threshold as a consequence of the irradiation of the contralateral hemisphere.

It is interesting to note that the onset of enhanced excitability (fourth day after the delivery of 24,000 rads of alpha particles) was coincident with pupil enlargement on the irradiated side in the absence of electrical stimulation. An example of this phenomenon is seen in Fig. 4 which shows a cat with the right pupil larger than the left. Attempts were made to reduce both pupils to the same size by using 0.5% isoptoeserine, but the enlarged pupil was resistant to this agent. A 1% isoptoatropine was effective in enlarging both pupils.

It has been found in doses below 32,000 rads delivered to the nucleus perifornicalis that the time course of the threshold voltage to evoke pupillodilation followed a biphasic pattern (Fig. 3). That is to say, after irradiation there occurred a decrease in the stimulus strength and then an increase in the threshold voltage to infinity. In these cases an imbalance in pupil size was coincident with the lowering of the threshold voltage (Fig. 4). Ultimately,

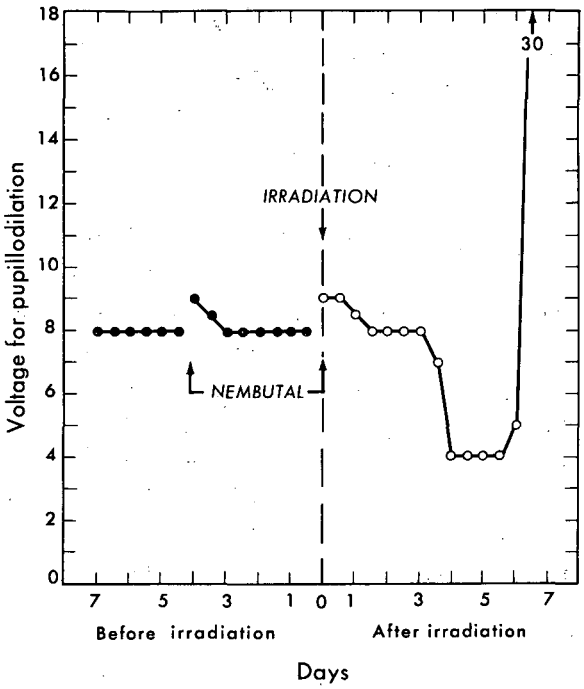

Figure 3. Variations in the stimulus strength to evoke pupillodilation before and after unilateral irradiation of the nucleus perifornicalis. In this case 24,000 rads of 910-MeV alpha particles produced a biphasic response in the threshold voltage with time. On the fourth day after local treatment with high-energy particles, the stimulus strength decreased to half of its control value. After 6 1/2 days electrical signals failed to produce pupillodilation. The implanted electrode in the contralateral hemisphere did not undergo a variation in threshold voltage as a consequence of ipsilateral irradiation.

MUB-3775

the response to electrical stimulation was lost (Table 1). It was of special interest to determine the dose of 910-MeV alpha particles that would immediately induce a loss of pupillodilation to electrical stimulation. While the cat was being irradiated at the 184-in. cyclotron, the beam was interrupted approximately every 10,000 rads. During this discontinuance of ionizing radiation, the threshold voltage to evoke pupillodilation with electrical stimulation was determined. In this procedure two cats lost their ability to respond to electrophysiological stimulation at 100,000 rads and one cat at 125,000 rads of high-energy particles. Animal survival was a severe problem with such high doses of irradiation.

The lowest dose of 910-MeV alpha particles that inhibited the action of the nucleus perifornicalis was 10,000 rads (Table 1), and this dose required 131 days to be effective. The nucleus perifornicalis of cats was irradiated with doses of less than 10,000 rads, but these doses gave no evidence of blocking the pupillodilation response evoked by electrical stimulation seven months after exposure to ionizing radiation.

In Fig. 5 has been plotted the logarithm of the dose delivered to the nucleus perifornicalis versus the postirradiation time in days for the loss of the pupillodilation response. It is clear that the relation between the logarithm of the delivered dose and the time for the blockage of the biological

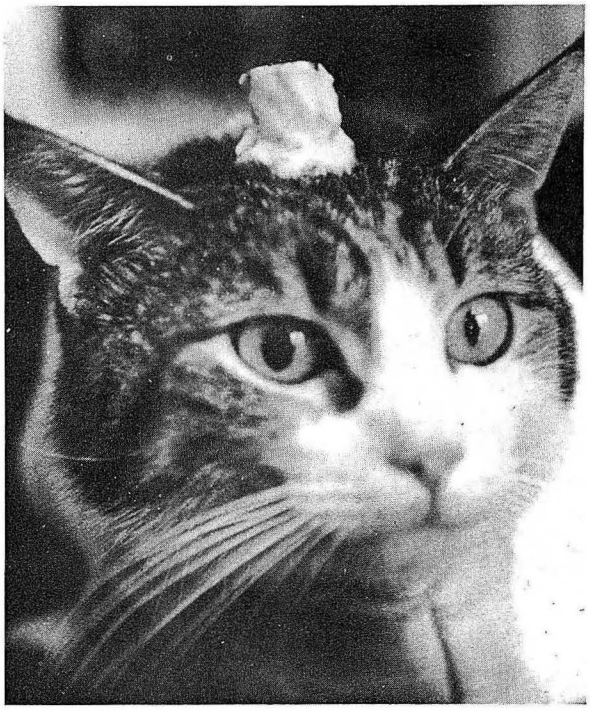

Figure 4. The action of cyclotron-accelerated alpha particles on the nucleus perifornicalis can be detected by an imbalance in pupil size. The pupil on the irradiated side develops an enlarged pupil coincident with the decrease of the stimulus threshold voltage.

JHL-3417

response is non-linear. Data to show that there was a loss of pupillodilation at 131 days for 10,000 rads is included in Table 1. The shape of the dose-response curve suggests an asymtote at 8,000 rads. However, this is not sufficient evidence to consider 8,000 rads as a minimum effective dose, although this interpretation is reasonable.

DISCUSSION

The physical properties of cyclotron-accelerated particles (negligible scatter, high penetration in parallel paths) in conjunction with a multiplane rotation technique, Tobias, Anger, and Lawrence (2), offer the advantage of generating discrete lesions within the central nervous system. Progress in the precise localization of lesions induced with high-energy irradiation has been aided by stereotaxically implanting animals, Gaffey (29). In the same study the effect of localized exposure of visual pathways (retina, optic tract and optic chiasma) to 910-MeV alpha particles was reported. We found then that with doses above 12,500-rad alpha particles that the latency period for blocking optic-tract transmission was a logarithmic function of the delivered dose. Promptly to block an evoked response to light stimuli required 200,000 rads. This was 100 times the dose necessary to immediately inhibit the electroretinogram with 910-MeV alpha particles. Thus, localized irradiation of these two components of the visual system revealed a significant difference in radiosensitivity.

Table 1. Relationship between the dose of alpha particles and the time for the suppression of the electrically evoked pupillodilation response

910-MeV alpha-particle dose (k rads)	Postirradiation time for pupillodilation loss
100	0
70	3 hrs
55	6 hrs
50	18 hrs
40	1 day
32	2 1/2 days
30	3
25	5
24	6 1/2
20	8
17.5	10
15.0	15
12.5	36
10.0	131

In the present work the technique for creating a discrete lesion in the nucleus perifornicalis was similar to our optic-tract irradiations. However, the volume of tissue irradiated was larger. In optic-tract irradiations the radius of the cyclotron's circular beam was 1/8-in.; in nucleus perifornicalis irradiations the radius was 1/4-in. As shown in Fig. 5, the logarithm of the dose of 910-MeV alpha particles versus the time for the suppression of the electrically induced pupillodilation was found to be non-linear. In optic-tract irradiations the survival time for photically evoked responses plotted against the logarithm of the delivered dose was linear above 12,500 rads. In optic-tract irradiations 20,000 rads proved effective in blocking transmission in 3 1/2 days. Local irradiations of the pupillodilation center with 20,000 rads required 8 days to inhibit electrically induced pupillodilation. Although these differences are real, i.e., these findings are repeatable, they are not of necessity evidence of a great difference in radiosensitivity. It is felt that these apparent differences are based on physical, not biological, differences. First, the electrophysiological techniques for assaying the efficiency of irradiation varied. In optic-tract studies the criteria for the effectiveness of ionizing radiation was the attenuation and suppression of an evoked bioelectric response. Bioelectric current in this instance was outgoing from the animal to the recording instruments. In experiments dealing with the sensitivity of the pupillodilation center to 910-MeV alpha particles, the current was ingoing to the animal from a stimulator. The end point in pupillodilation studies was the loss of a functional

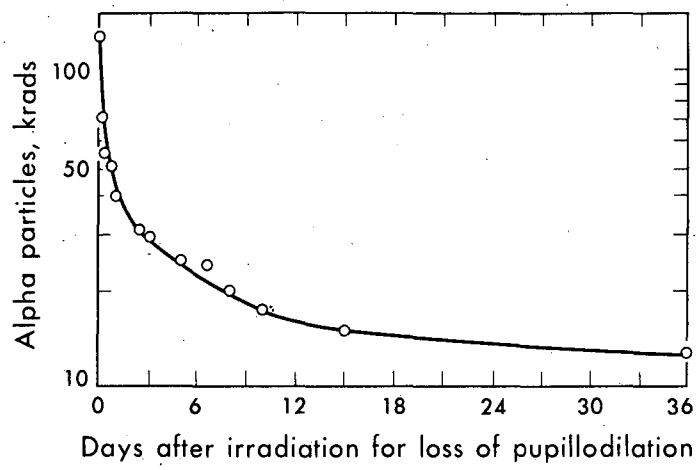

Figure 5. The logarithm of the dose of 910-MeV alpha particles delivered to the pupillodilation center is plotted against the time for the loss of the response to electrical stimulation. It is clear that there is not a linear relation between the logarithm of the dose and the survival time of the pupillodilation response.
MUB-3776

response to a controlled stimuli. The bipolar electrode producing this physiological response from the nucleus perifornicalis of the hypothalmus was actually in this structure. The current field between the stimulating electrodes extended over a volume with a diameter three times greater than the interelectrode distance, Bures, Petran and Zachar (34). Hence, with bipolar electrodes separated by 2 mm, it would be expected that a lesion would have to be a sphere 6 mm in diameter to suppress neural activity. It was for this reason that a circular beam with an aperature diameter of 6.3 mm was selected for nucleus perifornicalis irradiation. Our interpretation of the dose-response relationship of Fig. 5 is that the nonirritable tissue must be of a critical size to be effective, i.e., the volume of nonirritable cells must grow to a dimension greater than the current field distribution generated by the stimulating electrodes. When the dimension of nonirritability grew beyond the limits of current field, the animal would cease to respond to electrical stimulation. Therefore it is believed that a dose of 15,000 rads produced a suppression of the pupillodilation response after a period of 15 days because a sphere 6 mm in diameter had been made nonirritable. A dose of 30,000 rads rendered nonirritable a sphere 6 mm in diameter after a latency period of 3 days (Table 1).

The tips of the bipolar electrode in optic-tract irradiations were separated by 2 mm, as were those in nucleus perifornicalis studies. However, the bipolar electrode was used to record a propagated action potential of the optic tract, Gaffey (29). The stimulus in this case was a 10-μsec flash of light from a photo stimulator (Grass, Model PS-2) delivered at a fixed lamp-eye distance from the cat. The bioelectric signal detected on the optic tract in response to photic stimulation was fed to differential amplifier and suitable display instruments for analysis. In this case the length of optic-tract fiber involved was relatively small, i.e., for an interelectrode distance of 2 mm, approximately 3 mm of fiber length contributed to the recorded, travelling impulse. In the

instance of optic-tract irradiations with high-energy alpha particles, the latency period for irradiation blockage of conduction was the period required for the lesion to grow to a diameter of 3 mm. We found that it took 3 1/2 days to block optic-tract transmission with 20,000 rads of 910-MeV particles (29) and the same dose took 8 days to suppress the action of nucleus perifornicalis (Table 1). It is our contention that there is no real disparity here. In other words, a dose of 20,000 rads of high-energy alphas produced a 3 mm diameter sphere of inactive tissue in 3 1/2 days (optic-tract experiments) and the same dose of radiation produced a 6-mm diameter sphere of nonirritable tissue in 8 days (nucleus perifornicalis experiments).

It has been reported that the effect of high-energy-particle radiation on the central system depends on the volume of tissue irradiated. Haymaker (35) stated that with volumes greater than 1 mm in diameter circulatory disturbances play a primary role in pathogenesis. With irradiated volumes of tissue less than 1 mm diameter, Haymaker (35) restricts the effect of ionizing radiation to the neural elements. Using axonal material Gaffey (36) has shown that a minimum length of fiber must be irradiated in order to block impulse transmission. Millions of rads of high-energy alpha particles and protons failed to inhibit the propagation of action potentials of isolated sciatic nerves with a knife-edge beam less than 1 mm. The relevance of this finding to radiosurgery was investigated earlier by us (29). Midline bisection of the optic chiasma of cats was also attempted with 910-MeV alpha particle knife-edge beam. When the profile of the edge of this beam was limited to 0.5 mm, the optic chiasma transmission was not interrupted on the basis of electrophysiological data (29). However, a 2-mm-edge beam of cyclotron-accelerated alpha particles blocked cross-fiber transmission at the optic chiasma. To some extent this electrophysiological information tends to explain Zeman's, et al. (15) narrow-beam irradiations of mouse brain with deuterons.

SUMMARY

Contact with the pupillodilation center (nucleus perifornicalis of the hypothalmus) was made by insertion of bipolar electrodes through burr holes in the skull of cats. The leads from the left and right hemispheres were connected to a radio socket that was secured to the skull of an animal. Electrical stimulation of the pupillodilation center was made through the head socket of alert cats.

The Lawrence Radiation Laboratory's 184-inch synchrocyclotron served as a source of 910-MeV alpha particles. By a cross-fire-technique the pupillodilation center of the cat's brain was irradiated. This was accomplished by aligning the head of the cat in the path of the cyclotron beam with X rays so that the tip of the implanted electrode was both in the center of the high-energy beam and at the focus of a mechanical rotator. Head translations about this

focus of rotation concentrated irradiation in a discrete, spherical volume the diameter of the beam's aperature. Since the implanted electrode was in the center of this irradiated volume, the time-course for the blockage of pupillodilation could be studied as a function of the delivered dose of alpha particles. It was found that the action of electrical stimulation on the pupillodilation center could be inhibited immediately and irreversibly by 100,000 rads. Below 8,000 rads there was no detectable effect on the pupillodilation center even after seven months. In doses less than 32,000 rads the threshold voltage necessary to produce pupillodilation followed a biphasic pattern. A decrease in the threshold voltage was coincident with the appearance of pupil-size imbalance in the absence of electrical stimulation.

ACKNOWLEDGMENT

I am indebted to J. Howard, D. Love and W. Pratt for their cooperation in animal irradiations at the cyclotron.

This work was performed under the auspices of the U.S. Atomic Energy Commission and the National Aeronautics and Space Administration.

REFERENCES

1. Lawrence, E. O., and Livingston, M. S.; Phys. Rev. 40:19, 1932.
2. Tobias, C. A.; Anger, H. O., and Lawrence, J. H.; Am. J. Roentgenol. Radium Therapy Nucl. Med. 67:1, 1952.
3. Tobias, C. A.; Van Dyke, D. C.; Simpson, M. E.; Anger, H. O.; Huff, R. L., and Koneff, A. A.; Am. J. Roentgenol. Radium Therapy Nucl. Med. 72:1, 1954.
4. Leksell, L.; Acta Chir. Scand. 102:316, 1951.
5. Lawrence, J. H.; Cancer 10:795, 1957.
6. Tobias, C. A.; Hsu, K., and Born, J. L.; in Radiation Biology and Medicine, edited by W. D. Claus, Reading, Pa., Addison Wesley, 1958, p. 541-588.
7. Larsson, B.; Leksell, L.; Rexed, B.; Sourander, P.; Mair, W., and Andersson, B.; Nature 182:1, 222, 1958.
8. Leksell, L.; Larsson, B.; Andersson, B.; Rexed, B.; Sourander, P., and Mair, W.; Acta Radiol. 54:251, 1960.
9. Rexed, B.; Mair, W.; Sourander, P.; Larsson, B., and Leksell, L.; Acta Radiol. 53:289, 1960.
10. Andersson, B.; Larsson, B.; Leksell, L.; Mair, W.; Rexed, B., and Sourander, P.; in Response of the Nervous System to Ionizing Radiation, New York, Academic Press, 1962, p. 345.
11. Siegbahn, K., and Howard, F. T.; Nucl. Instr. Methods 18:1, 1962.
12. Larsson, B.; Leksell, L., and Rexed, B.; Acta Chir. Scand. 125:1, 1963.
13. Anderson, O. K.; Garcia, J.; Henry, J.; Riggs, C.; Roberts, J. H.; Thorell, B., and Tobias, C. A.; Radiation Res. 7:299, 1957.
14. Van Dyke, D. C., and Simpson, M. E.; Endocrinology 64:240, 1959.
15. Zeman, W.; Curtis, H. J.; Gebbard, E. L., and Haymaker, W.; Science 130:1, 760, 1959.

16. Zeman, W.; Samurajski, T., and Curtis, H. J.: Effects of Ionizing Radiation on the Nervous System, Vienna, International Atomic Energy Agency, 1962, p. 297.
17. Constable, J. D.; Lawrence, J. H.; Born, J. L.; Tobias, C. A.; Ariotti, P. E.; Sangalli, F.; Carlson, R. C., and Toch, P.; J. Am. Med. Assoc. 174:1720, 1960.
18. Lawrence, J. H.; Tobias, C. A.; Born, J. L.; Wang, C. C., and Linfoot, J. A.; J. Neurosurg. 19:717, 1962.
19. Lawrence, J. H.; Tobias, C. A.; Born, J. L.; Gottschalk, A.; Linfoot, J. A., and Kling, R. P.; J. Am. Med. Assoc. 186:236, 1963.
20. Malis, L. I.; Loevinger, R.; Kruger, L., and Rose, J. E.; Science 126:302, 1957.
21. Malis, L. I.; Kruger, L., and Rose, J. E.; Trans. Am. Neurol. Assoc., p. 70-80, 1958.
22. Malis, L. I.; Baker, C. P.; Kruger, L., and Rose, J. E.; J. Comp. Neur. 115: 212, 1960.
23. Malis, L. I.; Rose, J. E.; Kruger, L., and Baker, C. P.: Response of the Nervous System to Ionizing Radiation, New York, Academic Press, 1962, p. 359.
24. Janssen, P.; Klatzo, I ; Miguel, J.; Brustad, T.; Behar, A.; Haymaker, W.; Lyman, J.; Henry, J., and Tobias, C. A.; in Response of the Nervous System to Ionizing Radiations, edited by T. J. Haley and R. Snider, New York, Academic Press, 1962, p. 383
25. Rose, J. E.; Malis, L. I.; Kruger, L., and Baker C. P.; J. Comp. Neurol. 115:243, 1960
26. Hess, W. R.: The Functional Organization of the Diencephalon, New York, Grune & Stratton, 1957, p. 57.
27. Tisljar-Lentulis, G. M.; Atompraxis 10:367, 1961
28. Gaffey, C. T.: Response of the Nervous System to Ionizing Radiation, New York, Academic Press, 1962, p. 277.
29. Gaffey, C. T.; Bioelectric Sensitivity to Irradiation of the Retina and Visual Pathways, Lawrence Radiation Laboratory Report, UCRL-11005, 1963; in Response of the Nervous System to Ionizing Radiation, edited by T. Haley and R. Snider, Boston, Little, Brown and Company, 1964, p. 243-270.
30. Delgado, J. M. R.: Electrical Stimulation of the Brain, Austin, University of Texas, 1961, p. 25.
31. Birge, A C.; Anger, H. O., and Tobias, C. A.; in Radiation Dosimetry, New York, Academic Press, 1956, p. 623.
32. Born, J. L.; Anderson, A. O.; Birge, A. C.; Blanquet, P.; Brustad, T.; Carlson, R. A.; Van Dyke, D. C.; Fluke, D. J.; Garcia, J.; Henry, J. P.; Knisely, R. M.; Lawrence, J. H.; Riggs, C. W.; Thorell, B.; Tobias, C. A.; Toch, P., and Welch, G. P.; Progr. Nucl. Energy 2:189-206, 1959.
33. Welch, G. P., and Tobias, C. A.; Proceedings of the 3rd International Conference on Medical Electronics, London, Inst. Electronic Engineers, 1961, p. 465.

34. Bures, J.; Petran, M., and Zachar, J.; in Electrophysiological Methods in Biological Research, Praha, Academic Press, 1960, pp. 279, 388.
35. Haymaker, W.: Effects of Ionizing Radiation on the Nervous System, Vienna, International Atomic Energy Agency, 1962, p. 309-358.
36. Gaffey, C. T.; Radiation Res. 22:189, 1964.

Received November, 1964.

Serum Lipid-Lipoprotein Interrelationships between Males and Females

Norman K. Freeman, Frank T. Lindgren and Alicia M. Ewing

In a previous report (1) some interrelationships between serum lipids, serum-lipoprotein levels and lipoprotein composition were discussed. The data were obtained on sera from 32 normal males, aged 35 to 49 years, all employed at the Livermore site of Lawrence Radiation Laboratory. Since that time, the corresponding lipid and lipoprotein measurements have been made on sera from 16 normal females also aged 35 to 49 years and employed at the same laboratory. From these measurements, together with a more refined and detailed analysis of the lipoprotein spectra, it has been possible to establish a greater variety of lipid-lipoprotein interrelationships. This has been done independently for males and females in order to compare the corresponding correlation coefficients for the two sexes.

METHODS

Blood samples were drawn in the morning from subjects in a non-fasting state. The blood specimens were allowed to clot, and sera were separated in a clinical centrifuge. Ultracentrifugal procedures for the preparation and analysis of lipoprotein fractions have been described elsewhere (2,3). Low-density lipoproteins were also analyzed refractometrically (4). Lipid analysis of sera and of the separated lipoprotein fractions was carried out by infrared spectrophotometric methods (5,6). Total lipids were also determined gravimetrically.

Analysis of the lipoprotein patterns has been carried out with a computer program and the IBM 7094 computer. The details of this procedure are the subject of another report. Some of its salient features, however, will be given briefly here. Figure 1 shows a redrawn tracing of the appropriate Schlieren photograph taken during an analytic centrifuge run. The pattern, representing the low-density lipoprotein spectrum, is divided into a number of vertical strips whose widths represent S_f-rate intervals. There are 29 such intervals, or components, in the low-density lipoprotein spectrum and 15 in the high-density. The area of each strip between the salt background level and the Schlieren curve is a measure of the concentration of lipoprotein in that S_f-rate interval. Using the measured curve heights at each subdivision boundary as input data, the computer calculates the individual area, and by a summation process yields cumulative concentrations from which the step-wise integral curve

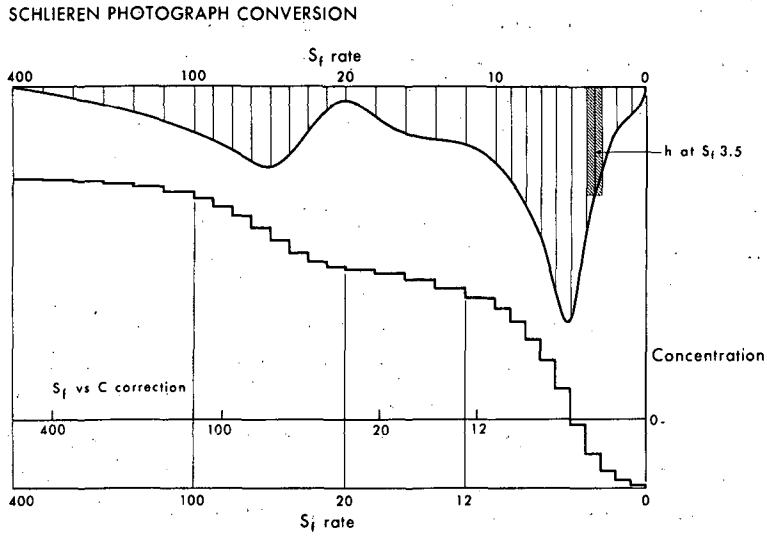

Figure 1. A stylized tracing of a low-density lipoprotein Schlieren pattern, showing the subdivision into 29 standard intervals. The computer-calculated integral curve (uncorrected) is shown below.

MUB-2566

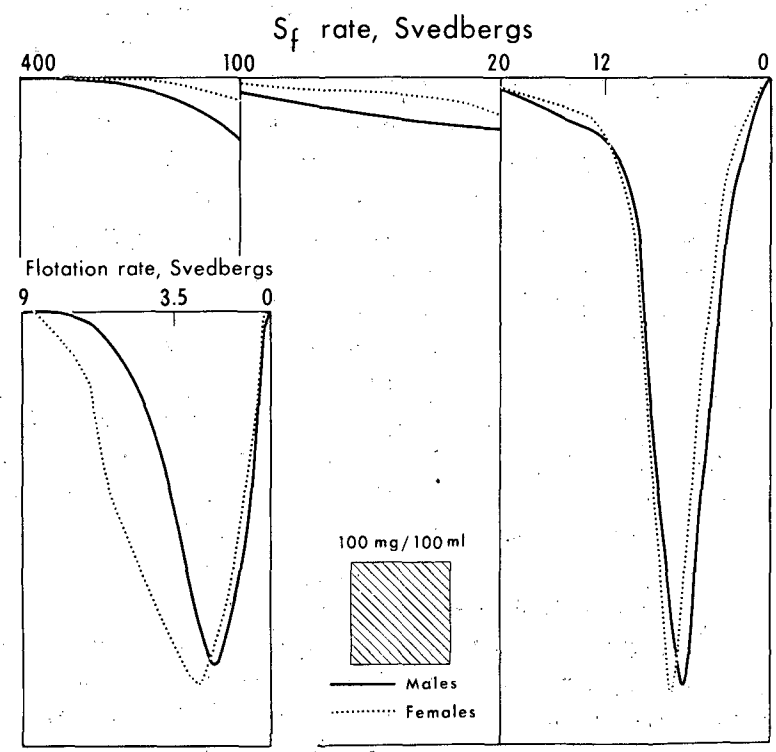

Figure 2. Comparison of average male and female serum-lipoprotein profiles, including both high-density and low-density classes. Curves have been constructed from concentration data for each of the 44 standard intervals, as determined by the computer, with all corrections as indicated in the text.

MUB-4024

shown in the lower part of Fig. 1 is constructed. The lipoprotein class represented by a given peak may be determined as the set of intervals between specified S_f-rates. The computer also makes the necessary calculations to correct for:

1) S_f versus C dependence
2) Johnston-Ogston effect
3) Standard conditions of viscosity and density
4) Base-of-cell position.

Each of the narrow S_f intervals into which the entire lipoprotein spectrum is divided can be regarded as a lipoprotein subclass, whose concentration then becomes one of the variables that may be correlated independently with all of the other measured values. Correlation coefficients (Pearson's product-moment) have been calculated for all pairs of variables with the computer. Of the 119 variables measured, those considered to be of primary relevance have been tabulated in Table 1, for both males and females. Correlation coefficients for this set of variables are given in Tables 2 and 3.

NORMAL LIPOPROTEIN PROFILES

From the mean values of lipoprotein concentrations at each of the 44 intervals, it is possible to construct a normal profile for a suitably selected population. This has been done for both males and females in the 35- to 49-year age range. The resulting profiles are shown in Fig. 2. One of the unique advantages of such a profile analysis is that, in addition to displaying gross differences in concentration and flotation rates, the more subtle features of the two distributions may be compared with one another. For example, the S_f 20-400 lipoprotein distribution for the females has a somewhat different shape from that of the males, being displaced toward the lower end of the S_f distribution. Similarly, comparison of the high-density lipoprotein spectra of the male and female groups reveals differences in concentration, mean F-rate and shape of the profile, particularly in the F 3.5-9.0 region of the distribution. F is used here to designate flotation in a general sense, inasmuch as S_f has been associated with flotation in a particular solution density (1.063 g/ml). Such lipoprotein profiles could presumably be constructed for various disease categories or physiological states and thereby provide valuable reference data for diagnostic purposes.

S_f RATE AND LIPOPROTEIN CONCENTRATIONS

A correlation of particular interest is the relationship between the S_f-rate of the peak of the S_f^o 0-12 lipoprotein class and the concentration of each narrow subclass of the entire lipoprotein distribution. In order to visualize this relationship, a plot has been made of these correlation coefficients for both male and female populations. These plots are shown in the lower part of Fig. 3.

Table 1. Mean values for serum lipids and lipoproteins and lipid composition of principal lipoprotein fractions

Variable no.	Males Mean	Males Standard dev.	Males Standard error	Females Mean	Females Standard dev.	Females Standard error	Units
1. STL (serum total lipid)	830.7	190.9	49.3	752.6	143.1	37.0	Mg/100 ml
2. STG (serum triglycerides)	173.2	122.0	31.5	110.4	65.4	16.9	" "
3. SCE (serum cholesteryl esters)	330.9	61.7	15.9	292.7	41.3	10.7	" "
4. SPL (serum phospholipids)	277.6	41.0	10.6	279.8	51.0	13.2	" "
5. VLD (very low-density lipoproteins)	174.0	157.4	40.6	75.7	69.1	17.9	" "
6. S_f 20-400 (lipoprotein fraction)	129.2	122.1	31.5	58.8	63.1	16.3	" "
7. VLDTG (very low-density lipoprotein triglycerides)	58.0	5.1	1.3	49.5	4.5	1.2	Wt% of total lipids
8. VLDCE (very low-density lipoprotein cholesteryl esters)	25.6	5.3	1.4	17.9	3.6	0.9	Wt% of total lipids
9. VLDPL (very low-density lipoprotein phospholipids)	19.6	1.7	0.5	25.0	2.5	0.6	Wt% of total lipids
10. S_f 0-20 (low-density lipoprotein fraction)	439.4	99.4	25.7	389.2	79.4	20.5	Mg/100 ml
11. S_f^o (rate of 0 - 20 peak)	6.32	0.92	0.24	7.34	0.75	0.19	Svedberg units
12. LDTG (low-density lipoprotein triglycerides)	7.8	2.7	0.7	8.4	2.4	0.6	Wt% of total lipids
13. LDCE (low-density lipoprotein cholesteryl esters)	55.6	2.0	0.5	52.9	1.3	0.3	" " "
14. LDPL (low-density lipoprotein phospholipids)	29.6	1.3	0.3	30.4	0.8	0.2	Wt% of total lipids
15. $F_{1.20}$ 0 - 9 (total high-density lipoproteins)	300.0	83.4	21.5	457.2	115.0	29.7	Mg/100 ml
16. $F_{1.20}$ 0 - 3.5 (high-density lipoprotein fraction)	230.0	52.8	13.6	238.3	52.7	13.6	Mg/100 ml
17. $F_{1.20}$ 3.5 - 9 (high-density lipoprotein fraction)	70.0	46.3	12.0	218.9	81.0	20.9	Mg/100 ml
18. Flotation rate of HDL peak	2.00	0.25	0.06	2.87	0.73	0.19	Svedberg units
19. HDLTG (high-density lipoprotein, triglycerides)	7.0	2.5	0.6	6.2	2.1	0.5	Wt% of total lipids
20. HDLCE (high-density lipoprotein, cholesteryl esters)	44.7	2.3	0.6	44.1	3.5	0.9	Wt% of total lipids
21. HDLPL (high-density lipoprotein, phospholipids)	43.1	1.1	0.3	43.3	2.0	0.5	Wt% of total lipids
22. A.I. (atherogenic index)*	69.6	27.6	7.1	51.4	14.1	3.6	A.I. units
23. S_f 0-400 (total low-density lipoproteins, ultracentrifuge)	575.2	185.7	47.9	448.5	99.0	25.6	Mg/100 ml
24. TLDL (total low-density lipoproteins, refractometry)	595.6	188.9	48.8	448.6	99.2	25.6	Mg/100 ml

*The ultracentrifugal atherogenic index (17) is given by: A.I. = $0.1(S_f^o$ 0-12) + 0.175 (S_f^o 12-400).

Table 2. Serum lipid, lipoprotein composition and lipoprotein interrelationships, 35-49 year males, 16 cases

Variable	1	2	3	4	5	6	7	8	9	10	11	12	13	14	15	16	17	18	19	20	21
1. STL																					
2. STG	0.87*																				
3. SCE	0.77*	0.37																			
4. SPL	0.91*	0.62*	0.91*																		
5. VLD	0.86*	1.00*	0.35	0.60†																	
6. S_f20-400	0.90*	0.98*	0.44	0.68*	0.98*																
7. VLDTG	0.28	0.35	0.04	0.23	0.34	0.25															
8. VLDCE	-0.29	-0.47	-0.03	-0.12	-0.46	-0.48	0.19														
9. VLDPL	-0.20	-0.30	0.02	-0.01	-0.32	-0.24	-0.81*	-0.04													
10. S_f0-20	0.59†	0.24	0.83*	0.69*	0.22	0.33	-0.25	-0.20	0.07												
11. S_f Rate	-0.63*	-0.76*	-0.25	-0.46	-0.77*	-0.76*	-0.32	0.59†	0.27	-0.10											
12. LDTG	0.41	0.65*	-0.11	0.21	0.61†	0.61†	0.13	-0.38	0.05	-0.06	-0.35										
13. LDCE	-0.01	0.02	0.05	-0.05	0.07	0.03	0.23	-0.18	-0.41	-0.08	-0.37	-0.55†									
14. LDPL	-0.65*	-0.81*	-0.19	-0.48	-0.79*	-0.79*	-0.29	0.68*	0.08	-0.09	0.83*	-0.68*	-0.06								
15. $F_{1.20}$0-9	-0.01	-0.32	0.35	0.34	-0.34	-0.28	0.34	0.55†	0.10	0.06	0.15	-0.43	0.13	0.22							
16. $F_{1.20}$0-3.5	0.10	-0.14	0.32	0.38	-0.15	-0.07	0.28	0.16	0.10	0.10	-0.19	-0.32	0.26	-0.12	0.88*						
17. $F_{1.20}$3.5-9	-0.13	-0.44	0.26	0.16	-0.46	-0.43	0.29	0.84*	0.03	0.00	0.52†	-0.42	-0.08	0.56†	0.81*	0.42					
18. F-Rate	-0.08	-0.10	-0.05	-0.05	-0.10	-0.14	0.17	0.41	-0.12	-0.19	0.48	0.08	-0.33	0.37	-0.04	-0.39	0.42				
19. HDLTG	0.75*	0.92*	0.24	0.49	0.90*	0.90*	0.18	-0.51†	-0.16	0.25	-0.65*	0.82*	-0.19	-0.79*	-0.49	-0.31	-0.54†	-0.09			
20. HDLCE	-0.58†	-0.81*	-0.06	-0.31	-0.79*	-0.80*	-0.03	0.47	-0.01	-0.08	0.52†	-0.79*	0.31	0.66*	0.50†	0.33	0.53†	0.12	-0.87*		
21. HDLPL	0.45	0.62*	-0.00	0.29	0.62†	0.63*	0.23	-0.30	-0.02	-0.05	-0.57†	0.52†	-0.15	-0.64*	-0.07	0.17	-0.34	-0.44	0.55†	-0.70*	
22. A.I.	0.95*	0.88*	0.67*	0.82*	0.87*	0.93*	0.09	-0.46	-0.16	0.66*	-0.64*	0.48	-0.03	-0.67	-0.20	-0.02	-0.35	-0.19	0.82*	-0.67*	0.48

* Significance, $P < 0.01$

† Significance, $P < 0.05$

Other values not significant

Table 3. Serum lipid, lipoprotein composition and lipoprotein interrelationships, 35 - 49 year females, 16 cases

Variable	1	2	3	4	5	6	7	8	9	10	11	12	13	14	15	16	17	18	19	20	21
1. STL																					
2. STG	0.86*																				
3. SCE	0.60†	0.20																			
4. SPL	0.97*	0.84*	0.48																		
5. VLD	0.85*	0.98*	0.22	0.84*																	
6. S_f20-400	0.77*	0.95*	0.16	0.74*	0.98*																
7. VLDTG	0.66*	0.64*	0.14	0.68*	0.65*	0.60†															
8. VLDCE	-0.51†	-0.57†	0.10	-0.60†	-0.58†	-0.54†	-0.67*														
9. VLDPL	0.27	0.23	0.35	0.24	0.26	0.27	0.35	-0.01													
10. S_f0-20	0.26	-0.03	0.76*	0.12	-0.01	-0.03	-0.05	0.47	0.48												
11. S_f Rate	0.21	-0.42	0.03	-0.18	-0.43	-0.52†	0.01	-0.08	-0.28	-0.20											
12. LDTG	0.49	0.81*	-0.27	0.52†	0.78*	0.81*	0.46	-0.62†	0.02	-0.41	-0.47										
13. LDCE	-0.22	-0.34	0.31	-0.32	-0.27	-0.25	-0.11	0.41	0.27	0.52†	0.19	-0.67*									
14. LDPL	-0.18	-0.15	-0.40	-0.17	-0.22	-0.25	-0.11	-0.16	-0.69*	-0.50†	-0.36	0.09	-0.29								
15. $F_{1.20}$0-9	0.71*	0.49	0.34	0.77*	0.49	0.38	0.61†	-0.67*	-0.09	-0.20	0.19	0.30	-0.40	0.12							
16. $F_{1.20}$0-3.5	0.73*	0.54†	0.50†	0.70*	0.54†	0.49	0.37	-0.52†	-0.01	-0.03	0.00	0.44	-0.52†	0.06	0.79*						
17. $F_{1.20}$3.5-9	0.53†	0.33	0.14	0.63*	0.33	0.21	0.63*	-0.61†	-0.12	-0.27	0.28	0.12	-0.22	0.13	0.90*	0.45					
18. F-Rate	-0.05	0.01	-0.23	0.04	0.06	0.04	0.51†	-0.13	0.11	-0.19	0.20	-0.13	0.34	-0.19	0.13	-0.39	0.47				
19. HDLTG	0.53†	0.86*	-0.14	0.52†	0.87*	0.91*	0.45	-0.52†	0.25	-0.19	-0.56†	0.89*	-0.34	-0.16	0.18	0.33	0.03	-0.03			
20. HDLCE	-0.79*	-0.93*	-0.05	-0.82*	-0.91*	-0.87*	-0.61†	0.63*	-0.03	0.20	0.40	-0.83*	0.49	-0.04	-0.58†	-0.53†	-0.46	-0.06	-0.80*		
21. HDLPL	0.77*	0.86*	0.13	0.79*	0.82*	0.76*	0.47	-0.61†	0.09	-0.24	-0.20	0.72*	-0.45	0.19	0.56†	0.61†	0.38	-0.16	0.69*	-0.87*	
22. A.I.	0.76*	0.75*	0.56†	0.65*	0.78*	0.79*	0.45	-0.15	0.52†	0.59†	-0.57†	0.41	0.12	-0.51†	0.17	0.36	-0.01	-0.09	0.64*	-0.58†	0.45

* Significance, $P < 0.01$
† Significance, $P < 0.05$
Other values not significant

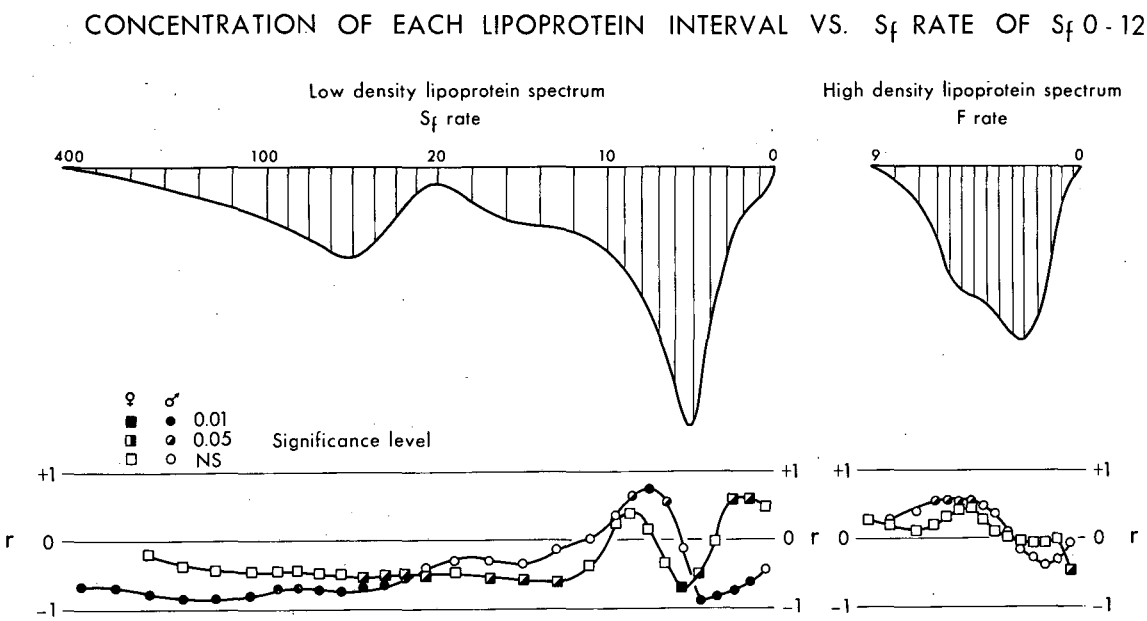

Figure 3. Correlations (for males and females) between concentrations of all lipoprotein subclasses and the S_f^o-rate of the major S_f 0-12 component.
MUB-4022

In the males, a significant inverse relationship is observed between the concentration of segments of the S_f 20-400 lipoprotein class and the S_f^o-rate of the S_f 0-12 component. In the female group only a borderline relationship is observed. In order to establish this relationship, or lack of it, more definitively, a much larger population study is needed. This should include sufficient numbers of females high in S_f 20-400 and males low in S_f 20-400 to allow a comparison based on matched levels of S_f 20-400 lipoproteins. The sinusoidal correlation pattern observed over the region of the S_f^o 0-12 major peak reflects the range of S_f^o-rate observed, as well as the significantly higher mean S_f^o-rate of the female as compared to the male group. Because of the limited numbers of cases in our study, it is not possible at this time to discuss definitively the significance of these S_f versus lipoprotein concentration relationships. However, Mills and Wilkinson (7) in a larger study of English males have observed an inverse relationship between S_f^o-rate of the S_f 0-12 component and total S_f 0-400 lipoprotein concentration. However, it should be pointed out that these workers observed considerably higher S_f^o-rates than we have, but both their method of calculating the S_f^o-rate and the F versus C dependence (including the K value) were different.

LIPOPROTEIN CONCENTRATIONS, COMPOSITION AND OTHER PARAMETERS

The lipid classes making up substantially all of the serum (or lipoprotein) lipids are cholesteryl esters, triglycerides, phospholipids and unesterified cholesterol, the first three of these comprising about 90% of the total.

The amount of unesterified fatty acids is negligibly small, except in the high-density fraction where it occurs to the extent of a few percent. Triglycerides, as measured, may contain small amounts of diglycerides and monoglycerides. The serum lipid and lipoprotein composition data given here (Table 1) are in terms of the three major components, which were determined by methods described in references (5,6).

The results of lipid analyses of the separated lipoprotein fractions are, in general, consistent with earlier composition data of Hillyard et al. (8), Lindgren et al. (9), and Bragdon et al. (10), except that a downward revision is indicated for the triglyceride content of both S_f 0-20 and HDL fractions. In S_f 0-20 the compensating percentage increase is distributed between cholesteryl esters and phospholipids, whereas in HDL a substantially larger value occurs for cholesteryl esters only. The lipoprotein concentrations given in Table 1 are also consistent with results that were obtained earlier in an extended study of a much larger population (11), except that the mean value for total HDL in both males and females appears to be significantly higher in the new data. In our current designation of the HDL sub-groups, this difference seems to be primarily in the faster-moving components, $F_{3.5-9.0}$. This fraction does not correspond precisely, however, with HDL_2 in the earlier nomenclature, so the distribution of this difference between the two HDL fractions is uncertain.

It may be noted in Table 1 that the lipoprotein composition data are essentially identical for males and females in both the high-density and S_f 0-20 classes. In the very low-density class ($S_f > 20$), females appear to have a higher percentage of phospholipid than males, and less triglycerides and cholesteryl esters. The mean level of VLD lipoproteins in females is less than half that found for males, but the fraction found in the range S_f 20-400 is nearly the same in both sexes. Within the S_f 20-400 class, however, there does appear to be a difference in the distribution. As indicated in Fig. 2, the S_f 20-400 lipoproteins in females are weighted more toward the slower-floating components. This observation is consistent with a higher average density and lower triglyceride content. Since the sera were obtained from individuals in the non-fasting state, some variability of both level and composition of the VLD lipoproteins is to be expected.

The lipid and lipoprotein parameters listed in Table 1 are those considered to be of principal interest. They were selected from a list of 119 variables actually measured, 44 of which are the individual segments of the total lipoprotein concentration profile. With the computer it has been possible to determine correlation coefficients between all pairs of the 119 variables. Some of these correlation coefficients have been used to construct the curves shown in the lower part of Fig. 3, which indicate relationships (previously described) between the flotation rate of the S_f^o 0-12 peak and concentrations of

certain lipoprotein subfractions. Tables 2 and 3 contain correlation coefficients between 22 of the principal variables that are listed in Table 1. These are given separately for males and females. Although a great many inferences might be drawn from a study of this array of numbers, it is pertinent here to consider only a few of the individual values and their possible meanings.

Some correlations involving triglycerides are of particular interest. Although a positive correlation of serum triglycerides and VLD lipoproteins would be expected, the observed values ($r = 0.99_5$, 0.98 for males and females respectively) are extremely high. By comparison, the corresponding r values for serum cholesteryl ester and S_f 0-20 lipoproteins are only 0.86 for males and 0.76 for females, despite the fact that for each lipoprotein class the corresponding lipid is the major component, representing half or more of the total lipid content. Consistent with these observations, and perhaps more important, are the correlations between serum triglycerides and the triglyceride content of each lipoprotein class. These coefficients are: VLD, 0.35 (M), 0.64 (F); S_f 0-20, 0.65 (M), 0.81 (F); HDL, 0.92 (M), 0.86 (F). By contrast, the correlation between serum cholesteryl ester and the percentage of cholesteryl ester in each lipoprotein class is absent or of a much lower order: VLD, -0.03 (M), 0.10 (F); S_f 0-20, 0.05 (M), 0.31 (F); HDL, -0.06 (M), -0.05 (F). The observation for triglycerides supports the hypothesis that a high level of VLD lipoproteins alters the composition of the S_f 0-20 and high-density lipoproteins, presumably by a transfer of triglycerides to them. At the same time, the percentage of cholesteryl esters in HDL lipoproteins drops, as indicated by a negative correlation coefficient with serum triglycerides. Examination of the original data suggests a saturation limit to the amount of triglyceride that can be taken up by the high-density lipoproteins. The mechanism of this transfer process is not clear, but its existence reemphasizes the importance of the high-density lipoproteins in the transport of triglycerides. Earlier studies by Nichols _et al_. (12) showed that triglyceride fed to human subjects could be identified in the triglyceride moiety of high-density lipoproteins within 5 hr after ingestion. More recently, the _in vitro_ experiments of Nichols and Smith (13), in which high-density lipoproteins were incubated with VLD lipoproteins or with fat emulsions, also serve to demonstrate this transfer. A binding capacity of high-density lipoproteins for a variety of substances, including triglycerides, has been observed by Ashworth and Green (14). The nature of this binding is not known, but Scanu and Hughes (15) have found that delipidized high-density lipoprotein exhibits an affinity for lipids.

In comparing the tables of correlation coefficients for our normal male and female populations, the values for a given pair of variables often differ markedly. Presumably, these differences can be rationalized on the basis of established sex differences in lipoprotein concentrations, composition, etc. For example, the correlation of serum total lipid with total HDL concentrations

is essentially zero (-0.01) in males, whereas in females the coefficient has a value of 0.71, significant at the 1% level. This suggests that for high serum-lipid levels, the excess lipid tends to be distributed predominantly in the low-density lipoproteins in males; in females a substantial amount occurs in high-density lipoproteins. This is also reflected in the correlations of serum total lipid with atherogenic index (A.I.), see Table 1. The coefficient for males, 0.95, is almost identical with the value (0.93) found by Nichols et al. (16) for a larger population of 88 normal males. The lower value of 0.76 observed here for females would seem to be a consequence of the incorporation of a greater proportion of excess lipid into HDL (which does not contribute to the calculated A.I.). It may also be noted that in females the correlation with A.I. is lower for each of the individual classes of serum lipids and low-density lipoproteins than it is in males.

It is hoped that the collected correlation coefficients will be useful in providing clues to lipoprotein behavior, or criteria for hypotheses in this area of study.

SUMMARY

Lipid and lipoprotein analyses have been carried out on the sera of 16 normal females ranging in age from 35 to 49 years. These data have been combined and compared with previous results on normal males of the same age range. With computer methods, concentrations have been determined for 44 lipoprotein subclasses. This permits the construction and comparison of mean lipoprotein profiles for male and female groups. In each group, correlations have been examined between concentrations of the subclasses and the S_f^o-rate of the major low-density lipoprotein peak. Correlation coefficients have also been tabulated for all pairs of 22 selected variables in each sex group. Some correlations of particular interest are discussed.

REFERENCES

1. Lindgren, F. T.; Freeman, N. K., and Wills, R. D.; Semiannual Report, Donner Laboratory, Lawrence Radiation Laboratory, UCRL-11184, 1963.
2. de Lalla, O., and Gofman, J. W.; in Methods of Biochemical Analysis, Vol. 1, edited by D. Glick, New York, Interscience, 1954, p. 459.
3. Freeman, N. K.; Lindgren, F. T., and Nichols, A. V.; in Progress in the Chemistry of fats and Other Lipids, Vol. 6, edited by R. T. Holman, W. O. Lundberg, and T. Malkin, London, Pergamon Press, Inc., 1963, p. 215.
4. Lindgren, F. T.; Nichols, A. V.; Freeman, N. K.; Wills, R. D.; Wing, L., and Gullberg, J. E.; J. Lipid Res. 5:68, 1964.
5. Freeman, N. K.; Ann. N. Y. Acad. Sci. 69:131, 1957.
6. Freeman, N. K.; J. Lipid Res. 5:236, 1964.
7. Mills, G. L., and Wilkinson, P. A.; Clin. Chim. Acta 8:701, 1963.

8. Hillyard, L. A.; Entenman, C.; Feinberg, H., and Chaikoff, I. L.; J. Biol. Chem. 214:79, 1955.
9. Lindgren, F. T.; Nichols, A. V., and Freeman, N. K.; J. Phys. Chem. 59:930, 1955.
10. Bragdon, J. H.; Havel, R. J., and Boyle, E.; J. Lab. Clin. Med. 48:36, 1956.
11. de Lalla O. F., and Gofman, J. W.; in Blood and Other Body Fluids, edited by D. S. Dittmer, Washington D. C., Federation of American Societies for Experimental Biology, 1961.
12. Nichols, A. V.; Rehnborg, C. S.; Lindgren, F. T., and Wills, R. D.; J. Lipid Res. 3:320, 1962.
13. Nichols, A. V., and Smith, L.; Semiannual Report, Donner Laboratory, Lawrence Radiation Laboratory, UCRL-11184, 1963.
14. Ashworth, L. A. E., and Green, C.; Biochim. et Biophys. Acta 70:68, 1963.
15. Scanu, A., and Hughes, W. L.; J. Biol. Chem. 235:2876, 1960.
16. Nichols, A. V.; Lindgren, F. T., and Gofman, J. W.; Geriatrics 12:130, 1957.
17. Gofman, J. W.; Strisower, B.; de Lalla, O.; Tamplin, A.; Jones, H. B., and Lindgren, F. T.; Modern Med. 11:119, 1953.

Received October, 1964.

The Effect of Very Low-Density Lipoproteins on Lipid Transfer in Incubated Serum

Alex V. Nichols and Lester Smith

An earlier report (1) from this laboratory has described a substantial increase in the glyceride content of high-density lipoproteins of d 1.063-1.21 (HDL) isolated from the lipemic serum of healthy subjects receiving a fat load. Since the serum concentration of the glyceride-rich very low-density lipoproteins of d < 1.006 (VLDL) was also markedly elevated in these subjects, the HDL-glyceride increase may have resulted from a transfer in vivo of glyceride from the VLDL to the HDL. The ability of HDL to bind additional glyceride has been demonstrated by Ashworth and Green (2) in experiments in which HDL species were exposed to Celite-dispersed glyceride. During in vitro incubation experiments, in which VLDL lipoproteins were added to serum samples low in glyceride content, Nichols and Smith (3) observed significant transfer of VLDL glyceride to HDL. Furthermore, this study showed a considerable reduction in the amount of cholesteryl esters bound to the HDL during uptake of glyceride by the HDL. In the present paper, we report our studies, in detail, on lipid transfer between all major human serum-lipoprotein classes, the VLDL, LDL (low-density lipoproteins of d 1.006-1.063) and HDL, in sera incubated with high amounts of added human VLDL lipoproteins. In addition, preliminary data describing the influence on lipid transfer of inhibition of the cholesterol esterifying enzyme of human serum (the serum fatty acid transferase, described by Glomset) (4) are presented.

MATERIALS AND METHODS

Serum for the incubation experiments was separated by methods previously described (5) from freshly-drawn blood of two fasting female subjects (D.P., age 43, and J.C., age 44) exhibiting low levels of VLDL lipoproteins. The VLDL lipoproteins, which were added to the above sera for lipid transfer studies, were rapidly separated ultracentrifugally (6) from the sera of two healthy male subjects (R.H., age 53, and D.D., age 40) having elevated levels of these lipoproteins. The sera of subjects D.P. and J.C. were incubated with VLDL from subjects R.H. and D.D. respectively.

Serum mixtures were incubated with gentle shaking in tightly-capped lusteroid tubes (6 ml) for 0 and 16 hr in a 37°C water bath. The experimental protocol consisted of duplicate incubation studies on a total of 4 ml of the following mixtures: a mixture of 3 ml of serum with 1 ml of a salt solution

(d 1.006); and on a mixture of 3 ml of serum with 1 ml of a salt solution (d 1.006) containing VLDL lipoproteins. In order to investigate lipid transfer when serum fatty acid transferase activity was inhibited, an additional incubation experiment was performed on a serum mixture, consisting of 3 ml serum (subject J.C.) and 1 ml of VLDL solution (subject D.D.), which contained 0.001 M of sodium p-hydroxymercuribenzoate (Sigma Chemical Co., St. Louis, Miss.).

At the end of the incubation period, 2 ml of salt solutions (d 1.006), containing appropriate amounts of sodium p-hydroxymercuribenzoate to yield a final concentration of 0.001 M of this compound, were added to each sample. The purpose of these solutions was to bring the mixture volumes to the 6 ml, as the first step in the ultracentrifugal isolation of the three major lipoprotein classes (7) and to inhibit the cholesterol esterifying activity of the serum fatty acid transferase (4). All salt solutions used in the preparative ultracentrifugal procedures contained 0.10 g/liter of the disodium salt of ethylenediaminetetraacetic acid. Evaluation of possible contamination of the LDL and the HDL fractions by VLDL lipids, resulting either from the incubation or ultracentrifugation procedures, was performed by control studies on solutions of VLDL lipoproteins alone. For incubated solutions of VLDL, ranging in glyceride concentrations between 300-450 mg/100 ml, the contamination of LDL and HDL fractions by VLDL lipids totalled on the average only 3 mg/100 ml and 1.5 mg/100 ml respectively. The above concentrations of total contaminating lipids, as well as all other lipid concentrations reported in this paper, are calculated for the volume comprising the incubation mixture (4 ml). The magnitude of these contaminations in the separate lipid classes is negligible relative to the concentration changes observed for lipid transfer in this investigation.

Lipids were extracted from the lipoprotein solutions by a modified method of Sperry and Brand (8), and each lipid extract was fractionated by silicic acid chromotography with the elution solvent mixtures described by Hirsch and Ahrens (9). The chromotographed lipids (cholesteryl esters, glycerides, unesterified cholesterol and phospholipids) were quantitated by an infrared spectrophotometric method reported by Freeman *et al*. (10).

RESULTS

LIPID CONCENTRATIONS IN VLDL, LDL AND HDL FRACTIONS ISOLATED FROM INCUBATED SERUM SOLUTIONS Table 1 shows the changes in lipid concentrations of the three major lipoprotein fractions following incubation of the sera from subjects D.P. and J.C. with saline solution (d 1.006). Cholesteryl ester concentrations increased in all three lipoprotein fractions in the incubated sera of both subjects. The largest increases in cholesteryl-ester concentrations were observed in the LDL fractions. Glyceride concentrations decreased in the VLDL but increased in the LDL and HDL of both serum samples. The glyceride concentration of the LDL of subject J.C. increased by about 41% following

Table 1. Change in lipid content of ultracentrifugal fractions isolated from incubated serum solutions

Lipid	Lipid concentration (in mg/100 ml)*					
	VLDL		LDL		HDL	
	Nonincubated	Incubated	Nonincubated	Incubated	Nonincubated	Incubated
Subject D.P.						
Cholesteryl esters	1.0(0.5)**	2.2(0.5)	65.1(2.3)	71.5(2.2)	60.7(1.1)	64.4(2.4)
Glycerides	3.9(0.2)	1.9(0.4)	9.7(0.6)	10.5(0.5)	4.4(0.4)	6.9(0.4)
Unesterified cholesterol	0.4(0.1)	0.5(0.1)	15.1(0.7)	11.9(0.2)	10.0(0.6)	7.3(0.5)
Phospholipids	1.2(0.2)	1.0(0.1)	38.3(2.9)	36.1(1.6)	78.2(1.1)	67.1(2.2)
Subject J.C.						
Cholesteryl esters	11.3(3.2)	16.3(3.5)	139.5(2.8)	150.8(3.0)	55.0(0.0)	60.5(2.5)
Glycerides	32.3(3.8)	16.3(2.0)	21.5(0.9)	36.3(1.5)	11.5(0.5)	13.8(0.9)
Unesterified cholesterol	5.5(1.0)	2.5(0.4)	27.3(1.1)	17.3(0.8)	6.3(0.4)	4.0(0.2)
Phospholipids	13.8(2.3)	8.3(1.6)	75.3(1.5)	60.0(2.0)	70.3(1.5)	57.5(1.2)

*Lipid concentrations tabulated in this and subsequent tables are concentrations of lipid present in the incubated volume. Incubation for 16 hr at 37°C.

**Values in parentheses in this and subsequent tables are standard errors of measurement $\sqrt{(S.E._M)}$ calculated from $S.E._M = \frac{\Sigma d^2}{2k}$ where d = difference between duplicates and k = number of pairs of duplicates. These values represent the estimate of the standard error for a single pair of duplicates.

incubation whereas the glyceride concentration in subject D.P.'s LDL fraction showed only an 8% increase. This difference in the subjects' percent response is probably due to the considerable difference in the initial VLDL glyceride concentration in the sera of these two subjects. The initial glyceride concentration of the VLDL fraction of subject J.C. is greater by approximately a factor of 8 than that of subject D.P.

Unesterified cholesterol concentrations were reduced in all three fractions in the serum of subject J.C.; and in the LDL and HDL fractions in the serum of D.P. following incubation. The unesterified cholesterol concentration in the VLDL of subject D.P. was extremely low, and for this reason it is not possible to determine the nature of its change following incubation. Phospholipid concentrations decreased in all three lipoprotein fractions in the incubated serum solutions of both subjects. The reductions in unesterified cholesterol and phospholipid concentrations can be explained as resulting from the activity of a serum-fatty acid transferase, described by Glomset (4). In this reaction fatty acids from the C-2 position of lecithin are transferred to

Table 2. Change in lipid content of ultracentrifugal fractions isolated from incubated serum containing added VLDL

Lipid	Lipid concentration (in mg/100 ml)					
	VLDL		LDL		HDL	
	Nonincubated	Incubated	Nonincubated	Incubated	Nonincubated	Incubated
Serum (subject D.P.) plus VLDL (subject R.H.)						
Cholesteryl esters	71.3(2.5)	124.4(2.3)	65.0(3.6)	53.3(2.3)	58.1(0.2)	35.6(1.0)
Glycerides	440.2(17.5)	365.4(9.0)	11.9(0.2)	39.7(0.2)	4.4(0.2)	38.0(0.8)
Unesterified cholesterol	31.0(4.2)	28.5(5.9)	14.9(0.7)	9.5(0.4)	9.7(0.1)	5.9(0.6)
Phospholipids	98.5(2.9)	82.7(1.8)	39.5(2.5)	38.3(2.4)	78.5(1.8)	66.8(1.3)
Subject J.C. plus VLDL (subject D.D.)						
Cholesteryl esters	109.5(2.2)	148.8(3.0)	142.0(2.8)	134.5(2.0)	56.5(1.3)	53.0(1.0)
Glycerides	310.8(9.3)	243.8(11.6)	22.8(0.8)	69.8(3.2)	12.8(0.6)	31.0(1.2)
Unesterified cholesterol	36.3(5.4)	25.8(3.6)	28.0(1.0)	25.8(1.5)	5.8(0.9)	4.0(0.6)
Phospholipids	113.8(2.3)	96.5(3.0)	72.0(2.2)	69.5(1.8)	68.3(1.4)	57.5(1.2)

unesterified cholesterol yielding cholesteryl esters and lysolecithin. The decrement in measured lipoprotein phospholipids results from (a) a migration (11) of some of the newly-formed lysolecithin from lipoprotein sites to the ultracentrifugal protein-residue fraction ($d > 1.21$) and (b) from an imcomplete recovery of the remaining lipoprotein-bound lysolecithin by the lipid extraction and processing procedures used.

LIPID CONCENTRATIONS IN VLDL, LDL AND HDL FRACTIONS ISOLATED FROM SERUM INCUBATED WITH ADDED VLDL. Table 2 shows the effects of incubation on the distribution of lipids bound to lipoproteins in serum mixtures of both subjects containing large amounts of added VLDL lipoproteins. Emphasis in this report is on the effects of very high or "saturation" concentrations of VLDL in the incubation media. In the present work, the concentrations of VLDL glyceride in the initial incubation mixtures, after the addition of the concentrated VLDL fractions, were 440.2 mg/100 ml with the serum of subject D.P. and 310.8 mg/100 ml with the serum of subject J.C.

Cholesteryl-ester concentrations in the VLDL fractions increased markedly in the incubation mixtures for both serum samples. Cholesteryl-ester concentrations in the LDL and HDL fractions were reduced in both samples. Thus, in spite of a definite net increase in the total cholesteryl-ester concentration in the incubation mixtures (18.9 mg/100 ml with serum of subject D.P. and 28.3 mg/100 ml with serum of subject J.C.), the cholesteryl esters of only the VLDL fractions were found to increase. These data show that the VLDL lipoproteins bind

not only some of the newly formed additional cholesteryl esters, arising from serum-fatty acid-transferase activity, but also some of the cholesteryl esters that were initially part of the LDL and HDL.

Considerable reductions in the glyceride concentrations of the VLDL fractions were observed following incubation in both serum mixtures. The glyceride concentrations in the LDL and HDL fractions, however, were markedly increased in both serum samples.

Unesterified cholesterol and phospholipid concentrations show the same qualitative changes, which indicate the presence of serum-fatty acid-transferase activity in the incubation systems. Since these two determinations are subject to the recovery limitations previously mentioned, quantitative interpretations of their changes will not be stressed.

LIPID CONCENTRATIONS IN VLDL, LDL AND HDL FRACTIONS ISOLATED FROM SERUM INCUBATED WITH ADDED VLDL AND SODIUM P-HYDROXYMERCURIBENZOATE Table 3 shows the effects of incubation on the distribution of lipoprotein lipids in the serum of subject J.C. containing added VLDL and an inhibitor of serum fatty acid transferase. These results indicate that the transfer of glycerides from VLDL to LDL and HDL, and the transfer of cholesteryl esters from the LDL and HDL to the VLDL can proceed in the absence of fatty acid-transferase activity. Inhibition of the enzyme activity is demonstrated by the relative constancy of the unesterified cholesterol and phospholipid concentrations in all three lipoprotein fractions. With the inhibitor present, the source of the cholesteryl esters of the VLDL fraction appears to be predominantly the cholesteryl esters of the HDL fraction, as indicated by the 26% reduction in the cholesteryl-ester concentration of this fraction. We also find, in agreement with the incubation studies of Minari and Zilversmit (12) on dog chylomicrons, a transfer of phospholipid from the VLDL to the HDL fraction in the absence of serum-fatty acid-transferase activity.

DISCUSSION

Glomset (11) and Rehnborg and Nichols (13) have described the distribution of cholesteryl esters among serum lipoproteins, following incubation of sera containing relatively low levels of VLDL lipoproteins. Their data, as well as those presented in this report, show an increase of cholesteryl esters in all three lipoprotein classes. These increases are attributed mainly to the activity of a serum fatty acid transferase and indicate that the cholesteryl esters produced are bound to serum lipoproteins during incubation. The data of this report, as well as those of Rehnborg and Nichols (13), also show that at relatively low levels of VLDL lipoproteins in the incubated serum there occurs a transfer of glyceride from the VLDL to the LDL and HDL. At the very high VLDL-lipoprotein concentrations used in this study, we find, in agreement with the above

Table 3. Change in lipid content of ultracentrifugal fractions isolated from incubated serum (subject J.D.) containing added VLDL (subject D.D.) plus sodium p-hydroxymercuribenzoate

Lipid	Lipid concentration (in mg/100 ml)					
	VLDL		LDL		HDL	
	Nonincubated	Incubated	Nonincubated	Incubated	Nonincubated	Incubated
Cholesteryl esters	101.3(2.0)	118.8(2.5)	142.9(2.3)	137.3(2.5)	56.7(1.2)	41.8(1.3)
Glycerides	303.6(6.1)	278.3(5.2)	21.3(0.6)	32.0(1.1)	11.0(0.7)	21.3(1.7)
Unesterified cholesterol	35.0(5.0)	32.8(4.3)	27.8(1.1)	26.3(1.3)	6.0(0.9)	6.0(0.8)
Phospholipids	116.0(2.1)	108.8(2.2)	77.5(1.6)	77.0(2.0)	73.5(2.5)	78.8(2.0)

observations, both an increased total serum-cholesteryl-ester concentration due to transferase activity and a considerable transfer of glycerides from the VLDL to the LDL and HDL. The distribution, however, of the cholesteryl esters among the major classes of lipoproteins is markedly different when elevated concentrations of VLDL are present in the incubation medium, for then the increased concentration of cholesteryl esters is found only in the VLDL, and the concentrations of cholesteryl esters in the LDL and HDL drop below their initial values. These data indicate that VLDL lipoproteins in high concentration bind not only some of the transferase-formed cholesteryl esters but also take up some of the cholesteryl esters initially bound to the LDL.

When the serum fatty acid transferase is inhibited by addition of sodium p-hydroxymercuribenzoate to the incubation system, some cholesteryl esters are still taken up by the VLDL and some glycerides are still transferred from them. This experiment shows that net lipid transfer can take place in the absence of transferase activity. In this case, we find for the VLDL a gain of approximately one mole of cholesteryl esters (assumed molecular weight of 651) for the loss of one mole of glyceride (assumed molecular weight of 885). For the LDL, we calculate a transfer of roughly two moles of cholesteryl esters for three moles of glyceride; and for the HDL, we calculate approximately two moles of cholesteryl esters for one mole of glyceride. It should be emphasized that these calculations for lipid substitution are very approximate and, although the inhibitor has removed possible complications due to transferase activity, the calculations are still subject to other complications in the incubation system. These complications include (a) the use of extremely high concentrations of VLDL, (b) the presence of all three major lipoprotein classes in the incubation solutions, and (c) difficulties in lipoprotein recovery during the ultracentrifugal procedures.

The physical transfer of cholesteryl esters and glycerides between human serum lipoproteins is apparently a basic property of these macromolecules.

Lindgren et al. (14) have observed a strong positive statistical correlation between serum VLDL concentrations and the HDL-glyceride contents in the serum of healthy male subjects. These observations, together with the preliminary data from our fat ingestion studies (1), suggest that similar physical lipid transfer may occur in vivo. From the available data, it is not possible to determine whether the suggested in vivo transfer is restricted only to the blood compartment or if other cellular or tissue compartments are also involved. If other compartments are involved, then the lipid-transfer reaction might play an active role in the transport of lipids from one compartment to another. Furthermore, this type of lipid-transfer reaction also could contribute to the accumulation of cholesteryl esters in tissue.

Minari and Zilversmit (12) found an increase in free cholesterol and a decrease in phospholipid on dog chylomicrons following 3-hr incubation with serum without detecting any transferase activity. The glyceride concentrations in their incubation mixtures were considerably lower than those used in the present study. Because of these differences in the incubation times and glyceride concentrations, it is probable that lipid transfer as described here would not be observed in their system. Furthermore, dog lymph chylomicrons may possibly not exhibit the same lipid-transfer properties as human VLDL. Thus, in our studies we have observed a markedly lower lipid transfer with a coconut oil emulsion (Ediol, Schenlabs Pharmaceuticals, Inc., New York, N.Y.), only roughly resembling chylomicrons, than with human VLDL or egg yolk lipoproteins when these were studied at comparable glyceride concentrations. It is very possible that considerable differences in lipid transfer properties exist between lipoprotein species of S_f greater than 400 and those of S_f 20-400. This question is currently under investigation.

Rowen (15) has reported that HDL are specifically degraded and their cholesteryl esters set free, when serum is incubated for 2 to 6 hr with a streptococcal extract. This degradation is associated with an increase in opalescence of the incubation mixture. The material, predominantly cholesteryl esters, responsible for the opalescence could be floated away from the parent solution upon preparative ultracentrifugation of the mixture. In these experiments the VLDL species were removed from the serum prior to incubation with the streptococcal extract. The mechanism whereby the extract degrades the HDL was not established in these investigations. More recently Rowen and Martin (16) have observed an enhancement of transferase activity in serum mixtures containing the extract. They suggest that disruption of HDL structure exposes lipids to the transferase and thus enhances its activity. Their observation of cholesteryl ester release by some form of lipoprotein degradation is of interest here since it is apparently another mechanism for initiating lipid transfer. It should be emphasized, however, that in all the experiments on lipid transfer reported by us in this paper, there was no observable increase in opalescence

nor any evidence of HDL degradation. The data in the present report describe a lipid-transfer process that occurs in incubated serum solutions between essentially intact lipoproteins.

SUMMARY

Incubation of human serum solutions low in glyceride content for 16 hr resulted in a net increase of cholesteryl esters in all three major human serum-lipoprotein classes, very low-density lipoproteins of d < 1.006 (VLDL), low-density lipoproteins of d 1.006-1.063 (LDL) and high-density lipoproteins of d 1.063-1.21 (HDL). Transfer of glycerides from the VLDL to the LDL and HDL was also observed during incubation. Reductions in lipoprotein unesterified cholesterol and phospholipids occurred during incubation and indicated the presence of serum-fatty acid-transferase activity in these solutions.

When serum was incubated in the presence of high concentrations of VLDL lipoproteins, the increase in cholesteryl esters was found only in the VLDL fraction. The VLDL apparently took up newly formed cholesteryl esters produced by serum-fatty acid-transferase activity, and accepted some cholesteryl esters initially bound to the LDL and HDL. When the transferase was inhibited with sodium p-hydroxymercuribenzoate, some of the cholesteryl esters, initially bound to the LDL and HDL, were still transferred to the VLDL. The HDL class was then the principal contributor of the cholesteryl esters. These observations indicate that reciprocal transfer of cholesteryl esters for glycerides in human serum lipoproteins can occur.

ACKNOWLEDGMENT

Supported in part by a research grant (HE 02029-09) from the National Heart Institute, U.S. Public Health Service and by the Atomic Energy Commission.

REFERENCES

1. Nichols, A. V.; Rehnborg, C. S.; Lindgren, F. T., and Wills, R. D.; J. Lipid Res. 3:320, 1962.
2. Ashworth, L. A. E., and Green, C.; Biochim. Biophys. Acta 70:68, 1963.
3. Nichols, A. V., and Smith, L.; Semiannual Report, Donner Laboratory, Lawrence Radiation Laboratory, UCRL-11184, 1963.
4. Glomset, J. A.; Biochim. Biophys. Acta 65:128, 1962.
5. deLalla, O. F., and Gofman, J. W.; in Methods of Biochemical Analysis, Vol. 1, edited by D. Glick, New York, Interscience Publishers, Inc., 1954, p. 459.
6. Lindgren, F. T.; Nichols, A. V., and Freeman, N. K.; J. Phys. Chem. 59:930, 1955.
7. Lindgren, F. T.; Nichols, A. V., and Wills, R. D.; Am. J. Clin. Nutr. 9:37, 1961.
8. Sperry, W. M., and Brand, F. C.; J. Biol. Chem. 213:69, 1955.
9. Hirsch, J., and Ahrens, E. H., Jr.; J. Biol. Chem. 233:311, 1958.

10. Freeman, N. K.; Lindgren, F. T.; Ng, Y. C., and Nichols, A. V.; J. Biol. Chem. 227:449, 1957.
11. Glomset, J. A.; Biochim. Biophys. Acta 70:389, 1963.
12. Minari, O., and Zilversmit, D. B.; J. Lipid Res. 4:424, 1963.
13. Rehnborg, C. S., and Nichols, A. V.; Biochim. Biophys. Acta, in press.
14. Lindgren, F. T.; Freeman, N. K., and Nichols, A. V.; in The Metabolism of Lipids as Related to Atherosclerosis, edited by F. Kummerow, Springfield, Thomas Publishing Co., 1964, p. 62.
15. Rowen, R.; J. Exptl. Med. 114:807, 1961.
16. Rowen, R., and Martin, J.; Biochim. Biophys. Acta 70:396, 1963.

Received October, 1964.

A General Computer Method for Statistical Analysis of Data

Alicia Ewing

In order to deal effectively with rapidly increasing amounts of experimental data, a computer program has been written in Fortran (1), which not only calculates the usual statistical parameters for a population but also automatically compares a group of related populations in order to identify significant differences between them. A population, as the term is used here, means a set of related cases, for example, "all animals subjected to treatment A". Each case (here an individual animal) consists of a number of measurements, usually one for each variable being studied. A group of related populations is considered to be populations from the same experiment (or from similar experiments), for example, the three populations "all animals subjected to treatment A", "all animals subjected to treatment B" and "all control animals" might make up a group, assuming that the variables have been recorded in the same order and units of measurement for each of the three populations. For flexibility of analysis, the group membership of each population and the population membership of each case can be defined by the arrangement of the input deck. This means that once data cards for all cases have been punched, a wide variety of breakdowns of the data can be analyzed merely by rearrangement of the input cards.

PROGRAM CALCULATIONS

The statistical terminology and notation used here are standard and may be found in most basic statistical texts (2,3). For each population of not more than 7,500 data items (number of cases times number of variables) the program will calculate the mean (μ), standard deviation (σ) and standard error of the mean, for each variable. The program then generates a six-part histogram for the intervals bounded by the points: $(\mu - 3\sigma)$, $(\mu - 2\sigma)$, $(\mu - \sigma)$, μ, $(\mu + \sigma)$, $(\mu + 2\sigma)$ and $(\mu + 3\sigma)$ for each variable. Any values less than $(\mu - 3\sigma)$ or greater than $(\mu + 3\sigma)$ are separately printed. This provides a means of checking the assumption of normal distribution, since the expected percentage of (normally-distributed) values within each such interval is well determined. If the normality assumption is untenable for a given variable, the subsequent program calculations involving this variable are probably invalid. Following the histogram calculations, the program computes the correlation coefficients (Pearson's r) for each pair of variables. The magnitude of r (which varies from -1 to +1) provides an indication of the degree of the linear relationship between the two variables; the sign of r is the sign of regression coefficient b_{xy} which can be computed from

r_{xy} by $b_{xy} = r_{xy} \frac{\sigma_y}{\sigma_x}$. All r's significant at either the five-percent or one-percent level are so labeled. In all these calculations, provisions are made in the program so that missing values for any of the variables will cause no difficulty; the results will be adjusted appropriately and the printed output will state the number of measurements used in each calculation.

In the usual case, a population will not consist of more than 7,500 data items. However, in the event that one does exceed this limit, the program will break the population data into blocks of no more than 7,500 items and perform the calculations described above on these blocks. When the calculations for the last block in such a population are completed, the program will combine all data and calculate μ, σ, and the standard error of the mean for each variable in the population as a whole.

As the programs perform calculations for a population, or a data-block, it writes the results on a magnetic "output" tape, which is subsequently converted to printed form. In addition, it temporarily stores μ, σ and n (the number of measurements) for each variable as computed from the data for an entire population on a second magnetic tape for reference by the part of the program, which performs comparisons between related populations. When the program senses the end of a group of related populations, it rewinds the second tape and reads the data for the populations in question. Then, selecting all possible pairs of populations in turn, it tests the two means for each variable in order to identify significant differences, using both the normal test, which is applicable for large values of n, and the t-test, which is preferable for variables with small numbers of observations. In addition, the program applies the F-test to the pair of standard deviations because any significant difference in the two σ's will invalidate the t-test. Significant values at either the five-percent or the one-percent level are marked, and the results are printed in tabular form for each pair of populations.

ACCURACY

Most of the program calculations are performed in floating point arithmetic, which can preserve the equivalent of eight significant digits. However, calculations involving the differences of very large values, such as sums of squares, are handled in double precision arithmetic, which preserves 16 significant digits. In computing significance levels for the t- and F-tests, the program searches stored tables of significant 'cutoff' points. Since, due to limited storage availability, it has not been feasible to store all such points, the significance levels must be regarded as approximations. In general, the program tends to err on the conservative side. Sufficient information is included with the output to allow reference to the complete statistical tables in doubtful cases. The significance levels for the normal test are exact.

OUTPUT IDENTIFICATION

In order to identify correctly computer-produced analyses at some later time, two labeling options can be used. The first provides for a population description consisting of 78 characters (including spaces), which can serve to identify the population in question. For example, TREATMENT B ANIMALS WITH BODY WEIGHT GREATER THAN MEAN might be such a description which, when included with the data cards for the population, will cause the program to repeat the description for ease of identification at the top of each page of output relating to the population. The second labeling procedure allows the use of one six-character (alphabetic or numeric) name for each variable; in the normal case, variable names are entered with the first population in each group and, from the point of view of the program, their entry serves to define the beginning of a new group. Thus, the careful use of the variable name option both enables the program to include the appropriate labels with the output and also provides a control over the comparisons that will be made.

RESTRICTIONS

In addition to the upper limit of 7,500 data items in the calculation of both histograms and correlation coefficients, the current version of the program is limited by the following restrictions: 1. no population may have more than 200 variables and 2. no more than 30 populations may be compared with one another at a time. These restrictions are a consequence of the amount of computer memory available on the IBM 7094 computer for storing data and intermediate results and, also, of the particular assignment (use) of such storage by the program. Some mutual adjustment of these limits is possible with program modification, for example, a decrease in the number of permissible variables would permit an increase in the size of the data block.

The limit on the number of populations to be compared could, even at this time, be increased, assuming that there are only a few variables in each population. However, as this maximum permits up to 435 (i.e., $n(n-1)/2$) comparisons between populations, this restriction should not prove serious. Should a group ever consist of more than 30 populations, the program will handle them in blocks of 30. It is anticipated that these restrictions will not affect the normal application of this program.

USAGE

Raw data for each case are transcribed onto standard data sheets in one of the formats acceptable to the program. Standard IBM cards are punched from the data sheets and grouped into the appropriate populations. The resulting card deck is then read by the IBM 1401 computer and written on a magnetic tape, which serves as input to the IBM 7094 program. Program output is also written on magnetic tape, which is subsequently printed by the 1401. To facilitate study of the output, it is possible to use the output tape as input to a

subsidiary program, which scans the tape and produces compact tables of results for specified variables. Such a program is currently used to read and reduce tables of correlation coefficients. Time required for the statistical calculations is quite variable, depending on both the total amount of data, the number of variables being studied and the number of populations to be compared. Most applications will probably require no more than 2 min of 7094 time. The 7094 computer is capable of executing more than 300,000 operations per second, not including operations for reading and writing magnetic tape.

SUMMARY

A flexible program for the statistical analysis of experimental data has been described. It is anticipated that such a program is, without modification, useful for computing standard statistical parameters and tests for a wide variety of application.

REFERENCES

1. Fortran General Information Manual, IBM Publications, Form F28-8074-1.
2. Hoel, P. G.; Introduction to Mathematical Statistics, New York, John Wiley & Sons, 1954.
3. Guilford, J. P.; Fundamental Statistics in Psychology and Education, New York, McGraw-Hill, 1956.

Received October, 1964.

STAFF PUBLICATIONS

Anger, H. O., and Davis, D. H.: Gamma-Ray Detection Efficiency and Image Resolution in Sodium Iodide, Rev. Sci. Instr. 35:693-697, 1964.

Anger, H. O., and Van Dyke, D. C.: Human Bone-Marrow Distribution Shown In Vivo by Iron-52 and the Positron Scintillation Camera, Science 144: 1587-1589, 1964.

Anger, H. O.: Scintillation Camera with Multichannel Collimators, J. Nucl. Med. 5:515-531, 1964.

Ashikawa, J. K.; Sondhaus, C. A.; Tobias, C. A.; Greenfield, A. G., and Paschkes, V.: Difference in Injury Mode, Dose-Rate Dependence and RBE of 730-MeV Protons, 100-kVp X Rays and 250-kVp X Rays, in Symposium on Biological Effects of Neutron and Proton Irradiations, Upton, N.Y., U.S. Brookhaven National Laboratory, Oct. 1963; Biological Effects of Neutron and Proton Irradiations, Vol. 1, Vienna, International Atomic Energy Agency, 1964, pp. 249-260.

Brustad, T.: Influence of H_2S on the Radiosensitivity of Enzymes and Microorganisms, Radiation Res. 22:421-430, 1964.

D'Angio, G. J.; Lawrence, J. H.; Gottschalk, A., and Lyman, J.: Relative Efficiency of High-LET Radiation (Bragg-Peak Lithium Ions) on Normal Rabbit Skin, Using Integral Dose as a Basis for Comparison, Nature 204:1267-1268, 1964.

Estable-Puig, J. F.; de Estable, R. F.; Tobias, C., and Haymaker, W.: Degeneration and Regeneration of Myelinated Fibers in the Cerebral and Cerebellar Cortex Following Damage from Ionizing Particle Radiation, Acta Neuropath. 4:175-190, 1964.

Evans, E. S.; Van Dyke, D. C., and Rosenberg, L. L.: Interaction of the Erythrocyte-Stimulating Factor with Calorigenic Hormones, Endocrinology 75: 758-764, 1964.

Freifelder, D.; Kleinschmidt, A. K., and Sinsheimer, R. L.: Electron Microscopy of Single-Stranded DNA: Circularity of DNA of Bacteriophage ϕX174, Science 146:254-255, 1964.

Freifelder, D., and Maaløe, O.: Energy Requirement for Thymineless Death in Cells of Escherichia Coli, J. Bacteriol. 88:987-990, 1964

Gaffey, C. T.: Bioelectric Sensitivity to Irradiation of the Retina and Visual Pathways, in International Symposium on the Response of the Nervous System to Ionizing Radiation, 2d, Los Angeles, 1963; Response of the Nervous System to Ionizing Radiation, edited by T. J. Haley and R. S. Snider, Boston, Little, Brown, 1964, pp. 243-270.

Glaeser, R. M., and Mel, H. C.: The Electrophoretic Behavior of Osmium Tetroxide-Fixed and Potassium Permanganate-Fixed Rat Erythrocytes, Biochim. Biophys. Acta 79:606-617, 1964.

Gottschalk, A., and Anger, H. O.: Letter to the editor, J. Nucl. Med. 5:569-570, 1964.

Gottschalk, A., and Anger, H. O.: The Sensitivity of the Positron Scintillation Camera for Detecting Simulated Brain Tumors with Gallium 68-EDTA, Am. J. Roentgenol. Radium Therapy Nucl. Med. 92:174-176, 1964.

Gutnisky, A.; Nohr, M. L., and Van Dyke, D.: Stimulation of Erythropoietin Production by Whole-Body Irradiation (Spleen Shielded), J. Nucl. Med. 5:595-605, 1964.

Jones, H. B.: Genetic Factors in Lung Disease, in Symposium on Aging of the Lung: Perspectives, Hahnemann Medical College, Philadelphia, Nov. 18-20, 1963; Aging of the Lung, edited by L. Cander, New York, Grune & Stratton, Inc., 1964, pp. 243-256.

King, J. L.: An Experiment in Progress with Mouse Populations, Genetics 50: 1211, 1964.

Lawrence, J. H.; Tobias, C. A.; Born, J. L.; Linfoot, J. A.; Kling, R. P., and Gottschalk, A.: Alpha and Proton Heavy Particles and the Bragg Peak in Therapy, Trans. Am. Clin. Climatol. Assoc. 75:111-116, 1964.

Manney, T. R.: Action of a Super-Suppressor in Yeast in Relation to Allelic Mapping and Complementation, Genetics 50:109-121, 1964.

Manougian, E.: Development of a Single Tracer Injection Method of C^{14}-Glucose Kinetic Studies in Humans, J. Nucl. Med. 5:746-762, 1964.

Manougian, E.; Pollycove, M.; Linfoot, J., and Lawrence, J. H.: C^{14}-Glucose Kinetic Studies in Normal, Diabetic, and Acromegalic Subjects, J. Nucl. Med. 5:763-795, 1964.

Mel, H. C.: On the Stability of Flow-Formed Interfaces, and a Diffusion-Gravity Controlled Enzyme-Substrate Reaction, Chem. Eng. Sci. 19:847-851, 1964.

Mel, H. C.: Stable-Flow Free Boundary (STAFLO) Migration and Fractionation of Cell Mixtures. III. Migration Principles--Sedimentation and Electrophoresis, J. Theoret. Biol. 6:307-324, 1964.

Nichols, A. V., Smith, L.; Rehnborg, C. S., and Francis, D.: Lipid Transfer by High-Density Lipoproteins of Human Serum In Vitro, Biochem. Biophys. Res. Commun. 17:512-516, 1964.

Person, D. A.; Sargent, T., and Isaac, E.: Thorotrast-Induced Carcinoma of the Liver, Arch. Surg. 88:503-510, 1964.

Rehnborg, C. S., and Nichols, A. V.: The Fate of Cholesteryl Esters in Human Serum Incubated In Vitro at 38°, Biochim. Biophys. Acta 84:596-603, 1964.

Rosenberg, L. L., and LaRoche, G.: Determination of Iodoamino Acid Composition of Rat Thyroidal Iodoprotein: Some Sources of Serious Error, Endocrinology 75:776-786, 1964.

Saito, H.; Sargent, T.; Parker, H. G., and Lawrence, J. H.: Normal Iron Absorption in Man, in International Society of Hematology, IX Congress, Mexico City, Sept., 1962; Proceedings, International Society of Hematology, Vol. 3, Mexico City, 1964, pp. 511-522.

Saito, H.; Sargent III, T.; Parker, H. G., and Lawrence, J. H.: Whole-Body Iron Loss in Normal Man Measured with a Gamma Spectrometer, J. Nucl. Med. 5: 571-580, 1964.

Sargent, T.; Linfoot, J. A.; Stauffer, H., and Lawrence, J. H.: Use of a Whole-Body Counter in Turnover Studies with Ca^{47}, J. Nucl. Med. 5:407-416, 1964.

Schooley, J. C., and Kelly, L. S.: Influence of the Thymus on the Output of Thoracic-Duct Lymphocytes, in The Thymus in Immunobiology, edited by R. A. Good and A. E. Gabrielsen, New York, Harper & Row, 1964, Chap. 11.

Sillesen, K.; Lawrence, J. H., and Lyman, J. T.: Heavy-Particle Ionization (He, Li, B, Ne) and the Proliferative Capacity of Neoplastic Cells In Vivo, Acta Isotopica 3:107-126, 1963.

Sondhaus, C. A.; Wallace, R. W.; Lyman, J. T.; Kase, K. W., and Steward, P. G.: Physical Parameters in Exposure of Large Animals to High-Energy Protons, in Symposium on Biological Effects of Neutron Irradiations, Upton, N.Y., U.S. Brookhaven National Laboratory, Oct. 1963; Biological Effects of Neutron and Proton Irradiations, Vol. 1, Vienna, International Atomic Energency Agency, 1964, pp. 231-247.

Tobias, C. A., and Todd, P.: Analysis of the Effects of High-LET Radiations on Various Strains of Cells, in Symposium on Biological Effects of Neutron Irradiations, Upton, N.Y., U.S. Brookhaven National Laboratory, Oct. 7-11, 1963; Biological Effects of Neutron and Proton Irradiations, Vol. 2, Vienna, International Atomic Energy Agency, 1964, pp. 410-428.

Tobias, C. A.; Lawrence, J. H.; Lyman, J.; Born, J. L.; Gottschalk, A.; Linfoot, J., and McDonald, L.: Progress Report on Pituitary Irradiation, in International Symposium on the Response of the Nervous System to Ionizing Radiation, 2d, Los Angeles, 1963; Response of the Nervous System to Ionizing Radiation, edited by T. J. Haley and R. S. Snider, Boston, Little, Brown, 1964, pp. 19-35.

Tobias, C. A., and Manney, T.: Some Molecular and Cellular Effects of Heavily Ionizing Radiations, Ann. N.Y. Acad. Sci. 114, Art. 1:16-31, 1964.

Van Dyke, D.; Anger, H., and Pollycove, M.: The Effect of Erythropoietic Stimulation on Marrow Distribution in Man, Rabbit, and Rat as Shown by Fe^{59} and Fe^{52}, Blood 24:356-371, 1964.

Winchell, H. S.; Pollycove, M.; Loughman, W. D.; Richards, V.; Kim, L., and Lawrence, J. H.: Homotransplantation Studies in Dogs Following Selective Lymphatic Ablation (abstract), in International Society of Blood Transfusion, Xth Congress, Stockholm, 1964; Abstracts, Stockholm, International Society of Blood Transfusion, 1964, P3 A:15.

Winchell, H. S.; Pollycove, M.; Kusubov, N.; Fawaaz, R.; Lawrence, J. H.: Iron Kinetics of Thoracic Duct Lymph, in International Society of Haematology, Xth Congress, Stockholm, Sweden, 1964; Abstracts, Stockholm, International Society of Haematology, 1964, F:34.

Yano, Y., and Anger, H. O.: A Gallium Positron Cow for Medical Use, J. Nucl. Med. 5:485-488, 1964.

Yokoro, K.; Kunii, A.; Furth, J., and Durbin, P. W.: Tumor Induction with Astatine-211 in Rats: Characterization of Pituitary Tumors, Cancer Res. 24:683-688, 1964.